

RATHISH RAJAN

Tailoring the Properties of Biocomposites by Silane Coupling Agents and Graphene Nanoplatelets

RATHISH RAJAN

Tailoring the Properties of Biocomposites
by Silane Coupling Agents and
Graphene Nanoplatelets

ACADEMIC DISSERTATION

To be presented, with the permission of
the Faculty of Engineering and Natural Sciences
of Tampere University,
for public discussion in the auditorium K1702
of Konetalo, Korkeakoulunkatu 6, Tampere,
on 9 September 2022, at 12 o'clock.

ACADEMIC DISSERTATION
Tampere University, Faculty of Engineering and Natural Sciences
Finland

<i>Responsible supervisor and Custos</i>	Professor Jyrki Vuorinen Tampere University Finland	
<i>Supervisor</i>	Professor Mikael Skrifvars University of Borås Sweden	
<i>Pre-examiners</i>	Doctor Parvez Alam The University of Edinburgh United Kingdom	Doctor Aart W. van Vuure KU Leuven Belgium
<i>Opponent</i>	Professor Patrik Fernberg Luleå University of Technology Sweden	

The originality of this thesis has been checked using the Turnitin OriginalityCheck service.

Copyright ©2022 Rathish Rajan

Cover design: Roihu Inc.

ISBN 978-952-03-2535-0 (print)
ISBN 978-952-03-2536-7 (pdf)
ISSN 2489-9860 (print)
ISSN 2490-0028 (pdf)
<http://urn.fi/URN:ISBN:978-952-03-2536-7>



Carbon dioxide emissions from printing Tampere University dissertations have been compensated.

PunaMusta Oy – Yliopistopaino
Joensuu 2022

Dedication

To my parents

Preface

This work was conducted at the former research unit of Tampere University of Technology in Kokkola, Finland (2011-2013), Technology Centre KETEK LTD in Kokkola, Finland (2013-2016) and Centria University of Applied Sciences in Kokkola, Finland (2017-2020). This thesis was part of the research projects ANACOMPO (Funded by the County Administrative Board of Norrbotten, Sweden, and the Regional Council of Lapland, Finland, in the EU Interreg IV-A North programme), ECOGEL-CRONOS (Funded by the EU Seventh Framework Programme FP7), and SMART-WPC (Funded by the County Administrative Board of Norrbotten, Sweden, and the Regional Council of Lapland, Finland, in the EU Interreg IV-A North programme).

I want to express my sincere gratitude to my supervisor and custos, Prof. Jyrki Vuorinen, for his guidance, insightful comments, patience and continuous support during this thesis's finalisation. I am deeply grateful to my co-supervisor, Prof. Mikael Skrifvars, for his motivation, enthusiasm and immense knowledge. His guidance helped me through the period of this study, in the publications of manuscripts and in finalising the thesis. I am thankful to retired Prof. Pentti Järvelä for allowing me to start my doctoral study under his supervision. I could not have imagined having better supervisors for my doctoral study. I am thankful to Prof. Kuruvilla Joseph, of the Indian Institute of Space Science and Technology, for inculcating in me the passion for research. I owe my deepest gratitude to the opponent and pre-examiners of this thesis

I am thankful to KETEK and CENTRIA UAS for permitting me to include the part of the project results in the publications that are part of this thesis. I am grateful to Dr Egidija Rainosalu, R & D Coordinator in CENTRIA UAS, for her continuous support and motivation throughout the thesis period. I am indebted to many of my colleagues at KETEK, CENTRIA UAS and Tampere University for their help in the lab and continuous motivation. I extend my gratitude to all of my co-authors for contributing to the publications. I thank all my friends for their constant support and encouragement.

I want to thank my parents and all my teachers for giving me the opportunities and experiences that shaped my life. I am deeply in debt to my parents, Mr G. Rajan and Mrs Geetha Bai. K., for selflessly encouraging me to explore new directions in my life and search for my destiny. I thank my sister and her family for being there during the ups and downs in my life. My deep and sincere gratitude to my wife and my boys for their patience, unparalleled love, help, support and sacrifices that made this thesis possible. Above all, I praise God, the almighty, to provide me with this opportunity and grant me the capability to proceed successfully.

Kokkola, 12.8.2022

Rathish Rajan

Abstract

The increase in environmental awareness and stringent regulations from concerned governing bodies are the main driving forces for the growing interest in biomaterials. The development of environment-friendly bio-composites and their application in various industrial sectors has steadily increased during the last few decades. Wood-based, natural, and man-made fibres are used to manufacture bio-composites. The polymer matrix can be thermoset resins like epoxy (EP) or unsaturated polyester resin (UPR), or thermoplastic polymers like polypropylene (PP), polyethylene (PE) and polyvinyl chloride (PVC).

The primary resource to produce regenerated cellulose fibre (RCF) or man-made cellulose fibres is wood. The regenerated cellulose fibres, which are commonly named viscose or rayon, possess high purity, uniformity and reproducibility of their properties. Compared to lignocellulosic fibres, the benefit of man-made cellulose is that it is available in continuous filaments.

When it comes to the lignocellulosic fibre or regenerated cellulose fibre reinforced composites, the interface between fibre and matrix polymer plays a vital role. The hydrophilic wood-based fibres and hydrophobic thermoplastic polymer composites result in structurally weak composites due to the non-compatible interaction across the interface. Though the chemical modification techniques for wood fibre based composites are well-known, that of RCF-based composites requires more research. Few studies report the use of the chemical modification of viscose fabric to be used in composite production. The chemicals used in the modification step necessitate waste treatment, which involves extra energy consumption,

time and money. Hence an environmentally friendly and sustainable approach to improve fibre-matrix adhesion is necessary.

In the Nordic countries with abundant raw material sources, the forest industry explores new applications for the produced side-streams. The building and construction, automotive and household commodities are the primary markets for wood-plastic composites (WPCs). By exploring new markets for WPC's, the composite industry and the forest industry will gain larger markets and better commercial profits from wood and its by-products. One approach for finding a new market for WPC's is to develop extrinsically conductive composites containing conductive fillers. The research in functionalising the WPC is in the developing stage, and it requires profound research.

This thesis aims to improve the interfacial adhesion in viscose fabric/thermoset resin-based composites by chemically modifying the viscose fabric. In another approach, the thermoset resin (epoxy resin) is modified with an appropriate silane coupling agent as an alternative to fibre surface modification, and its effect on various properties of composites is studied. Another objective of the study is to produce and characterise wood-plastic composites containing electrically and thermally conductive nanofillers. The effect of incorporating graphene nanoplatelets (GNP) on various properties of polypropylene-based WPC is studied. These types of composites can be a sustainable solution for the extrinsically conductive polymer market.

The silane coupling agents such as 3-aminopropyltriethoxysilane (APTES), 3-methacryloxypropyltrimethoxysilane (MPS) and also acetylation

treatment are adopted to modify the viscose fabrics. The unsaturated polyester-based composites prepared from viscose fabric modified by APTES in ethanol medium increased the flexural strength and notched Charpy impact strength by 18% and 115%, respectively. The water absorption studies revealed that the APTES modification significantly delayed and reduced the total absorbed water compared to all other composites.

As an alternative to the fibre modification method, epoxy resin was modified by APTES to produce viscose fabric reinforced composites. The epoxide content determination and FTIR results from this study show that resin modification efficiency was better at 70°C compared to modification done at room temperature. The APTES was mixed directly into the epoxy resin, eliminating any process waste in the modification stage. The tensile strength and elongation at break of the composites prepared using APTES-modified epoxy resin increased by 14% and 41%, respectively. The Charpy impact strength of APTES-modified epoxy resin based viscose fabric composites increased by 115%.

The effect of GNP on various properties of WPC was studied. The addition of graphene into PP-based WPC yielded an anti-static/dissipative WPC compound at a graphene loading of 15 wt%. The surface resistivity of PP/wood/graphene composite decreased by several orders of magnitude from 1014 Ω /sq to 106 Ω /sq. While achieving the desired electrical properties, the tensile strength of hybrid WPC decreased by 25%. The thermal conductivity of WPC containing 20 wt% wood filler and 15 wt% GNP increased by 130% compared to WPC comprising 20 wt% wood filler.

List of Publications

- I. **Rajan, R.**, Riihivuori, J., Skrifvars, M., & Järvelä, P. (2014) Effect of viscose fabric modification on the mechanical and water absorption properties of composites prepared through vacuum infusion. *Journal of Reinforced Plastics and Composites* 33 (15), 1416-1429. <https://doi.org/10.1177/0731684414534748>
- II. **Rajan, R.**, Rainosalo, E., Thomas, S.P., Ramamoorthy SK., Zavašnik, J., Vuorinen, J., & Skrifvars, M. (2018) Modification of epoxy resin by silane-coupling agent to improve tensile properties of viscose fabric composites. *Polymer Bulletin* 75, 167-195. <https://doi.org/10.1007/s00289-017-2022-2>
- III. **Rajan, R.**, Rainosalo, E., Ramamoorthy SK., Thomas, S.P., Zavašnik, J., Vuorinen, J., & Skrifvars, M. (2018) Mechanical, thermal, and burning properties of viscose fabric composites: Influence of epoxy resin modification. *Journal of Applied Polymer Science* 135 (36), 46673 (1-12). <https://doi.org/10.1002/app.46673>
- IV. **Rajan, R.**, Näkki, J., Layek, R., Rainosalo, E. (2021) Wood plastic composites with improved electrical and thermal conductivity. *Wood Science and Technology* 55, 719-739. <https://doi.org/10.1007/s00226-021-01275-9>

Author contributions

Article I - The author planned the experiments with Riihivuori. The first author did the chemical modification of viscose fabric. The second author conducted composite preparation and characterisation. The author interpreted the results and wrote the manuscript. Prof. Skrifvars and Prof. Järvälä took part in writing, as well as commented and approved the manuscript.

Article II – The author planned and conducted the experiments, interpreted the results and wrote the manuscript. Dr Ramamoorthy conducted the tensile testing of composites and Dr Zavašnik conducted the SEM analysis. All other authors contributed in writing, commenting and approving the manuscript.

Article III – The author planned and conducted the experiments, interpreted the results and wrote the manuscript. Dr Ramamoorthy conducted the 3-point bending test and Dr Zavašnik conducted the SEM analysis. All other authors contributed in writing, commenting and approving the manuscript.

Article IV - The author planned and conducted the experiments, interpreted the results and wrote the manuscript. Dr Layek performed the thermal conductivity analysis and Dr Näkki conducted the SEM analysis. All the authors contributed in writing, commenting and approving the manuscript.

List of Symbols and Abbreviations

AKD	Alkyl ketene dimer
APTES/APS	3-aminopropyltriethoxysilane
ASTM	American Society for Testing and Materials
ATR	Attenuated total reflectance
CNT	Carbon nanotubes
DP	Degree of polymerisation
DSC	Differential scanning calorimetry
EP	Epoxy
ESD	Electrostatic discharge
EU	European Union
FTIR	Fourier-transform infrared spectroscopy
GCN	Graphitic carbon nitride
GNP	Graphene nanoplatelets
GNP-MB	Graphene nanoplatelet masterbatch
GRP	Glass fibre reinforced plastics
HDPE	High-density polyethylene
ISO	International Organization for Standardization
IUPAC	International Union of Pure and Applied Chemistry
MAPP	Maleic anhydride grafted polypropylene
MB	Masterbatch

MEKP	Methyl ethyl ketone peroxide
MPS	3-Methacryloxypropyltrimethoxysilane
NFRP	Natural fibre reinforced polymer composites
NMMO	<i>N</i> -methyl morpholine oxide
PBS	Polybutylene succinate
PE	Polyethylene
PHR	Parts per hundred resin
PLA	Polylactic acid
PMMA	Polymethyl methacrylate
PP	Polypropylene
PVC	Polyvinyl chloride
RCFs	Regenerated cellulose fibres
SCA	Silane coupling agent
SEBS-g-MA	Styrene block copolymer grafted with maleic anhydride
SEM	Scanning electron microscopy
TGA	Thermogravimetric analysis
UPR	Unsaturated polyester resin
VE	Vinyl ester resin
WPC-MB	Wood-plastic composite masterbatch
WPCs	Wood-plastic composites

Contents

Preface	iii
Abstract	v
List of publications	ix
Author's contribution	xi
List of symbols and abbreviations	xiii
1. INTRODUCTION.....	1
1.1. Viscose fibre reinforced composites	6
1.2. Wood-plastic composites	11
1.3. Chemical modifications	14
1.3.1. Fibre modifications	15
1.3.2. Resin modifications	18
1.4. Functional fillers in wood-plastic composite	20
1.5. Justification.....	24
2. AIM OF THE STUDY	27
3. EXPERIMENTAL.....	30

3.1.	Materials.....	30
3.1.1.	Viscose fabric based composites.....	30
3.1.2.	Functionalised wood-plastic composite.....	31
3.2.	Methods	32
3.2.1.	Viscose fabric modification.....	32
3.2.2	Epoxy resin modification	34
3.2.3.	Preparation of unsaturated polyester-based composites	35
3.2.4.	Preparation of epoxy-based castings and composites.....	36
3.2.5.	Preparation of hybrid wood-plastic composites	38
3.3.	Characterisation	40
4.	RESULT AND DISCUSSIONS	51
4.1.	Unsaturated polyester/viscose fabric composite.....	51
4.1.1.	Mechanical properties	51
4.1.2.	Water absorption test.....	54
4.2.	Epoxy/viscose fabric composites.....	56
4.2.1.	Modification of epoxy resin	56
4.2.2.	Tensile properties	60

4.2.3. Tensile fractography.....	64
4.2.4. Charpy impact strength.....	66
4.2.5. Burning properties.....	70
4.3. Hybrid wood-plastic composite	72
4.3.1. Tensile properties	72
4.3.2. Surface resistivity	76
4.3.3. Thermal conductivity	81
5. CONCLUSIONS AND FUTURE WORK.....	83
REFERENCES.....	86

1 Introduction

A global action plan to avoid climate change by limiting global warming has been set out in the Paris Agreement, which entered into force on November 2016 [1]. The European Union (EU) is already acting to achieve the target by 2030 (2030 climate and energy framework) by reducing greenhouse gas emissions by at least 40% [2]. The European Commission foresees a competitive EU industry and circular economy as a critical enabler to reduce greenhouse gas emissions [3]. By reducing the energy needs and process emissions, by increasing recycling rates, and through new materials like composites that can replace energy-intensive materials, this goal can be reached [3].

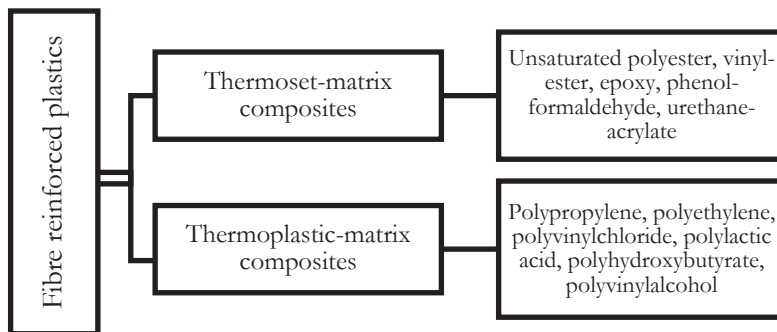


Figure 1: Classification of fibre reinforced plastics based on the type of polymer matrix

Composite materials are one of the most advanced and adaptable engineering materials known to man [4]. Composite materials are macroscopic combinations of two or more distinct materials having a discrete and recognisable interface separating them [5]. A composite material consists of a reinforcing phase embedded in a bulk phase called the matrix. While the matrix gives the composite its shape, surface appearance, environmental tolerance and overall durability, the fibrous reinforcement bears most of the structural loads, thus primarily providing macroscopic stiffness and strength [4]. The matrix may be metallic, ceramic or polymeric in origin.

The interface between the matrix and the reinforcing phase has a significant role in determining the composite's mechanical properties. The interface is the boundary between two phases of different chemistry and microstructure. Such boundaries mostly have chemical and mechanical interactions, and therefore we can also define a separate region, called the interphase, which is the volume of material affected by the interactions at the interface [6]. The interphase is formed when a polymer matrix (grey) interacts with the filler/fibre (black), as seen in Figure 2 (a). The interphase may be a bulk matrix or have different properties formed from its interaction with the matrix. When the volume fraction increases, as seen in Figure 2 (b), or if the size of the filler/fibre decreases at the same volume fraction as shown in Figure 2 (c), it is possible that the interphase is now predominant and forms a continuous phase. In this case, the interphase acts as the effective matrix material with the original bulk matrix seen as a discontinuous phase [6].

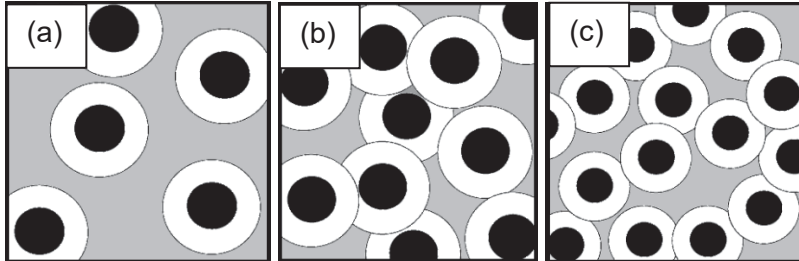


Figure 2: Interphase in polymer composites (a) at low-volume filler content, (b) at high-volume filler content and (c) small-size filler at high-volume content (Adapted from [6])

Polymer matrix composites are the most common because of their reasonable cost, relative ease of manufacture and considerable weight savings. They exhibit greater specific strength and specific modulus compared to metal matrix composites [7]. The matrix binds the reinforcing materials together and helps transfer mechanical loads from weak matrices to stronger reinforcements. Polymer composites are mainly divided into thermoplastic and thermosetting composites based on their thermal processing characteristics, as seen in Figure 1. The main type of thermoplastic composites produced in Europe uses short glass fibre as reinforcement (1.47 mt in 2017) [8]. Polypropylene and polyamide are the most popular commercial thermoplastic matrices for short glass fibre reinforced composite production [8]. Thermosetting resins have superior bonding and forming characteristics due to the chemistry involved. Thermosetting resins, available in liquid forms, offer a combination of low cost and ease in processing compared to thermoplastics. Although most of the thermoset resins require high temperature for processing, some of the thermoset resins, including the most commonly used unsaturated polyester resins, are processable at room temperature. The most common thermoset resins used

for composite production are phenolic, epoxy and unsaturated polyester resins.

Biocomposites play an essential role in various industries, being an alternative to materials gathered from crude oil resources. Biocomposites are produced by embedding natural fibres of plant or animal origin in a bio-based or synthetic polymer matrix. A market study conducted by the nova-Institute shows that the European production of biocomposites was 410,000 tonnes in 2018 (Figure 3) [9]. The production of glass fibre reinforced plastics (GRP) reported in 2017 is 1.12 million tonnes, and it is predicted to grow by 2.1% to a total volume of 1.14 million tonnes in 2018 [8, 10]. The overall annual growth rate of biocomposites was about 3% in 2012 – 2017 [9].

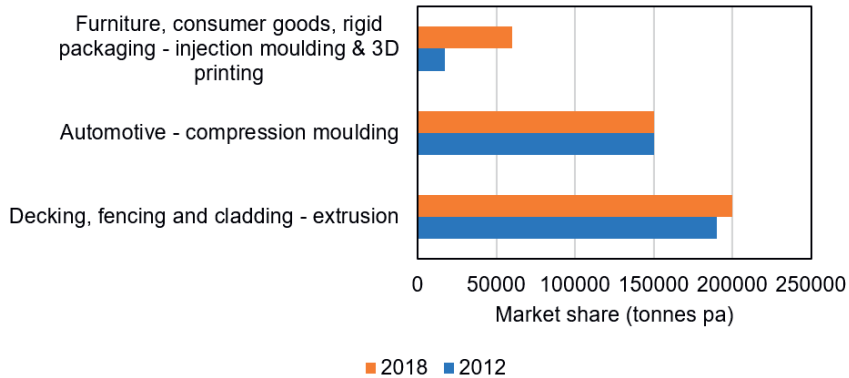


Figure 3: Production of biocomposites in Europe in 2012 (blue) and 2018 (orange) (Adapted from [9])

Bio-based natural fibre reinforced polymer composites (NFRPs) are of great interest, as natural fibres are abundant in nature, renewable, biodegradable, and reduce dependency on fossil fuel when considering the conventional carbon fibre production [11, 12]. The NFRPs are also often characterised as environment-friendly or green materials due to their origin. Numerous studies in the literature focus on using various natural fibres to produce reinforced polymer composites [13].

Applications of NFRPs are mainly for non-structural or semi-structural applications. Staiger and Tucker [14] defined semi-structural applications as those that require the component to support its weight and bear external loads such as soft loads or impacts. Due to the limitations of utilising the full advantage of natural fibres' mechanical properties, the demand for biocomposites in structurally demanding applications is limited. These properties are not entirely achievable due to naturally occurring structural defects within the fibre, defects introduced during processing of the fibre and chemical incompatibilities with the polymer matrix. Conducting more research on NFRPs, focused on improving their properties, is essential. NFRPs have increasing market demand, especially among automobile companies looking for lightweight materials with sound damping properties [15-17].

The new environmental regulations from the governing authorities have forced the manufacturers to shift the focus from non-biodegradable raw materials to more sustainable ones. In this context, abundant, renewable and biodegradable natural fibres will be a better choice over non-degradable synthetic fibres in composite production. The classification of lignocellulosic fibres based on the part of the tree/plant from where it is separated is seen in Figure 4 [18].

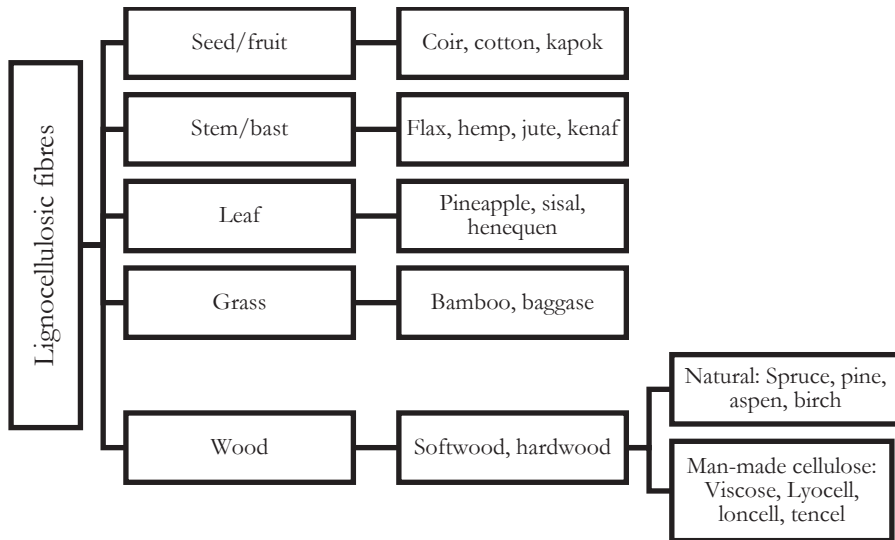


Figure 4: Classification of lignocellulosic fibres based on the part of the plant/tree (Adapted from [18])

1.1 Viscose fibre reinforced composites

Regenerated cellulose fibres (RCF) production, such as viscose, has existed since the late 19th century [19]. Although the conventional source for the production of RCFs is wood [19], non-conventional sources such as bamboo [20], bagasse [21] and bacterial cellulose [22] are also utilised. The wood cellulose for viscose production is prepared mainly through the Kraft pulping process and sulphite process. The Kraft pulping process is an alkaline process in which sodium hydroxide and sodium sulphide are active delignification agents [23]. The sulphite process utilises sulphur dioxide with varying cation, liquor pH and cooking temperature for the

delignification of wood. The various processes involved in the pulping of wood are well described by Lönnberg [23].

The traditional method of producing regenerated cellulose fibre is the viscose process. The Lyocell process, which was introduced later, has several environmental benefits compared to the viscose process. First patented in 1893, the viscose still maintains its unique position among man-made fibres. The viscose process involves converting wood pulp into a spinnable high-viscosity solution termed “dope” and then to longer filaments with desired properties [24]. The pulp is first soaked in a strong alkali solution of 17 – 19% sodium hydroxide to convert cellulose to alkali cellulose or sodium cellulose. The obtained swollen mass is pressed to achieve a precise alkali to cellulose ratio. In the next step, the alkali cellulose is aged under controlled conditions of time and temperature to depolymerise the cellulose by oxidation to the desired degree of polymerisation (DP). The aged alkali cellulose is treated with carbon disulphide to form sodium cellulose xanthate. The sodium cellulose xanthate is dissolved in dilute sodium hydroxide to yield a viscous orange-coloured solution, from which the name viscose originated. After filtration, deaeration and ripening to the desired coagulation point known as a salt index, the viscose solution is ready for spinning. The viscose filaments form when the viscose solution extrudes through the tiny holes of a spinneret into a spin bath consisting of sulphuric acid, sodium sulphate, zinc sulphate and water. Finally, the viscose filaments are neutralised, bleached and washed before surface finishing is applied [24].

The Lyocell process resulted from the high demand to develop a cellulose fibre that exhibits an improved cost to performance ratio compared to the viscose process. The increased environmental awareness also acted as a

driver for developing the Lyocell process in the 1980s. Likewise, viscose fibre, the source of Lyocell fibre, is also wood pulp. As described by White [25], in the Lyocell process the wood pulp is directly dissolved in hot *N*-methyl morpholine oxide (NMMO) by avoiding an intermediate step in the process. This process also recovers >99% of the NMMO solvent to reduce the effluent and is eco-friendlier than the traditional viscose process.

Regenerated cellulose fibres predominately used as textile fabric and cord yarn in car tyres are currently emerging as reinforcement in thermoplastic and thermoset biocomposites. Carrillo et al.[26] studied various properties of short Lyocell fibre reinforced HDPE composites with respect to fibre content and chemical treatment of the fibres. The tensile testing showed that the Lyocell fibre reinforced composite's tensile modulus increased with increasing fibre content (6.6 – 29.9 wt%) compared to neat HDPE. They analysed the effect of the chemical modification of Lyocell fibre on tensile strength and found that the strength of the composites made from 6.6 wt% Lyocell modified by PMMA grafting is higher and the results are statistically significant compared to neat HDPE and HDPE/Lyocell composite. The tensile strength of the composites made from untreated Lyocell fibres decreased with increasing fibre content compared to neat HDPE. Although the silane modification improved the tensile strength, it was still below the tensile strength of neat HDPE. These results indicate a low adhesion between fibre and matrix, even after chemical modification with the silane coupling agent. The amount of silane (MPS) used in this study was 5 wt% (w.r.t. weight of fibre). The decreased adhesion might be due to the excess amount of silane, forming a layer on the fibre surface and hence preventing effective stress transfer.

Reinhardt et al. [27] prepared a bio-based composite using PLA as the matrix and unidirectional viscose fibre as reinforcement (50 vol%) via filament winding and the film stacking method. The tensile strength and modulus of continuous viscose-PLA composites increased by 127% and 133%, respectively, compared to neat PLA. Elongation at break of continuous viscose-PLA composites increased by 11% compared to neat PLA. PLA- and PBS-based viscose fibre composites were prepared with a fibre content of 10, 30 and 50 wt% [28]. The tensile test results showed that strength increases with the increase of the fibre content in both PLA and PBS composites. This study reported that the viscose fibre reinforced composites performed better in tensile strength than flax and hemp reinforced composites. The main factor for improved strength of viscose fibre composites as discussed in the article is the good dispersion of Cordenka fibres compared to flax and hemp, which improved the fibre-matrix adhesion. The impact strength of PLA reinforced with viscose fibre significantly increased compared to neat PLA. However, the same reinforcement resulted in decreased impact strength for PBS composites. This discrepancy is explained by the brittle nature of both polymers. The viscose fibre reinforcement improved the impact resistance of low-impact resistant PLA. The ductility of the viscose fibre is much higher than the flax and hemp fibre, which results in increased impact strength.

Behners et al. [29] reported the photochemical surface treatment of viscose fabric using pentaerythritol triacrylate or allyl diallylphthalate. The effect of modification on various properties of viscose fabric/polypropylene composites was studied. The modification of the viscose fibres and resultant PP-based composites showed improved fibre-matrix adhesion and interfacial shear strength, which improved tensile and impact strength compared

to untreated viscose fabric composites. The mechanical properties' improvement is explained based on the improved wettability and increased affinity to non-polar polymers like PP.

Ramamoorthy et al. [30] studied the effect of silane and alkali treatment of viscose fibre on lactic acid based thermoset composites' properties. They reported that 10 wt% silane treatment increased the tensile strength from 80.86 MPa (untreated) to 91.43 MPa. The water absorption for the composites decreased 10% after the silane treatment. The composites' impact strength increased with the increase in silane content. The studies mentioned above point out the need for modifying the RCF fibres before using them in the production of biocomposites. Mader et al. [31] studied the effect of surface properties and fibre-matrix adhesion on epoxy/viscose composites' impact strength. They compared the variations in impact strength of composites based on two different viscose fibres (with and without oily avivage). They found that the avivage decreased the impact strength by 6% due to increased fibre-matrix adhesion. The improved adhesion resulted in shorter debond length and subsequently pull-out length, resulting in lower energy absorption [31]. In another study, Santamala et al. [32] compared epoxy/unidirectional Lyocell composites' mechanical properties to flax and glass fibre composites. The Lyocell composites showed comparable tensile properties to flax composites. This study highlighted the necessity of improving the adhesion through RCF fibre modifications to achieve better mechanical properties than those found in their study [32].

The hydrophilic properties of RCFs lead to weak interphase in hydrophobic thermoplastic polymer composites, resulting in structurally weak composites. When cellulose fibre based composites are exposed to water, the water penetrates through voids in the composite and is absorbed due to

the hydrophilic hydroxyl groups in the fibre. The composite properties diminish when the swelling of cellulose fibre creates stress at the interface region, leading to the microcracking mechanism in the matrix around the swelled fibre. Excessive exposure of composites to water finally results in ultimate debonding between the fibre and the matrix [33]. Compared to lignocellulosic fibres, RCF has a more amorphous region through which water absorption can occur. Chemical modification of RCFs is essential to reduce the water absorption and increase the interfacial adhesion between fibre and matrix. Though the chemical modification techniques for wood fibre based composites are well-known, those of RCF-based composites require more research. Few studies, including those mentioned above, have reported the chemical modification of viscose fabric used in composite production.

1.2 Wood-plastic composites

Wood is a naturally abundant material. The cellulose fibres embedded in a lignin matrix coupled with hemicellulose form a natural composite [34]. The wood-plastic composites are manufactured predominantly from synthetic thermoplastic polymers and wood flour or fibres. Natural wood fibre or wood flour can be extracted from a virgin source and is often a byproduct of sawmills or recycled wood. The obtained materials are processed further into a final filler-like form suitable for composite processing by chipping and grounding if required. The wood flour is usually less than 1 mm in length and has a wide distribution of length to diameter ratio known as the aspect ratio. Instead of long individual fibres, these particles comprise bundles of short fibres. [35].

The wood flour is in particulate form or very short in length. The benefits of wood flour compared to wood fibre is its relatively high bulk density, free-flowing nature, low cost and the availability for manufacturing of WPCs. Wood fibres as reinforcement will increase mechanical properties such as strength, elongation and impact resistance [36]. Processing issues, such as feeding and metering low bulk density fibres, limit the use of wood fibres in WPC production.



Figure 5: Commercial wood-plastic composite products (a) hollow profile for decking from UPM Biocomposites (b) kitchen utensils from Stora Enso and (c) wood-plastic cutleries from Akvila (Source: Company websites)

The wood species and size of wood particles highly influence the properties of WPCs. The commonly used wood species are aspen, spruce, pine, maple and oak. Migneault et al. [37] investigated the effect of wood fibre surface chemistry on the tensile properties, flexural strength and impact resistance of WPC. The six different fibres used were trembling aspen wood, black spruce wood, white birchwood, trembling aspen bark, black spruce bark and bleached cellulose pulp. They stated that the fibres with

higher carbohydrate content on the surface led to composites with high strength compared to the fibres with more lignin or extractives. According to the literature, the WPCs based on hardwood species performed better in tensile strength than the softwood species' wood filler [38]. The results show an increase in tensile strength of 5%, 10%, 5% for 20 wt%, 30 wt%, and 50 wt% filler loading, respectively, when compared to ponderosa pine. The increase in tensile strength for hardwood fibre based WPC can be associated to the higher cellulose content when compared to softwood. According to Schwarzkopf and Burnard [39], another aspect related to the wood species selection is the microstructure of the wood. The effective surface area for interaction with the polymer and the polymer penetration into the wood structure affect the composite properties.

Typically, both recycled and virgin grade thermoplastic polymers are used in WPC production [40]. The polypropylene (PP) based WPCs dominate the European WPC market [41]. Polypropylene is the most chosen virgin grade of plastic, while polyethylene is in demand as recycled plastic in WPC production [42]. The WPCs are used largely as decking, and PVC-based WPCs are mainly used as the windows and doors [41].

Several chemical modification methods are employed to improve various properties of WPCs. Yeh et al. [43] reported that the optimal maleic anhydride grafted polypropylene (MAPP) content is 2% for WPC containing 50% wood filler. When the MAPP content was 2 wt%, the tensile strength increased to 41 MPa from 22 MPa for WPC without MAPP. They studied the synergistic effect of MAPP and SEBS-g-MA (styrene block copolymer grafted with maleic anhydride) on tensile and impact strength. The combination of MAPP (2%) and SEBS-g-MA (1%) slightly decreased the tensile

strength compared to MAPP alone, while considerably improving the impact strength of WPC.

Wang et al. [44] investigated four different silanes' efficiency in improving the polypropylene WPCs' mechanical properties. Compared to WPC with untreated fibre, the fibre treated with silane alone did not improve WPC properties. But, in the presence of dicumyl peroxide, composites treated with 3-methacryloxypropyltrimethoxysilane (MPS) and allyltrimethoxysilane exhibited an increase of up to 90, 60 and 50% in flexural, tensile and impact strength, respectively.

Poplar wood was modified with the alkyl ketene dimer (AKD) coupling agent to prepare polypropylene-based WPC. In this study, Zhang [45] investigated the coupling agent's influence in improving mechanical properties. Compared to WPC with 70% fibre without any coupling agent, WPC with 5% AKD as a coupling agent improved the tensile strength and modulus of WPC by 41% and 45%, respectively. The impact strength of WPC with coupling agent increased 38% compared to WPC without a coupling agent. The improvement in the performance of AKD-coupled composites was attributed to the higher surface area coverage of the wood fibres' surface by the lactone groups and the long carbon chain, enhancing the interfacial adhesion between wood fibres and plastics.

1.3 Chemical modifications

As already discussed, the main drawback of natural fibres compared to glass fibre and carbon fibre is the poor mechanical properties due to non-uniformity in the fibre properties. Lignocellulosic fibres are hydrophilic in

nature due to the presence of strongly polarised hydroxyl groups. These non-treated hydrophilic fibres are incompatible with most of the hydrophobic polymers used in composites. The incompatibility is a critical issue because when adhesion between fibre and matrix is weak, the stress transfer is insufficient. Hence, strong interfacial adhesion is essential to achieve better performance of the material. Various physical and chemical modification methods can improve interfacial bonding. The primary approach to enhance the interfacial adhesion is to modify the fibre's surface by different chemical treatments [13, 46-48] and by physical methods such as corona treatment and plasma treatment, to name a few examples [49, 50].

In general, the interfacial adhesions between a fibre and a matrix resin in fibre reinforced composites are chemical, physical or mechanical adhesion [51]. The chemical adhesion proceeds through the formation of chemical bonds between fibre and matrix. The primary approach for improving the chemical bonding between fibre and matrix resin is the surface modification of fibre through chemical treatment methods such as alkali treatment, acetylation and coupling agent treatment [52-55].

1.3.1 Fibre modifications

The hydroxyl groups present in the glucose units building up the cellulose polymer are available for modification. The cellulose fibre has a hydrophilic surface which is chemically modifiable by reactions with the hydroxyl groups. Through the chemical treatments, these hydroxyl groups undergo reaction and introduce new chemical moieties which could effectively interact with the matrix. Mercerisation, isocyanate treatment, permanganate treatment, acrylation, acetylation, silane treatment, peroxide treatment, benzoylation treatment and maleated coupling agents are examples of the

chemical treatments adopted for modification of the natural fibres [56-58]. In general, after chemical treatment, the fibre-matrix adhesion in the produced fibre reinforced composites is improved. Among the chemical treatments, mercerisation, acetylation, and silane coupling agent treatments are the most reported fibre modification methods in the literature. The acetylation and silane coupling agent modifications of lignocellulosic fibres are briefly discussed below due to their relevance to this study.

Acetylation is an attractive method for modifying the surface of natural fibres. It involves making them more hydrophobic by introducing acetyl groups. Acetylation, first used in hardwood, showed that it reduced the swelling of wood in water. This method is studied more than any other modification methods for lignocellulosic fibres. The reaction occurs between hydroxyl groups of cellulose fibre with the acetyl group (Figure 6). This substitution reaction renders fibre into a hydrophobic state. The hydroxyl groups in the crystalline region of cellulose do not react, as the acetylating agent cannot access these. In contrast, the hydroxyl groups that react with acetic anhydride are those of the lignin, hemicelluloses, and those located in amorphous domains of the cellulose [53].



Figure 6: Schematic representation of acetic anhydride modification of lignocellulosic fibre [59, 60]

Silane coupling agents (SCA) have a general chemical structure of $R(4-n)-Si-(R'X)_n$ ($n=1, 2$), where R is alkoxy, X is an organic functional group and R' is the alkyl bridge connecting the silicon atom and organic functional group. This bifunctionality of organosilanes facilitates an effective coupling between cellulosic fibres and polymer matrices. In natural fibre composites, the most commonly used silanes are trialkoxysilanes [52, 59] with amino, mercapto, glycydoxy, vinyl or methacryloxy organic functional groups.

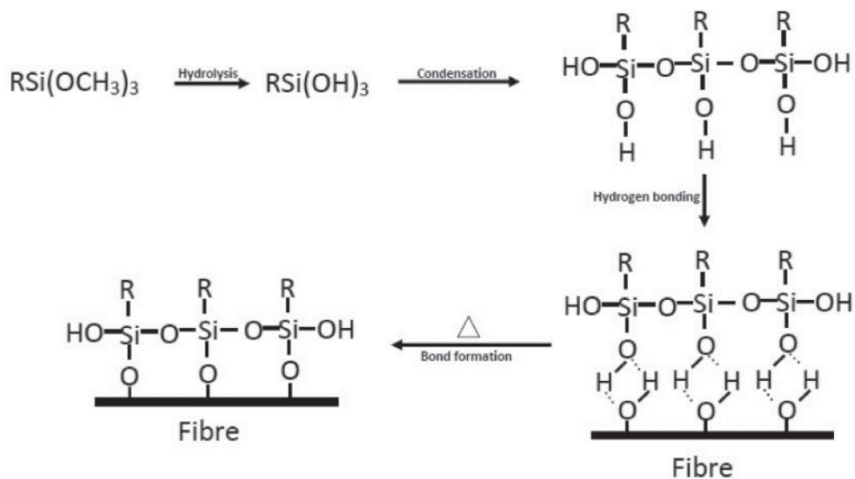


Figure 7: Reaction between the silane coupling agent and lignocellulosic fibre [59]

The mechanism for the coupling of organosilanes with cellulosic fibres initiates through the hydrolysis of silanes in the presence of water, yielding reactive silanol groups (Figure 7). During the hydrolysis, the silanols' self-condensation can also occur; however, it is advisable to control the self-condensation to leave the silanols available to be adsorbed with hydroxyl

groups of cellulosic fibres. The reactive silanols are adsorbed to the hydroxyl group on the cellulosic fibre surface through hydrogen bonding. Finally, under high temperature, the hydrogen bonds between silanols and the fibre hydroxyl group get converted to covalent -Si-O-C- bonds while liberating water [52, 59]. The effective interaction of silane-treated fibre is highly dependent on the reactivity and compatibility between organo-functionality of silane and reactivity of resin.

1.3.2 Resin modifications

Resin or matrix modification is another approach to improve fibre/matrix adhesion in polymer composites. Numerous studies related to modifying the thermoplastic polymers through the grafting method are reported in the literature [61-63]. The post-modification of polyolefins with polar or functional groups is common in producing polyolefins with functional or reactive chemical groups. The grafting of reactive groups onto thermoplastics decreases hydrophobicity and improves the compatibility with the fibre reinforcement. Among various methods, high shear rate reactive extrusion is widely used for producing grafted thermoplastics [64]. The grafting of maleic anhydride onto polypropylene involves; (1) thermal decomposition of peroxide and formation of primary radicals; (2) PP macroradical formation through hydrogen abstraction predominantly from tertiary carbon of PP backbone; (3) covalent bonding of maleic anhydride onto PP; (4) termination of reaction through hydrogen abstraction from another tertiary carbon [65]. Several studies report the usage of grafted polymers as a compatibiliser in NFRP [66-68].

Thermoset resins like unsaturated polyester (UPR), vinyl ester (VE) and epoxy (EP) are the main type of resins used to manufacture thermoset

composites. The modification of thermoset resins can be done by selecting the appropriate modifying agent compatible with the resin's available reactive chemical groups. SCA can act as a modifying agent that will react with thermoset resin functionality and the fibre surface via chemical bonding or physical attraction. Reactive groups with a higher chemical affinity towards fibre hydroxyls are introduced into the matrix resin through the resin modification. The SCA's organic functionalities can form chemical bonds with compatible reactive groups in the matrix resin, while the hydrolysable alkoxy groups can react with the fibre surface. Thus, an improved fibre-matrix adhesion is achievable through the matrix resin modification approach [69].

Mostly, the chemical modification of thermoset resin is done to improve the toughness of the resin. Aziz et al. [70] modified unsaturated polyester resin to improve its compatibility with kenaf fibre in the composite. The reference (type A) used in this study was a commercial polyester resin named Crystic 2-406PA. Compared to type A resin, type B resin was hydrophilic in nature. The type C and type D resins contained additional monomers, 2,3-epoxypropyl methacrylate and 2-hydroxyethyl methacrylate, respectively, to improve resin/kenaf fibre adhesion. They found that the resin modification significantly increased the composite's mechanical properties due to improved fibre-matrix adhesion.

Yang et al. [71] studied the mechanical properties of carbon fibre reinforced epoxy composites prepared from the resins modified with different types of silane coupling agents (SCA). They found that matrix modification improved the tensile strength and flexural properties of carbon fibre composites by 4% and 44%, respectively. Wei-Gang et al. [72] modified epoxy resins with SCA to improve the corrosion resistance and epoxy coatings'

adhesion on the aluminium surface. The water resistance of epoxy coatings on metal substrates improved after the silane treatment [73]. The potential of SCAs, poly-siloxanes, silsesquioxanes, silica and silicates in the modification of epoxy resin has been reported [74]. The research related to the silane modification of epoxy resin is mostly in coatings to improve flexibility, adhesion, corrosion resistance and water resistance.

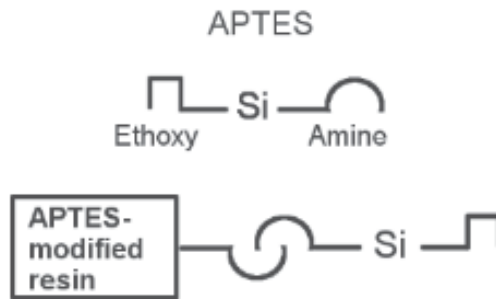


Figure 8: Schematic representation of 3-aminopropyltriethoxysilane reaction with epoxy resin [75]

1.4 Functional fillers in wood-plastic composite

Wood-plastic composite (WPC) material consisting of wood fibres and cellulose fibre from pulp are used currently in industrial sectors like building and construction for decking, railing, flooring, cladding, and window frames, to name but a few. Demand for WPCs is also increasing in furni-

ture, consumer goods, household electronics and automotive parts production. WPCs' functionalisation will open new markets for WPCs, and ultimately the composite and forest industry will benefit from this. Hybrid composites are a combination of three or more materials to achieve specific properties. For example, the combination of glass fibre with carbon fibre at an optimal ratio can result in composites with good mechanical properties at a lower cost. The preparation of hybrid composites by combining carbon and other inorganic fillers is another strategy [76, 77]. Combining two or more fillers can be beneficial so that the final product's properties can result from synergistic effects between the fillers. Therefore, the hybrid composites exhibit multi-functionality, since the two fillers' combined properties can lead to new material production with quite a diverse set of properties [76]. The hybridisation of WPC with functional inorganic fillers and nanofillers is also of interest, since these fillers may impart exceptional functionality to the WPC by increasing the thermal or electrical conductivities of otherwise low conductive WPC. However, the lack of interaction between the synthetic fibres/inorganic filler/nanofiller, wood fibres, and matrix limits the effective reinforcement. A better understanding of the interaction between these components in hybrid WPC is the subject of both scientific and practical interest.

Song et al. [78] studied the effect of varying graphite loading from 10-40% on the flexural properties and impact strength of the WPC based on 30% of bamboo flour. The flexural strength of the hybrid composite decreased with increasing graphite content. The composites' flexural strength decreased from 38.8 MPa to 30.5 MPa at a graphite content of 40 wt%. The flexural modulus of the hybrid composite doubled compared to the HDPE/bamboo flour composite, indicating the improvement in the WPC's stiffness due to the graphite's addition. The HDPE/bamboo flour

composites with 40 wt% of graphite exhibited a volume resistivity of 31.2 Ω .cm. Among the different graphite loading, only 40% of graphite showed an EMI-SE of 20 dB in the frequency range of 30 – 3,000 MHz.

Lei et al. [79] studied the effect of different concentration of graphitic carbon nitride (GCN) on the 40% wood flour filled WPC's properties. The results from their study showed that the composite's tensile modulus increased by 142.9% compared to WPC containing 5 wt% of GCN. The tensile strength of the hybrid composite with 3 wt% of GCN exhibited a 4% increase compared to WPC, whereas the flexural strength showed a decreasing trend with increasing GCN content. The flexural strength of WPC was 47.4 MPa and it decreased to 43.8 MPa when the GCN content was 10 wt%.

Faruk et al. [80] used two different approaches to incorporate nanoclay in WPC. Nanoclay reinforced HDPE was used as a matrix for the wood-plastic composite to improve the composite's mechanical properties. The flexural strength of WPC increased from 28.9 MPa to 33.5 MPa through the addition of 5 wt% of nanoclay. The flexural modulus of the hybrid WPC increased compared to neat WPC. The coupling agent improved the flexural strength and the modulus of both neat and hybrid WPC. They found that using the HDPE/nanoclay as a WPC matrix is the best approach to incorporate the nanoclay into WPC.

Lee et al. [81] incorporated nanoclay into the WPC to improve various properties. The addition of 1-phr nanoclay increased the tensile properties (16.4 MPa to 33.7 MPa) and the impact strength (5.5 kJ/m² to 8.8 kJ/m²) when compared to neat WPC. The increase in tensile properties was at-

tributed to the higher dispersion and exfoliation of nanoclay in the PP matrix achieved after the addition of MAPP. The drastic increase in the impact strength of WPC containing 2 phr nanoclay and 3% MAPP was ascribed to the coupling effect of MAPP at the interfaces.

Graphene has received much interest in recent years due to its exceptional mechanical, thermal and electrical properties. Graphene is a two-dimensional allotrope of carbon made up of a single layer of sp^2 hybridised carbon atoms [82, 83]. The structures with several layers of carbon atoms are called graphene nanoplatelets (GNP), which are used as nanofillers to improve the various properties of polymer nanocomposite [84]. Different methods, such as in-situ, solution casting and melt mixing, are used to prepare thermoplastic polymer-based nanocomposites [83]. Since melt mixing is a well-established processing technique in the plastic industry, many reports on graphene and graphite-based polymer nanocomposites produced by this method are found in the literature [85, 86]. Those studies indicate that graphene's addition improves the nanocomposites' mechanical properties at a lower filler content. However, for the nanocomposites prepared by the melt mixing method, the electrical percolation threshold is reached at a higher GNP loading. Hence the electrical conductivity in graphene-based nanocomposites is achieved by sacrificing mechanical properties up to a certain degree [83].

Some studies have reported the influence of GNP on the various properties of WPC. Most of those studies focused on the effect of GNP on mechanical and thermal properties. Sheshmani et al. [87] studied the polypropylene/wood/GNP system and reported that the tensile and flexural properties of the hybrid composites increased at 0.8 wt% of GNP content. They

also found that by increasing GNP content to 3-5 wt%, the strength decreased due to agglomeration. The composites' electrical conductivity or thermal conductivity was not studied. In another study, researchers developed PVC/wood/GNP composites to be used as electromagnetic interference shielding material [88]. This study showed that maximum electromagnetic interference shielding (26 dB) for composites was achieved with GNP loading of 9 wt%.

1.5 Justification

The hydrophilic nature of lignocellulosic fibres is due to the non-crystalline cellulose, hemicellulose, pectin and the fibres' porous morphology [89]. The hydrophilic nature of fibre can result in incompatibility with hydrophobic matrix resins like polypropylene [90]. This results in natural fibre composite's inferior mechanical properties, which can be significantly evident in the long-term-used application. The water uptake by natural fibres can be associated with the amorphous regions of the cellulose and with the hydrophilic non-cellulosic components. Due to the close packing of the cellulosic chains and the hydrogen bonding between the hydroxyl groups, there are less accessible hydroxyl groups in the crystalline region, which eventually decreases water absorption in the crystalline region of fibres.

The degree of crystallinity for viscose fibres is in the range of 27–41% [91], which is lower than that of some other natural cellulose fibres like flax and hemp. RCFs, similar to lignocellulosic fibres, absorb moisture through the amorphous cellulose hydroxyl groups in the fibre [92]. This results in relatively increased water uptake by viscose fibres and points out the necessity

of interfacial modification in viscose fibre based polymer composites. In order to be considered in semi-structural and structural applications, the RCF composites need to overcome the polymer incompatibility issues by controlling RCF fibres' hydrophilicity. The chemical modification of fibres can generate waste from the modification process, requiring waste treatment. Also, some of the fibre chemical modification methods are time-consuming and expensive. As an alternative to the chemical modification of fibre, a resin modification approach that is quicker and generates less process waste can also be utilised. Thus, research on conventional thermoset resins (epoxy, unsaturated polyester) based RCF composites suitable for automotive and other structural applications is highly relevant.

The interest in environment-friendly wood-plastic composites (WPC) has been steadily increasing in various industrial sectors over the last few decades [93]. The primary market for wood-plastic composites is building and construction, the automotive industry, and the furniture industry [93]. Wood-plastic composites are used to produce non-load bearing products like household appliances and load-bearing products similar to decking. In Finland, the forest industry is strong and growing steadily [94]. The sawmills generate by-products, including wood chips, wood flour and bark [95]. These by-products are utilised primarily for energy recovery and for producing fibre board, particle board and WPCs [95].

Incorporating functional properties such as thermal and electrical properties will open a new market for WPCs in addition to the current applications. The hybridisation of WPC with conductive fillers and nanofillers is of interest, since these fillers may impart unique functionality to the WPC by increasing the thermal or electrical conductivity of otherwise insulative WPC. However, the lack of interaction between the conductive fillers,

wood fibre/flour and matrix limits the effective reinforcement. A better understanding of the interaction between these components in hybrid WPCs is the subject of both scientific and practical interest.

This thesis falls in line with global and EU (2030 climate and energy framework) demand for limiting global warming. The thesis research has studied and developed lightweight composite materials that could be a prospective replacement for automotive parts, materials for building and construction, and ESD-safe WPC products. The research focuses on the interfacial modification in thermoset composites via fibre surface modification and thermoset resin modification. The study will also develop wood-plastic composites (WPCs) with functional properties that can open a new market for WPCs.

2 Aim of the study

This thesis aims to study various properties of environment-friendly and light-weighted composites with viscose fabric and wood flour as reinforcement and conventional thermoset resins (epoxy and unsaturated polyester) and thermoplastic (polypropylene) as a matrix. The obtained findings should allow the development of biocomposites for automotive applications and ESD-safe products, and for thermal management.

The more detailed aims are the following:

- To understand the chemistry behind the modification of viscose fabric by acetylation and silane coupling agents. The effect of such chemical modifications on thermoset composites' various properties will be studied.
- The modification of thermoset resin by the addition of modifying agents into the resin that yields less process waste will be evaluated as an environmentally friendly alternative, considering the environmental impact of the process waste after the fibre chemical modification. The effect of resin modification on the various properties of resin and composites will be studied.
- To study the possibilities of expanding wood-plastic composites' utilisation in applications requiring electrical and thermal conductivity. Graphene nanoplatelets (GNP) will be used as conductive filler to produce conductive wood-plastic composites using the conventional melt processing method. The effect of conductive fillers on various properties of composites will be studied.

The main research questions are the following:

1. What is the influence of fabric modification on various properties of viscose fabric/unsaturated polyester resin composites?
2. How protective is gelcoat coating for viscose fabric reinforced thermoset composites?
3. Can the resin modification method be better or an alternative to the fabric modification method?
4. How does the incorporation of graphene nanoplatelets influence various properties of WPCs?

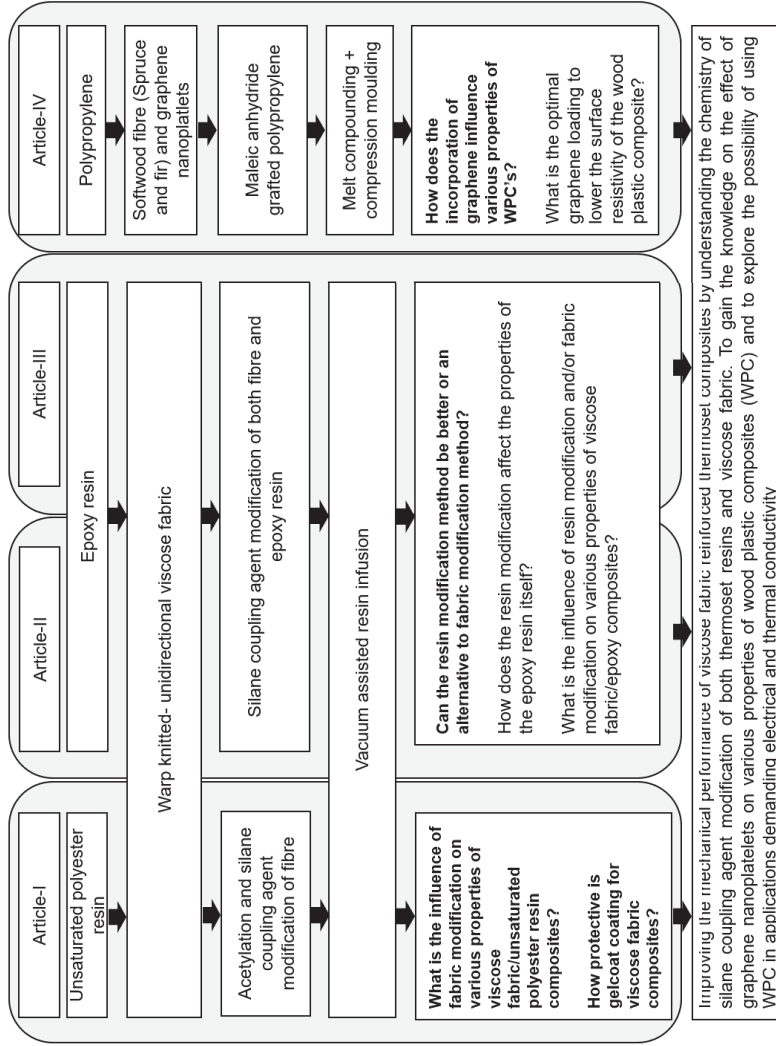


Figure 9: Outline of the thesis including the experiments, research questions and overall objective

3 Experimental

3.1 Materials

3.1.1 Viscose fabric based composites

Reinforcement - The fabric used in the production of thermoset composites is made from Cordenka 610F viscose yarn with the twist Z40, 2440 dtex linear density and 1,350 filaments (Cordenka, Germany). The yarn was processed into unidirectional fabrics with a surface weight of 223 g/m² by warp knitting (Engtex, Sweden), as seen in Figure 10 (Article I, II & III).

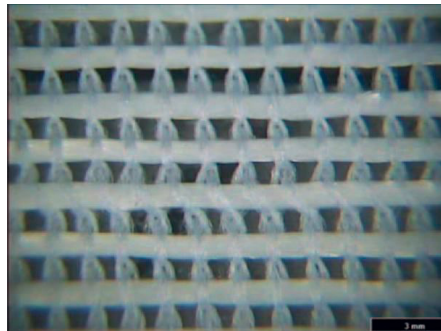


Figure 10: Warp-knitted fabric with the thick weft yarn in the horizontal direction and the thin polyester yarn in the vertical direction [59]

Thermoset resins - An unsaturated polyester resin (Envirez[®]M8600 TA) with a biomass content of 13% was purchased from Ashland Inc, Finland. The density of the resin given by the supplier was 1.1 g/cm³. Methyl ethyl ketone peroxide (MEKP) was used as a catalyst. The gelcoat surface resin used in the accelerated water absorption study was based on unsaturated

polyester (Maxguard®NP) (Article I). Prime 20LV, an epoxy resin manufactured by Gurit Ltd, was used to produce viscose fabric composites (Article II & III). An amine hardener (Prime 20LV slow) was used to cure the castings and composites.

Chemicals – 3-aminopropyltriethoxysilane (APS; 99% purity) from Acros Organics was used as a coupling agent to modify the viscose fabric surface (Article I, II, III). 3-methacryloxypropyltrimethoxysilane (Sigma Aldrich) was another SCA used to modify the viscose fabric (Article I). Acetic anhydride obtained from Merck was used for the acetylation of the viscose fabric (Article I). All the chemicals used for the titration method to determine the epoxide content of the epoxy resin was of reagent grade and used as received (Article II & III).

3.1.2 Functionalised wood-plastic composite

WPC masterbatch – The WPC masterbatch containing 50% (by weight) wood flour and polypropylene (PP) was purchased from a masterbatch producer. The softwood flour consists of spruce and fir with a maximum size of 500 µm. About 3% (by weight) of additives are included in the composition (Article IV).

GNP masterbatch – The graphene nanoplatelet (GNP) masterbatch containing 30% (by weight) of GNP in polypropylene (PP) was purchased from NanoXplore, Canada. The masterbatch GNP is heXo-G V20 with an average thickness of 20 nm (40 layers) and a flake size of 50 µm. The PP used in the masterbatch is an impact copolymer 4220H from Pinnacle Polymers (Article IV).

Polypropylene – The PP in WPC masterbatch and the PP used to dilute the WPC masterbatch was Moplen EP240H, an impact-resistant copolymer produced by LyondellBasell. The main properties of both Moplen EP240H and 4220H are tabulated in Table 1.

Table 1: Physical properties of two impact-resistant polypropylene used in this study

Properties	Moplen EP240H	4220H
Density (g/cm ³)	0.9 (ISO 1183)	0.9 (ASTM D1505)
Tensile modulus (MPa)	1100 (ISO 527-1-2)	-
Tensile Stress at Yield (MPa)	23.0 (ISO 527-1-2)	24.2 (ASTM D638)
Tensile Strain at Yield (%)	8.0 (ISO 527-1-2)	6.0% (ASTM D638)
MFR (g/10 min) (230°C/2.16 kg)	2.0 (ISO 1133)	20.0 (ASTM D1238)

3.2 Methods

3.2.1 Viscose fabric modification

The viscose fabric was chemically modified using 3-aminopropyltriethoxysilane (APTES), 3-methacryloxypropyltrimethoxysilane (MPS) and acetic anhydride.

APTES: APTES was added either to an ethanol/distilled water solution or distilled water to yield a 2 vol% silane concentration in the solution.

Fabric dipped in the silane solution for 5 min was then dried at room temperature for 30 min. Then, the fabrics were oven-dried at 110°C and kept in sealed plastic bags until composite preparation (Article I, II & III).

Table 2: Modification of viscose fabrics and designations for composites

Code	Fabric modification method	Composites code	Resin
APS 95-5	Fabrics treated with 2 vol% APS in (95:5) ethanol/distilled water solution (v/v)	C-APS1 (Article I)	Unsaturated polyester
		RS0-FS2-C (Article I & II)	Epoxy
APS 50-50	Fabrics treated with 2 vol% APS in (50:50) ethanol/distilled water solution (v/v)	C-APS2	Unsaturated polyester
APS water	Fabrics treated with 2 vol% APS in distilled water.	C-APS3	Unsaturated polyester
MPS	Fabrics treated with 0.5 vol% MPS silane in distilled water	C-MPS	Unsaturated polyester
Acetylation	Acetic anhydride treatment	C-acetylation	Unsaturated polyester

MPS: The viscose fabric was treated in an aqueous solution with an MPS concentration of 0.5 vol%. The MPS was dissolved in distilled water acidified with acetic acid to maintain the pH at 4.5. The solution was stirred well for 15 min to form a clear homogeneous solution. Then the fabric was immersed in the solution for one hour. Finally, the fabric was dried for 24

h at 60°C to remove traces of methanol resulting from the methoxy silane's hydrolysis (Article I).

Acetylation: The fabrics pre-dried at 70°C for 16 h were dipped into a glass beaker with acetic anhydride for 1 min. The excess anhydride was drained off by placing the fabrics on a stainless-steel mesh for 3 min. Finally, the treated fabrics were dried at 110°C for two hours (Article I).

3.2.2 Epoxy resin modification

The epoxy resin was mixed with 1, 3, and 5 wt% of APTES. No solvents or catalysts were used in the modification of resin. The modification was done for one hour at room temperature and 70°C. Epoxy resin and the appropriate amount of silane was weighed into a plastic container equipped with a magnetic stirrer and stirred for one hour at room temperature. The resin and an appropriate amount of silane were weighed into a round bottom flask equipped with a reflux condenser for the modifications done at a temperature of 70°C. The stirring continued for one hour in a water bath maintained at a temperature of 70°C (± 3) (Article II & III).

Table 3: Reaction conditions for modification of epoxy resin and designations

APTES (wt%)	Temperature (°C)	Designation		
		Resin	Castings	Composites
0	-	RS0	RS0-CC	RS0-C
1	23	RS1-RT	RS1-RT-CC	-
	70	RS1-70	RS3-RT-CC	RS1-70-C
3	23	RS3-RT	RS3-RT-CC	-
	70	RS3-70	RS3-70-CC	RS3-70-C
5	23	RS5-RT	RS5-RT-CC	-
	70	RS5-70	RS5-RT-CC	RS5-70-C

3.2.3 Preparation of unsaturated polyester-based composites

The composites were fabricated through the vacuum-assisted resin infusion method. The whole process overview is shown in Figure 11. Three replicated composites were made from each type of modified viscose fabric by using identical process conditions. Before the infusion, the fabrics used for lamination were dried in an oven at 70°C for 16 h. The viscose fabrics were stacked as straight as possible on each other to form a unidirectional four-layer lay-up [± 0]₄. A vacuum pressure of -0.3 bar was applied, and it was ensured that there was no leakage in the vacuum bag. The resin was then mixed with 1.2 vol% of MEKP and added to the resin container to start the infusion. The infusion process was completed in approximately 15-20 min at room temperature. The composites were first cured for 24 hours at room temperature and then post-cured at 70°C for 3 hours.

Composites were also made to evaluate the effectiveness of the protective gelcoat surface resin in preventing water absorption. The gelcoat was applied on the glass plate before the fabrics' lay-up for the vacuum infusion process. The gelcoat used here is a white-coloured unsaturated polyester resin used to form the composite surface in contact with the environment. The application of gelcoat was done in a dustless and well-ventilated place at 18°C-25°C. The gelcoat was applied by using spacers to achieve a layer thickness of approximately 0.5 mm. The gelcoat was mixed with 1.5 wt% of MEKP and cured for 4 – 5 hours at room temperature after forming the layer. The vacuum infusion was done one day after the gelcoat application by following the procedure mentioned above. These composites were made with viscose fabric, which has not undergone any chemical modifications. The composite's surface without gelcoat and the edges were covered with two topcoat layers, applied with a paintbrush. Similar to gelcoat,

the topcoat also forms the composite surface that protects the composite against weathering and chemicals. When gelcoat is applied in the mould, topcoats are used as a finish coat on the composite part's inner side.

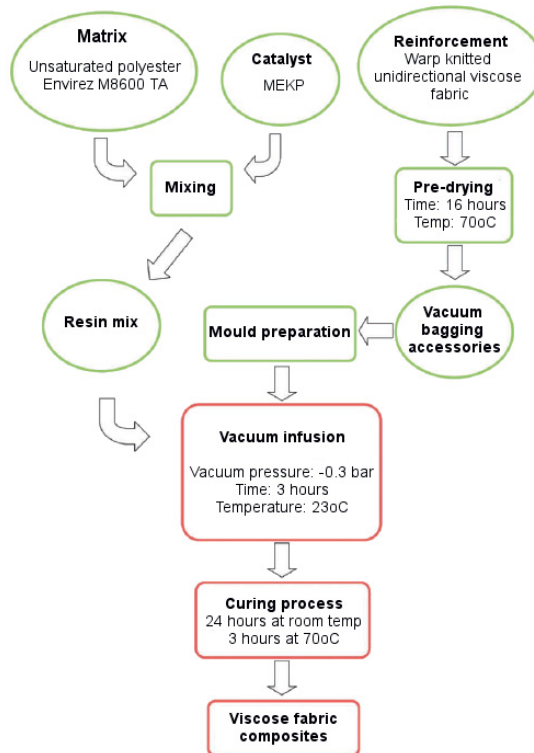


Figure 11: An overview of unsaturated polyester resin/viscose fabric composite production [59]

3.2.4 Preparation of epoxy-based castings and composites

The cured castings (without fibre reinforcement) and epoxy/viscose fabric composites were prepared from epoxy resin modified by APTES. For

comparison, the composites were also prepared from unmodified epoxy resin and APTES-modified viscose fabrics. Cured castings and composites with unmodified viscose fabric as reinforcement were prepared from unmodified epoxy resin as a reference.

Cured castings: Cured castings were prepared using a metal mould with dimensions specified for a dog-bone shaped tensile specimen (ISO 527-2) [96]. After proper mixing, the resin was poured into the metal mould and left for curing. The epoxy resin was mixed with the hardener in a 100:26 ratio (by weight). The curing was done for 7 hours at 65°C and later post-cured at 80°C for 2 hours.

Composites: Modified epoxy-based composites were prepared through the vacuum-assisted resin infusion method. Four layers of warp-knitted unidirectional viscose fabric were carefully laid [$\pm 0/\pm 90/\pm 0/\pm 90$] on top of each other in four layers on the mould surface. Later, the vacuum bagging was completed and the resin infusion was done. The resin infusion was done in a climate chamber at 65°C and by applying a vacuum pressure of 0.1 bar. The composites were cured the same way as cured castings, and the same amount of hardener was used for curing the composites. The fibre weight and volume percentage in the composites were 38–42% and 31–35%, respectively. The thickness of the composites was 2.2–2.4 mm.

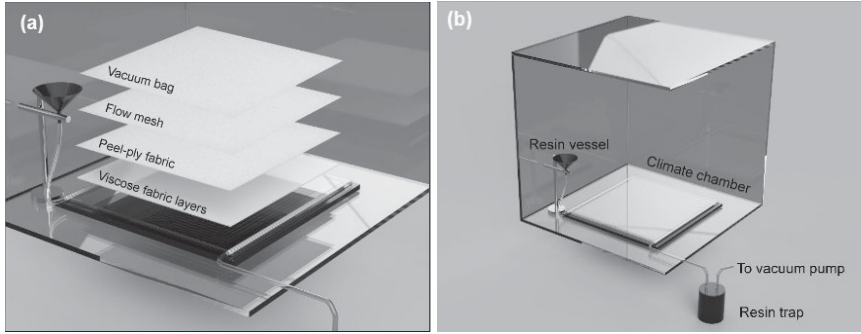


Figure 12: Schematic representation of (a) vacuum bag and (b) composite preparation by vacuum-assisted resin infusion in an oven [69]

3.2.5 Preparation of hybrid wood-plastic composites

The hybrid WPCs were prepared through two-stage melt compounding in a co-rotating intermeshing twin-screw extruder, ZSK 18 MEGAlab, from Coperion, Germany. The extruder's barrel length was 72 mm, and the outer diameter of the screw was 18 mm ($D_o/D_i = 1.55$).

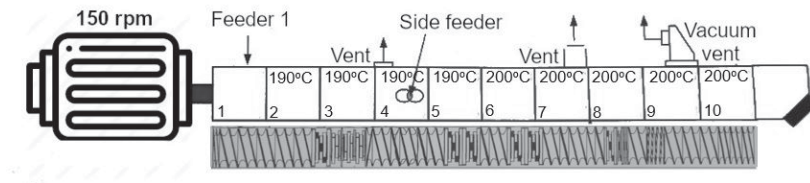


Figure 13: Extrusion set-up and screw configuration for processing hybrid wood-plastic composites

The pre-mixed wood-plastic composites containing 24 wt% (WPC1), 30 wt% (WPC2) and 40 wt% (WPC3) wood flour were prepared by diluting WPC-MB (50 wt% wood flour) with Moplen EP240H. In the second stage,

WPC1 (83.5 wt%)/GNP-MB (16.5 wt%), WPC2 (66.6 wt%)/GNP-MB (33.4 wt%) and WPC3 (50 wt%)/GNP-MB (50 wt%) were melt mixed to produce PP-W20-G5, PP-W20-G10 and PP-W20-G15, respectively. The pre-mixed WPC was fed from the main feeder and GNP-MB was fed from the side feeder. The compounding was done at a screw speed of 150 rpm and the total feed rate was 5 kg/h. The extruder temperature was set 190°C-200°C as seen in Figure 13. The extrudate was cooled in water and finally pelletised and saved for further use. The designations and composition of hybrid wood-plastic composites are listed in Table 1 (Article IV).

Table 4: Designations and composition of hybrid wood-plastic composites

Composites	PP (wt%)	Wood flour (wt%)	GNP (wt%)
PP	100	0	0
PP-W20	80	20	0
PP-W20-G5	75	20	5
PP-W20-G10	70	20	10
PP-W20-G15	65	20	15

The WPC plates were made by hot pressing the PP-W20 and hybrid WPC pellets (Figure 14). The pressing was done in a manual hydraulic hot press at a temperature of 220°C for 3 min with a press load of 3.5 MPa. Initially, a pre-heating time of 15 min was given before the load was applied to remove the moisture. The plates' size was 200 mm x 200 mm, with a 3.6 – 3.8 mm thickness. These plates were later CNC machined to test specimens.



Figure 14: The wood-plastic composite pellets containing 20 wt% of wood flour (PP-W20) and wood-plastic composite pellets containing 20 wt% wood flour and 15 wt% graphene nanoplatelets (PP-W20-G15)

3.3 Characterisation

3.3.1 Tensile properties

Tensile properties of unsaturated polyester resin/viscose fabric composite were determined in accordance with ISO-527-2 [96] by using a Messphysik tensile testing machine equipped with a 10 kN load cell. The test was done at ambient conditions at a test speed of 5 mm/minute. The sample thickness was in the range of 2-3 mm, depending on the modification of the fibre utilised. Tensile strength, modulus and elongation at break are reported from an average of five specimens (Article I).

The tensile properties of modified epoxy cured castings were done in accordance with ISO-527-2 [96] by using a Tiratest 2705 tensile tester equipped with a 5 kN load cell. The average thickness of the casting was 4 mm and the test was conducted at a speed of 2 mm/minute (Article II).

The tensile testing of epoxy/viscose fabric composite was done using a Tinius Olsen H10KT tensile testing machine. The test was conducted in accordance with ISO 527-2 [96]. The average thickness of the specimen was 2.3 mm. The tensile properties are reported from an average of six specimens (Article III). The tensile test was performed in a Tiratest 2705 tensile testing machine equipped with a 5 kN load cell. The test was carried out at room temperature with a speed of 5 mm/minute. The length of the sample was 150 mm and the length of the narrow portion was 80 mm. The thickness of tensile specimens was 3.6 mm – 3.8 mm. Tensile properties are calculated as an average of six specimens. Tensile modulus is calculated from the stress-strain curve slope in the strain interval between 0.05% and 0.25% using the chord slope method.

3.3.2 Flexural properties

The flexural properties of the unsaturated polyester resin/viscose fabric composite were done in accordance with ISO 178 [97] (Article I). The Messphysik MIDI 10-20/4 x 11 tensile tester equipped with a 1 kN load cell was used to do the three-point bending test. The dimension of the specimen used for testing was 80 mm (l) x 15 mm (w) x 2 mm (h). The span length was 50 mm. The test was carried out at ambient condition with a 2 mm/min crosshead speed, and the average values from five specimens are reported.

The three-point bending test for epoxy resin/viscose fabric was done according to the ISO 14125:1998 [98] standard using a Tinius Olsen H10KT universal testing machine (Article III). The dimensions of the specimens were 80 mm x 15 mm (length x width). The thickness of the specimen was

2.3 mm. The test was done at a speed of 10 mm/minute. The span length was 64 mm.

3.3.3 Charpy impact test

Impact resistance of unsaturated polyester resin/viscose fabric composite was measured using a CEAST Resil 5.5J impact testing machine, in accordance with ISO 179 [99] (Article I). The dimension of the specimen was 80 mm (l) x 10 mm (w) x 2 mm (h). The test was done edgewise with a 2 mm notch. The results are presented from an average of three specimens.

The Charpy impact test of epoxy resin/viscose fabric composite was done using Comotech QC-639D testing machines. The test was done in accordance with ISO 179 (Article III). The test was done edgewise without a notch. The dimension of the specimen was 80 mm (l) x 10 mm (w) x 2.3 mm (h). The results are presented from an average of five specimens.

3.3.4 Dynamic mechanical analysis

The dynamic mechanical properties of epoxy resin/viscose fabric composite were analysed using Netzsch DMA 242 (Article III). The measurement was done in tensile mode at a frequency of 1 Hz. The dimension of the specimen was 30 mm (l) x 5 mm (w) x 2.3 mm (h). The free length of the specimen was 10 mm. The test temperature ranged from 25°C to 130°C at a heating rate of 2°C/min.

3.3.5 Water absorption test

The gravimetric water absorption test was done in accordance with ISO 62: 2008 [100] to evaluate the performance of unsaturated polyester/viscose fabric composite (Article I). The test was done at room temperature. The weight gain percentage was calculated from Equation (1).

$$C = [(m_2 - m_1)/m_1 \times 100] \quad (1)$$

NB: m_1 – the mass of the specimen before immersion in water; m_2 – the mass of the specimen after immersion in water for a specified time.

The dimension of the specimen was 90 mm x 90 mm. For each batch of composite, three specimens were tested, and the average value is reported. The edge of the specimens was sealed with topcoat paint. The test was continued until the specimen was saturated or until 102 (2,448 hours) days. An accelerated water absorption test was done to evaluate surface gelcoat and topcoat performance in preventing water absorption. The samples after the test were visually analysed for changes or blister formation on the gelcoat and topcoat surface and deformation of the composite after testing. Weight gain during the test was determined to study the protection efficiency of the gelcoat on the water absorption of the composite laminates. The side of the composite without gelcoat and the edges were sealed with a topcoat. The composites were cut into 100 mm x 100 mm specimens with 2.3 mm thickness. One set of specimens with the dimensions mentioned above was drilled to make three circular holes in the middle of the specimen to study the water absorption. Another set without holes was evaluated for any blister formation or deformation in the composite after

an accelerated water absorption test. The container was placed in a climate chamber at 65°C for four weeks to accelerate the water absorption.

3.3.6 Epoxide content of the epoxy resin

The epoxide content of modified epoxy resin was determined according to manual titration procedures in accordance with ASTM D1652-11 [101] (Article II). The neat or modified epoxy resin was dissolved in methylene chloride and then titrated with standard perchloric acid in the presence of an excess of tetraethylammonium bromide. The sample (0.4 g) was titrated with a perchloric acid reagent to a sharp blue to the green endpoint, stable for approximately 30 s. The volume of perchloric acid consumed during titration was recorded. The weight percent epoxide and epoxy equivalent weight were calculated according to Equation (2) and (3). The value reported is the average of two measurements.

$$E = 4.3 \times V \times N/W \quad (2)$$

$$W_{EEW} = 43 \times 100/E \quad (3)$$

NB: E – weight percent epoxide; W_{EEW} – epoxy equivalent weight; V – the volume of perchloric acid reagent used to titrate the sample (ml); N - normality of perchloric acid reagent; the constant 4.3 is the theoretical molecular weight of the epoxide ring 43 adjusted to 4.3 for the calculation to percent epoxide; W – the weight of the epoxy resin (g) (Article II).

3.3.7 Viscosity of epoxy resin

The viscosity of the neat and modified epoxy resin was measured using an Anton Paar MCR 301 rheometer (Article II). The test was done at a temperature range of 25°C – 65°C at a constant shear rate of 10 s⁻¹. The measurement was done using a 25 mm plate-plate spindle configuration with a gap distance of 1 mm. The value reported is the average of two measurements.

3.3.8 Wettability of cured epoxy castings

The wettability of cured epoxy castings was evaluated by measuring the contact angle of the castings' surface using a contact angle measurement instrument, OCA20 from Dataphysics GmbH (Article II). The static contact angle of ultra-pure water on cured epoxy was measured at room temperature by a sessile drop method. The contact angle value was taken 10 s after depositing the drop on the epoxy surface. The results are reported as the average of five measurements with a corresponding standard deviation.

3.3.9 FTIR spectroscopy

APTES-modified epoxy resin, cured castings and epoxy/viscose fabric composites were measured by ATR-FTIR spectroscopy (Article II). The spectra from resins and cured casting surface were recorded on an ATR PerkinElmer-Spectrum One spectrometer. Signals of eight scans at a resolution of 4 cm⁻¹ were averaged before the Fourier transformation. The spectrum was recorded over a range of 4,000–650 cm⁻¹. The spectra from the epoxy/viscose fabric composites' surface were recorded on a Bruker Optics-Tensor 27 spectrometer equipped with a diamond ATR accessory.

Signals of 32 scans at a resolution of 4 cm^{-1} were averaged over a range of $4,000\text{--}400\text{ cm}^{-1}$.

3.3.10 Differential scanning calorimetry

The glass transition temperature of cured epoxy castings was determined using a Netzsch DSC 204. The samples were heated from 25°C to 250°C at a rate of $10^\circ\text{C}/\text{minute}$ and then cooled. In the second heating scan, the sample was heated from 25°C to 250°C at a rate of $10^\circ\text{C}/\text{minute}$. The sample size was $10\text{--}11\text{ mg}$ and the test was conducted in a nitrogen atmosphere. The glass transition temperature from the second heating scan of the cured castings is reported (Article II). The effect of cooling rate on melting and crystallisation behaviour of the hybrid wood-plastic composites containing $20\text{ wt}\%$ wood flour and $15\text{ wt}\%$ GNP was determined using a Netzsch DSC 204 in a nitrogen atmosphere. The sample mass for all the composites was 10 mg (± 2). The first heating was done from a temperature of 25°C to 220°C at a rate of $40^\circ\text{C}/\text{min}$, followed by isothermal heating for 20 min representing the press time of the composites. The cooling was done at two different cooling rates of $2^\circ\text{C}/\text{min}$ or $40^\circ\text{C}/\text{min}$. The second heating was performed at $40^\circ\text{C}/\text{min}$ (Article IV).

3.3.11 Scanning electron microscopy

The tensile fractured surface of epoxy/viscose fabric composites was investigated by FE-SEM (Jeol JSM-7600F) at 5 keV using a below-the-lens (LEI) secondary electrons detector (SE) to minimise charging on the fibres (Article II). The impact fractured surface of epoxy/viscose fabric composites was studied with a scanning electron microscope (SEM; JSM-5800, Jeol Inc., Tokyo, Japan) operating at a low accelerating voltage (5 keV) to

minimise the beam damage of the polymer (Article III). The examination of the platinum-coated tensile fracture surface of hybrid wood-plastic composites was performed on a JEOL JCM-6000 Neoscope scanning electron microscope with an electron acceleration voltage of 15 kV. For polished cross-section surfaces of hybrid wood-plastic composites, the examination was made without a coating and an acceleration voltage of 1 kV to reduce the charging of the surface on the Zeiss EVO 50VP scanning electron microscope (Article IV).

3.3.12 Thermogravimetric analysis

The thermal decomposition of epoxy/viscose fabric was studied using a thermogravimetric analyzer, Netzsch TG 209C. The test was conducted in a nitrogen atmosphere by heating from 25°C to 800°C at 10°C/minute. The sample mass for all the composites was 20 mg (± 2) (Article III).

3.3.13 Burning rate test

The burning rate test was done in accordance with ISO 3795:1998 [102], which describes the method to determine the burning behaviour of interior materials in road vehicles, tractors, and machinery for agriculture and forestry (Article III). The sample was held horizontally in a U-shaped holder, and the free end of the sample was exposed to a low-energy flame for 15 s in a combustion chamber. The test is finished when the flame extinguishes, or within the time in which the flame passes a measured distance. The specimen dimensions for epoxy/viscose fabric were 138 mm (l) x 60 mm (w) x 2.3 mm (h) and for functional WPC 138 mm (l) x 60 mm (w) x 4 mm (h). The result is reported from an average of three specimens.



Figure 15: A viscose fabric/epoxy composite sample tested for determining the burning rate

3.3.14 Surface resistivity

The surface resistivity measurement of hybrid wood-plastic composites was done according to ASTM D257 – 07: Standard Test Method for DC Resistance or Conductance of Insulating Materials [103] (Article IV). Surface resistivity was measured by applying a voltage potential across the insulator sample's surface and measuring the resultant current (I). The electrode system is a circular flat metal plate type concentric ring electrode Vermason H108C (upper electrode) and H116BC (lower electrode). The power supply was a TRACOPOWER MHV12 – 0.5 K6000P, 500 volts. The voltmeter used was a Fluke 45 Dual display multimeter, and the ammeter was a Keithley model 6485 Picoammeter. The measurement was done at 500 V and in a room maintained at a temperature of $21^{\circ}\text{C} \pm 2$. The current reading from the picoammeter was noted 60 s after the start of measurement. The surface resistivity measurement of all other samples was

done following the same procedure. Two plates, each with 100 mm x 100 mm and 3.6 – 3.8 mm thickness, were measured for all the samples. The results are an average of four measurements done from both surfaces of the two plates. The surface resistance of PP-W20-G15 prepared by slow and fast cooling was measured following the same procedure explained above, except that the thickness of test samples was 2 mm and the test voltage was 100 V. The surface resistivity was calculated from Equation (4).

$$\text{Surface resistivity } \rho_s = \frac{\pi (D1+D2)}{(D2-D1)} R_s \quad (4)$$

Where D1 is the outer diameter of the inner ring in cm; D2 is the inner diameter of the outer ring in cm; R_s is measured resistance in ohms.

3.3.15 Thermal conductivity

A Netzsch LFA 467 device with Proteus LFA software was used to measure the samples' thermal diffusivity and CP(T) at 25°C (Article IV). Before the measurements, the surface of the sample was coated using a graphite spray. The samples' rear surface was heated by exposing a short light xenon laser pulse on the rear surface, and the temperature change of the opposite side of the sample was detected using an infrared detector. The thermal diffusivity was calculated using Equation (5) [104].

$$a=0.1338 d^2/t_{1/2} \quad (5)$$

where *a* = the thermal diffusivity; *d* = thickness of the sample, and *t*^{1/2} = time at the half signal height.

$$k(T) = \alpha(T) \times c_p(T) \times \rho(T) \quad (6)$$

The thermal conductivity of the samples was computed at 25°C using Equation (6). Where $k(T)$, $\alpha(T)$, $c_p(T)$ and $\rho(T)$ are the thermal conductivity, thermal diffusivity, specific heat capacity and experimental density of the sample, respectively. The density of PP, PP-W20, PP-G15 and PP-W20-G15 was measured as 0.90, 0.94, 0.97, and 1.04, respectively.

4 Results and discussion

The most important findings from this study are presented and discussed in Chapter 4. The first section analyses and discusses the effectiveness of the viscose fabric's chemical surface modification in improving various properties of the unsaturated polyester-based composite. The second section will discuss the resin modification method's viability as an alternative to the chemical surface modification method. The third section focuses on evaluating and discussing the results of hybrid WPCs.

4.1 Unsaturated polyester/viscose fabric composite

4.1.1 Mechanical properties

In terms of flexural strength, the C-APS1 composite performed best among all the epoxy/viscose fabric composites studied in this thesis (Figure 16). Compared to the C-untreated composite, improvement in flexural strength (22%) was visible from the results. The C-APS2 and C-APS3 composites also exhibited an increase of 6% and 7%, respectively. The C-MPS composites exhibited lower flexural strength among all the composites tested. As expected, the flexural strength of all the composites decreased after water absorption.

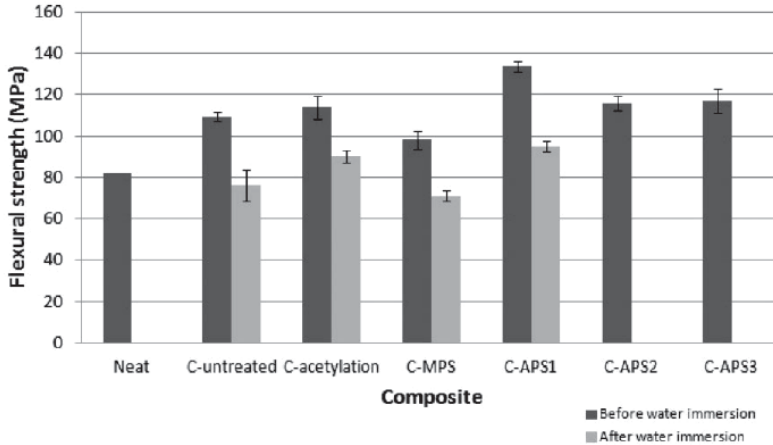


Figure 16: Effect of chemical modification on flexural strength of unsaturated polyester/viscose fabric composite [59]

The improvement in the flexural strength might be due to improved adhesion between viscose fabric and UP-resin caused by possible chemical bonding between the modified viscose fabric and the UP-resin. APTES silane might have undergone physical and chemical reactions with the reactive sites in unsaturated polyester resin, resulting in good adhesion between fibre and the unsaturated polyester matrix. The amine reaction with polyester may occur by adding the hydrogen atom of the amino group to the carbon atom in the carbon double bond, with the balance of the amine adding to the other carbon. Since polyester contains free carboxyl groups, part of the amine may also remain combined as a salt [105]. The amine in APTES may react with the carbon double bond in the polyester. This reaction is more favoured at 20°C to 150°C [106]. The cure temperature and post-cure temperature used to prepare composites were 23°C and 70°C, respectively. Thus, it is assumed that the reaction between APTES and UP-resin resulted in an improvement of properties. The better flexural strength

of C-APS1 after water immersion can be ascribed to the improved water resistance of the modified fabric.

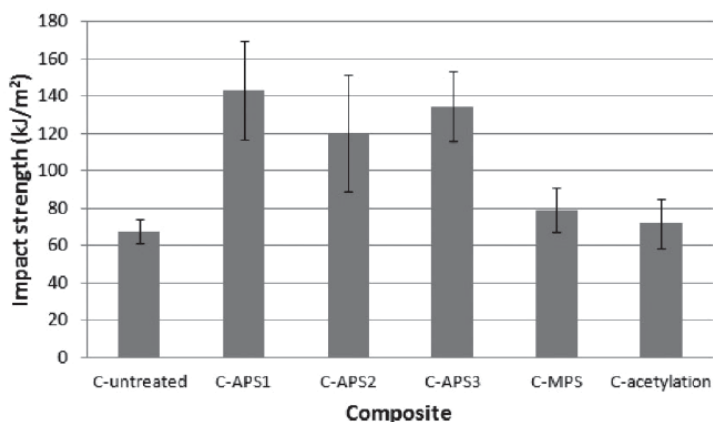


Figure 17: Effect of chemical modifications on the impact resistance of unsaturated polyester/viscose fabric composite [59]

The tensile strength of the C-APS1 composite decreased by 25% (114 MPa) compared to the C-untreated composite (152 MPa). It has been reported in the literature [107] that the tensile strength of single fibres is reduced after chemical treatment with amino-functional silane. During the chemical modification of cellulose, the reaction occurs at the amorphous region or in the crystalline region's border. The diffusion of modification reagent into the celluloses' crystalline domain is impossible. However, the reagent can react with the cellulose molecule chain ends close to the surface of crystallites by opening some of the hydrogen-bonded cellulose chains [108]. Thus, new amorphous domains are formed from the crystalline region. The decrease in crystallinity results in reduced tensile properties of the fibre [107]. Therefore, it can be assumed that the chemical treatment with

APTES decreased the crystallinity of the fibre, leading to a decrease in the tensile strength of the composites.

The Charpy impact strength of UPR/viscose fabric composites increased when using APTES-modified viscose fabric (Figure 17). Three different APTES modification methods adopted in this study resulted in a two-fold increase in impact strength. Among the three APTES modification methods, APS1 showed the most improvement. The regenerated cellulose fibres are proved to be very tough materials, which manifests as a high work to fracture and high failure strain [109]. In literature, it is found that the fracture toughness of composites with knitted fabric reinforcement is increased due to the uniaxially inlaid yarns in the fabric [110]. Therefore, the structure of the reinforcement has influenced the impact strength of all the composites under study. The notable improvement in the fracture toughness of APTES silane-modified composites can be ascribed to improved fibre-matrix interactions.

4.1.2 Water absorption test

All the composites reached saturation point in the duration of the test time (102 days). The composites, with the exception of C-APS1, showed a rapid increase in water absorption in the test's initial period. The improved water resistance of C-APS1 is seen in Figure 18. The mass gain at the end of the test for C-APS1 was 2% less when compared to C-untreated composites.

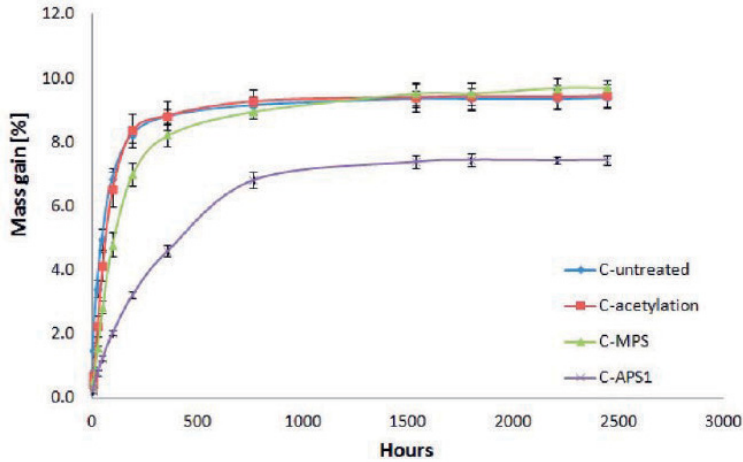


Figure 18: Effect of chemical modifications on the water uptake of unsaturated polyester/viscose fabric composite [59]

The improvement in water resistance of C-APS1 justifies the results from the 3-point bending test of composites done after water immersion. The decrease in flexural strength was smaller in C-APS1 compared to any other composites. This indicates the effectiveness of APTES modification in reducing water absorption. C-APS1 composites were prepared by using viscose fabric modified with the APS 95-5 treatment. This finding points out that the modification in the ethanol/water medium modified the fibre surface and penetrated the yarn filaments, making the fabric more resistant towards the water. The reaction between the cellulosic fabric and the APTES may proceed via hydrolysis of the ethoxy groups in silane, which further form highly reactive silanols. Silanols form a hydrogen bond with the hydroxyl group of fabric, and after that, in the presence of heat, a covalent bond is formed between fabric and silane. The amino group present in the silane is supposed to form a chemical or physical bond with unsatu-

rated polyester resin, thus forming a bridge between the fabric and the polymer. A deformation in the tested plates, except for C-APS1 composites, was observed by visual inspection after the test. This observation ascertains the improvement in water resistance characteristics of the C-APS1 composite after silane modification of viscose fabric.

The APTES modification of viscose fabric was successful in improving various properties of its UP-resin based composites. The bending strength and the composites' impact resistance increased notably when compared to composites based on untreated viscose fabrics. The APTES modification of fabric is an excellent method for improving the water resistance of UP-resin based composites.

4.2 Epoxy/viscose fabric composites

4.2.1 Modification of epoxy resin

The effectiveness of APTES in modifying epoxy resin was evaluated by determining the epoxide content of modified resin. The weight percent epoxide decreased by increasing the content of APTES in the modification (Figure 19).

The epoxide content decreased by 2.6% and 3.4% for RS5-RT and RS5-70, respectively, compared to RS0 resin (unmodified). The epoxy equivalent weight (EEW) increased to 211 g/mol for RS5-70 from 184 g/mol for RS0 resin. The decrease in epoxide content indicates the grafting of APTES onto the epoxy resin by the reaction between amine in silane and epoxide in the resin.

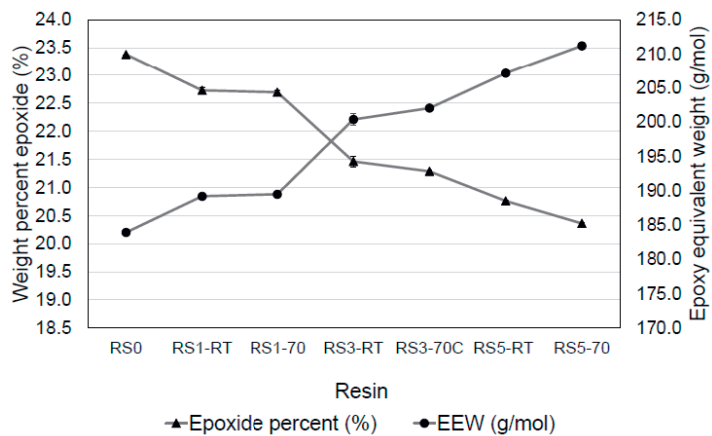


Figure 19: Effect of APTES modification on the epoxide content of epoxy resin [75]

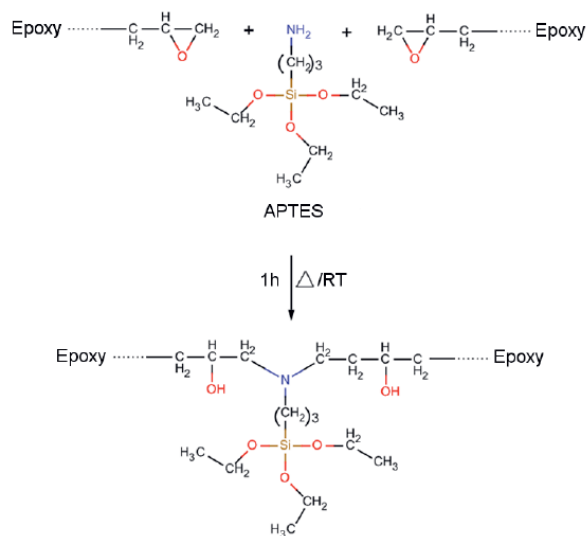


Figure 20: Possible chemical reaction during the grafting of APTES silane onto the epoxy resin [75]

The reaction is assumed to proceed through a primary amine in APTES reacting with the epoxy oxirane ring, forming a secondary amine and a hydroxyl group. The formed secondary amine will further react with another oxirane ring, resulting in the silane grafting, as shown in Figure 20 [73, 111]. Similar observations are made by other researchers about the modification of epoxy resin by APTES [112]. This finding is supported by an increase in the viscosity of modified resins. The viscosity of the RS5-70 resin doubled when compared to RS0 resin. The reaction between APTES and epoxy resin is assumed to be similar to the reaction between the epoxy resin and amine hardener. During the cure reaction of epoxy resin, the viscosity increases with time and temperature due to the cross-linked network formation [113]. The increase in viscosity of modified resin supplements the results obtained from the epoxide content determination test.

The FTIR spectra of RS0 resin and RS5-70 are seen in Figure 21. The spectra of modified resins seem to be similar to that of RS0 resin, with a few variations. A new absorption band appears at $1,077\text{ cm}^{-1}$ for resins modified with 5 wt% APTES (RS5-70). Previous studies assign this band to Si-O-C linkage, indicating that the ethoxy group in the APTES silane remains unreacted in the modified resin [114]. The absence of an absorption band in a range of $1,040\text{ cm}^{-1}$ to $1,020\text{ cm}^{-1}$ and 990 cm^{-1} to 945 cm^{-1} confirms that silanols (Si-OH) are not present in the modified resin. The absence of an absorption band corresponding to siloxane in the region also confirms that the ethoxy group is unreacted. The major observation from Figure 21 (b) and (c) compared to Figure 21 (a) is the disappearance of the absorption band at $1,077\text{ cm}^{-1}$ which is assigned to the unreacted ethoxy group in modified resin. This indicates that during curing, the resin's ethoxy group has reacted, forming an improvement in the fibre-matrix adhesion.

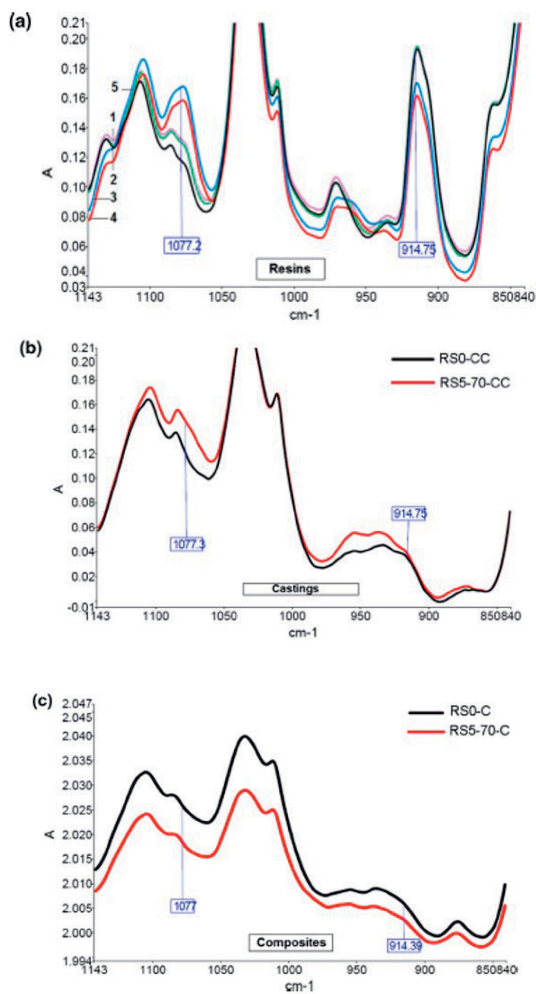


Figure 21: FTIR spectra of epoxy resin, cured castings and composites in the region 1,140–840 cm⁻¹ (a) resins—1: RS1-70, 2: RS0, 3: RS5-RT, 4: RS5-70, 5: RS1-RT (b) castings and (c) composites [75]

4.2.2 Tensile properties

The tensile strength of cured epoxy castings is shown in Figure 22. The tensile strength decreases with an increase in APTES content irrespective of the temperature used in the modification. Compared to resin modification at room temperature, the tensile strength of resins modified at 70°C decreased. The epoxide content determination test results point out that there is less oxirane oxygen in the modified resins compared to unmodified epoxy resin. Therefore, during the cure reaction with amine hardener, comparatively less oxirane is available for crosslinking reaction with an amine. The decreased cross-link density might have decreased the tensile strength of the cured epoxy castings. In general, thermoset resins with low cross-link density exhibit low tensile strength [115]. It is observed that there was no significant change in terms of elongation at break of the modified cured castings when compared to RS0-CC.

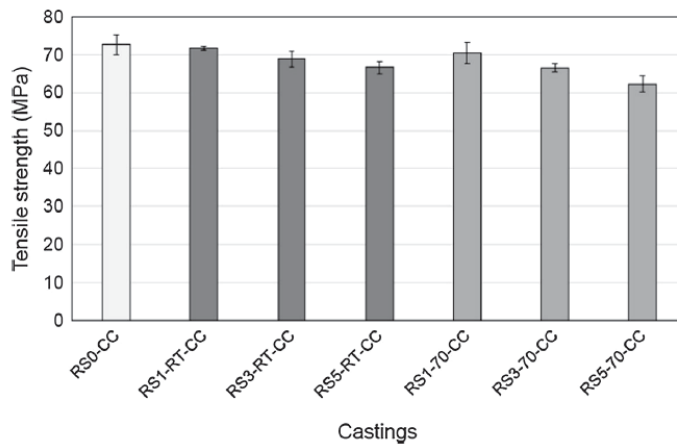


Figure 22: Effect of resin modification on tensile strength of cured castings [75]

The tensile strength of epoxy/viscose fabric composites is shown in Figure 23. The tensile strength of RS3-70-C and RS5-70-C increased by 14% and 11%, respectively, compared to RS0-C composites. Meanwhile, the tensile strength of RS0-FS2-C decreased by 22%. The ethoxy group's presence after modification of resin was evident from the FTIR analysis (Figure 21.a). However, the FTIR analysis of composites shows that the absorption band around $1,077\text{ cm}^{-1}$, corresponding to the ethoxy group found in modified resins, disappeared in the case of composites. This observation indicates that the ethoxy group grafted to the epoxy resin has undergone reaction during the composites' curing. As discussed above, it is essential to note that the modification of epoxy resin with 3 wt% and 5 wt% of APTES decreased the tensile strength of the cured castings. A notable difference is found when the same resins are used to prepare viscose fabric reinforced composites. The tensile strength of RS3-70-C and RS5-70-C increased by 14% and 11%, respectively. The increase in composites' strength is obviously due to the improved adhesion between viscose fabric and modified epoxy resin.

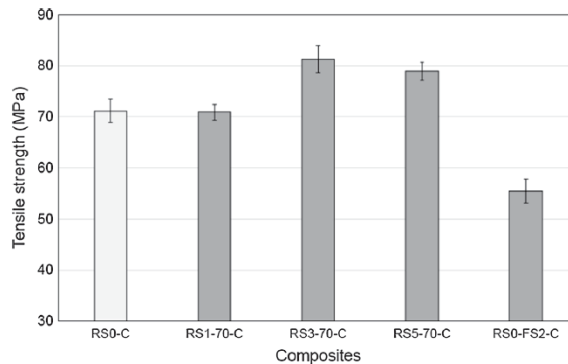


Figure 23: Effect of resin modification on tensile strength of epoxy/viscose fabric composites [75]

The elongation at break of the composites is shown in Figure 24. The elongation seems to be increasing with increased APTES content in epoxy resin. Compared to the RS0-C composite, the elongation at break of RS3-70-C and RS5-70-C increased by 29% and 41%, respectively. In contrast, there was a 40% decrease in elongation of the RS0-FS2-C composite. The elongation of the reinforcing fibre influences more the elongation at break. Compared to native lignocellulosic fibre, the elongation at break of viscose fibre used in this study is significantly higher [116]. The improved fibre-matrix adhesion also has contributed to the improvement in elongation at break of the composites.

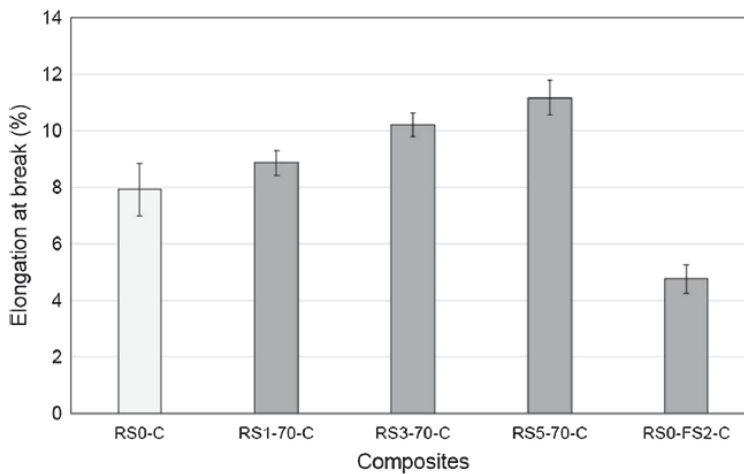


Figure 24: Effect of resin modification on the elongation of the epoxy/viscose fabric composites [75]

The percentage of change in tensile properties of composites fabricated with chemically modified fibres are tabulated and compared with the results obtained from this study (Table 5). The literature data for comparison is restricted to those studies that have reported improved tensile properties after chemical modification. The improvement in tensile strength of composites prepared from APTES-modified epoxy resin is similar to composites prepared from chemically modified lignocellulosic fibres [117, 118].

Table 5: A comparison of the influence of fibre modification and resin modification approaches on the tensile strength of corresponding composites [75]

Composites	Chemical modification	Change in tensile strength (%)
Grewia tilifolia/epoxy	NaOH (5 wt%)	5.8
Flax/epoxy	NaOH (5 wt%)	21.9
Bamboo/epoxy	NaOH (5 wt%)	32.8
Grewia tilifolia/epoxy	APTES (1 vol%) in acetone	14
Bamboo/epoxy	MPS (0.5 wt% in deionised water)	15.1
Viscose/epoxy	APTES (2 vol% in ethanol/water)	-22.0
Viscose/modified epoxy	APTES (3 wt%)	14.0
Viscose/modified epoxy	APTES (5 wt%)	10.8

4.2.3 Tensile fractography

The tensile fracture surfaces of the RS0-C and RS5-70-C composites are shown in Figure 25 and Figure 26, respectively. The filament bundle pull-off in the non-load-bearing 90° layers of RS0-C can be seen from 25 (a). The single filaments in the 90° layer bundle appear to be clean, with the less resin-covered region and fibre splitting. The resin-rich region seems smooth and shiny, but the resin region near polyester knit yarn exhibits micro-textures resembling river lines. The load-bearing 0° plies are observed to be more rugged. The internal cracking within the bundle and bundle de-bonding along the fibre–matrix interface is visible from Figure 25 (b). The image analysis of RS0-C composites indicates that the adhesion between viscose yarns and the epoxy resin is weak.

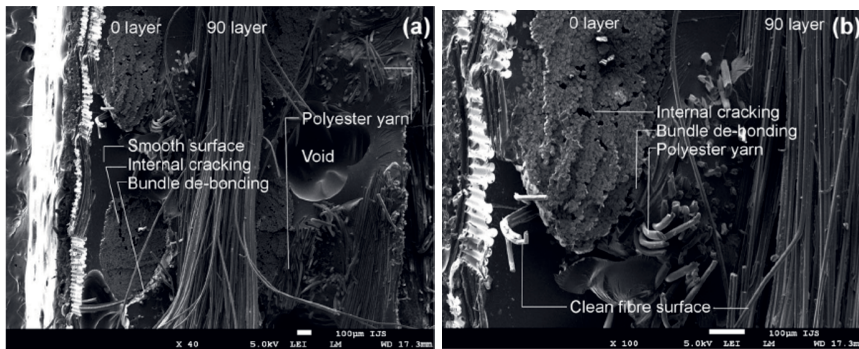


Figure 25: Tensile fracture surface of the reference epoxy/viscose fabric composite made from unmodified resin and unmodified fabric [75]

The tensile fracture surface of RS5-70-C is shown in Figure 26. The 90° layer bundle filaments are well embedded in the matrix resin with less splitting than the RS0-C composite. This indicates an improved fibre–matrix adhesion in RS5-70-C. The internal cracking within the bundle and the

splitting in load-bearing 0^0 layers are less in the case of RS5-70-C when compared to RS0-C composites. The resin-covered 0^0 layer bundles can be seen in Figure 26 (b).

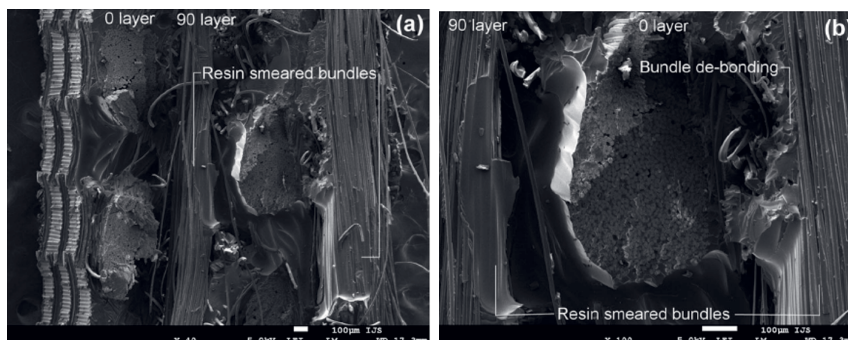


Figure 26: Tensile fracture surface of epoxy/viscose fabric composite prepared from epoxy resin modified by 5% APTES and unmodified fabric [75]

In general, failure modes like fibre fracture, delamination between the layers, ply splitting or matrix cracking can occur in cross-ply laminates [119, 120]. When under tension, the first failure in a cross-ply laminate is the ply-cracking in the non-load-bearing 90^0 layers [121]. On the other hand, the fibre breakages and internal bundle cracking are the main failures occurring in the load-bearing 0^0 layers. The failure modes discussed above are observed from the fracture surface of the composites obtained in this study. In general, a lack of matrix resin on the fibre surface, a higher degree of filament pull-out, and matrix cracking within the fibre bundles are taken as evidence of insufficient fibre–matrix adhesion [122]. When the fibre–matrix adhesion improved after resin modification, the degree of de-bonding was lower in the case of RS5-70-C composites. The presence of knit yarn

in the boundary of the bundle initiated the de-bonding in that particular region. The knit yarns are reported to act as initiation sites for damage development in composites with knitted fabric as reinforcement [123]. The observations made from the SEM analysis indicate an improved fibre-matrix adhesion, and it also supplements the tensile results discussed in the previous section.

4.2.4 Charpy impact strength

The Charpy impact strength of epoxy/viscose fabric composites is shown in Figure 27. The strength of RS1-70-C and RS3-70C increased by 18% and 37%, respectively, compared to the RS0-C composite. The impact strength of RS5-70-C doubled when compared to RS0-C. On the other hand, the impact strength of RS0-FS2-C decreased by 48% compared to RS0-C composites.

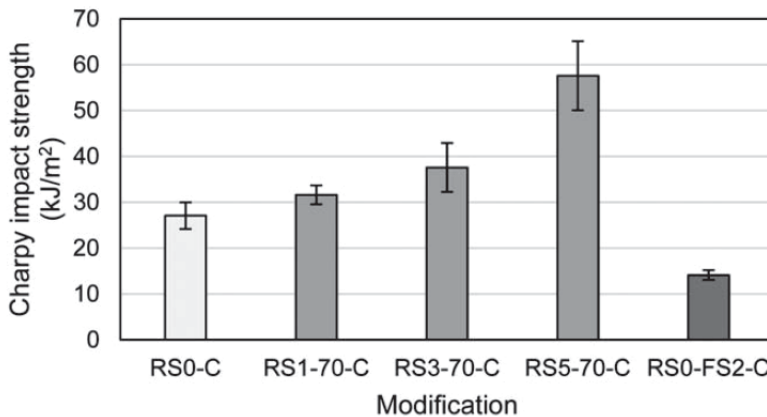


Figure 27: Effect of modifications on Charpy impact strength of epoxy/viscose fabric composites [69]

There are several factors governing the impact resistance of the composite materials. Among those, strength and stiffness of fibre, matrix toughness, thickness, lay-up, impact velocity, and support conditions are of major importance [124]. When a composite is tested under impact, a part of the energy related to the impact is used for elastic deformation of the composite. The remaining energy is dissipated through different failure mechanisms like fibre breakage, fibre–matrix de-bonding, delamination, and matrix resin cracking [124]. The impact fracture surface analysis through SEM is supposed to provide the information on the type of fractures occurred in the composites.

The fractography analysis (Figure 28) supports the experimental results obtained from the Charpy impact testing. Among the modified resin-based composites, the impact strength of RS5–70-C composites almost doubled compared to RS0-C composites. The improvement in the toughness of the resin is evident when comparing the resin-rich areas of the RS0-C composites and RS5–70-C composites. The resin-rich region in the RS5–70-C composite was much more impact-resistant when considering the matrix crack formation observed in the RS0-C composites. Also, the microtextures indicating the shear failure in the resin-rich region is also indicating the improved impact resistance of the epoxy composite after the APTES modification. The impact failure surface with evidence of shear failure shows improved impact resistance. Thus, it is assumed that the epoxy resin modification with compatible SCAs like APTES improves the toughness of the resultant composite.

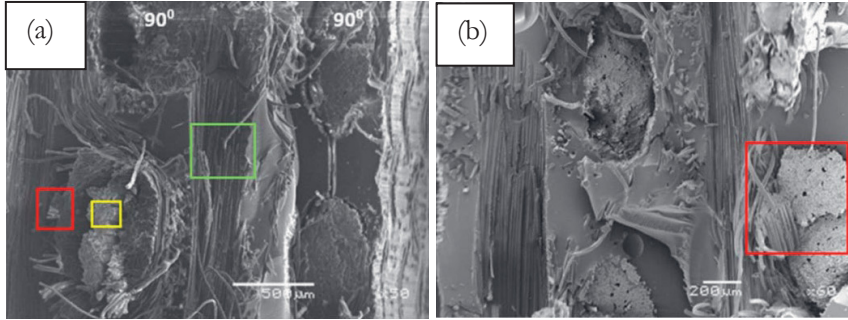


Figure 28: SEM images from impact fracture surface of (a) RS0-C and (b) RS5-70-C

The damping factor $\tan \delta$ is often associated with the impact resistance of the natural fibre composites [125]. A high $\tan \delta$ value indicates that the material is more viscous and has high energy dissipation potential, whereas a low $\tan \delta$ is associated with a highly elastic material capable of storing energy within its structure. Several authors have explained the increase in impact resistance of NFRP composites based on an increase in area and height of the $\tan \delta$ peak [125]. A large area under the $\tan \delta$ peak indicates a great degree of molecular mobility, which translates into better damping properties, meaning that the material can better absorb and dissipate energy. As seen from Figure 29, the area under the $\tan \delta$ curve for RS0-FS2-C is smaller among all the other composites. This explains the lowest impact resistance of RS0-FS2-C when compared to other composites.

A shift in glass transition temperature is observed in the composites after the APTES modification. There was a decrease of about 7°C in T_g of the RS1-70-C composite with respect to the RS0-C composite. The glass transition temperature T_g of the RS3-70-C and RS5-70-C composites in-

increased 16°C when compared to the RS0-C composite. There was an increase of 6°C in T_g of the RS0-FS2-C composite with respect to the RS0-C composite. The increase in glass transition temperature of the composite can be taken as a measure of interfacial interaction. The higher the T_g , the stronger the fibre–matrix adhesion. Similar kinds of observations for natural fibre reinforced composites have been reported in the literature [125, 126]. In addition to the polymer and the fibre, the interfacial adhesion between the fibres also has significant influence on the impact resistance of composites. The results obtained in this study indicate that the impact resistance of the viscose fibre based composites increases with improved interfacial adhesion, as seen from the increase in the glass transition temperature.

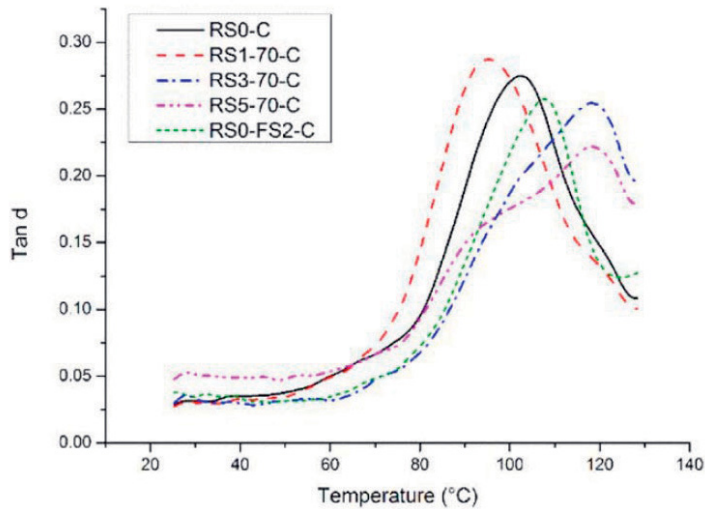


Figure 29: Effect of modifications on the tan d value of the viscose fabric [69]

4.2.5 Burning properties

The burning rate of epoxy/viscose fabric composites can be seen in Figure 30. The burning rate of the RS5-70-C composite increased by 18% compared to the RS0-C composite. A general trend observed from the results is that with an increase in APTES content in the modification of resin, the composites' burning rate increased. The composite prepared from APTES-modified viscose fabric (RS0-FS2-C) exhibited the lowest burning rate among all the composites. There was a decrease of about 8% in the burning rate for the RS0-FS2-C composite compared to RS0-C composites. This shows that APTES fabric modification has effectively reduced the burning rate of the composite. The deformation of samples after the test was prominent in RS3-70-C and RS5-70-C composites.

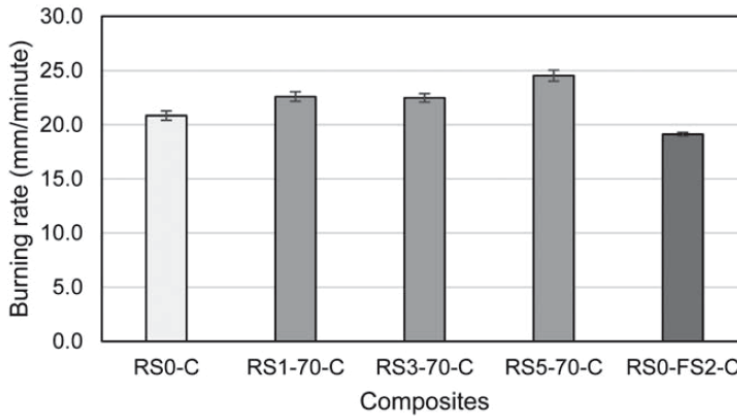


Figure 30: Effect of modifications on the burning behaviour of epoxy/viscose fabric composites [69]

The $\tan \delta$ curve in Figure 29 shows an increase in T_g for RS3-70-C and RS5-70-C composites, and an increase in T_g is correlated to an increase in

cross-link density. Since high energy is required to break highly cross-linked structures, the chamber's maximum temperature recorded during the test for RS3–70-C and RS5–70-C composites was higher compared to other composites. The flame-retardant properties of composites are adversely affected by the increase in cross-link density [127]. High crosslink density can make the network structure too rigid to produce charred layers during combustion, thus increasing its flammability.

The T_g of the RS0-FS2-C composite is lower than RS3–70-C and RS5–70-C composites. Therefore, the cross-link density is assumed to be low in RS0-FS2-C composites compared to RS3–70-C and RS5–70-C composites. However, the low burning rate of RS0-FS2-C composites can be more influenced by the modification of viscose fabric by APTES. The decrease (62.8% to 55.6%) in crystallinity of sisal [128] and Lyocell fibres [129] after APTES modification is reported in the literature. The decrease in crystallinity in cellulose fibre results in a reduction of levoglucosan, which is evolved as highly flammable fluid tar. One recommendation made by Kozłowski and Władka-Przybylak [130] to decrease the flammability of the cellulose fibre is to decrease the crystallinity of the cellulosic fibres. Therefore, the APTES modification of viscose fabric is expected to play a vital role in reducing the burning rate. According to ECE Reg. No 118 and directive 95/28/CE, the result of the horizontal burning tests conducted according to ISO 3795 shall be satisfied if the burning rate is not more than 100 mm/min [131]. Therefore, all the epoxy/viscose fabric composites can be assigned as satisfactory in the burning test irrespective of modifications.

4.3 Hybrid wood-plastic composite

4.3.1 Tensile properties

The tensile strength of neat PP, PP-W20 and PP-Wood-GNP hybrid composites is shown in Figure 31. The strength of hybrid composites decreased gradually by increasing the GNP content. The strength of PP-W20-G10 and PP-W20-G15 decreased by 10% and 20%, respectively, when compared to PP-W20.

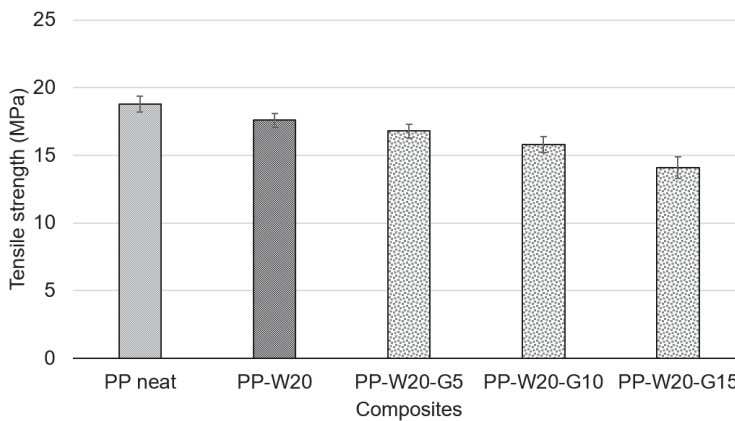


Figure 31: Effect of increasing GNP loading on the tensile strength of hybrid WPC [83]

GNP's capability in enhancing the tensile properties of composites is explained based on the effect of graphene structure, dispersion of fillers, and filler-matrix adhesion [76]. The analysis of hybrid composites indicates that GNP fillers' presence influences the composites' tensile strength. The strength of PP-W20-G10 and PP-W20-G15 decreased (approx. 2 MPa and

4 MPa, respectively) when compared to the tensile strength (18 MPa) of PP-W20. However, given the total filler content of PP-W20-G10 and PP-W20-G15 composites are 30 wt% and 35 wt%, respectively, the decrease in tensile strength is quite apparent. Idumah and Hassan [132] studied the kenaf fibre/GNP/PP composite system and reported using 5 wt% MAPP improved polymer for kenaf fibre adhesion. However, GNP's adhesion to polymer was weak due to the lack of any chemical bond formation between GNP and MAPP. A similar observation is made from the tensile fracture surface analysis of the wood fibre/GNP/PP composite system under this study. The tendency of graphene to agglomerate has created stress concentration in the composite that leads to failure of composites in tensile load. The decrease in tensile properties due to GNP's restacking at 5 wt% loading has been reported elsewhere [132]. In this study, the GNP loadings in hybrid WPC are above 5 wt%. Thus, the decrease in tensile strength can be attributed to the agglomeration of the GNP and lack of chemical interaction between GNP and polymer.

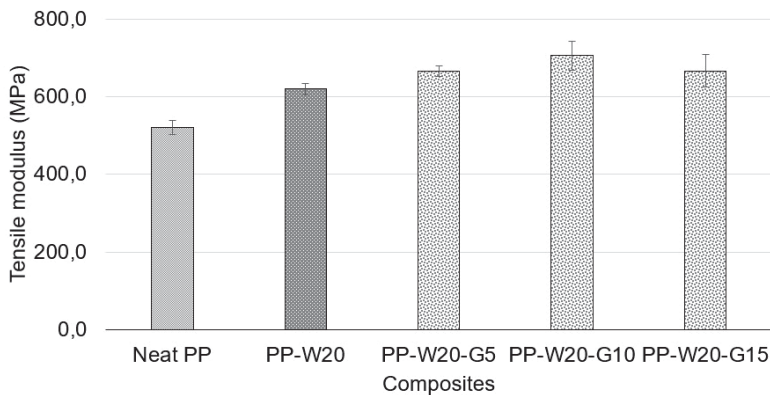


Figure 32: Effect of increasing GNP loading on tensile modulus of hybrid WPC [83]

Young's modulus of hybrid composites increased 35% compared to PP neat and 14% compared to PP-W20, as seen in Figure 32. The graphene is a two-dimensional layer of carbon that possesses high stiffness [133]. The reinforcing effect of graphene increases with increasing graphene content up to 10% by weight and then decreased. When compared to PP-W20, the elastic modulus of hybrid composite has improved. This indicates that the incorporation of GNP into wood-plastic composite improved the stiffness of composites. The tensile modulus of graphene is 1 TPa [134], and the increase in stiffness with GNP incorporation up to an optimal concentration of filler in nanocomposites and hybrid composites are also reported in the literature [135, 136]. The enhancement in the modulus can be attributed to the stiffness difference between the polymer and the graphene. The increase in stiffness with GNP incorporation up to an optimal concentration of filler in hybrid composites is also reported in the literature [135].

SEM images from the tensile fracture surface are shown in Figure 33 (a-f). The surface of wood flour in the wood-plastic composite containing 20 wt% flour seems to show good compatibility with PP (Figure 33 a & b). The wood flour surface appears to be rough and wetted with the polymer. Also, there is no fibre pull-out observed from the SEM analysis. These observations indicate good adhesion between PP and wood flour in the presence of MAPP as a compatibilising agent. The study of the surface of both PP-G15 and PP-W20-G15 revealed clusters of agglomerated particles appearing in different sizes. The GNP's surface was clean without any polymer covering, indicating low compatibility between the polymer and the GNP. Figure 33 (f) shows that the partially pulled out and broken fibres seem to be coated with the polymer, indicating better adhesion between wood flour and PP in the hybrid composites. Simultaneously, the GNP surface is

found to be without any polymer covering, which means low compatibility with the PP in PP-W20-G15. A similar observation can be made from Figure 33 (d).

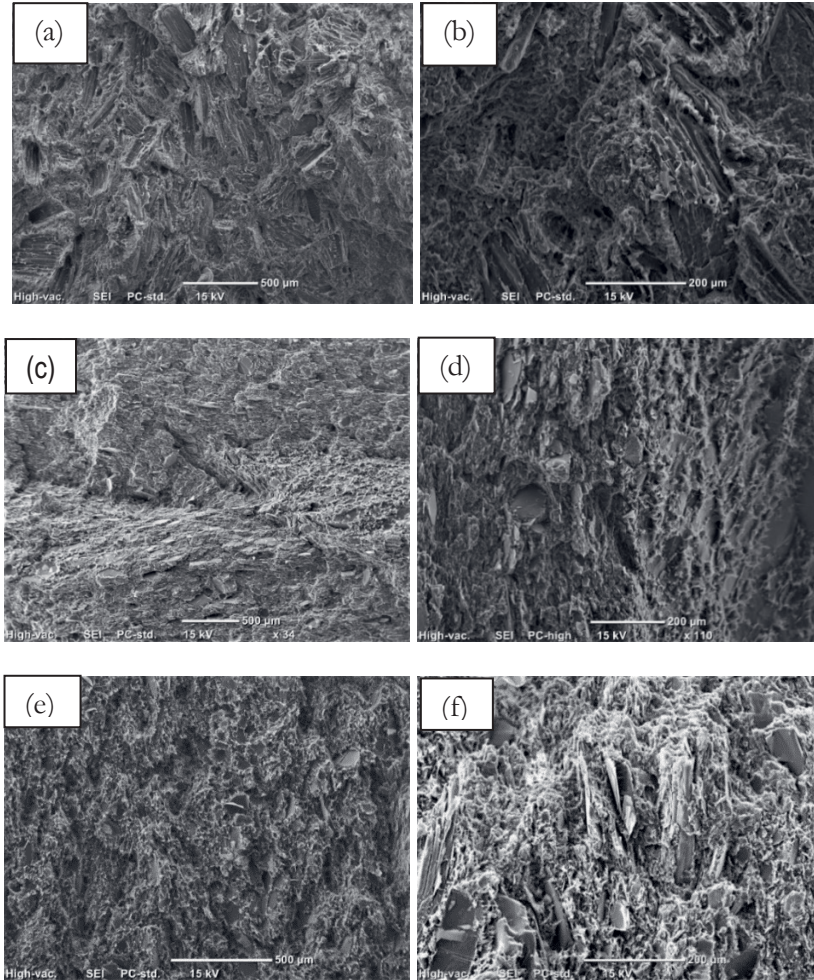


Figure 33: SEM images from the tensile fractured surface of (a), (b) PP-W20 (c), (d) PP-G15 and (e), (f) PP-W20-G15 [83]

4.3.2 Surface resistivity

The surface resistivity of PP/GNP and hybrid WPCs is listed in Table 6. The percolation threshold is reached with a filler loading of 15% by weight in PP/GNP and hybrid composites. The surface resistivity of PP/GNP and hybrid composites decreased several orders of magnitude to $10^8 \Omega/\text{sq}$ and $10^6 \Omega/\text{sq}$, respectively. The results from surface resistivity measurements indicate that the surface conductivity increased by incorporating GNP in both PP and WPC containing 20% by weight of wood filler.

Table 6: Effect of GNP on the surface resistivity of PP/GNP and hybrid WPCs [83]

Composites	Surface resistivity (Ω/sq)	SD
PP neat	1.19E+14	5.34E+12
PP-W20	1.08E+14	6.19E+12
PP-G5	1.05E+14	7.25E+12
PP-G10	1.00E+14	3.55E+12
PP-G15	8.83E+08	8.43E+08
PP-W20-G5	4.96E+14	6.67E+12
PP-W20-G10	4.48E+14	1.90E+13
PP-W20-G15	2.90E+06	2.05E+06

The electrical conduction mechanism in the insulating polymer/conductive filler composites is described based on percolation theory. The electrical conductivity in those composites is due to free electron movement through conductive fillers' conductive path at a critical filler loading. There

is a sudden increase in electrical conductivity at this critical filler loading, after which it gets saturated. This critical filler concentration is known to be the electrical percolation threshold concentration [137].

In general, an uncoated insulator sample accumulates charge during the examination. SEM images from a cross-section of GNP-filled PP-G15 and PP-W20-G15 acquired with 1 kV show brighter areas (Figure 34 c & d). This observation can be explained as the “reverse” charging characteristic, where the local field effect in a conductive composite enhances the relative secondary electron emission in the isolated conductive grains [138]. Similar observations in polymer/carbon nanofiller filled composites are reported elsewhere [139, 140]. Due to this phenomenon, the conductive filler is seen brighter in a dark insulating matrix. Due to a low acceleration voltage of 1 kV, both the penetration depth of primary electrons and escape depth of secondary electrons (SE) are low, and only near-surface information is obtained. The brighter GNP (15 wt%) is seen in Figure 34 (c) and (d). In Figure 34 (d), the GNP is seen to be even better distributed in the presence of 20 wt% wood flour. The charging phenomenon directly represents the GNP's electrically conductive path in the PP matrix. The results from the SEM analysis support the findings from the surface resistivity measurements.

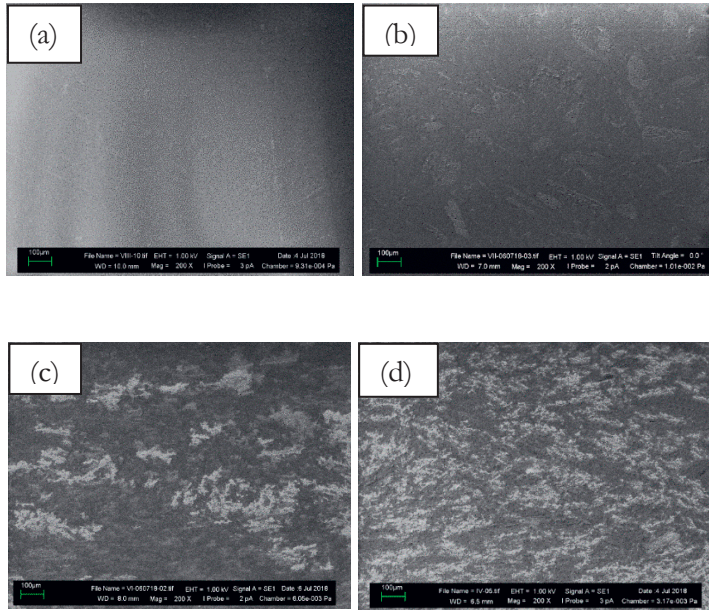


Figure 34: SEM images from polished surface of (a) PP neat (b) wood-plastic composite – PP-W20 (c) antistatic composites filled with GNP (PP-G15) (d) anti-static/dissipative wood-plastic composite filled with wood flour and GNP (PP-W20-G15) [83]

It is worth noting that the WPC containing 20% (by weight) is more conductive than PP with the same loading (15% by weight) of GNP. The total insulating components (PP and wood) in both PP-G15 and PP-W20-G15 are 85 wt%. With the total amount of conductive filler in both PP/GNP and hybrid composite being the same, the decreased surface resistivity of hybrid composite is due to the good distribution of GNP in the presence of wood filler. Good distribution of GNP helped in forming a more effective conductive path in the PP-W20-G15 hybrid composite. Based on the

results obtained and according to the literature [141], the PP filled with 15 wt% of GNP and WPC containing 15 wt% GNP can be used as anti-static packaging for sensitive electronics and in wood-plastic composite products to prevent the build-up of static electricity.

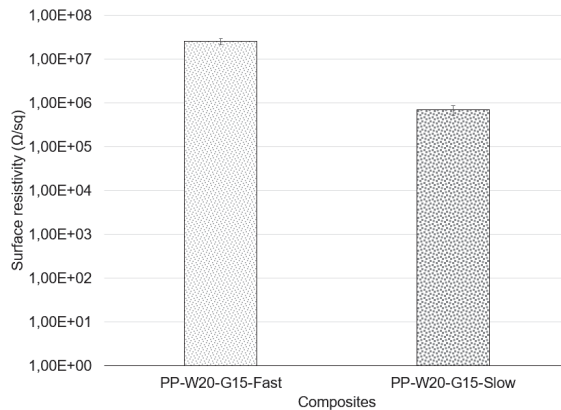


Figure 35: Effect of cooling rate on the surface resistivity of hybrid WPCs [83]

The surface resistivity of PP-W20-G15 was found to be influenced by the processing conditions during the hot pressing. The effect of varying cooling rate during the compression moulding was studied by using two different cooling rates; (1) fast cooling in which the composites were cooled at a rate of $\approx 14^\circ\text{C}/\text{minute}$ by running water and air through the channels in the top and bottom platens in the hydraulic press and (2) slow cooling at a rate of $\approx 0.7^\circ\text{C}/\text{minute}$, in which the composites were left in the press to cool down to 23°C without using cooling water or air. The composite produced under slow cooling exhibits low surface resistivity ($6.97\text{E}+05$) compared to the composite made under fast cooling ($2.52\text{E}+07$), as seen in Figure 35. Since there is no variation in GNP or wood flour content in the

two composites, the lowering of resistivity can be related to polypropylene's crystallisation behaviour.

DSC analysis was done on the granulates of neat polymer and composites to study the effect of fast and slow cooling on its thermal behaviour. A cooling rate of 2°C/minute and 40°C/minute was used to represent slow cooling and fast cooling, respectively. It should be noted that the result presented in Table 7 does not precisely represent the processing conditions used in this study. When comparing two different cooling rates, a notable difference in crystallisation temperature and the degree of crystallinity of PP can be observed from Table 7. The decrease in surface resistivity of PP-W20-G15-Slow produced using slow cooling can be correlated to the increase in the degree of crystallinity.

It is documented that the formation of the conductive path is easier in highly crystalline thermoplastics compared to those with a higher amorphous phase [142]. According to Kalaitzidou et al. [143], the degree of crystallinity and the type of crystals, the size of the crystals, and nucleating effect of GNP can affect the percolation threshold and electrical resistivity of PP-based composites. They found that the slow cooling resulted in larger but fewer crystals than fast cooling, in which a large number of small crystals were formed [143]. A similar observation about decreased resistivity in slow cooled PP/CNT composites was made by Wang et al. [144]. They reported that most of the CNT was prevented from participating in the nucleation of PP crystals by using an external nucleating agent, and therefore more CNT was available for forming a conductive path.

Table 7: Effect of cooling rate on the melt temperature, crystallisation temperature and degree of crystallinity [83]

Composites	T_m (°C)		T_c (°C)		χ (%)	
	Fast	Slow	Fast	Slow	Fast	Slow
PP neat	169	170	106	128	30	34
PP-W20	172	169	104	129	29	34
PP-G15	175	174	106	131	30	37
PP-W20-G15	170	172	108	132	30	36

Therefore, the decreased resistivity of PP-W20-G15-Slow compared to PP-W20-G15-Fast is due to an increase in crystallinity and fewer but large crystallites formed during slow cooling. It is assumed that the wood flour participated in the nucleation of PP crystals, allowing most of the GNP to form a conductive path in slow cooled PP-W20-G15 by decreasing the surface resistivity.

4.3.3 Thermal conductivity

The thermal conductivity of polypropylene (PP neat) and composites is shown in Figure 36. The incorporation of 15 wt% GNP in wood-plastic composites with 20 wt% wood filler has significantly increased thermal conductivity by 130% (PP-W20-G15). The increase in thermal conductivity is attributed to the better distribution of GNP in hybrid composites in the presence of wood flour, as seen from Figure 36.

The GNP has high thermal conductivity, and it is reported that incorporation of GNP in the polymer matrix can lead to an increase in thermal conductivity [145]. The main factors affecting the heat conduction in polymer composites containing GNP are lateral size and thickness, interfacial ther-

mal resistance, GNP dispersion, surface functionalisation and GNP concentration [146]. The heat transfer in polymer composites containing low GNP, where fillers cannot connect, depends on the interfacial interaction of graphene and polymer [146]. Effective interaction between polymer and graphene can decrease the interfacial thermal resistance and improve the phonon transfer between polymer and graphene. In polymer composites with higher GNP loading, like those used in this study, the heat conduction is through the thermally conductive path formed by the GNP-GNP contact. Once the composite makes contact with the heat source, the heat transfers quickly through the GNP's thermal conduction path. There was no critical loading or percolation threshold identified in the case of PP/GNP and PP/GNP/wood flour hybrid composites. An increase in the thermal conductivity in both systems containing 15 wt% of GNP was observed. Although there was an increase in PP and WPC's thermal conductivity after the addition of 15 wt% GNP, these materials are still not suitable for use in applications requiring heat dissipation.

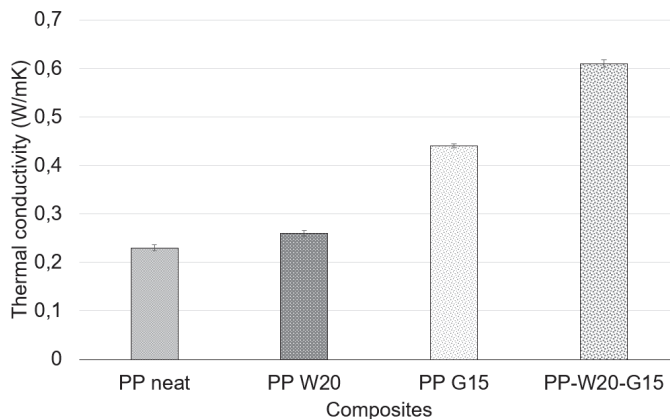


Figure 36: Effect of GNP loading on the thermal conductivity of wood-plastic composites [83]

5 Conclusions and future work

This thesis's main objective was to investigate the suitability of different chemical modification methods in improving the fibre-matrix adhesion in viscose fabric reinforced thermoset composites. From the results in this thesis, it is evident that the interfacial adhesion between matrix resin and fibre reinforcement plays a vital role in determining the properties of natural fibre composites. The effectiveness of acetylation and silane coupling agents to surface modify the viscose fabric was studied to address research question 1 (Article 1). The results showed that the 3-aminopropyltriethoxysilane (APTES) treatment was best among the fibre modification methods chosen in this study. APTES modification significantly improved mechanical and water resistance of viscose fabric/unsaturated polyester composites (VF/UPR) through improved fibre-matrix adhesion. The use of gel-coat and topcoat reduced the water uptake in VF/UPR composites, as seen from the accelerated water absorption test (research question 2).

To address research question 3, the effectiveness of epoxy resin modification as an environmentally friendly alternative for the chemical fibre modification method was studied (Article II and III). The epoxy resin modification by APTES decreased the tensile strength of cured resin. However, the tensile strength and elongation at break increased when APTES-modified epoxy resin was used to fabricate viscose fabric/epoxy composites. It is worth mentioning that the impact strength of viscose fabric/epoxy composites doubled after APTES modification of epoxy resin. These results indicate that modifying the resin with coupling agents compatible with the chemical functionality of thermoset resin is an alternative to conventional chemical methods for modifying regenerated cellulose fibres.

Another objective of this thesis was to develop anti-static wood-plastic composites (WPC) suitable for ESD-safe applications. Research question 4 was addressed by studying the influence of graphene nanoplatelets on tensile properties, surface resistivity and thermal conductivity of wood-plastic composites produced by the melt compounding method (Article IV). The anti-static WPC with a surface resistivity of $10^6 \Omega/\text{sq}$ was developed with a decrease in tensile strength and improved stiffness. The thermal conductivity of anti-static wood-plastic composites almost doubled when compared to polypropylene. The presence of wood flour helped achieve a better distribution of GNP compared to composites containing GNP alone. The developed anti-static WPC can be used to produce anti-static containers and ESD-safe chairs for the electronic industry, and for making anti-static pipes that are exposed to a less humid environment.

Although this thesis's findings act as a basis for developing wood-based fibre reinforced polymer composites with improved mechanical, physical and electrical properties, there are a few aspects that require further research. It is worth studying suitable coupling agents to modify commonly used thermoset resins like unsaturated polyester resin and vinyl ester resin. Based on laboratory experiments, it was estimated that less process waste is generated in the resin modification method compared to fibre chemical modification methods like acetylation, alkali treatment and silane coupling agent modification. The environmental impact of both fibre modification and the resin modification approach needs to be validated by conducting a life cycle assessment study. Since the melt processing technique was selected, a relatively high graphene content was used to reach the desired electrical resistivity for anti-static WPC. When considering the economy,

studies are needed to improve melt processing conditions to reach the percolation threshold at lower graphene content. Alternatively, cost-efficient conductive fillers to develop anti-static WPC need to be selected.

References

- [1] J. Rogelj, M.d. Elzen, N. Höhne, T. Fransen, H. Fekete, H. Winkler, R. Schaeffer, F. Sha, K. Riahi, M. Meinshausen, Paris Agreement climate proposals need a boost to keep warming well below 2 °C, *Nature*, Vol. 534, Iss. 7609, 2016, pp. 631-639. <https://www.nature.com/articles/nature18307>.
- [2] European Commission European council conclusions 23/24 October 2014, http://www.consilium.europa.eu/uedocs/cms_data/docs/pressdata/en/ec/145397.pdf.
- [3] European Commission A Clean Planet for all - A European strategic long-term vision for a prosperous, modern, competitive and climate neutral economy, European Commission, Brussels, <https://eur-lex.europa.eu/legal-content/EN/TXT/PDF/?uri=CELEX:52018DC0773&from=EN>.
- [4] B.T. Astrom, *Manufacturing of Polymer Composites*, 1st ed. Routledge, London, 1997, 469 p.
- [5] T.J. Reinhart, Overview of Composite Materials, in: S.T. Peters (ed.), *Handbook of Composites*, Springer US, Boston, MA, 1998, pp. 21-33.
- [6] D.A. Jesson, J.F. Watts, The Interface and Interphase in Polymer Matrix Composites: Effect on Mechanical Properties and Methods for Identification, *Polymer Reviews*, Vol. 52, Iss. 3, 2012, pp. 321-354. <https://doi.org/10.1080/15583724.2012.710288>.
- [7] M.M. Dawoud, Introductory Chapter: Background on Composite Materials, in: Anonymous (ed.), *Characterizations of Some Composite Materials*, IntechOpen, Rijeka, 2019, pp. Ch. 1.

[8] E. Witten, V. Mathes, The European GRP Market in 2018, AVK –Industrievereinigung Verstärkte Kunststoffe e.V., 2018, 1-59 p. Available: https://www.avk-tv.de/files/20181115_avk_ccev_market_report_2018_final.pdf.

[9] Nova-Institute PRESS RELEASE (EN/DE): Biocomposites performing great – not only for lightweight construction! nova-Institute, <http://nova-institute.eu/press/>.

[10] AVK Composites Germany The European GRP market in 2016, <https://www.materialstoday.com/composite-industry/comment/the-european-grp-market-in-2016/>.

[11] J.P. Patel, P.H. Parsania, 3 - Characterization, testing, and reinforcing materials of biodegradable composites, in: N.G. Shimpi (ed.), Biodegradable and Biocompatible Polymer Composites, Woodhead Publishing, 2018, pp. 55-79.

[12] B.S. Gupta, M. Afshari, 15 - Polyacrylonitrile fibers, in: A.R. Bunsell (ed.), Handbook of Properties of Textile and Technical Fibres (Second Edition), Woodhead Publishing, 2018, pp. 545-593.

[13] K.L. Pickering, M.G.A. Efendy, T.M. Le, A review of recent developments in natural fibre composites and their mechanical performance, Composites Part A: Applied Science and Manufacturing, Vol. 83, 2016, pp. 98-112. Available (accessed ID: 271638): <http://www.sciencedirect.com/science/article/pii/S1359835X15003115>.

[14] M.P. Staiger, N. Tucker, 8 - Natural-fibre composites in structural applications, in: K.L. Pickering (ed.), Properties and Performance of Natural-Fibre Composites, Woodhead Publishing, 2008, pp. 269-300.

[15] R. Dunne, D. Desai, R. Sadiku, J. Jayaramudu, A review of natural fibres, their sustainability and automotive applications, Journal of Reinforced Plastics and Composites, Vol. 35, Iss. 13, 2016, pp. 1041-1050.

Available (accessed doi: 10.1177/0731684416633898; 26):
<https://doi.org/10.1177/0731684416633898>.

[16] M. Noryani, S.M. Sapuan, M.T. Mastura, M.Y.M. Zuhri, E.S. Zainudin, Material selection criteria for natural fibre composite in automotive component: A review, IOP Conference Series: Materials Science and Engineering, Vol. 368, 2018, pp. 12002. <http://stacks.iop.org/1757-899X/368/i=1/a=012002>.

[17] F.M. AL-Oqla, S.M. Sapuan, Natural fiber reinforced polymer composites in industrial applications: feasibility of date palm fibers for sustainable automotive industry, Journal of cleaner production, Vol. 66, 2014, pp. 347-354. <http://dx.doi.org/10.1016/j.jclepro.2013.10.050>.

[18] M.F.M. Alkbir, S.M. Sapuan, A.A. Nuraini, M.R. Ishak, Fibre properties and crashworthiness parameters of natural fibre-reinforced composite structure: A literature review, Composite Structures, Vol. 148, 2016, pp. 59-73. Available (accessed ID: 271517): <http://www.sciencedirect.com/science/article/pii/S0263822316300034>.

[19] J. Chen, Chapter 4 - Synthetic Textile Fibers: Regenerated Cellulose Fibers, in: R. Sinclair (ed.), Textiles and Fashion, Woodhead Publishing, 2015, pp. 79-95.

[20] J. Chen, K. Wang, F. Xu, R. Sun, Effect of hemicellulose removal on the structural and mechanical properties of regenerated fibers from bamboo, Cellulose, Vol. 22, Iss. 1, 2015, pp. 63-72. Available (accessed ID: Chen2015): <https://doi.org/10.1007/s10570-014-0488-8>.

[21] N. Phinichka, S. Kaenthong, Regenerated cellulose from high alpha cellulose pulp of steam-exploded sugarcane bagasse, Journal of Materials Research and Technology, Vol. 7, Iss. 1, 2018, pp. 55-65. <http://www.sciencedirect.com/science/article/pii/S2238785416301831>.

[22] Q. Gao, X. Shen, X. Lu, Regenerated bacterial cellulose fibers prepared by the NMMO·H₂O process, Carbohydrate Polymers, Vol. 83, Iss.

- 3, 2011, pp. 1253-1256. <http://www.sciencedirect.com/science/article/pii/S0144861710007629>.
- [23] B. LÖNNBERG, 2 - Industrial cellulose, in: C. Woodings (ed.), *Regenerated Cellulose Fibres*, Woodhead Publishing, 2001, pp. 22-36.
- [24] A.G. WILKES, 3 - The viscose process, in: C. Woodings (ed.), *Regenerated Cellulose Fibres*, Woodhead Publishing, 2001, pp. 37-61.
- [25] P. WHITE, 4 - Lyocell: the production process and market development, in: C. Woodings (ed.), *Regenerated Cellulose Fibres*, Woodhead Publishing, 2001, pp. 62-87.
- [26] F. Carrillo, X. Colom, X. Cañavate, Properties of Regenerated Cellulose Lyocell Fiber-Reinforced Composites, *Journal of Reinforced Plastics and Composites*, Vol. 29, Iss. 3, 2010, pp. 359-371.
<https://doi.org/10.1177/0731684408097777>.
- [27] M. Reinhardt, J. Kaufmann, M. Kausch, L. Kroll, PLA-Viscose-Composites with Continuous Fibre Reinforcement for Structural Applications, *Procedia Materials Science*, Vol. 2, 2013, pp. 137-143.
<http://www.sciencedirect.com/science/article/pii/S2211812813000175>.
- [28] S. Frackowiak, J. Ludwiczak, K. Leluk, Man-Made and Natural Fibres as a Reinforcement in Fully Biodegradable Polymer Composites: A Concise Study, *Journal of Polymers and the Environment*, Vol. 26, Iss. 12, 2018, pp. 4360-4368. Available (accessed ID: Frackowiak2018): <https://doi.org/10.1007/s10924-018-1301-9>.
- [29] T. Bahners, M. Kelch, B. Gebert, X.L. Osorio Barajas, T.C. Schmidt, J.S. Gutmann, J. Müssig, Improvement of fibre–matrix adhesion in cellulose/polyolefin composite materials by means of photo-chemical fibre surface modification, *Cellulose*, Vol. 25, Iss. 4, 2018, pp. 2451-2471. Available (accessed ID: Bahners2018): <https://doi.org/10.1007/s10570-018-1724-4>.

- [30] S.K. Ramamoorthy, F. Bakare, R. Herrmann, M. Skrifvars, Performance of biocomposites from surface modified regenerated cellulose fibers and lactic acid thermoset bioresin, *Cellulose*, Vol. 22, Iss. 4, 2015, pp. 2507-2528. Available (accessed ID: Ramamoorthy2015): <https://doi.org/10.1007/s10570-015-0643-x>.
- [31] A. Mader, A. Kondor, T. Schmid, R. Einsiedel, J. Müssig, Surface properties and fibre-matrix adhesion of man-made cellulose epoxy composites – Influence on impact properties, *Composites Science and Technology*, Vol. 123, 2016, pp. 163-170. <http://www.sciencedirect.com/science/article/pii/S0266353815301603>.
- [32] H. Santamala, R. Livingston, H. Sixta, M. Hummel, M. Skrifvars, O. Saarela, Advantages of regenerated cellulose fibres as compared to flax fibres in the processability and mechanical performance of thermoset composites, *Composites Part A: Applied Science and Manufacturing*, Vol. 84, 2016, pp. 377-385. <http://www.sciencedirect.com/science/article/pii/S1359835X16000683>.
- [33] Z.N. Azwa, B.F. Yousif, A.C. Manalo, W. Karunasena, A review on the degradability of polymeric composites based on natural fibres, *Materials & Design*, Vol. 47, 2013, pp. 424-442. <http://www.sciencedirect.com/science/article/pii/S0261306912007832>.
- [34] P. Zadorecki, A.J. Michell, Future prospects for wood cellulose as reinforcement in organic polymer composites, *Polymer Composites*, Vol. 10, Iss. 2, 1989, pp. 69-77. <https://onlinelibrary.wiley.com/doi/abs/10.1002/pc.750100202>.
- [35] F.C. Campbell, Introduction to Composite Materials, in: F.C. Campbell (ed.), *Structural composite materials*, ASM International, Ohio, USA, 2010, pp. 1-29.
- [36] C.M. Clemons, R.M. Rowell, D. Plackett, K. Segerholm, Chapter 13: Wood/Nonwood Thermoplastic Composites, in: R. Rowell (ed.),

Handbook of wood chemistry and wood composites, second edition, CRC press, 2012, pp. 473.

[37] S. Migneault, A. Koubaa, P. Perré, B. Riedl, Effects of wood fiber surface chemistry on strength of wood–plastic composites, *Applied Surface Science*, Vol. 343, 2015, pp. 11-18. Available (accessed ID: 271533): <http://www.sciencedirect.com/science/article/pii/S0169433215005462>.

[38] M.J. Berger, N.M. Stark, Investigations of Species Effects in an Injection-Molding-Grade, Wood-Filled Polypropylene, The Fourth International Conference on Woodfiber-Plastic Composites, May 12–14, 1997, Forest Products Society, Madison, Wisconsin, pp. 19-25.

[39] M.J. Schwarzkopf, M.D. Burnard, Wood-Plastic Composites—Performance and Environmental Impacts, in: Anonymous (ed.), *Environmental Impacts of Traditional and Innovative Forest-based Bioproducts*, Springer, Singapore, 2016, pp. 19-43.

[40] A.A. Klyosov, Composition of Wood–Plastic Composites: Cellulose and Lignocellulose Fillers, in: Anonymous (ed.), *Wood-Plastic Composites*, John Wiley & Sons, Ltd, 2007, pp. 75-122.

[41] A. Eder, M. Carus, Global Trends in Wood-Plastic Composites (WPC), *Bioplastics Magazine*, 2013, pp. 1-17.

[42] A. Haider, A. Eder, Markets, Applications, and Processes for Wood Polymer Composites (WPC) in Europe, *Markets, Applications, and Processes for Wood Polymer Composites (WPC) in Europe*.

[43] S. Yeh, K. Kim, R.K. Gupta, Synergistic effect of coupling agents on polypropylene-based wood–plastic composites, *Journal of Applied Polymer Science*, Vol. 127, Iss. 2, 2013, pp. 1047-1053. Available (accessed doi: 10.1002/app.37775; 19): <https://doi.org/10.1002/app.37775>.

- [44] Q. Wang, Z. Xiao, W. Wang, Y. Xie, Coupling pattern and efficacy of organofunctional silanes in wood flour-filled polypropylene or polyethylene composites, *Journal of Composite Materials*, Vol. 49, Iss. 6, 2015, pp. 677-684. <https://doi.org/10.1177/0021998314525065>.
- [45] H. Zhang, Effect of a novel coupling agent, alkyl ketene dimer, on the mechanical properties of wood-plastic composites, *Materials & Design*, Vol. 59, 2014, pp. 130-134. <https://www.sciencedirect.com/science/article/pii/S0261306914001666>.
- [46] M.J. John, R.D. Anandjiwala, Recent developments in chemical modification and characterization of natural fiber-reinforced composites, *Polymer Composites*, Vol. 29, Iss. 2, 2008, pp. 187-207. <https://onlinelibrary.wiley.com/doi/abs/10.1002/pc.20461>.
- [47] C.A.S. Hill, *Wood Modification: Chemical, Thermal and Other Processes*, John Wiley & Sons, Ltd, Chichester, England, 2006, 260 p.
- [48] J. Cruz, R. Fanguero, Surface Modification of Natural Fibers: A Review, *Procedia Engineering*, Vol. 155, 2016, pp. 285-288. Available (accessed ID: 278653): <http://www.sciencedirect.com/science/article/pii/S1877705816321713>.
- [49] D. Sun, Surface Modification of Natural Fibers Using Plasma Treatment, in: S. Kalia (ed.), *Biodegradable Green Composites*, Wiley-Blackwell, 2016, pp. 18-39.
- [50] B. Enciso, J. Abenojar, M.A. Martínez, Influence of plasma treatment on the adhesion between a polymeric matrix and natural fibres, *Cellulose*, Vol. 24, Iss. 4, 2017, pp. 1791-1801. <https://link.springer.com/article/10.1007/s10570-017-1209-x>.
- [51] J.L. Thomason, The interface region in glass fibre-reinforced epoxy resin composites: 1. Sample preparation, void content and interfacial

strength, *Composites*, Vol. 26, Iss. 7, 1995, pp. 467-475. Available (accessed ID: 272911): <http://www.sciencedirect.com/science/article/pii/001043619596804F>.

[52] Y. Xie, C.A.S. Hill, Z. Xiao, H. Militz, C. Mai, Silane coupling agents used for natural fiber/polymer composites: A review, *Composites Part A: Applied Science and Manufacturing*, Vol. 41, Iss. 7, 2010, pp. 806-819. Available (accessed ID: 271638): <http://www.sciencedirect.com/science/article/pii/S1359835X10000850>.

[53] M. El Boustani, F. Brouillette, G. Lebrun, A. Belfkira, Solvent-free acetylation of lignocellulosic fibers at room temperature: Effect on fiber structure and surface properties, *Journal of Applied Polymer Science*, Vol. 132, Iss. 29, 2015, Available (accessed doi: 10.1002/app.42247; 02): <https://doi.org/10.1002/app.42247>.

[54] V. Fiore, G. Di Bella, A. Valenza, The effect of alkaline treatment on mechanical properties of kenaf fibers and their epoxy composites, *Composites Part B: Engineering*, Vol. 68, 2015, pp. 14-21. Available (accessed ID: 271637): <http://www.sciencedirect.com/science/article/pii/S1359836814003576>.

[55] M. Cai, H. Takagi, A.N. Nakagaito, Y. Li, G.I.N. Waterhouse, Effect of alkali treatment on interfacial bonding in abaca fiber-reinforced composites, *Composites Part A: Applied Science and Manufacturing*, Vol. 90, 2016, pp. 589-597. Available (accessed ID: 271638): <http://www.sciencedirect.com/science/article/pii/S1359835X16302810>.

[56] Y. Xie, C.A.S. Hill, Z. Xiao, H. Militz, C. Mai, Silane coupling agents used for natural fiber/polymer composites: A review, *Composites Part A: Applied Science and Manufacturing*, Vol. 41, Iss. 7, 2010, pp. 806-819. <http://www.sciencedirect.com/science/article/pii/S1359835X10000850>.

[57] S. Kalia, K. Thakur, A. Celli, M.A. Kiechel, C.L. Schauer, Surface modification of plant fibers using environment friendly methods for their

application in polymer composites, textile industry and antimicrobial activities: A review, *Journal of Environmental Chemical Engineering*, Vol. 1, Iss. 3, 2013, pp. 97-112. <http://www.sciencedirect.com/science/article/pii/S2213343713000213>.

[58] M.M. Kabir, H. Wang, K.T. Lau, F. Cardona, Chemical treatments on plant-based natural fibre reinforced polymer composites: An overview, *Composites Part B: Engineering*, Vol. 43, Iss. 7, 2012, pp. 2883-2892. <http://www.sciencedirect.com/science/article/pii/S1359836812002922>.

[59] R. Rajan, J. Riihivuori, E. Rainosalo, M. Skrifvars, P. Järvelä, Effect of viscose fabric modification on the mechanical and water absorption properties of composites prepared through vacuum infusion, *Journal of Reinforced Plastics and Composites*, Vol. 33, Iss. 15, 2014, pp. 1416-1429. Available (accessed doi: 10.1177/0731684414534748; 05): <https://doi.org/10.1177/0731684414534748>.

[60] C.A.S. Hill, Khalil, H. P. S. A., M.D. Hale, A study of the potential of acetylation to improve the properties of plant fibres, *Industrial Crops and Products*, Vol. 8, Iss. 1, 1998, pp. 53-63. <https://www.sciencedirect.com/science/article/pii/S0926669097100127>.

[61] R.P. Singh, Surface grafting onto polypropylene — a survey of recent developments, *Progress in Polymer Science*, Vol. 17, Iss. 2, 1992, pp. 251-281. Available (accessed ID: 271613): <http://www.sciencedirect.com/science/article/pii/007967009290024S>.

[62] J.J. Robin, C. Boyer, B. Boutevin, C. Loubat, Synthesis and properties of polyolefin graft copolymers by a grafting “onto” reactive process, *Polymer*, Vol. 49, Iss. 21, 2008, pp. 4519-4528. Available (accessed ID: 271607): <http://www.sciencedirect.com/science/article/pii/S0032386108006873>.

[63] M. Zhang, R.H. Colby, S.T. Milner, T.C.M. Chung, T. Huang, W. deGroot, Synthesis and Characterization of Maleic Anhydride Grafted

Polypropylene with a Well-Defined Molecular Structure, *Macromolecules*, Vol. 46, Iss. 11, 2013, pp. 4313-4323.
<https://doi.org/10.1021/ma4006632>.

[64] J. Bonilla-Cruz, M. Dehonor, E. Saldívar-Guerra, A. González-Montiel, Polymer Modification: Functionalization and Grafting, in: E. Saldívar-Guerra, Vivaldo-Lima Eduardo (ed.), *Handbook of Polymer Synthesis, Characterization, and Processing*, Wiley-Blackwell, 2013, pp. 205-223.

[65] F. Kučera, J. Petruš, P. Poláček, J. Jančář, Controlled reactive modification of polypropylene with maleic anhydride via solvent-free technique, *Polymer Degradation and Stability*, Vol. 168, 2019, pp. 108934.
<http://www.sciencedirect.com/science/article/pii/S014139101930254X>.

[66] D.M. Panaitescu, Z. Vuluga, M. Ghiurea, M. Iorga, C. Nicolae, R. Gabor, Influence of compatibilizing system on morphology, thermal and mechanical properties of high flow polypropylene reinforced with short hemp fibers, *Composites Part B: Engineering*, Vol. 69, 2015, pp. 286-295. Available (accessed ID: 271637): <http://www.sciencedirect.com/science/article/pii/S1359836814004545>.

[67] M.R. Nevare, P.D. Tatiya, P.P. Mahulikar, V.V. Gite, Effect of maleated polypropylene as a compatibilizer and hyperbranched polyester as a processing aid on polypropylene-wood flour biocomposites, *Journal of Vinyl and Additive Technology*, Vol. 24, Iss. 2, 2018, pp. 179-184. Available (accessed doi: 10.1002/vnl.21544; 03): <https://doi.org/10.1002/vnl.21544>.

[68] A. Ferrer, I.C. Hoeger, X. Lu, O.J. Rojas, Reinforcement of polypropylene with lignocellulose nanofibrils and compatibilization with biobased polymers, *Journal of Applied Polymer Science*, Vol. 133, Iss. 34, 2016, Available (accessed doi: 10.1002/app.43854; 03): <https://doi.org/10.1002/app.43854>.

[69] R. Rajan, E. Rainosaló, S.K. Ramamoorthy, S.P. Thomas, J. Zavašnik, J. Vuorinen, M. Skrifvars, Mechanical, thermal, and burning

properties of viscose fabric composites: Influence of epoxy resin modification, *Journal of Applied Polymer Science*, Vol. 135, Iss. 36, 2018, pp. 46673. Available (accessed <https://doi.org/10.1002/app.46673>; 04): <https://doi.org/10.1002/app.46673>.

[70] S.H. Aziz, M.P. Ansell, S.J. Clarke, S.R. Panteny, Modified polyester resins for natural fibre composites, *Composites Science and Technology*, Vol. 65, Iss. 3, 2005, pp. 525-535. Available (accessed ID: 271518): <http://www.sciencedirect.com/science/article/pii/S0266353804002027>.

[71] J. Yang, J. Xiao, J. Zeng, L. Bian, C. Peng, F. Yang, Matrix modification with silane coupling agent for carbon fiber reinforced epoxy composites, *Fibers and Polymers*, Vol. 14, Iss. 5, 2013, pp. 759-766. <https://link.springer.com/article/10.1007/s12221-013-0759-2>.

[72] W. Ji, J. Hu, L. Liu, J. Zhang, C. Cao, Improving the corrosion performance of epoxy coatings by chemical modification with silane monomers, *Surface and Coatings Technology*, Vol. 201, Iss. 8, 2007, pp. 4789-4795. Available (accessed ID: 271621): <http://www.sciencedirect.com/science/article/pii/S025789720601111X>.

[73] W. Ji, J. Hu, L. Liu, J. Zhang, C. Cao, Water uptake of epoxy coatings modified with γ -APS silane monomer, *Progress in Organic Coatings*, Vol. 57, Iss. 4, 2006, pp. 439-443. Available (accessed ID: 271377): <http://www.sciencedirect.com/science/article/pii/S0300944006002189>.

[74] J.J. Chruściel, E. Leśniak, Modification of epoxy resins with functional silanes, polysiloxanes, silsesquioxanes, silica and silicates, *Progress in Polymer Science*, Vol. 41, 2015, pp. 67-121. Available (accessed ID: 271613): <http://www.sciencedirect.com/science/article/pii/S007967001400094X>.

[75] R. Rajan, E. Rainosalo, S.P. Thomas, S.K. Ramamoorthy, J. Zavašnik, J. Vuorinen, M. Skrifvars, Modification of epoxy resin by

silane-coupling agent to improve tensile properties of viscose fabric composites, *Polymer Bulletin*, Vol. 75, Iss. 1, 2018, pp. 167-195. Available (accessed ID: Rajan2018): <https://doi.org/10.1007/s00289-017-2022-2>.

[76] D.G. Papageorgiou, I.A. Kinloch, R.J. Young, Mechanical properties of graphene and graphene-based nanocomposites, *Progress in Materials Science*, Vol. 90, 2017, pp. 75-127. Available (accessed ID: 271965): <http://www.sciencedirect.com/science/article/pii/S0079642517300968>.

[77] E. Watt, M.A. Abdelwahab, M.R. Snowdon, A.K. Mohanty, H. Khalil, M. Misra, Hybrid biocomposites from polypropylene, sustainable bio-carbon and graphene nanoplatelets, *Scientific Reports*, Vol. 10, Iss. 1, 2020, pp. 10714. Available (accessed ID: Watt2020): <https://doi.org/10.1038/s41598-020-66855-4>.

[78] J. Song, W. Yang, F. Fu, Y. Zhang, The Effect of Graphite on the Water Uptake, Mechanical Properties, Morphology, and EMI Shielding Effectiveness of HDPE/Bamboo flour composites, *BioResources*, Vol. 9, Iss. 3, 2014, pp. 3955-3967. <https://www.openaire.eu/search/publication?articleId=doajarticles::c4d83726785b5b6f7ed1182b9f120ee2>.

[79] B. Lei, Y. Zhang, Y. He, Y. Xie, B. Xu, Z. Lin, L. Huang, S. Tan, M. Wang, X. Cai, Preparation and characterization of wood-plastic composite reinforced by graphitic carbon nitride, *Materials & Design* (1980-2015), Vol. 66, 2015, pp. 103-109. Available (accessed ID: 271569): <http://www.sciencedirect.com/science/article/pii/S0261306914008292>.

[80] O. Faruk, L.M. Matuana, Nanoclay reinforced HDPE as a matrix for wood-plastic composites, *Composites Science and Technology*, Vol. 68, Iss. 9, 2008, pp. 2073-2077. Available (accessed ID: 271518): <http://www.sciencedirect.com/science/article/pii/S0266353808000997>.

[81] H. Lee, D.S. Kim, Preparation and physical properties of wood/polypropylene/clay nanocomposites, *Journal of Applied Polymer Science*, Vol. 111, Iss. 6, 2009, pp. 2769-2776. Available (accessed doi: 10.1002/app.29331; 03): <https://doi.org/10.1002/app.29331>.

[82] M. Nasrollahzadeh, Z. Issaabadi, M. Sajjadi, S.M. Sajadi, M. Atarod, Chapter 2 - Types of Nanostructures, in: M. Nasrollahzadeh, S.M. Sajadi, M. Sajjadi, Z. Issaabadi, M. Atarod (ed.), *Interface Science and Technology*, Elsevier, 2019, pp. 29-80.

[83] R. Rajan, J. Näkki, R. Layek, E. Rainosalo, Wood plastic composites with improved electrical and thermal conductivity, *Wood Science and Technology*, 2021, Available (accessed ID: Rajan2021): <https://doi.org/10.1007/s00226-021-01275-9>.

[84] S. Paszkiewicz, A. Szymczyk, Chapter 6 - Graphene-Based Nanomaterials and Their Polymer Nanocomposites, in: N. Karak (ed.), *Nanomaterials and Polymer Nanocomposites*, Elsevier, 2019, pp. 177-216.

[85] H. Zhang, W. Zheng, Q. Yan, Y. Yang, J. Wang, Z. Lu, G. Ji, Z. Yu, Electrically conductive polyethylene terephthalate/graphene nanocomposites prepared by melt compounding, *Polymer*, Vol. 51, Iss. 5, 2010, pp. 1191-1196. <http://www.sciencedirect.com/science/article/pii/S003238611000056X>.

[86] H. Kim, C.W. Macosko, Processing-property relationships of polycarbonate/graphene composites, *Polymer*, Vol. 50, Iss. 15, 2009, pp. 3797-3809. <http://www.sciencedirect.com/science/article/pii/S0032386109004558>.

[87] S. Sheshmani, A. Ashori, M. Arab Fashapoyeh, Wood plastic composite using graphene nanoplatelets, *International Journal of Biological Macromolecules*, Vol. 58, 2013, pp. 1-6. <http://www.sciencedirect.com/science/article/pii/S0141813013001335>.

[88] I. Karteri, M. Altun, M. Gunes, Electromagnetic interference shielding performance and electromagnetic properties of wood-plastic nanocomposite with graphene nanoplatelets, *Journal of Materials Science: Materials in Electronics*, Vol. 28, Iss. 9, 2017, pp. 6704-6711. Available (accessed ID: Karteri2017): <https://doi.org/10.1007/s10854-017-6364-1>.

- [89] A. Céline, S. Freour, F. Jacquemin, P. Casari, The hygroscopic behavior of plant fibers: a review, *Frontiers in Chemistry*, Vol. 1, 2014, <https://www.frontiersin.org/articles/10.3389/fchem.2013.00043/full>.
- [90] G. Cantero, A. Arbelaiz, R. Llano-Ponte, I. Mondragon, Effects of fibre treatment on wettability and mechanical behaviour of flax/polypropylene composites, *Composites Science and Technology*, Vol. 63, Iss. 9, 2003, pp. 1247-1254. <http://www.sciencedirect.com/science/article/pii/S0266353803000940>.
- [91] P. Zugenmaier, *Crystalline Cellulose and Derivatives: Characterization and Structures*, Springer-Verlag, Berlin Heidelberg, 2008, 285 p.
- [92] J. Park, T. Lee, J. Back, S. Jang, H. Kim, M. Skrifvars, Phenyl silane treatment and carding process to improve the mechanical, thermal, and water-absorption properties of regenerated cellulose lyocell/polylactic acid bio-composites, *Composites Part B: Engineering*, Vol. 167, 2019, pp. 387-395. <http://www.sciencedirect.com/science/article/pii/S1359836818344895>.
- [93] M. Carus, A. Partanen, *Natural fibre-reinforced plastics: establishment and growth in niche markets*. Hürth: Nova Institute GmbH. 2018 Mar. <https://edepot.wur.nl/494568>
- [94] Natural Resources Institute Finland The boom in the forest sector continues – the wood market heats up, <https://www.luke.fi/en/news/the-boom-in-the-forest-sector-continues-the-wood-market-heats-up/>.
- [95] M.K. Hassan, A. Villa, S. Kuittinen, J. Jänis, A. Pappinen, An assessment of side-stream generation from Finnish forest industry, *Journal of Material Cycles and Waste Management*, Vol. 21, Iss. 2, 2019, pp. 265-280. Available (accessed ID: Hassan2019): <https://doi.org/10.1007/s10163-018-0787-5>.

- [96] ISO 527-2: 2012, Plastics—Determination of Tensile Properties—Part 2: Test Conditions for Moulding and Extrusion Plastics, International Organization for Standardization-ISO, 2012, p.11.
- [97] ISO 178: 2010—Plastics—Determination of Flexural Properties, International Standards Organization-ISO, 2010, p.19.
- [98] ISO 14125: 1998, Fibre reinforced plastic composites—determination of flexural properties, International Standards Organization-ISO, 1998, p.18.
- [99] ISO 179–1: 2010, Plastics—Determination of Charpy Impact Properties, Part 1: Non-Instrumented Impact Test, International Organization for Standardization-ISO, 2010, p.22.
- [100] ISO 62: 2008, Plastics—Determination of Water Absorption, International Organization for Standardization-ISO, 2008, p.15.
- [101] ASTM D1652-11, Standard Test Method for Epoxy Content of Epoxy Resins, ASTM International, 2011, p.4.
- [102] ISO 3795:1989, Road vehicles, and tractors and machinery for agriculture and forestry Determination of burning behaviour of interior materials, International Organization for Standardization-ISO, 1989, p.6.
- [103] ASTM D257-07, Standard Test Methods for DC Resistance or Conductance of Insulating Materials, ASTM International, 2007, p.18.
- [104] W.J. Parker, R.J. Jenkins, C.P. Butler, G.L. Abbott, Flash Method of Determining Thermal Diffusivity, Heat Capacity, and Thermal Conductivity, *Journal of Applied Physics*, Vol. 32, Iss. 9, 1961, pp. 1679-1684. <https://aip.scitation.org/doi/10.1063/1.1728417>.
- [105] K. Li, R. Qiu, W. Liu, Improvement of Interfacial Adhesion in Natural Plant Fiber-reinforced Unsaturated Polyester Composites: A Critical Review, *Reviews of Adhesion and Adhesives*, Vol. 3, Iss. 1, 2015, pp. 98-

120. <https://www.ingentaconnect.com/content/scrive-ner/raa/2015/00000003/00000001/art00003>
<https://doi.org/10.7569/RAA.2015.097301>.

[106] S.J. Kenson, Reaction products of polyesters and primary amines, US2969335A, 24.01.1961, 4 p.

[107] M.A. Sawpan, K.L. Pickering, A. Fernyhough, Effect of various chemical treatments on the fibre structure and tensile properties of industrial hemp fibres, *Composites Part A: Applied Science and Manufacturing*, Vol. 42, Iss. 8, 2011, pp. 888-895. Available (accessed ID: 271638): <http://www.sciencedirect.com/science/article/pii/S1359835X11000789>.

[108] V. Tserki, N.E. Zafeiropoulos, F. Simon, C. Panayiotou, A study of the effect of acetylation and propionylation surface treatments on natural fibres, *Composites Part A: Applied Science and Manufacturing*, Vol. 36, Iss. 8, 2005, pp. 1110-1118. Available (accessed ID: 271638): <http://www.sciencedirect.com/science/article/pii/S1359835X05000345>.

[109] R. Adusumali, M. Reifferscheid, H. Weber, T. Roeder, H. Sixta, W. Gindl, Mechanical Properties of Regenerated Cellulose Fibres for Composites, *Macromolecular Symposia*, Vol. 244, Iss. 1, 2006, pp. 119-125. Available (accessed doi: 10.1002/masy.200651211; 14): <https://doi.org/10.1002/masy.200651211>.

[110] K.H. Leong, S. Ramakrishna, Z.M. Huang, G.A. Bibo, The potential of knitting for engineering composites—a review, *Composites Part A: Applied Science and Manufacturing*, Vol. 31, Iss. 3, 2000, pp. 197-220. Available (accessed ID: 271638): <http://www.sciencedirect.com/science/article/pii/S1359835X99000676>.

[111] S. Ananda Kumar, Sankara Narayanan, T. S. N., Thermal properties of siliconized epoxy interpenetrating coatings, *Progress in Organic Coatings*, Vol. 45, Iss. 4, 2002, pp. 323-330. Available (accessed ID: 271377): <http://www.sciencedirect.com/science/article/pii/S0300944002000620>.

[112] S. Seraj, Z. Ranjbar, A. Jannesari, Synthesis and characterization of an anticratering agent based on APTES for cathodic electrocoatings, *Progress in Organic Coatings*, Vol. 77, Iss. 11, 2014, pp. 1735-1740. Available (accessed ID: 271377): <http://www.sciencedirect.com/science/article/pii/S0300944014001908>.

[113] P.J. Halley, M.E. Mackay, Chemorheology of thermosets—an overview, *Polymer Engineering & Science*, Vol. 36, Iss. 5, 1996, pp. 593-609. <https://onlinelibrary.wiley.com/doi/abs/10.1002/pen.10447>.

[114] J.M. Hu, W.G. Ji, L. Liu, J.Q. Zhang, C.N. Cao, Improving the Corrosion Performance of Epoxy Coatings by Modification with “Active” and “Non-active” Silane Monomers, in: K.L. Mittal (ed.), *Silanes and Other Coupling Agents*, Volume 5, CRC Press, 2009, p. 203.

[115] H. Dodiuk, S.H. Goodman, 1 - Introduction, in: H. Dodiuk, S.H. Goodman (ed.), *Handbook of Thermoset Plastics (Third Edition)*, William Andrew Publishing, Boston, 2014, pp. 1-12.

[116] R. Adusumali, M. Reifferscheid, H. Weber, T. Roeder, H. Sixta, W. Gindl, Mechanical Properties of Regenerated Cellulose Fibres for Composites, *Macromolecular Symposia*, Vol. 244, Iss. 1, 2006, pp. 119-125. <https://onlinelibrary.wiley.com/doi/abs/10.1002/masy.200651211>.

[117] J. Jayaramudu, G.S.M. Reddy, K. Varaprasad, E.R. Sadiku, S.S. Ray, A.V. Rajulu, Mechanical properties of uniaxial natural fabric *Grewia tiliifolia* reinforced epoxy based composites: Effects of chemical treatment, *Fibers and Polymers*, Vol. 15, Iss. 7, 2014, pp. 1462-1468. <https://link.springer.com/article/10.1007/s12221-014-1462-7>.

[118] P.K. Kushwaha, R. Kumar, Effect of Silanes on Mechanical Properties of Bamboo Fiber-epoxy Composites, *Journal of Reinforced Plastics and Composites*, Vol. 29, Iss. 5, 2010, pp. 718-724. <https://doi.org/10.1177/0731684408100691>.

[119] E.S. Greenhalgh, Fibre-dominated failures of polymer composites, in: Anonymous (ed.), Failure analysis and fractography of polymer composites, 2010, pp. 107-163.

[120] S.T. Pinho, P. Robinson, L. Iannucci, Fracture toughness of the tensile and compressive fibre failure modes in laminated composites, Composites Science and Technology, Vol. 66, Iss. 13, 2006, pp. 2069-2079. Available (accessed ID: 271518): <http://www.sciencedirect.com/science/article/pii/S026635380600011X>.

[121] P.W.R. Beaumont, Cracking Models; Broken Parts, Applied Composite Materials, Vol. 13, Iss. 5, 2006, pp. 265-285. <https://link.springer.com/article/10.1007/s10443-006-9022-y>.

[122] S. Deng, L. Ye, Influence of Fiber-Matrix Adhesion on Mechanical Properties of Graphite/Epoxy Composites: I. Tensile, Flexure, and Fatigue Properties, Journal of Reinforced Plastics and Composites, Vol. 18, Iss. 11, 1999, pp. 1021-1040. Available (accessed doi: 10.1177/073168449901801105; 10): <https://doi.org/10.1177/073168449901801105>.

[123] G.A. Bibo, P.J. Hogg, M. Kemp, Mechanical characterisation of glass- and carbon-fibre-reinforced composites made with non-crimp fabrics, Composites Science and Technology, Vol. 57, Iss. 9, 1997, pp. 1221-1241. Available (accessed ID: 271518): <http://www.sciencedirect.com/science/article/pii/S0266353897000535>.

[124] J. J. Andrew, S. M. Srinivasan, A. Arockiarajan, H. N. Dhakal, Parameters influencing the impact response of fiber-reinforced polymer matrix composite materials: A critical review, Composite Structures, Vol. 224, Iss. 15, 2019, p. 111007. <https://www.sciencedirect.com/science/article/abs/pii/S0263822318343575>.

[125] L.A. Pothan, Z. Oommen, S. Thomas, Dynamic mechanical analysis of banana fiber reinforced polyester composites, Composites Science and Technology, Vol. 63, Iss. 2, 2003, pp. 283-293. Available (accessed

ID: 271518): <http://www.sciencedirect.com/science/article/pii/S0266353802002543>.

[126] M. Jawaid, H. A. Khalil, O. S. Alattas, Woven hybrid biocomposites: dynamic mechanical and thermal properties. *Composites Part A: Applied Science and Manufacturing*, Vol. 43, Iss. 2, 2012, pp. 288-93. <https://www.sciencedirect.com/science/article/pii/S1359835X11003605>

[127] S.V. Levchik, E.D. Weil, Thermal decomposition, combustion and flame-retardancy of epoxy resins—a review of the recent literature, *Polymer International*, Vol. 53, Iss. 12, 2004, pp. 1901-1929. <https://onlinelibrary.wiley.com/doi/abs/10.1002/pi.1473>.

[128] M.Z. Rong, M.Q. Zhang, Y. Liu, G.C. Yang, H.M. Zeng, The effect of fiber treatment on the mechanical properties of unidirectional sisal-reinforced epoxy composites, *Composites Science and Technology*, Vol. 61, Iss. 10, 2001, pp. 1437-1447. <http://www.sciencedirect.com/science/article/pii/S026635380100046X>.

[129] S.K. Ramamoorthy, M. Skrifvars, M. Rissanen, Effect of alkali and silane surface treatments on regenerated cellulose fibre type (Lyocell) intended for composites, *Cellulose*, Vol. 22, Iss. 1, 2015, pp. 637-654. Available (accessed ID: Ramamoorthy2015): <https://doi.org/10.1007/s10570-014-0526-6>.

[130] R. Kozłowski, M. Władyska-Przybylak, Flammability and fire resistance of composites reinforced by natural fibers, *Polymers for Advanced Technologies*, Vol. 19, Iss. 6, 2008, pp. 446-453. <https://onlinelibrary.wiley.com/doi/abs/10.1002/pat.1135>.

[131] M. Försth, H. Modin, B. Sundström, A comparative study of test methods for assessment of fire safety performance of bus interior materials, *Fire and Materials*, Vol. 37, Iss. 5, 2013, pp. 350-357. <https://onlinelibrary.wiley.com/doi/abs/10.1002/fam.1116>.

- [132] C.I. Idumah, A. Hassan, Characterization and preparation of conductive exfoliated graphene nanoplatelets kenaf fibre hybrid polypropylene composites, *Synthetic Metals*, Vol. 212, 2016, pp. 91-104. <http://www.sciencedirect.com/science/article/pii/S0379677915301752>.
- [133] J.R. Potts, D.R. Dreyer, C.W. Bielawski, R.S. Ruoff, Graphene-based polymer nanocomposites, *Polymer*, Vol. 52, Iss. 1, 2011, pp. 5-25. Available (accessed ID: 271607): <http://www.sciencedirect.com/science/article/pii/S0032386110010372>.
- [134] de Sousa, Daniel Eurico Salvador, C.H. Scuracchio, de Oliveira Barra, Guilherme Mariz, A.d.A. Lucas, Chapter 7 - Expanded graphite as a multifunctional filler for polymer nanocomposites, in: K. Friedrich, U. Breuer (ed.), *Multifunctionality of Polymer Composites*, William Andrew Publishing, Oxford, 2015, pp. 245-261.
- [135] S. Sheshmani, A. Ashori, M. Arab Fashapoyeh, Wood plastic composite using graphene nanoplatelets, *International Journal of Biological Macromolecules*, Vol. 58, 2013, pp. 1-6. Available (accessed ID: 271248): <http://www.sciencedirect.com/science/article/pii/S0141813013001335>.
- [136] H. Kim, A.A. Abdala, C.W. Macosko, Graphene/Polymer Nanocomposites, *Macromolecules*, Vol. 43, Iss. 16, 2010, pp. 6515-6530. <https://doi.org/10.1021/ma100572e>.
- [137] S.N. Tripathi, G.S.S. Rao, A.B. Mathur, R. Jasra, Polyolefin/graphene nanocomposites: a review, *RSC Advances*, Vol. 7, Iss. 38, 2017, pp. 23615-23632. <https://pubs.rsc.org/en/content/articlelanding/2017/ra/c6ra28392f>.
- [138] K.T. Chung, J.H. Reisner, E.R. Campbell, Charging phenomena in the scanning electron microscopy of conductor-insulator composites: A tool for composite structural analysis, *Journal of Applied Physics*, Vol. 54, Iss. 11, 1983, pp. 6099-6112. <https://aip.scitation.org/doi/abs/10.1063/1.331946>.

- [139] J. Syurik, O.A. Ageev, D.I. Cherednichenko, B.G. Konoplev, A. Alexeev, Non-linear conductivity dependence on temperature in graphene-based polymer nanocomposite, *Carbon*, Vol. 63, 2013, pp. 317-323. <http://www.sciencedirect.com/science/article/pii/S000862231300609X>.
- [140] Y.V. Syurik, M.G. Ghislandi, E.E. Tkalya, G. Paterson, D. McGrouther, O.A. Ageev, J. Loos, Graphene Network Organisation in Conductive Polymer Composites, *Macromolecular Chemistry and Physics*, Vol. 213, Iss. 12, 2012, pp. 1251-1258. <https://onlinelibrary.wiley.com/doi/abs/10.1002/macp.201200116>.
- [141] S.K.H. Gulrez, M.E.A. Mohsin, H. Shaikh, A. Anis, A.M. Pulose, M.K. Yadav, E.H.P. Qua, S.M. Al-Zahrani, A review on electrically conductive polypropylene and polyethylene, *Polymer Composites*, Vol. 35, Iss. 5, 2014, pp. 900-914. <https://onlinelibrary.wiley.com/doi/abs/10.1002/pc.22734>.
- [142] I. Chodak, I. Krupa, "Percolation effect" and mechanical behavior of carbon black filled polyethylene, *Journal of Materials Science Letters*, Vol. 18, Iss. 18, 1999, pp. 1457-1459. Available (accessed ID: Chodak1999): <https://doi.org/10.1023/A:1006665527806>.
- [143] K. Kalaitzidou, H. Fukushima, P. Askeland, L.T. Drzal, The nucleating effect of exfoliated graphite nanoplatelets and their influence on the crystal structure and electrical conductivity of polypropylene nanocomposites, *Journal of Materials Science*, Vol. 43, Iss. 8, 2008, pp. 2895-2907. Available (accessed ID: Kalaitzidou2008): <https://doi.org/10.1007/s10853-007-1876-3>.
- [144] J. Wang, Y. Kazemi, S. Wang, M. Hamidinejad, M.B. Mahmud, P. Pötschke, C.B. Park, Enhancing the electrical conductivity of PP/CNT nanocomposites through crystal-induced volume exclusion effect with a slow cooling rate, *Composites Part B: Engineering*, Vol. 183, 2020, pp. 107663. <http://www.sciencedirect.com/science/article/pii/S135983681934733X>.

[145] A. Li, C. Zhang, Y. Zhang, Thermal Conductivity of Graphene-Polymer Composites: Mechanisms, Properties, and Applications, *Polymers*, Vol. 9, Iss. 9, 2017, p.437. <https://www.mdpi.com/2073-4360/9/9/437>.

[146] A. Li, C. Zhang, Y. Zhang, A. Li, C. Zhang, Y. Zhang, Thermal Conductivity of Graphene-Polymer Composites: Mechanisms, Properties, and Applications, *Polymers*, Vol. 9, Iss. 9, 2017, pp. 437. <https://www.mdpi.com/2073-4360/9/9/437>.

PUBLICATION

I

Effect of viscose fabric modification on the mechanical and water absorption properties of composites prepared through vacuum infusion


Rathish Rajan, Johanna Riihivuori, Egidija Rainosalo, Mikael Skrifvars, Pentti Järvelä

Journal of Reinforced Plastics & Composites (2014) 33 (15), 1416–1429

<https://doi.org/10.1177/0731684414534748>

Publication reprinted with the permission of the copyright holders.

Effect of viscose fabric modification on the mechanical and water absorption properties of composites prepared through vacuum infusion

Journal of Reinforced Plastics and Composites
2014, Vol. 33(15) 1416–1429
© The Author(s) 2014
Reprints and permissions:
sagepub.co.uk/journalsPermissions.nav
DOI: 10.1177/0731684414534748
jrp.sagepub.com


R Rajan^{1,2}, J Riihivuori¹, E Rainosalo², M Skrifvars³ and P Järvelä¹

Abstract

Viscose fabric-reinforced unsaturated polyester composites were successfully prepared through vacuum infusion process. Unidirectional viscose fabric was modified by two different organosilane coupling agents and by acetylation treatment. The main objective was to study the influence of fabric treatment on the mechanical and water absorption properties of the composites. Flexural, tensile and impact properties of composites were studied. The results from mechanical testing of composites pointed out that 3-aminopropyltriethoxy silane treatment increased the flexural and impact strengths of the composites with respect to untreated fabric composite. The impact strength of 3-aminopropyltriethoxy silane-treated fabric composites almost doubled compared to the value of untreated fabric composite. Among all the composites under study, those with fabrics treated by 2 vol% 3-aminopropyltriethoxy silane in ethanol/water (95:5) solution exhibited significant improvement in water uptake resistance. An unsaturated polyester gelcoat and topcoat were applied as the outer surface on the composites with untreated fabric. This was done in order to investigate the visual surface appearance and evaluate the gelcoat and topcoat effect on water absorption after accelerated water immersion test. The regenerated cellulose fibre as reinforcement shows high potential to be used as an alternative for natural bast fibres, especially, when toughness of material matters. Chemical treatment of regenerated cellulose fibres could result in improvement in properties of polymer composites, considering that the appropriate treatment method is selected for the corresponding fibre–matrix system.

Keywords

Viscose fibre, regenerated cellulose, chemical modification, silane coupling agent, fabric composite, mechanical properties, gelcoat, water absorption

Introduction

Natural fibre reinforcement offers many advantages over its synthetic counterpart and is usually used in the form of short and continuous fibre reinforcement. Short fibre-reinforced thermoplastic and thermoset composites are widely explored research areas.^{1–3} However due to brittleness, the bast fibre-reinforced composites exhibit poor impact strength. Hence, application of this kind of composites is limited to interior parts in automotive industry or in non-structural application.⁴ Continuous fibre reinforcements such as unidirectional, non-crimped fabrics and woven fabrics are good choice in development of high-performance

composites. The regenerated cellulose fibres, which are commonly named as viscose or rayon, possess high purity, uniformity and reproducibility of their

¹Department of Material Sciences, Tampere University of Technology, Tampere, Finland

²Technology Centre Ketek Ltd, Kokkola, Finland

³School of Engineering, University of Borås, Borås, Sweden

Corresponding author:

M Skrifvars, School of Engineering, University of Borås, Borås S-50190, Sweden.

Email: mikael.skrifvars@hb.se

properties.⁵ They are also available as continuous filaments, which can be processed into woven or warp-knitted textile fabrics. Since the regenerated cellulose fibres could form composites without compromising the benefits provided by natural fibres and considering that it can overcome the drawback of natural fibre in certain aspects, regenerated cellulose fibres could be a better alternative or a parallel choice for lignocellulosic fibres in composite manufacturing.⁶

Lignocellulosic fibres are mainly composed of cellulose, hemicellulose, pectins, lignin and waxes. These fibres are hydrophilic due to the hydrophilic nature of the hemicelluloses, pectin and also due to the porous morphology of the fibres. This hydrophilic nature can result in incompatibility between these fibres and the matrix resin, which is commonly hydrophobic polymer, for example polypropylene. This indeed leads to inferior mechanical properties of the natural fibre composite, which can be, especially, evident in long-term-used application. The absorption of water by natural fibres can be related to the amorphous regions of the cellulose and to the hydrophilic non-cellulosic components. In the crystalline region, there are less available hydroxyl groups, due to the close packing of the cellulosic chains, and the hydrogen bonding between the hydroxyl groups, eventually resulting in lesser water absorption. The degree of crystallinity for viscose fibres, as reported in literature, is in the range of 27–41%,^{7,8} which indicates rather high water absorption and higher hydrophilicity. Hence, the modification of the hydroxyl groups on the viscose fibre is an essential factor when fabricating a composite with lower water absorption and good fibre–matrix interaction. A chemical modification of the viscose fibre may improve the compatibility with reactive thermoset resins like unsaturated polyester resin. Several chemical methods utilized for the modification of natural fibres have been reported in literature. Methods such as acetylation,^{9,10} peroxide treatment^{11,12} and usage of silane coupling agents^{13–15} might also be suitable for viscose fibre treatment. Eventually, the chemical modification reduces the hydrophilic nature of the cellulosic fibres through functionalization of the free hydroxyl groups in the fibre. For instance, in the organosilane coupling agents the silane alkoxy group reacts with the hydroxyl group on the cellulose, while the organofunctional group on the other end of the silane is available for reaction with the matrix resin in the composite.

Organosilanes have a general chemical structure of $R_{(4-n)}-Si-(R'X)_n$ ($n = 1, 2$), where R is alkoxy, X is any organofunctionality and R' is the alkyl bridge connecting the silicone atom and organofunctionality. This bifunctionality of organosilanes facilitates an effective coupling between cellulosic fibres and polymer matrices. In natural fibre composites, most commonly used

silanes are trialkoxysilanes¹³ with amino, mercapto, glycydoxy, vinyl or methacryloxy groups as the organic functionality. The mechanism for the coupling of organosilanes with cellulosic fibres is initiated through the hydrolysis of silanes in presence of water yielding reactive silanol groups. During the hydrolysis, self-condensation of the silanols can also take place; however, it is advisable to control the self-condensation in order to leave the silanols available to be adsorbed with hydroxyl groups of cellulosic fibres. The reactive silanols are adsorbed to the hydroxyl group on cellulosic fibre surface through hydrogen bonding. Finally under higher temperature, the hydrogen bonds between silanols and fibre hydroxyl group get converted to covalent $-Si-O-C-$ bonds while liberating water.¹³ The effective interaction of silane-treated fibre is highly dependent on the reactivity and compatibility between organofunctionality of silane and reactivity of resin.

Vacuum-assisted resin infusion techniques have become popular in manufacturing polymer composites. In literature, vacuum infusion is known under different names that basically involve similar technology in which the impregnation of a dry reinforcement is done by a liquid polymer resin transported under vacuum.¹⁶ In this process, the resin is drawn into a preform by external air-pressure, which forces the resin to flow into the mould, from which the air has been evacuated by vacuum. The low cost tooling and scalability to very large structures has made vacuum infusion method a very attractive fabrication technology. It also minimizes the void contents inside the moulded composites, reduces volatile organic compound emissions and results in less production waste than other moulding techniques.¹⁷

Regenerated cellulose fibre-reinforced thermoplastic composites have been investigated with mostly biodegradable polymers as matrix material.^{18,19} Reports related to conventional thermoplastics reinforced with regenerated cellulose composites are also seen in literature.^{20,21} However, the studies on regenerated cellulose fibre/thermoset composites are very few.^{6,22–24} Chemical modification of regenerated cellulose fibre-based fabrics and the study of its influence on the properties of composites are seldom found in literature.²⁵ This study reports the effect of two different silane coupling agents and acetylation modification of warp-knitted unidirectional viscose fabrics on the mechanical and water absorption properties of unsaturated polyester composites. An unsaturated polyester-based gelcoat and topcoat were applied on the surface of the composites reinforced with untreated viscose fabrics. The intention was to evaluate the effect of these protective coatings on the visual appearance of the composite surface and the water absorption properties through accelerated water absorption test.

Experimental

Materials

Viscose yarn with the twist Z40, 2440 dtex linear density and 1350 filaments (Cordenka[®] CR) was obtained from Cordenka GmbH, Germany. The yarn was processed by warp knitting into unidirectional fabrics (Figure 1) with a surface weight of 223 g/m² (Engtex, Sweden). An unsaturated polyester resin (Envirez[®] M8600 TA) with a biomass content of 13% was purchased from Ashland Inc, Finland. Density of the resin given by the supplier was 1.1 g/cm³. Methyl ethyl ketone peroxide (MEKP) was used as a catalyst. The gelcoat was based on unsaturated polyester (Maxguard[®] NP) and topcoat was supplied by Ashland Inc, Finland. The chemicals used for fibre surface modification were 3-aminopropyltriethoxy silane (APS; 99% purity) obtained from Acros Organics, 3-methacryloxypropyltrimethoxy silane (MPS) obtained from Sigma–Aldrich and acetic anhydride obtained from Merck. All the other chemicals used in this study were of analytical grade and were used without further purification. For the vacuum infusion, sealant tapes, peel-ply fabric, injection fabric, plastic film for vacuum bagging and mould releasing agent (Chemlease[®] manufactured by Chem Trend) were supplied by Kevra Oy, Finland. The plastic connecting tubes used in vacuum infusion process were obtained from Etra Oy, Finland.

Chemical treatments

Two different organosilanes were used for the fibre surface treatment, APS and MPS. Different treatment

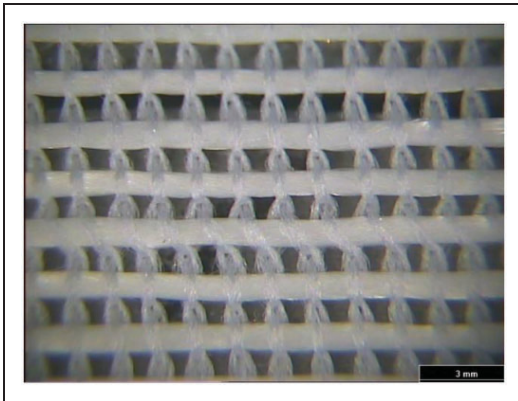


Figure 1. The fabricated warp-knitted fabric with the thicker weft viscose yarn in the horizontal direction, and the thin polyester warp yarn in the vertical direction.

procedures were opted to carry out the treatments and those are listed in Table 1. Acetylation of the fabric was done with acetic anhydride. A general reaction method for silane modification of fibre is shown in Figure 2.

APS treatment. APS was added either to an ethanol/distilled water solution or to distilled water, according to the corresponding treatments (Table 1) to yield a 2 vol% silane concentration in solution. Fabrics were dipped in a plastic container containing the silane solution for 5 min and then dried at room temperature. After 30 min, the fabrics were oven-dried at 110°C and kept in sealed plastic bags until composite preparation. The reaction between the cellulosic fabric and the APS silane may proceed by hydrolysis of the organosilane ethoxy groups which further form highly reactive silanols. Silanols form hydrogen bond with hydroxyl group of fabric, and thereafter in the presence of heat, a covalent bond is formed between fabric and silane. The amino group present in the silane is supposed to form chemical or physical bond with unsaturated polyester resin, thus forming a bridge between fabric and the polymer.

MPS treatment. Fabrics were treated in aqueous solution with 0.5 vol% MPS concentration. The reaction solution was prepared by dissolving MPS in distilled water acidified with acetic acid to maintain the pH at 4.5. The solution was further stirred for 15 min to form a clear homogeneous solution. Then the fabrics were immersed in the solution for 1 h. Finally, the fabrics were dried for 24 h at 60°C to remove traces of methanol resulted from hydrolysis of the methoxysilane.^{26,27} A general reaction mechanism for the silane modification of the fabric is given in Figure 2. The unsaturation in MPS may react with styrene in the presence of the initiator

Table 1. Details on different kinds of chemical treatment.

Treatment	Treatment condition
APS 95-5	Fabrics treated with 2 vol% APS in (95:5) ethanol/distilled water solution (v/v)
APS 50-50	Fabrics treated with 2 vol% APS in (50:50) ethanol/distilled water solution (v/v)
APS water	Fabrics treated with 2 vol% APS in distilled water.
MPS	Fabrics treated with 0.5 vol% MPS silane in distilled water
Acetylation	Acetic anhydride treatment

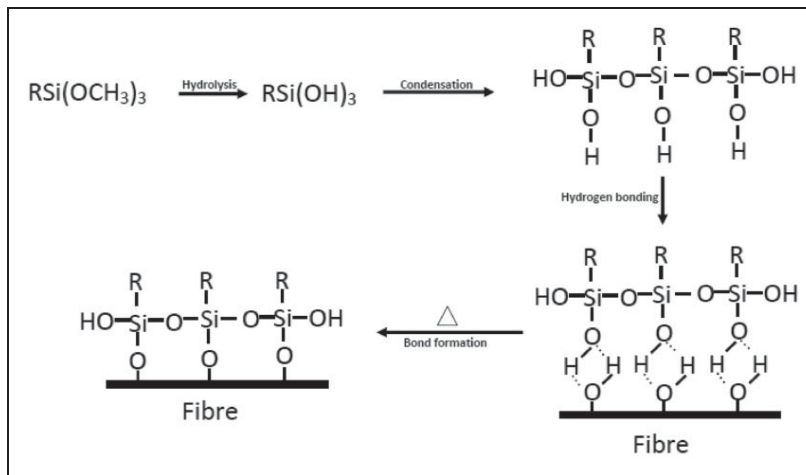


Figure 2. Organosilane coupling agent reaction with a cellulosic natural fibre.¹³

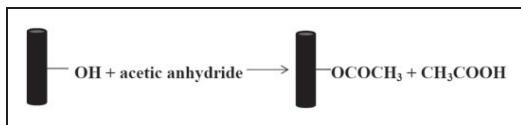


Figure 3. Acetylation of a cellulosic natural fibre using acetic anhydride.²⁹

during the curing of unsaturated polyester resin, thus forming a stable chemical bond with the resin.

Acetylation treatment. Fabrics pre-dried at 70°C for 16h were dipped into glass beaker with acetic anhydride for 1 min. The excess anhydride was drained off by placing the fabrics on a stainless steel mesh for 3 min. Finally, the treated fabrics were dried at 110°C for 2h.²⁸ Figure 3 represents the reaction mechanism for the acetylation of cellulose with acetic anhydride. Hydroxyl groups present on the surface of the fabric are supposed to be substituted with a carbonyl group through an esterification reaction.

Preparation of composites through vacuum infusion method

The composites were fabricated through vacuum infusion method, which is an efficient method to prepare high-quality composites. The whole process overview is shown in Figure 4. Three replicated composites were made from each type of modified viscose fabric, by using identical process conditions. The laminate was laid up with four layers of fabric and a flow-enhancing fabric was used on the peel ply to enhance resin flow

and distribution through the viscose fabrics. This helped in achieving better wettability at low vacuum pressure for viscose composites. Before infusion, the fabrics to be used for lamination were dried in an oven at 70°C for 16h. It is assumed that by drying the fabric, it is easier to remove any moisture present in the fabric. If moisture is present in the fabric, it might evaporate during the infusion process and leads to formation of voids.

The fabrics were laid-up on high-glossy glass plates with the dimensions of $250\text{ mm} \times 300\text{ mm}$. After cleaning the glass surface, a release agent was applied on it. Then a two-sided sealant tape was attached on four sides of the glass plate in order to fixate the vacuum bag film. In the space formed by the sealant tape, four layers of viscose fabric were placed and stacked as straight as possible on each other to form a unidirectional lay-up [$\pm 0^\circ/\pm 0^\circ/\pm 0^\circ/\pm 0^\circ$]. Then, the resin flow enhancing fabrics followed by the peel-ply fabric were placed on the top of viscose fabrics. Since rectangular lay-up was used, the connection tubes for vacuum and resin were fixed parallel to each other as shown in Figure 5(a). Finally, the fabric lay-up was covered with vacuum bag plastic film sealed to the two-sided sealant tape attached to the glass plate edges, thus making a closed system, which can be evacuated by vacuum. The vacuum infusion setup is shown in Figure 5(b). The infusion process was carried out in a well-ventilated place. Vacuum tubes were connected from resin vessel to the inlet tube and further to resin trap and to the vacuum pump. A vacuum pressure was applied near to -0.3 bar . After ensuring that there was no leak in the vacuum bag, the resin was mixed with 1.2 vol% of MEKP and added into resin vessel. The resin

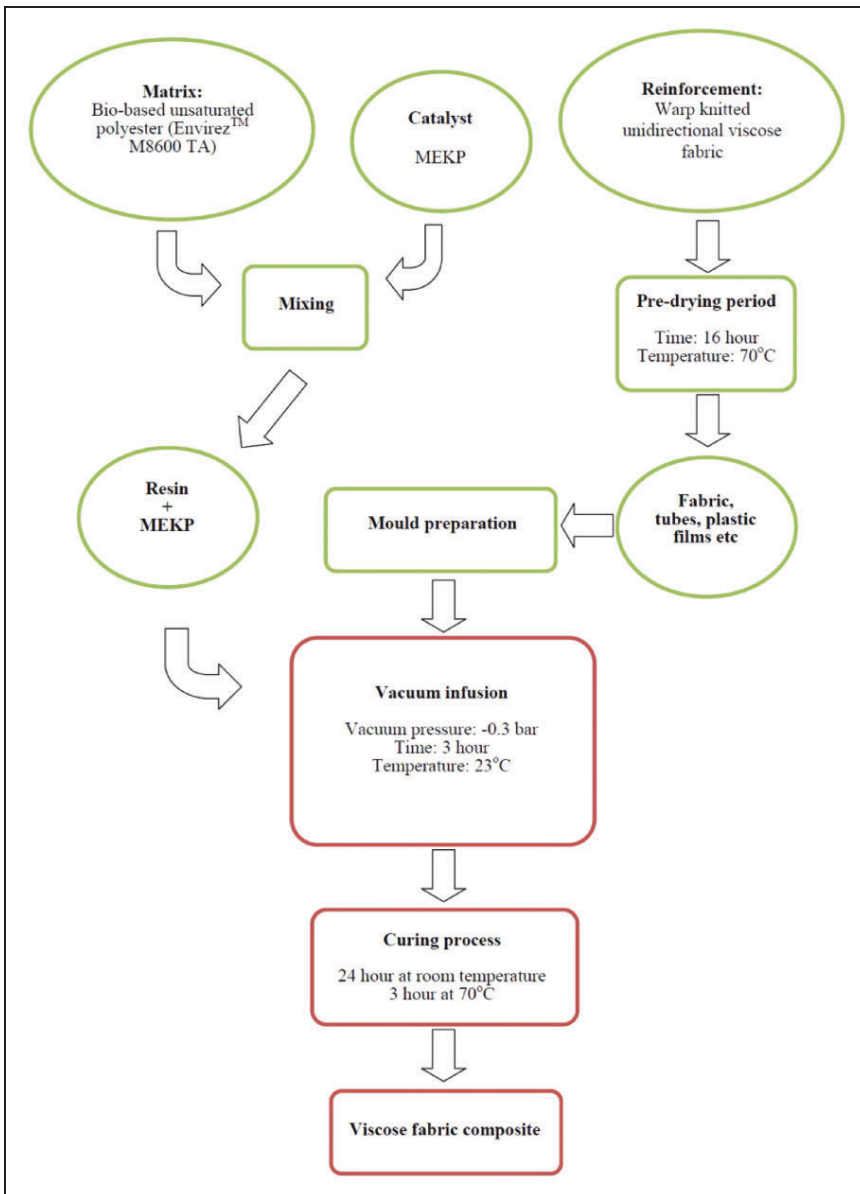


Figure 4. Schematic overview of the used preparation process for the viscose fabric composite.

was then allowed to flow through the tubes and through the fabrics. Any excess resin coming out from the impregnated fabrics was collected in resin trap. After infusion was completed and the fabrics were fully impregnated, the resin inlet tube was closed with a clamp. The connected vacuum pump was left working for 3 h after completing the infusion to achieve

constant vacuum pressure and to remove still remaining air bubbles in the composite. The whole infusion process took approximately 15–20 min at ambient conditions. The laminates were kept at room temperature for 24 h and then at 70°C for 3 h to completely cure the resin. The designation of each composite and corresponding treatment method is tabulated in Table 2.

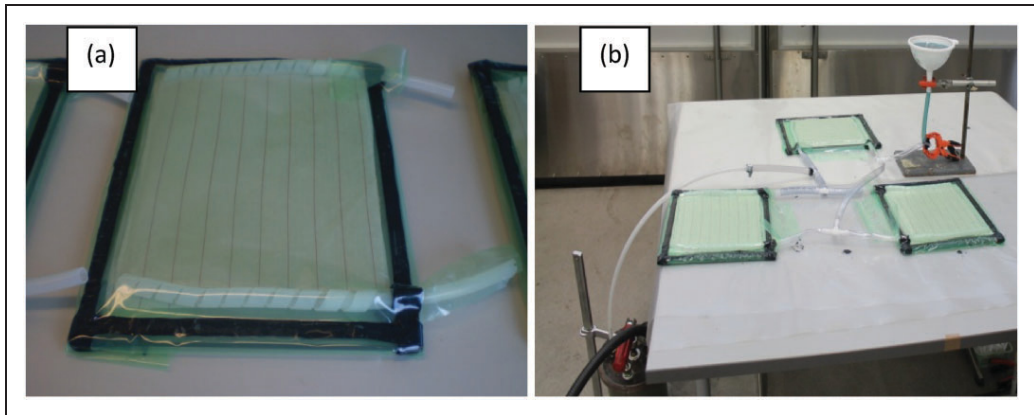


Figure 5. (a) Mould ready for infusion and (b) whole vacuum infusion setup.

Table 2. Designation of viscose fabric composites and respective chemical treatments.

Composite	Treatment
C-untreated	Composite with viscose fabric without treatment
C-APSI	Composite with APS 95-5 treated viscose fabric
C-APS2	Composite with APS 50-50 treated viscose fabric
C-APS3	Composite with APS water treated viscose fabric
C-MPS	Composite with MPS treated viscose fabric
C-acetylation	Composite with acetylated viscose fabric

Composites with gelcoat and topcoats

The preparation of viscose composite laminates coated with a protecting gelcoat and topcoat was also part of this study. The gelcoat and the topcoat are unsaturated polyester resins, which are applied in the process, so that they form the outermost surface. The aim was to investigate their effect on the water absorption and visual appearance of the laminates before and after their exposure to water at accelerated conditions. This is of particular practical interest, as unsaturated polyester resin composites are commonly used in applications where the surface is exposed to water or humidity. Prior to the lay-up of the fabrics for the vacuum infusion process, the gelcoat was applied on the glass plate. To get a good quality gelcoat surface, it is important to have a perfectly clean mould with no defects. The gelcoat was, therefore, applied in a dustless

and well-ventilated place at 18–25°C temperature. Normally, thickness of the gelcoat layer is between 0.5 and 3 mm, and in this study 0.5 mm thickness was applied. In order to achieve this thickness, a 0.5-mm metal sheet was placed parallel on the mould. After applying the releasing agent, gelcoat thoroughly mixed with 1.5 wt% of MEKP was spread carefully with a plastic tool on the mould and rolled with a stainless steel ruler as uniform as possible. Gelcoat was left to cure for 4–5 h at room temperature, until the surface was non-sticky. The vacuum infusion was done one day after gelcoat application. Procedure for vacuum infusion was exactly same as the one described above for the composites. In this part of the study, viscose fabric without any chemical treatment was used, and the resin used was the same (Envirez M8600 TA). The surface of the composite without gelcoat and the edges of composite were covered with two layers of topcoat, which was applied with a paintbrush. After vacuum infusion and curing period, laminates were cut into size of 100 mm × 100 mm for the accelerated water absorption tests.

Characterization of viscose fabric composites

Flexural properties

The flexural properties of the composites before and after water immersion were determined by a three-point bending test method according to ISO 178 standard. Messphysik MIDI 10–20/4 × 11 tensile testing machine equipped with 1-kN load was used for the testing. The specimens with size of

80 mm × 15 mm × 2 mm (length, width and average thickness) were used for testing. The test was carried out at ambient temperature with a crosshead speed of 2 mm/min and with a span length of 50 mm. Flexural strength and modulus were determined from five test specimens and average values were calculated and reported.

Tensile properties

Tensile properties were determined according to ISO 527-1 by using Messphysik tensile machine equipped with a 10-kN load cell. Tensile test specimens were machined in a shape of dog bone through laser. Dimensions of the testing area were 70 mm of length of narrow portion, 10 mm of width of narrow portion and 2–3 mm of an average thickness. Overall, length of the specimens was 150 mm and gauge length was 50 mm. The test was carried out at ambient temperature with a testing speed of 5 mm/min. Tensile strength, modulus and elongation at break, was taken from average of five specimens and is reported.

Charpy impact strength

Impact strength is defined as the ability of a material to resist fracture under stress applied at high speed and is directly related to the toughness of material. Toughness means the ability of the material to absorb applied energy. Charpy impact tests for viscose composite specimens were carried out using CEAST Resil 5.5J impact testing machine. Tests were done according to ISO 180 standard. It was very challenging to test the impact properties of the viscose composites due to their very tough nature. First, impact test was carried out with the specimens in size of 80 mm × 15 mm × 2 mm. However, the specimens did not break even with 50 J loading, which forced to make the specimens thinner with a width of 10 mm. Notches were also machined according to standard in depth of 2 mm. Finally, impact test was carried out with specimens having dimensions of 80 mm × 10 mm × 2 mm with 2 mm notches. Impact loading was done using a 5 J non-instrumented hammer, and edgewise. Three specimens each for different viscose composites were tested. As this is less number of the test specimens than which is recommended in the standard, the result may be influenced by this. The impact strength (kJ/m²) was calculated following equation (1) considering the remaining width after notching

$$a_{cU} = E_c/hb_N \times 10^3 \quad (1)$$

where ' E_c ' indicates the corrected energy absorbed by breaking the test specimen (J), ' h ' is the thickness of the test specimen in millimetres and ' b_N ' is the remaining width of the test specimen in millimetres after notching.

Water absorption test of composites

A gravimetric water absorption test was carried out in accordance with ISO 62 to determine water absorption behaviour of the viscose composite specimens at room temperature. The water content of each test specimen was determined by calculating their change in mass during the testing time. The weight gain percentage was calculated according to the Equation (2).

$$c = m_2 - m_1/m_1 \times 100\% \quad (2)$$

where ' m_1 ' is the mass of the test specimen in milligrams after drying and before immersion in water and ' m_2 ' is the mass of the test specimen after immersion at selected time periods. The composites were cut into 90 mm × 90 mm square-shaped plates, and for each composite type, three specimens were made. After that, the edges of the specimens were sanded and sealed with topcoat paint. This was done in order to prevent water absorption through the cut edges into laminates through the fibres. Before starting the test, all the specimens were conditioned to constant mass by keeping in an oven at 50 ± 2°C for three days, and then specimens were allowed to cool in a desiccator for two days at room temperature. After the conditioning, the specimens were placed in a container filled with distilled water at 23 ± 2°C. The first weighing was done after 2 h, and this was repeated 11 times; the last weighing was done after 102 days (2448 h). Each weighing was done to the nearest 0.1 mg within a minute of being removed from water, and the specimens were wiped off with lint-free tissue paper before placing it on the scale. It was seen that weighing after 2 and 6 h was necessary, because the composites have a high diffusion coefficient for water. The test continued until the saturation was reached, or until 102 days, if the test specimens did not reach saturation point completely. After finishing the test, the test specimens were dried in an oven at 50°C for 24 h and cooled in a desiccator for 2 h, and finally weighed to compare their weight difference to initial weight of the test specimens before water immersion.

Accelerated water absorption/aging test

An accelerated aging test was carried out for the composites which were coated with gelcoat and topcoat.

The aim of this test was to study the visual appearance, blister formation on the surfaces and deformation of the composite after testing. Weight gain during the test was determined in order to study the protection efficiency of the coatings on the water absorption of the composite laminates.

The blistering formation on the gelcoat surface is the most common phenomena caused mainly by osmosis. It is a common problem in marine applications, in which exterior surface of boat hulls are coated with gelcoat being exposed to water for a long period of time. The gelcoat-covered composites were cut into size of 100 mm × 100 mm specimens, and two-layered topcoat was applied on the side with no gelcoat. The cut edges of the specimens were also covered with the topcoat in order to prevent the water absorption through the edges. One set of specimens were drilled to make three circular holes in the middle of the test specimen in order to study the effect of cut holes on water uptake. This was done as it is common to fast other components by bolts in drilled holes, and these might cause water absorption. The specimens were weighed before they were placed in a container with 12 L of distilled water. The container was placed in a climate chamber at 65°C for four weeks, in order to accelerate the water absorption. These conditions are far by the conditions marine composite products are exposed to. Distilled water was used due to its more aggressive properties compared to sea water. Keeping the gelcoat specimens immersed in water at 50°C for 50 days corresponds to exposure conditions at 19°C for 30 days. If the temperature had been lowered, the test might have taken

even years. Weight of the specimens was taken after four weeks, when the test was finished.

Results and discussion

Flexural properties

Flexural strength of the prepared viscose composite specimens before and after water immersion test along with flexural strength of cured Envirez M8600 is shown in Figure 6. Before water immersion, the C-APS1 composite exhibits the highest strength (133.9 MPa) among all the composites. There is an increase in strength of 22% when compared to untreated fabric composite (C-untreated). In comparison with untreated fabric composite, the C-APS2 and C-APS3 composites show an increase of 6% and 7%, respectively. The MPS treated fabric composite (C-MPS) shows the weakest flexural strength (98.3 MPa). The flexural modulus is shown in Figure 7. Untreated viscose composite (C-untreated) and acetylated viscose fabric composites (C-acetylation) exhibit similar flexural stiffness with 5.5 and 5.3 GPa, respectively. Among the different APS treatments, APS 95-5 treated fabric composite (C-APS1) shows higher flexural modulus than for C-APS2 and C-APS3 composites. The composites made from the MPS treated viscose fabric (C-MPS) exhibit the flexural stiffness of 4.7 GPa. Water immersion test was conducted for C-untreated, C-APS1, C-MPS and C-acetylation composites. The flexural strength of all composites decreased after water immersion test. The percentage

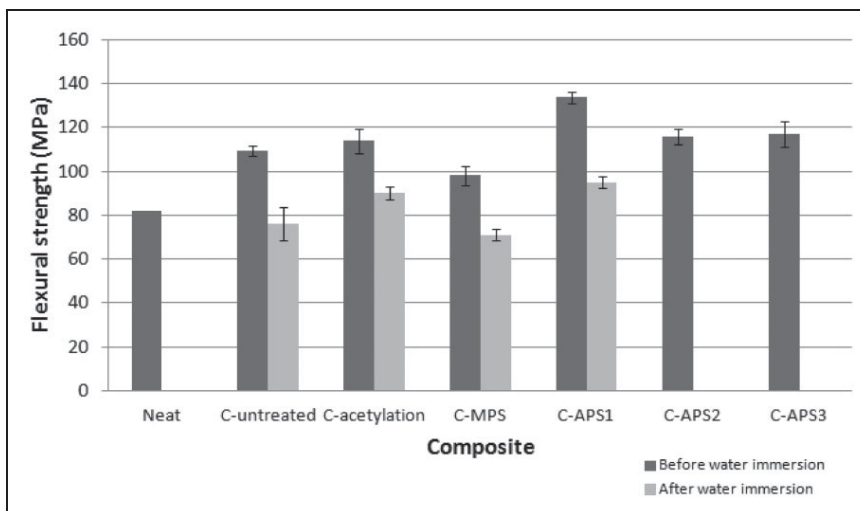


Figure 6. Flexural strength of composites made from differently treated viscose reinforcements.

of reduction compared to non-immersed samples for C-untreated, C-APS1, C-MPS and C-acetylation composites are 30.4%, 28.9%, 27.6% and 20.7%, respectively.

The flexural strength results indicate that the APS 95-5 treatment significantly improved flexural strength for composites compared to composites made from untreated viscose (C-untreated). This indicates an improved adhesion between matrix and fibre modified with organosilane containing amino functional group. It could be assumed that the APS silane has undergone physical and chemical reactions with the reactive sites in unsaturated polyester resin, thus resulting in a good adhesion between fibre and unsaturated polyester matrix. The reaction of amine with polyester may occur by the addition of the hydrogen atom of amine group to the carbon atom in the carbon double bond and balance of the amine adds to other carbon.³⁰ Since polyester contains free carboxyl groups, part of the amine may also remain combined in as a salt.³¹ C-APS2 and C-APS3 composites exhibit lower flexural properties compared to C-APS1 composites. The results from this study point out the significance of the ethanol concentration in the reaction medium for APS silane treatment. The higher the concentration of alcohol, the higher is the effect of modification on fibre and finally improving the properties of resultant composite. Against the expectations, MPS silane treatment of fabrics lowered the properties of C-MPS composites compared to C-untreated composites. It is reported that MPS silane is more compatible with unsaturated polyester matrix than APS.^{32,33} The results from this study shows that the fibre treatment in water medium for MPS was not effective to form a better interaction between fibre and polyester resin. It is possible that the concentration of MPS silane used was excess for the modification of fibre and could be considered that a

physisorbed MPS layer is formed on the surface of chemisorbed layer. This layer acts as a lubricant, and failure occurs in this region through slippage of physisorbed MPS chains.³⁴ It is also possible that the physisorbed layer prevents the chemisorbed silane from reacting with resin,³⁵ thus resulting in a composite with inferior properties.

The water absorption during 102 days resulted in a weak fibre–matrix interface, thus resulting in the reduction of flexural properties after water immersion test. The decrease in properties with increase in water absorption is ascribed to the formation of hydrogen bond between the water molecules and cellulose fibre. Viscose fibers have typically low moisture resistance; however, the APS 95-5 silane treatment of the viscose fabric have obviously reduced the number of free hydroxyl groups on the surface of fibre and therefore made it more resistant to water absorption. The water absorption of composites also depends on possible defects formed during manufacturing, such as voids. Through voids, water uptake is easily initiated, which negatively influences the properties of composite.

Tensile properties

Tensile testing results are presented in Table 3. The value for neat unsaturated polyester is taken from manufacturer data. It is seen that the untreated fabric gives composites showing highest tensile strength (152.2 MPa) among all composites. The composites made from acetylated fabrics (C-acetylation) proved to give best tensile strength (148 MPa) among the treated fabric composites. MPS treated fabric composites (C-MPS) exhibited the lowest value (98 MPa), while APS 95-5 treated fabric composite (C-APS1) shows a 25% reduction in tensile strength compared to

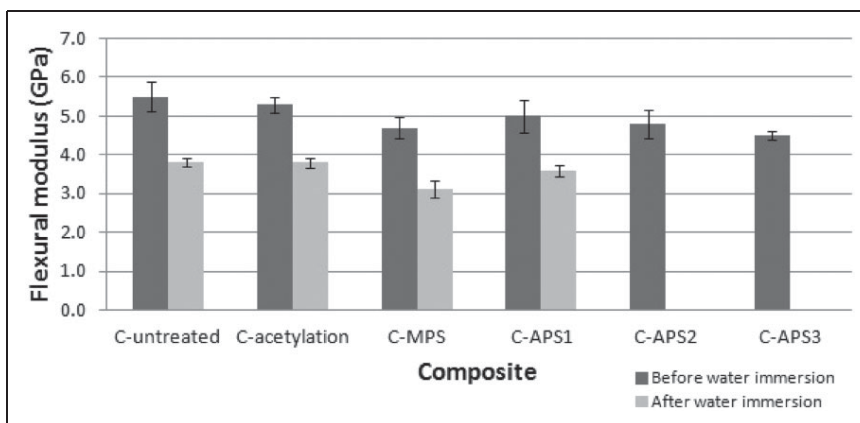


Figure 7. Flexural modulus of viscose composites.

Table 3. Tensile properties of viscose/unsaturated polyester composites.

Composite	Tensile strength (MPa)	Tensile modulus (GPa)	Elongation at break (%)
Neat unsaturated polyester	55	3.4	2.6
C-untreated	152.2 ± 5.2	4.9 ± 1.8	9.6 ± 0.5
C-acetylation	148.9 ± 7.3	4.8 ± 1.9	10.1 ± 0.4
C-MPS	98.9 ± 6.4	4.2 ± 1.8	13.1 ± 1.1
C-APS1	114.1 ± 2.5	3.7 ± 1.1	10.0 ± 0.4

untreated fabric composites (114.1 MPa). It is seen from the results that all silane treatments have reduced the tensile strength, while acetylation does not seem to make any improvement in the tensile strength of composites. A similar trend is also seen in the results of tensile modulus. Untreated fabric composite (C-untreated) and acetylated fabric composites (C-acetylation) exhibit the highest values, 4.9 and 4.8 GPa, which are very close to each other. However, APS 95-5 treated fabric composite (C-APS1) exhibits the lowest tensile modulus, 3.7 GPa. Standard deviation is high in each case. There was an obvious yield point in the stress-strain curves of viscose composites, which indicates the tough nature of the composites. Elongations at break are also presented in Table 3. All the composites show similar values, except the MPS treated fabric composites (C-MPS), which exhibits improved elongation at break.

The tensile properties of the composites largely depend on the properties of the reinforcement fibre. The tensile strength of single lignocellulosic fibre has been reported to be reduced after treatment with amino functional silanes and after acetylation.³⁶ In the chemical modification of cellulose, the reaction takes place at amorphous region or at the edge of crystalline region. Since the reagent is not able to diffuse into the crystalline region, it reacts with the chain ends close to the surface of crystallites resulting in opening up of some of the hydrogen bonded cellulose chains and consequently new amorphous domains are formed from the crystalline region.³⁷ The decrease in crystallinity will reduce the fibre tensile properties.³⁶ As already mentioned, the degree of crystallinity for viscose fibre is in range of 27–41%. It could be then assumed that the formation of additional amorphous domains through the chemical treatment of viscose fabric will reduce the tensile properties of the viscose yarn. Since the tensile properties of composite were studied in the direction of inlaid viscose yarn, the inferior tensile properties of yarn might be a reason for decrease in tensile properties of composite except for elongation at break. The elongation at break for the inlaid viscose yarn (Cordenka CR[®]) is reported to be

much higher than for the lignocellulosic fibre.⁶ The reinforcing effect of the viscose yarn is seen from the value for elongation at break from all the studied composites. It should be noticed that tensile properties for the untreated viscose yarns or for warp-knitted fabrics were not studied in this investigation. Another factor which might have influenced the results is the machining of the tensile specimen. The number of viscose yarns in the narrow test region varied from 6 to 7 in each layer of fabric through the length in test direction because the inlaid yarns were not aligned straight. Moreover, four layers of warp-knitted fabrics were not stitched together, and the viscose yarn was not held tightly enough by the polyester yarn.

Charpy impact test

Notched Charpy impact strength of viscose composites are shown in Figure 8. All the composites reinforced with APS silane-treated fabric shows a significant increase in the notched impact strength value. Impact strength of C-APS1 composite is 143.3 kJ/m², while impact strength of untreated composite is 67.6 kJ/m². There is an increase of 53%, 44% and 49% in impact strength of C-APS1, C-APS2 and C-APS3 composites, respectively, when compared to untreated composites. An improvement of 14% is seen for C-MPS fabric composites against C-untreated composites. However, acetylated and untreated composites have almost similar impact strength values.

The regenerated cellulose fibres are proved to be very tough materials, which are shown as high work to fracture and as a high failure strain. The impact strength is clear advantage when using viscose fabric reinforcements, and viscose is highly recommended to use, when great fracture toughness is needed in a composite product.³⁸ These results also indicate a good interaction between the chemically modified viscose fibres and the unsaturated polyester resin which improves the impact strength of the composites significantly. It could be assumed that APS silane is a good surface modifier for viscose fibre and thereby can be utilized as reinforcement in polymer composites including

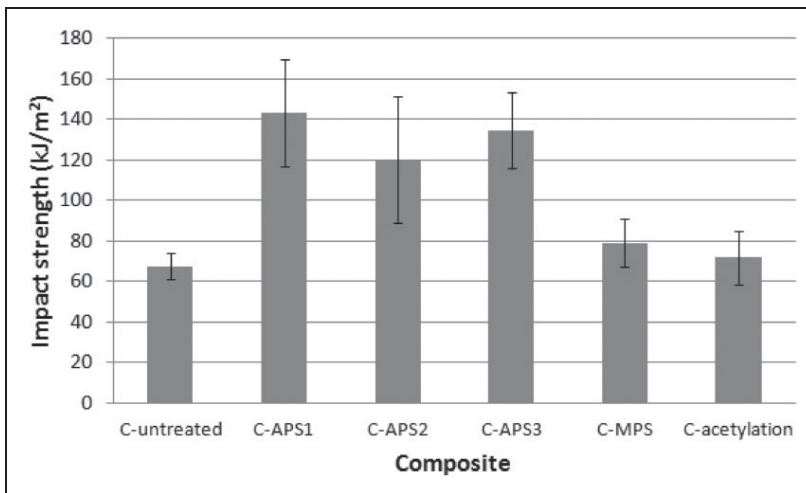


Figure 8. Charpy impact strength of viscose composite specimens.

unsaturated polyester matrix. In general, the knitted structure of fabric used in this study is thought to exhibit improved mechanical properties of composites owing to the uniaxially inlaid yarns in the fabric.³⁹ The fracture toughness of knitted fabric composites is also reported to increase with the number of layers used in the composite in contrast to composites with one layer of fabric.⁴⁰ Thus, both the structure of the reinforcement and the APS silane treatment have favoured the production of composites with increased impact resistance.

Gravimetric water absorption

The composite test specimens were kept immersed in water for 2448 h (102 days). During that time, the weight of the test specimens was taken at particular interval of time. The test was stopped at the saturation point, at which the weight of the specimens reached equilibrium through water absorption.

The mass gain for the composites as a function of water exposure time in hours is illustrated in Figure 9. Water absorption showed a sharp increase at the beginning of the test and attained equilibrium after three months. All the tested specimens reached the water absorption equilibrium point during the testing period. C-untreated and C-acetylated fabric composites show similar water absorption behaviour, with a pretty fast absorption during the first eight days. Water absorption of C-APS1 composite is obviously slower and is not showing a sharp mass gain at the beginning of the test as the other composites did. The total mass gain at the end of the test was the lowest in C-APS1 composite with water absorption of 7.44%. C-MPS

composite has the highest water absorption of 9.7%. The improvement in water resistance of C-APS1 composite may be related to the effective modification of viscose fabric with APS silane. The APS 95-5 treatment, in which APS was dissolved in a (95:5) ethanol/water solution might have modified not only the surface of yarns but also may have penetrated into the yarn filaments, therefore making the fabric more resistive against the water uptake. Bending of the test specimens was visible for all the composites except C-APS1. It is considered that higher the water absorption, higher is the chance of structural deformation of the specimen. The results obtained from water absorption studies point out the formation of good interaction between the unsaturated polyester resin and the APS silane-modified viscose fabric.

Blister formation on gelcoat and topcoat viscose fabric/Unsaturated polyester composites

Accelerated water absorption test was carried out for composites coated with gelcoat and topcoat to study blister formation on the composite surface. The thickness of the gelcoat layer was 0.5 mm. Figure 10(a) and (b) represents photographs of gelcoat surface on the viscose composite specimens before (a) and after (b) test. No blisters were observed on the gelcoat surface after four-week immersion in water at 65°C. However, a noticeable observation is the patterns of viscose fabrics, which are visible on the gelcoat surface after the test period. This is probably due to the very thin gelcoat layer. There were no remarkable changes on the topcoat surface; however, large number of cracks on the edges of the specimen which was covered with topcoat

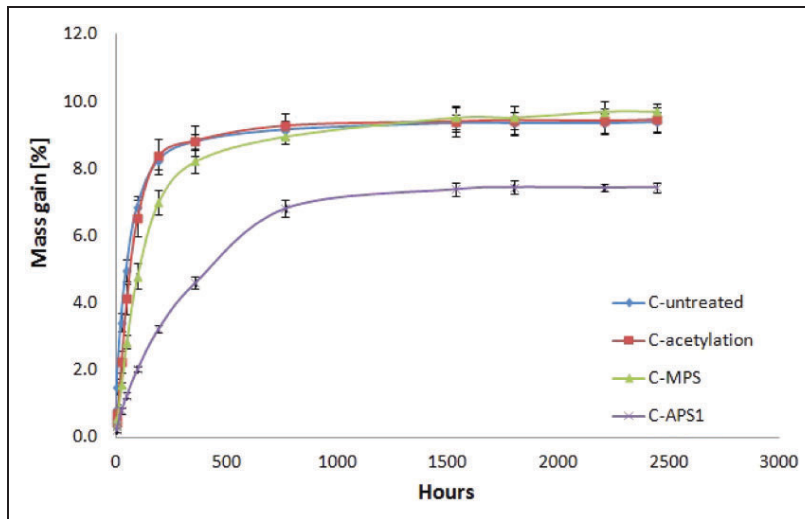


Figure 9. Mass gain (%) of viscose composite specimens as a function of time after 2448 h (102 days).

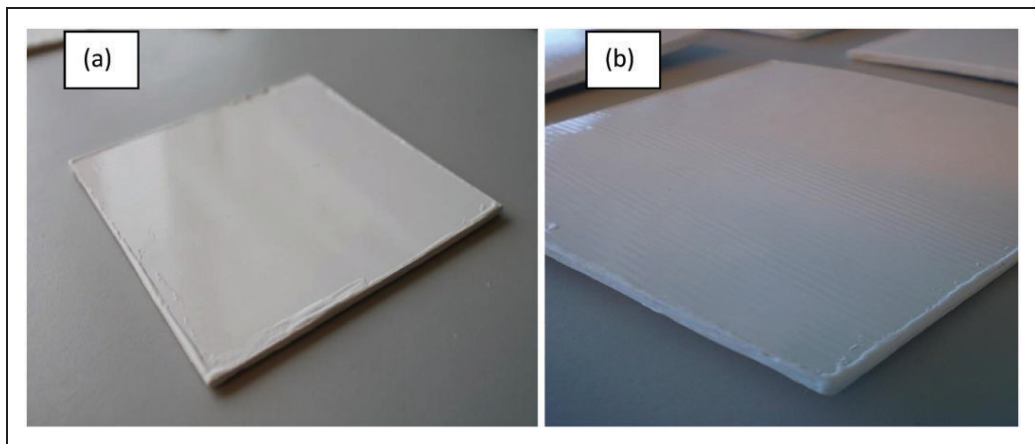


Figure 10. Digital photograph of gel-coat surface (a) before test and (b) with pattern of viscose fabric visible after test.

were visible. This could have influenced on the water absorption.

Landowski et al.⁴¹ have studied the effect of the different thicknesses of the gelcoat on the blister formation. In the study, it was reported that the number of blister was the same regardless of gelcoat layer thickness. They have also concluded that the use of 1 or 1.5 mm thickness for the gelcoat could provide a better protection for the laminate against water absorption, even though blistering rate remains same.

The mass gain of viscose composite immersed in water at 65°C for four weeks is presented in Figure 11. It is observed that the mass gain of composites

with gelcoat is much lower compared to the gravimetric water absorption test of treated and untreated composites discussed in preceding section, even though the testing conditions are different (discussed in 'gravimetric water absorption' section). The untreated fabric composite (C-untreated) without gelcoat and topcoat attained 5% water absorption after two days of water absorption at ambient conditions. Although the untreated fabric composite with gelcoat and topcoat took four weeks to attain same level of water absorption and in latter case, it is worth to note that test was done at accelerated conditions. It can therefore be assumed that gelcoat and topcoat have provided a

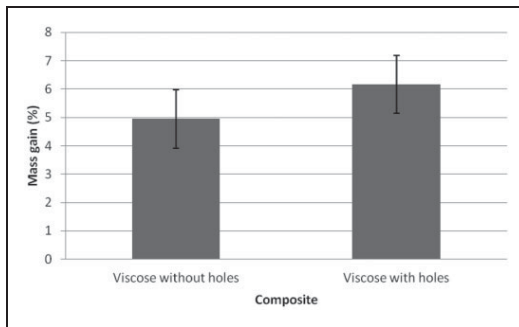


Figure 11. Mass gain (%) of the gel-coated specimens after four-week accelerated water test.

rather good protection against water uptake through the laminate surface. As expected, the mass increase was the lowest in the viscose composite specimens without any drilled holes. The water absorption in these composites might have been initiated through the edges on which topcoat was applied. One explanation for this is the formation of cracks on the edges of the specimen during the test period, which could have provided fast water absorption through the edges. Thicker gelcoat layer could have provided a better protection against water absorption. This was also studied by Landowski et al.⁴¹ According to their studies, water uptake in specimens with the thicker gelcoat layer was less than the specimens with a gelcoat layer of 0.5 mm.

Conclusions

Chemically modified unidirectional warp-knitted viscose fabrics and unsaturated polyester resin composites were successfully prepared through vacuum infusion method. Silane and acetylation treatment of the viscose fabrics has resulted in a significant improvement in mechanical properties, such as the flexural and impact strengths, and also improved the water resistance properties of unsaturated polyester composites. From these results, it could be concluded that the amino functional silane, APS is suitable for modifying the viscose fibre. This study also points out the influence of higher concentration of ethanol in the reaction media for modification with the trialkoxysilanes containing ethoxy groups. It is worth to note that the regenerated cellulose fibre has a clean surface with many reactive sites for an effective modification compared to lignocellulosic fibre. The reduction in water absorption of APS 95-5 treated composite was more efficient than for other chemically treated fabric composites. The gelcoat surface of the composite contained no blister formation and also the use of gelcoat and topcoat reduced the water uptake as was seen from accelerated water absorption test. It could be concluded that chemical treatment of

regenerated fibres could result in improvement in properties of composites, considering that the appropriate treatment method is selected for the corresponding fibre–matrix system.

Funding

This work is supported by EU Interreg IVA North program (304-11500-12), The County Administrative Board of Norrbotten, Sweden and Regional Council of Lapland, Finland, for the project ANACOMPO.

Conflict of Interest

None declared.

References

1. Bos LH, Mussig J and van den Oever MJA. Mechanical properties of short-flax-fibre reinforced compounds. *Compos Part A* 2006; 37: 1591–1604.
2. Herrera-Franco PJ and Valadez-González A. A study of mechanical properties of short natural-fibre reinforced composites. *Compos Part B* 2005; 36: 597–608.
3. Kaddami H, Dufresne A, Khelifi B, et al. Short palm tree fibres – thermoset matrices composites. *Compos Part A* 2006; 37: 1413–1422.
4. Wambua P, Ivens J and Verpoest I. Natural fibres: can they replace glass in fibre reinforced plastics? *Compos Sci Technol* 2003; 63: 1259–1264.
5. Lenz J, Shurz J and Eichinger D. Properties and structure of lyocell and viscose-type fibers in the swollen state. *Lezinger Berichte* 1994; 9: 19–25.
6. Mader A, Volkmann E, Einsiedel R, et al. Impact and flexural properties of unidirectional man-made cellulose reinforced thermoset composites. *J Biobased Mater Bioenergy* 2012; 6: 481–492.
7. Zugenmaier P. Crystalline cellulose and cellulose derivatives – characterization and structures. In: Timell TE and Wimmer R (eds) *Springer series in wood science*. Germany: Springer, 2008, chapter 7, pp. 207–220.
8. Colom X and Carrillo F. Crystallinity changes in lyocell and viscose-type fibres by caustic treatment. *Eur Polym J* 2002; 38: 2225–2230.
9. Andersson M and Tillman A-N. Acetylation of jute: effects on strength, rot resistance and hydrophobicity. *J Appl Polym Sci* 1989; 37: 3437–3447.
10. Ebrahimzadeh PR. *Dynamic mechanical studies of wood, paper and some polymers subjected to humidity changes*. PhD thesis, Chalmers University of Technology, Sweden, 1997.
11. Sreekala MS, Kumaran MG, Joseph S, et al. Oil palm fibre reinforced phenol formaldehyde composites: influence of fibre surface modifications on the mechanical performance. *Appl Compos Mater* 2000; 7: 295–329.
12. Sreekala MS, Kumaran MG and Thomas S. Water sorption in oil palm fibre reinforced phenol formaldehyde composites. *Compos Part A* 2002; 33: 763–777.
13. Xie Y, Hill CAS, Xiao Z, et al. Silane coupling agents used for natural fibre/polymer composites: a review. *Compos Part A* 2010; 41: 806–819.

14. Van de Weyenberg I, Ivens J, De Coster A, et al. Influence of processing and chemical treatment of flax fibres on their composites. *Compos Sci Technol* 2003; 63: 1241–1246.
15. Li X, Tabil LG and Panigrahi S. Chemical treatments of natural fibre for use in natural fibre-reinforced composites: a review. *J Polym Environ* 2007; 15: 25–33.
16. Goren A and Atas C. Manufacturing of polymer matrix composites using vacuum assisted resin infusion molding. *Arch Mater Sci Eng* 2008; 34: 117–120.
17. Khattab A. *Exploratory development of VARIM process for manufacturing high temperature polymer matrix composites*. PhD Thesis, University of Missouri, 2005.
18. Graupner N, Herrmann SA and Mussig J. Natural and man-made cellulose fibre-reinforced poly(lactic acid) (PLA) composites. *Compos Part A* 2009; 40: 810–821.
19. Bax B and Mussig J. Impact and tensile properties of PLA/Cordenka and PLA/flax composites. *Compos Sci Technol* 2008; 68: 1601–1607.
20. Ganster J, Fink H-P and Pinnow M. High-tenacity man-made cellulose fibre reinforced thermoplastics – injection moulding compounds with polypropylene and alternative matrices. *Compos Part A* 2006; 37: 1796–1804.
21. Carrillo F, Colom X and Canavate X. Properties of regenerated cellulose lyocell fibre-reinforced composites. *J Reinf Plast Compos* 2010; 29: 359–371.
22. Meredith J, Coles RS, Powe R, et al. On the static and dynamic properties of flax and Cordenka epoxy composites. *Compos Sci Technol* 2013; 80: 31–38.
23. Lehtiniemi P, Dufva K, Berg T, et al. Natural fibre-based reinforcements in epoxy composites processed by filament winding. *J Reinf Plast Compos* 2011; 30: 1947–1955.
24. Ramamoorthy SK, Kundu CK, Adekunle K, et al. Properties of green composites with regenerated cellulose fibre and soybean-based thermoset for technical applications. *J Reinf Plast Compos* 2014; 33: 193–201.
25. Rojo E, Alonso MV, Dominguez JC, et al. Alkali treatment of viscose cellulosic fibres from eucalyptus wood: structural, morphological, and thermal analysis. *J Appl Polym Sci* 2013; 130: 2198–2204.
26. Kushwaha PK and Kumar R. Effect of silanes on mechanical properties of bamboo fibre-epoxy composites. *J Reinf Plast Compos* 2010; 29: 718–724.
27. Sever K, Sarikanat M, Seki Y, et al. The mechanical properties of γ -methacryloxypropyltrimethoxy silane-treated jute/polyester composites. *J Compos Mater* 2010; 44: 1913–1924.
28. Rowell RM. A simplified procedure for the acetylation of hardwood and softwood flakes for flakeboard production. *J Wood Chem Technol* 1986; 6: 427–448.
29. Hill ASC, Abdul Khalil HPS and Hale MD. A study of the potential of acetylation to improve the properties of plant fibres. *Ind Crop Prod* 1998; 8: 53–63.
30. Tesoro GC, Ferry D, Lee WK, et al. Polyolefins of improved dye affinity modified with unsaturated polyester resin. Patent 3317633, USA, 1967.
31. Simons JK. Reaction products of polyesters and primary amine. Patent 2969335, USA, 1961.
32. Abdelmouleh M, Boufi S, Belgacem MN, et al. Modification of cellulose fibers with functionalized silanes: effect of the fiber treatment on the mechanical performances of cellulose–thermoset composites. *J Appl Polym Sci* 2005; 98: 974–984.
33. Uma Devi L, Bhagawan SS and Thomas S. Mechanical properties of pineapple leaf fiber-reinforced polyester composites. *J Appl Polym Sci* 1997; 64: 1739–1748.
34. Park R and Jang J. Effect of surface treatment on the mechanical properties of glass fibre/vinylester composites. *J Appl Polym Sci* 2004; 91: 3730–3736.
35. Hanada H, Fujihara K and Harada A. The influence of sizing conditions on bending properties of continuous glass fibre reinforced polypropylene composites. *Compos Part A* 2000; 31: 979–990.
36. Swapan MA, Pickering KL and Fernyhough A. Effect of various chemical treatments on the fibre structure and tensile properties of industrial hemp fibres. *Compos Part A* 2011; 42: 888–895.
37. Cantero G, Arbelaiz A, Llano-Ponte R, et al. Effects of fibre treatment on wettability and mechanical behaviour of flax/polypropylene composites. *Compos Sci Technol* 2003; 63: 1247–1254.
38. Adusumali R-B, Reifferscheid M, Weber H, et al. Mechanical properties of regenerated cellulose fibres for composites. *Macromol Symp* 2006; 244: 119–125.
39. Leong KH, Ramakrishna S, Huang ZM, et al. The potential of knitting for engineering composites – a review. *Compos Part A* 2000; 31: 197–220.
40. Karger-Kocsis J, Czigan T and Mayer J. Fracture behaviour and damage growth in knitted carbon fibre fabric reinforced polyethylmethacrylate. *Plast Rubber Compos Process Appl* 1996; 25: 109.
41. Landowski M, Budzik M and Imielińska K. Water sorption and blistering of GFRP laminates with varying structures. *Adv Mater Sci* 2013; 12: 23–29.

PUBLICATION II

Modification of epoxy resin by silane-coupling agent to improve tensile properties of viscose fabric composites

Rathish Rajan, Egidija Rainosalo, Selvin Thomas P, Sunil Kumar Ramamoorthy,
Janez Zavasnik, Jyrki Vuorinen, Mikael Skrifvars

Polymer Bulletin (2018) 75, 167–195

<https://doi.org/10.1007/s00289-017-2022-2>

Publication reprinted with the permission of the copyright holders.

Modification of epoxy resin by silane-coupling agent to improve tensile properties of viscose fabric composites

Rathish Rajan^{1,2,3} · Egidija Rainosalo³ ·
Selvin P. Thomas⁴ · Sunil Kumar Ramamoorthy^{5,6} ·
Janez Zavašnik⁷ · Jyrki Vuorinen¹ · Mikael Skrifvars⁵

Received: 19 October 2016/Revised: 23 March 2017/Accepted: 11 April 2017
© Springer-Verlag Berlin Heidelberg 2017

Abstract The modification of epoxy resin by 3-aminopropyltriethoxysilane (APTES) to improve the tensile properties of warp knitted viscose fabric composites is reported in this study. The study evaluates the efficiency of modification methods adopted to modify the epoxy resin and the influence of the resin modification on various properties of the cured castings. The influence of matrix resin modification on the tensile properties of viscose fabric composite is compared to those prepared from chemically modified fibre. The efficiency of the modification was determined through titration method to determine the epoxide content of epoxy resin, viscosity measurement and FTIR. The effect of APTES modification on various properties of cured castings is studied through differential scanning calorimeter, contact angle measurement and tensile testing. The addition of APTES into the epoxy resin decreased the epoxide content in the resin as evident from the titration method. The tensile strength of cured castings decreased after the resin modification. The tensile

Electronic supplementary material The online version of this article (doi:10.1007/s00289-017-2022-2) contains supplementary material, which is available to authorized users.

✉ Mikael Skrifvars
mikael.skrifvars@hb.se

¹ Department of Materials Science, Tampere University of Technology, 33101 Tampere, Finland

² Technology Centre KETEK, 67100 Kokkola, Finland

³ Centria University of Applied Sciences, 67100 Kokkola, Finland

⁴ Chemical Engineering Technology Department and Advanced Materials Laboratory, Yanbu Research Center, Royal Commission Yanbu Colleges and Institutes, Yanbu Alsinaiah 41612, Kingdom of Saudi Arabia

⁵ Swedish Centre for Resource Recovery, University of Borås, 50190 Borås, Sweden

⁶ Swerea IVF AB, Box 104, 431 22 Mölndal, Sweden

⁷ Centre for Electron Microscopy and Microanalysis, Jožef Stefan Institute, 1000 Ljubljana, Slovenia

strength and elongation at break of the viscose fabric composites prepared from modified resin, increased up to 14 and 41%, respectively. The improved adhesion of APTES-modified epoxy resin to the viscose fibre is confirmed from SEM analysis of tensile fracture surface.

Keywords Epoxy · Modification · APTES · Silane coupling agent · Viscose · Tensile · Composites · Regenerated cellulose

Introduction

The mechanical performance of a composite depends on the properties of the constituents and on the interfacial bonding between the fibre and the matrix. The fibre–matrix adhesion determines how much external stress can be transferred to the load bearing fibres [1]. Thus, the stress concentrations are reduced which result in the improvement of the overall mechanical properties of composites. The interfacial adhesion between a fibre and a matrix resin can be classified as chemical adhesion, physical adhesion, or mechanical adhesion [2]. The chemical adhesion proceeds through the formation of chemical bonds between fibre and matrix. The main approach for improving the chemical adhesion between fibre and matrix resin is the surface modification of fibre through wet chemical treatment methods such as alkali treatment, acetylation, coupling agent treatment or reactive gas treatment methods such as corona treatment and cold plasma treatment [3–7]. These surface treatment methods can improve the adhesion between the fibre and the matrix by bringing their surface energy to comparable values. In both cases, this is achieved by incorporating suitable functional groups and by changing the surface morphology by etching. Wide ranges of chemical modification methods to modify fibre to improve the physical properties of composites are discussed in literature [1, 8, 9].

Among various chemical methods available, silane coupling agent modification is a commonly utilised method to modify the glass fibre surface [10, 11] and lignocellulosic fibre surface [4, 12, 13]. Silane coupling agents have a general chemical structure of $R_{(4-n)}-Si-(R'X)_n$ ($n = 1, 2$), where R is alkoxy (ethoxy, methoxy), X is any organofunctional group such as amino, methacryl, epoxy, or vinyl and R' is the alkyl bridge connecting the silicon atom and the organofunctional group [5, 12]. Trialkoxysilanes are the type of organo-functional silanes commonly used in the surface modification of lignocellulosic fibres [12]. The alkoxy group in the silane can form a chemical bond with the lignocellulosic fibre surface. The completion of coupling reaction of the silane grafted on the fibre surface depends on the reactivity between the organo-functionality of silane and the matrix resin. There are several studies which report the lignocellulosic fibre surface modification with silane coupling agent [14, 15]. These studies reported that the fibre modification with silanes had resulted in the improvement of various physical properties of the thermoplastic and thermoset composites.

The present study differs from the practice of prior art in a way that the silane coupling agent is not used as a fibre surface modifier. Instead, it is directly mixed in the thermoset resin to prepare an alkoxy silane containing thermoset resin. From the

composite processing point of view, this is a benefit, as resin modification can be done much easier compared to a surface treatment of a reinforcement. It is well understood from the literature that the chemical surface modification deteriorates the strength of natural fibres [16–18]. Direct mixing of silane coupling agent with epoxy resin and using it in composite preparation is assumed to be eco-friendly and energy efficient. The direct mixing of silane coupling agent with resin and using the modified resin in composite preparation creates less process waste compared to the fibre modification method. The alkali solution or silane solution used to modify the fibre requires waste treatment, which includes additional cost and consumes more energy. Through the matrix resin modification, reactive sites are introduced in the backbone of matrix resin with a higher chemical affinity towards the hydrophilic cellulosic fibre surface without deteriorating the strength of the cellulosic fibre. The organic functionalities such as amino, methacrylate, epoxy, or vinyl groups present in the silane, are capable of forming chemical bonds with compatible reactive moieties in the matrix resin, while the hydrolysable alkoxy groups are capable of reacting with the fibre surface. Thus, it is anticipated to have a good fibre–matrix adhesion through the modification of thermoset resins by silane coupling agents.

Several approaches to modify epoxy resins have been reported in the literature [19–22]. Most of those studies are focused on improving the toughness of the epoxy resin. To improve the crack resistance and prevent interlaminar failure, the epoxy resin has been toughened with elastomers, thermosets, thermoplastics, particulates or by other miscellaneous methods [19–24]. Epoxy resins have been modified by silane coupling agents to improve the corrosion resistance and the adhesion of epoxy coatings on the aluminium surface [25]. The water resistance of epoxy coatings on metal substrates has been improved through silanes [26]. The potential of silane coupling agents, polysiloxanes, silsesquioxanes, silica and silicates in modification of silane has been reported [27]. Most of the studies related to the silane modification of epoxy resin are in the area of coatings to improve the flexibility, adhesion and/or corrosion resistance. The modification of epoxy resin by silane for use as matrix resin in polymer composites are rarely found in literature. Epoxy resins have been modified with different types of silane coupling agents and the resulting mechanical properties of its composite with carbon fibre were studied by Yang et al. [28]. They reported that the matrix modification improved the tensile strength and flexural properties of carbon fibre composites by 4 and 44%, respectively. Kaynak et al. [29] modified epoxy resins by hydroxyl-terminated polybutadiene and reported improvement in mechanical properties, especially the toughness of the composites.

Modification agents, which are specifically used to improve a particular property, can adversely affect other important resin characteristics, which are relevant for composite manufacturing. Thus, studies on the effect of modification on various properties of silane coupling agent modified epoxy resin, cured castings and composites are of special interest. The studies on modification of epoxy resin by silane coupling agent for using it as the matrix resin in regenerated cellulose fibre reinforced composites are rarely reported. The main objective of this investigation was to modify an epoxy resin with an amino functional tri-alkoxysilane and to assess the effect of the modification on the various properties of the resin and cured

castings. In addition, the tensile properties of modified epoxy/viscose fabric composites are compared with the epoxy/modified viscose fabric to identify the best approach to improve fibre–matrix adhesion.

Experimental

Materials

Prime 20LV, an epoxy resin manufactured by Gurit Ltd was used for modification and composite preparation. An amine hardener (Prime 20LV slow) was used to cure the castings and composites. The main properties of the Prime 20LV resin as given by the manufacturer are listed in Table 1 [30]. The silane-coupling agent for epoxy resin modification was 3-aminopropyltriethoxysilane (APTES; 99% purity). All the chemicals used for the titration method to determine the epoxide content of the epoxy resin was of reagent grade and used as received. The fabric used as the reinforcement in the preparation of composites for the tensile test was based on Cordenka 610F viscose yarn with the twist Z40, 2440 dtex linear density and 1350 filaments (Cordenka, Germany). The yarn was processed by warp knitting into unidirectional fabrics with a surface weight of 223 g/m² (Engtex, Sweden).

Resin modification method

The epoxy resin modification was done by mixing the epoxy resin with 1, 3, and 5 wt% of APTES. No solvents or catalysts were used in the modification of resin. The modification was done for 1 h at room temperature and at 70 °C. Epoxy resin and the appropriate amount of silane were weighed into a plastic container equipped with a magnetic stirrer and were stirred for 1 h at room temperature. For the modifications done at 70 °C, the resin and an appropriate amount of silane were weighed into a round bottom flask equipped with a reflux condenser. Stirring was done for 1 h in a water bath maintained at a temperature of 70 °C (±3).

Table 1 Properties of epoxy resin and its cured castings according to the resin supplier

Properties of resin	Resin	Hardener
Mix ratio (by weight)	100	26
Viscosity at 25 °C (cP)	600–640	15–17
Density (g/cm ³)	1.123	0.936
<i>Properties of cured castings</i>		
<i>T_g</i> Ult (DMTA) (°C)	87–89	
HDT (°C)	68	
Tensile strength (MPa)	73	
Tensile modulus (GPa)	3.5	
Strain to failure (%)	3.5	
Cured density (g/cm ³)	1.144	

Viscose fabric modification method

The viscose fabric modification was done following the procedure explained in our previous study [5]. APTES was added to an ethanol/distilled water (95:5) solution to yield a 2 vol% silane concentration in solution. After 15 min, the fabrics were dipped in a plastic container containing the reaction solution for 5 min and then dried at room temperature. After 30 min, the fabrics were oven-dried at 110 °C for 30 min and cooled in a desiccator.

Preparation of cured castings

A metal mould with dimensions specified for dog-bone shaped tensile specimen according to the ISO 527-2 was placed on the polished glass plate and the edges were sealed with two-sided sticky tape. After proper mixing, the resin was poured into the metal mould. The castings were cured at 65 °C for 7 h and post-cured at 80 °C for 2 h. The epoxy resin was mixed with the hardener in 100:26 ratio (by weight).

Preparation of composites

Composites were prepared by vacuum assisted resin infusion method. The mould release agent was applied on a steel mould. The mould was then polished and used after another 30 min. Four layers of warp knitted unidirectional viscose fabric were carefully laid ($\pm 0/\pm 90/\pm 0/\pm 90$) (Fig. 1) one after another on the mould surface and finally the vacuum bagging was completed and the infusion was done. The infusion was done in a climate chamber at 65 °C and by applying a vacuum pressure of 0.1 bar. The composites were cured same way as in the case of cured castings and the same amount of hardener was used for curing the composites. The fibre weight percentage in the composites was 38–42%. The thickness of the composites was 2.2–2.4 mm. The details of the modification and designations of the modified resin, cured castings and composites are given in Table 2.

Fig. 1 Schematic representation of fabric lay-up in viscose fabric composite

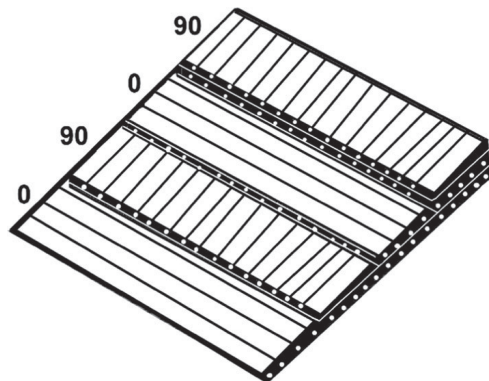


Table 2 Details of modification and designations of resins, castings, and composites

Modification		Designation		
Silane	Description	Resin	Cured castings	Composites
0 wt%	No modification	RS0	RS0-CC	RS0-C
1 wt%	Resin modified at room temperature	RS1-RT	RS1-RT-CC	NA
3 wt%	Resin modified at room temperature	RS3-RT	RS3-RT-CC	NA
5 wt%	Resin modified at room temperature	RS5-RT	RS5-RT-CC	NA
1 wt%	Resin modified at 70 °C	RS1-70	RS1-70-CC	RS1-70-C
3 wt%	Resin modified at 70 °C	RS3-70	RS3-70-CC	RS3-70-C
5 wt%	Resin modified at 70 °C	RS5-70	RS5-70-CC	RS5-70-C
2 vol%	Fabric treated at room temperature and dried at 110 °C	NA	NA	RS0-FS2-C

Characterization

Epoxide content of epoxy resin

The epoxide content of the epoxy resin was determined according to manual titration method described in ASTM D1652-11. The resin was dissolved in methylene chloride and then titrated with standard perchloric acid in the presence of an excess of tetraethylammonium bromide. The hydrogen bromide generated in situ by the reaction of the perchloric acid with the quaternary ammonium halide rapidly opens the epoxide ring. Therefore, the quantity of perchloric acid consumed can be taken as a measure of epoxy content. The sample was titrated with a perchloric acid reagent to a sharp blue to green end point which was stable for approximately 30 s. The volume of perchloric acid consumed during titration was recorded. The weight percent epoxide and epoxy equivalent weight were calculated according to Eqs. (1) and (2), respectively.

$$E = 4.3 \times V \times N/W \quad (1)$$

$$W_{\text{EEW}} = 43 \times 100/E \quad (2)$$

where, E and W_{EEW} are weight percent epoxide and epoxy equivalent weight, respectively. V is the volume of perchloric acid reagent used to titrate the sample (ml), N is normality of perchloric acid reagent, the constant 4.3 is the theoretical molecular weight of the epoxide ring 43, adjusted to 4.3 for the calculation to percent epoxide; and W is the weight of the epoxy resin used (g). The value reported is average of two measurements.

Viscosity measurements

The viscosity of unmodified RS0 and silane modified epoxy resins was measured using an Anton Paar MCR 301 rheometer at a constant shear rate of 10 s^{-1} from 25

to 65 °C. The measurements were done with a 25 mm plate–plate measuring system at a gap distance of 1 mm. The values reported are average of two measurements.

Contact angle measurements

The contact angle of the surface of the castings was measured to determine the wettability of the cured epoxy resin after silane modification. The measurements were done using a contact angle measurement instrument, OCA20 from Dataphysics GmbH. The static contact angle of ultra pure water on cured epoxy was measured at room temperature by a sessile drop method. The contact angle value was taken 10 s after depositing the drop on the epoxy surface. The results are reported as the average of five measurements with corresponding standard deviation.

FTIR spectroscopy

ATR-FTIR spectroscopy was used to characterise the APTES silane modification of the epoxy resin and to characterise the surface of modified cured epoxy castings and composites. The spectra from resins and cured casting surface were recorded on an ATR PerkinElmer-Spectrum One spectrometer. Signals of eight scans at a resolution of 4 cm⁻¹ were averaged before Fourier transformation. The spectrum was recorded over the range 4000–650 cm⁻¹. The spectra from the surface of epoxy/viscose fabric composites were recorded on Bruker Optics-Tensor 27, spectrometer equipped with diamond ATR accessory. Signals of 32 scans at a resolution of 4 cm⁻¹ were averaged over the range 4000–400 cm⁻¹.

Differential scanning calorimetry (DSC)

The glass transition temperature from the cured castings was determined using a Netzsch 204 DSC. The samples were first heated from 25 to 250 °C at a rate of 10 °C/min and then cooled. The second heating was run from 25 to 250 °C at a rate of 10 °C/min. Heating of cured epoxy resin samples to remove any prior thermal history and then cooling before second heat cycle was reported elsewhere [31]. The sample size was 10–11 mg and test was conducted in a nitrogen atmosphere. The glass transition temperature from the second heating scan of the cured castings is reported.

Tensile properties of modified cured castings

The tensile testing of the modified cured castings was conducted according to ISO 527-2:2012 using a Tiratest 2705 tensile testing machine equipped with a 5 kN load cell. The cured casting specimen dimensions were 80 mm of the length of the narrow portion, 10 mm of the average width of narrow portion and 4 mm of an average thickness. The gauge length was 50 mm and overall length of the specimen was 150 mm. The testing was carried out at ambient temperature with a testing speed of 2 mm/min. The tensile properties are calculated as the average of five specimens.

Tensile properties of composites

Tensile tests for composites were carried out using Tinius Olsen H10KT universal testing machine. The load cell was 10 kN and test speed was 10 mm/min. Dumb-bell shaped specimens were tested and ISO 527-2:2012 standard was followed. Overall length was 150 mm with the parallel-sided portion of about 60 mm. The width at the parallel-sided portion was 10 mm. The gauge length was 50 mm. The tensile properties are calculated as an average of six specimens.

Scanning electron microscopy (SEM)

Samples for SEM observations were mounted perpendicular on Al-support base with conductive tape, allowing observing the fractured surface. The conductive amorphous carbon paint was used to make contacts with the upper surface; afterwards the samples were coated with few nano-meters thick layer of amorphous carbon (Balzers SCD 050 sputter coater) to achieve conductivity for electrons. The fractured surface was investigated with FE-SEM (Jeol JSM-7600F) at 5 keV using below-the-lens (LEI) secondary electrons detector (SE) to minimize charging on the fibers.

Results and discussion

Epoxide content of modified resin

The modification of epoxy resin by APTES silane was verified by epoxide content determination according to ASTM D1652-11. The results are shown in Fig. 2. The weight percent epoxide of RS0 resin, RS1-RT resin and RS1-70 resin was determined to be 23.4, 22.7, and 22.7%, respectively. Irrespective of modification temperatures, the epoxide content of resin after modification with 1 wt% APTES decreased slightly when compared with unmodified epoxy resin. Compared to RS0 resin, a decrease of 1.9 and 2.1% in the epoxide content of RS3-RT (21.5%) resin and RS3-70 (21.3%) resin, respectively, was recorded. The epoxide content in RS5-RT resin and RS5-70 resin was 20.8 and 20.4%, respectively. Compared to RS0 resin, there was a decrease of 2.6 and 3.4% in epoxide content of RS5-RT and RS5-70, respectively. Correspondingly, the epoxide equivalent weight (EEW) increased to 211 g/mol for RS5-70 from 184 g/mol for RS0. The decrease in epoxide content and an increase in epoxide equivalent weight after addition of APTES into epoxy resin confirms the grafting of APTES onto the epoxy resin. The reaction is assumed to proceed by a primary amine in APTES reacting with oxirane ring forming a secondary amine and a hydroxyl. The formed secondary amine will further react with another oxirane ring, resulting in the grafting of the silane as shown in Fig. 3 [26, 32]. Seraj et al. [33] modified epoxy resin by APTES to use in cathodic electro-

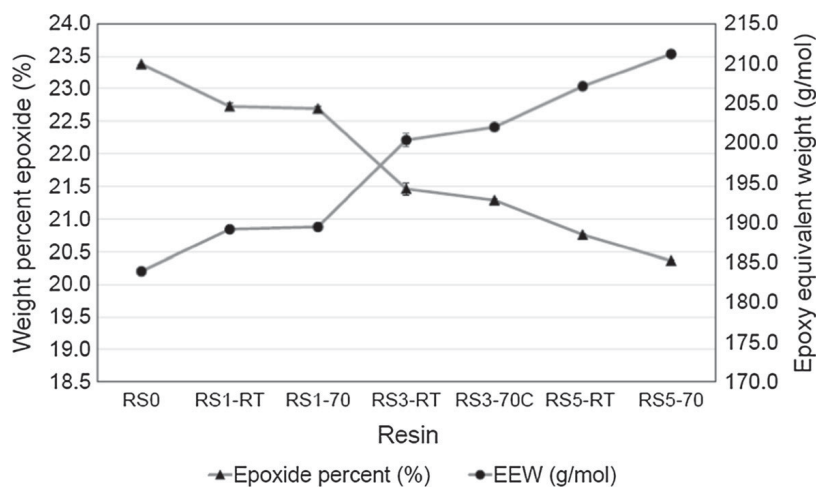


Fig. 2 Epoxide equivalent weight of EP unmodified and silane coupling agent modified epoxy resin

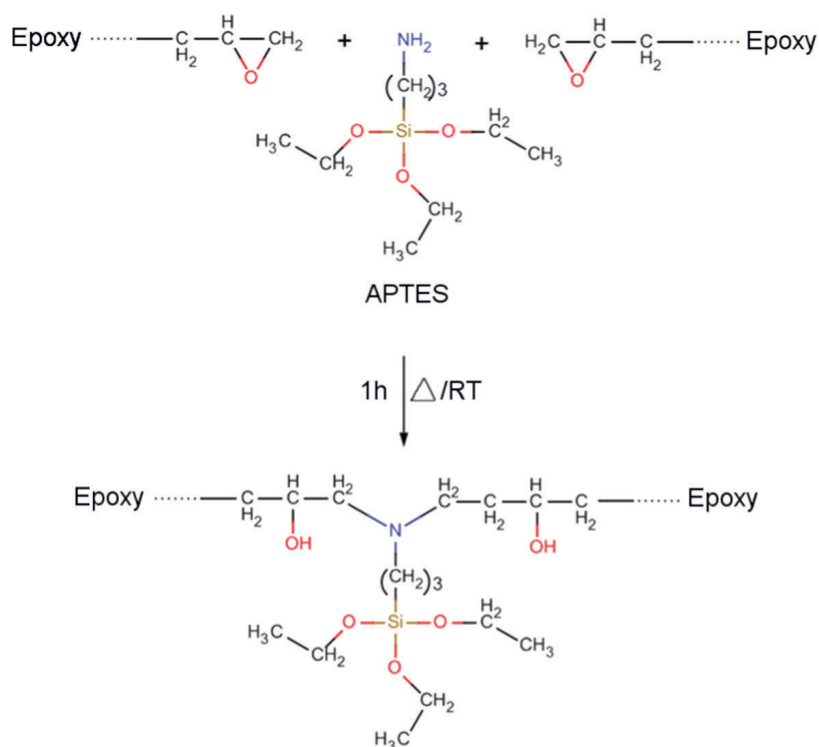


Fig. 3 Coupling reaction between 3-aminopropyltriethoxysilane and epoxide in epoxy resin

coating application. They also made a similar observation that the reaction of APTES with epoxide in resin increased the epoxide equivalent weight. It was also noticed that the reaction was more favoured at 70 °C compared to room temperature when the APTES content was 3 and 5 wt%.

Viscosity of modified resins

The viscosity of RS0 and modified epoxy resins exhibited a decreasing trend with an increase in temperature, as shown in Table 3. The viscosity of the epoxy resin increased with increase in silane content used in resin modification. At room temperature and at the processing temperature (65 °C) the viscosity of 5% APTES-modified epoxy resins was doubled when compared to the value for RS0 epoxy resin. During the cure reaction, viscosity of the thermoset resins will initially decrease due to thermal effects and then eventually increase with rise in the time or temperature due to the formation of cross-linked network [34]. Since the reaction between APTES and epoxide is similar to that of epoxy cure reaction with amine hardener, the increase in viscosity of APTES-modified epoxy resin is attributed to the coupling reaction occurred between silane-amine and epoxide of epoxy resin. The increase in viscosity of modified resin supplements the results obtained from the epoxide content determination test, that a reaction occurred between the epoxy resin and APTES.

FTIR analysis of resins, castings and composites

All the characteristic IR bands for epoxy resin are found in RS0 resin. The absorption bands at 1508 and 1608 cm^{-1} are assigned to the aromatic ring in epoxy resin. The absorption band corresponding to stretching of C–H of the epoxide ring is at 3057 cm^{-1} . The absorption band at 914 and 830 cm^{-1} is assigned to the C–O and C–O–C stretching of epoxide group [25, 35]. In epoxy resin, the broad band around 3500 cm^{-1} is assigned to O–H stretching of hydroxyl groups in epoxy resin [33, 36]. It was observed that in the case of RS5-70, the intensity of band at 3481 cm^{-1} corresponding to hydroxyl group increased compared to that of RS0. This indicates the formation of hydroxyl groups via epoxide reaction with silane-amine, as shown in Fig. 3. Similar observation was made by Seraj et al. in their study related to modification of epoxy resin by APTES [33]. A comparison of RS0 resin and RS5-70 resin spectra is shown in Fig. 4.

The spectra obtained for modified resins seem to be almost similar to RS0 resin with few variations. There is a new absorption band appearing at 1077 cm^{-1} for

Table 3 Effect of silane modification on the viscosity of epoxy resin

Modification	Viscosity (cP)	
	25 °C	65 °C
RS0	614	36
RS1-RT	704	38
RS1-70	716	61
RS3-RT	872	48
RS3-70	891	48
RS5-RT	1170	59
RS5-70	1185	61

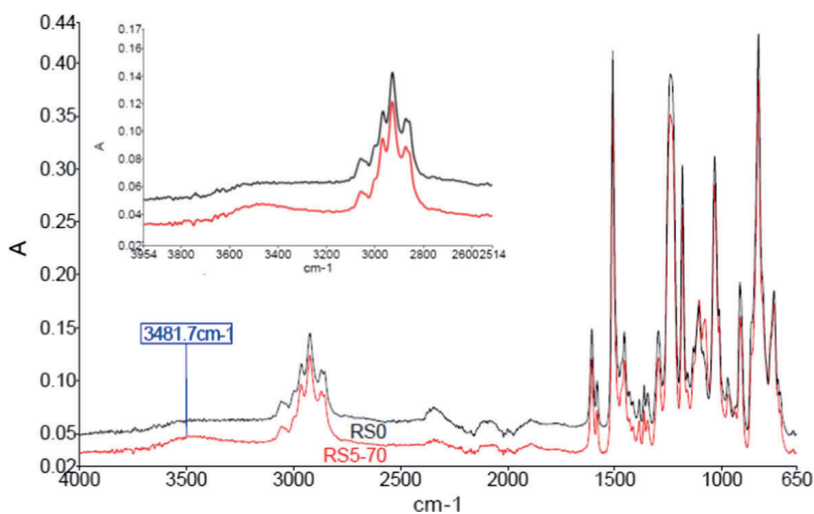


Fig. 4 FTIR spectra of RS0 and RS5-70 resins and inset in the region 3954–2514 cm^{-1}

resins modified with 5 wt% APTES. Some previous studies assign this band to Si–O–C linkage indicating that the ethoxy group in the APTES silane remains unreacted in the modified resin [37]. The absence of absorption band in the region 1040–1020 cm^{-1} and 990–945 cm^{-1} confirms that silanols (Si–OH) are not present in the modified resin. The absence of absorption band corresponding to siloxanes (Si–O–Si) in the region 1090–1010 cm^{-1} also confirms that the ethoxy group in modified epoxy resin is unreacted [35]. The absorption bands corresponding to the ethoxy and epoxide groups are shown in Fig. 5a. Generally, it is considered that the peak around 914 cm^{-1} for epoxy resin corresponds to the epoxide group in epoxy resin [25, 32]. It is seen from Fig. 5a that the intensity of the band at 914 cm^{-1} is decreasing in the case of RS5-RT resin and RS5-70 resin. However, compared to RS0 resin, no difference was noticed in the case of RS1-RT resin and RS1-70 resin.

The absorption bands which remain invariable in a reaction which corresponds to the linkages that do not take part in the cure reaction is used as a quantitative reference for analysing cure reaction of epoxy. This is because the absorption of these bands does not change during the reaction [38–41]. Dividing the area of the reactive band by the area of reference band corrects the variation in mass and thickness of the sample. The normalized area ratio can then be used to compare different spectra. In this study, the absorption band at 1508 cm^{-1} corresponding to the aromatic ring in the epoxy resin is used as a reference band. The peak area of 914 cm^{-1} corresponding to epoxide from all the spectrums were measured by keeping the baseline and integration region constant at 928–883 cm^{-1} . The area ratio of the absorption band of epoxide (914 cm^{-1}) to reference band (1508 cm^{-1}) and the area of absorption band at 914 cm^{-1} are shown in Table 4. The peak area corresponding to epoxide for RS1-RT and RS1-70 resins does not change compared to RS0 resin. However, peak area for RS5-RT and RS5-70 resins decreased considerably when compared to RS0 resin. The decrease in the area of the reactive band (914 cm^{-1}) and the decrease in the area ratio, especially for RS5-RT and RS5-

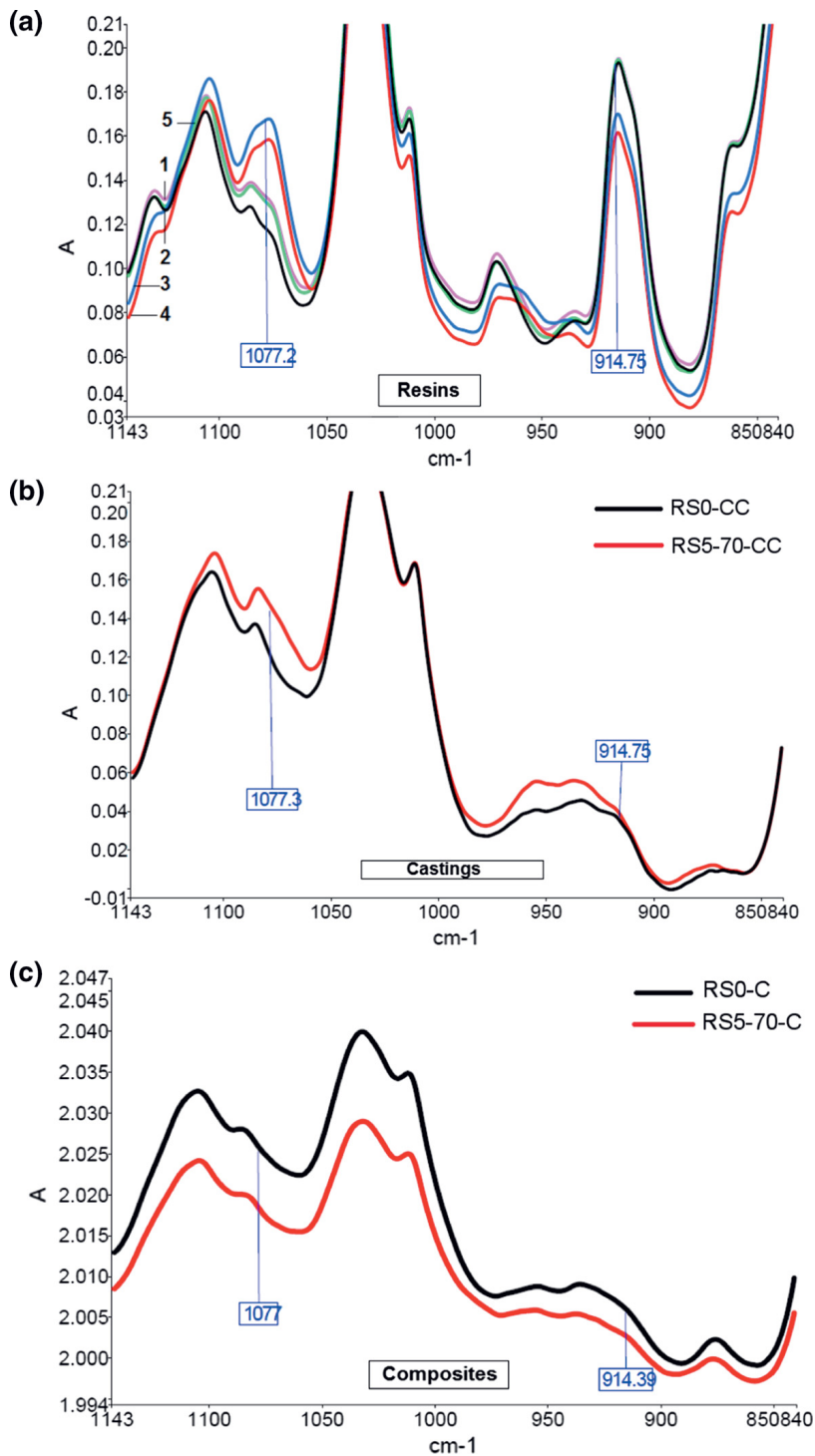


Fig. 5 FTIR spectra of epoxy resin, cured castings and composites in the region 1140–840 cm^{-1}
a resins—1: RS1-70, 2: RS0, 3: RS5-RT, 4: RS5-70, 5: RS1-RT **b** castings and **c** composites

Table 4 Peak area for resins at 914 cm^{-1} and area ratio of reactive band and reference band

Resin	Peak area	Area ratio (914 /1508 cm^{-1})
RS0	2.43	0.45
RS1-RT	2.40	0.44
RS1-70	2.38	0.45
RS5-RT	2.00	0.40
RS5-70	1.98	0.39

70 resins compared to RS0 resin confirm that the epoxide reacted with an amine in the APTES by resulting in a reduction of epoxide in the modified resins. The results from ATR-FTIR is supporting the results obtained from the epoxide content determination test.

Figure 5b, c compares the FTIR spectrum of castings and composites prepared from RS-0 and RS5-70 resins. The major difference in spectra of both castings and composites was in the region 1140–840 cm^{-1} . The disappearance of the absorption band at 1077 cm^{-1} in the case of RS5-70-CC castings and composites can be seen in Fig. 5b, c. This absorption band is assigned to the unreacted ethoxy group in modified resin (Fig. 5a). The tensile test results of composites which will be discussed later, shows significant improvement in tensile properties which indicate that the ethoxy group have undergone reaction with viscose fabric. Another notable difference seen from Fig. 5b, c is the disappearance of the absorption band at 914 cm^{-1} corresponding to the epoxide in epoxy resin. This indicates that both castings and composites prepared from the modified resin have achieved proper cure as similar in the case of those made from unmodified resin.

Glass transition temperature of cured castings

The glass transition temperature of cured castings is given in Fig. 6. The T_g is reported from the midpoint temperature of second heating scan. The ultimate T_g for the castings made from 3 and 5% APTES silane modified epoxy resin slightly decreased when compared to RS0-CC casting. The lowering of T_g after silane modification of epoxy resin has been explained based on the introduction of the flexible silane molecule into the resin structure [42]. According to epoxide titration, the epoxide content in epoxy resin decreased with increase in the APTES silane content. The epoxide content is relatively lower in the modified resins and therefore, less oxirane oxygen takes part in the crosslinking reaction with amine hardener during the curing of the resin. This has resulted in cured castings with low degree of crosslinking in the case of an epoxy resin modified with a higher concentration of APTES silane. The crosslink density is considered to be influencing the T_g of the thermoset resin. A cured system with lower crosslink density is supposed to have lower glass transition temperature [43]. Please refer to Figure S7 and S8 for DSC thermogram of unmodified and modified cured castings.

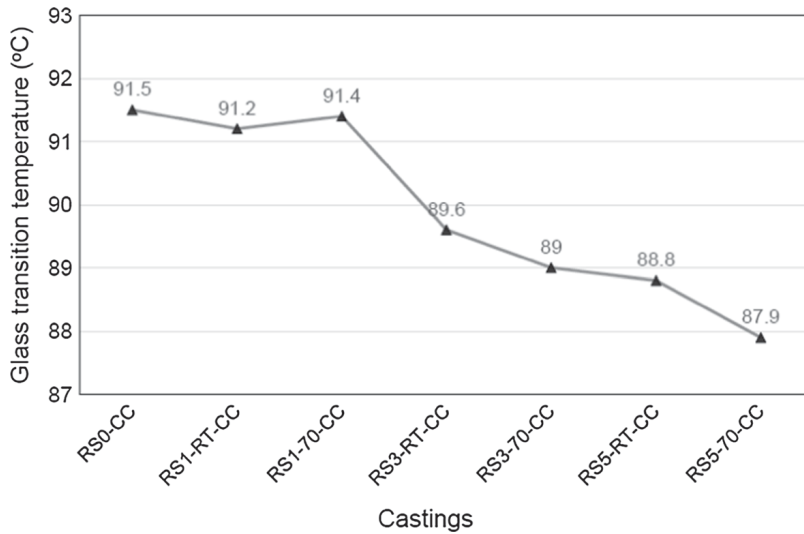


Fig. 6 Effect of APTES modification on the glass transition temperature of cured castings

Contact angle measurements of cured castings

The contact angle measurement of modified epoxy castings was done to determine the wetting properties of cured castings after modification. The contact angles obtained for the modified and RS0-CC epoxy casting surfaces are given in Fig. 7. The contact angle of water on silane modified cured castings seems to be increasing with the silane modification. The contact angle gives an indication of wettability of

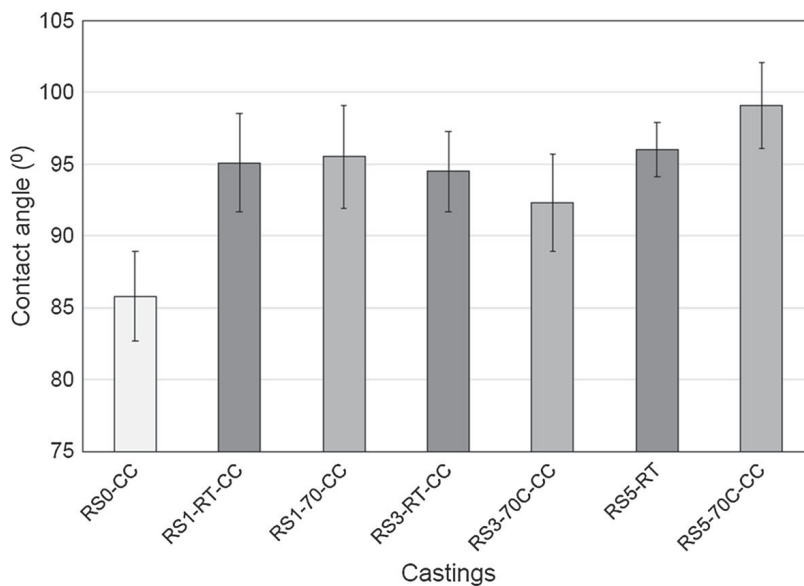


Fig. 7 Static water contact angle of modified and unmodified cured epoxy castings

the used liquid on a solid surface. Although epoxy resins have good physical properties, one of its main drawbacks comparing to other commonly used thermoset resin such as unsaturated polyester resins are its low resistivity against water. The water absorption of epoxy resin is related to the presence of hydroxyl groups formed in the ring opening reaction of the epoxide with the amine hardener [44]. A possible explanation for the hydrophobization by silane modification could be the migration of hydrophobic silicon to the surface of cured resin. Honaman et al. [45] modified epoxy coating with amino functional siloxanes and silanes including APTES. They found that the modified epoxy coating has poor recoatability. This phenomenon was explained based on the migration of silicon to the surface of amino functional silane modified bisphenol A epoxy coating. It is widely considered that the more hydrophobic a solid surface is the lower is its wettability. Considering these facts, it could be assumed that the APTES silane modification has increased the hydrophobicity of cured modified epoxy resin compared to the cured unmodified resin.

Tensile properties of cured epoxy castings

The tensile strength of cured castings is as shown in Fig. 8. The tensile strength of RS0-CC casting was determined to be 73 ± 2.6 MPa. The tensile strength of the castings prepared from room temperature modified resins decreased in an order of RS1-RT-CC (72 ± 0.5 MPa) > RS3-RT-CC (69 ± 2.1 MPa) > RS5-RT-CC (67 ± 1.6 MPa). There was no significant change observed in tensile strength of RS1-70-CC (70 ± 2.8 MPa) castings when compared to RS0-CC castings. However, the tensile strength decreased with further increase of APTES content for resins modified at 70 °C. The tensile strength recorded for RS3-70-CC and RS5-70-CC are 67 ± 1.0 and 62 ± 2.1 MPa, respectively. Irrespective of the modification

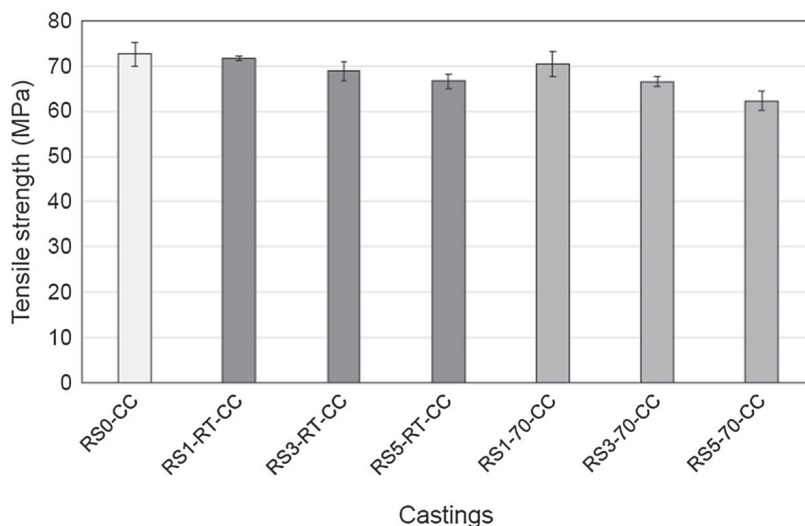


Fig. 8 Effect of APTES modification on the tensile strength of cured castings

temperatures, the tensile strength of modified castings decreased with an increase in APTES content. The effect of modification temperature on the tensile strength of castings was found to be influenced by the APTES content. The change in tensile strength among RS1-RT-CC and RS1-70-CC and RS3-RT-CC and RS3-70-CC was less significant considering the standard deviation in the results obtained. Whereas, compared to RS5-RT-CC, there is a small decrease in tensile strength of RS5-70-CC.

According to the epoxide content determination test, the epoxide content of epoxy resin decreased with an increase in APTES content, regardless of modification temperatures. For this reason, a relatively low amount of oxirane oxygen will take part in the crosslinking reaction with amine hardener in the case of modified cured castings. This will result in cured castings with lower crosslink density compared to casting prepared from RS0 resin. Crosslink density is a critical parameter governing the properties of the cured resins. Generally, thermoset resins with lower cross-link density are considered to have lower tensile strength [46]. The decrease in the tensile strength of cured castings with increasing APTES content is correlated with the decrease in epoxide content of resin with an increase in APTES content. Thus, it is deduced that lower tensile strength of modified cured castings is due to low cross-link density induced by the APTES grafting on the epoxy resin.

The elongation at break of the APTES-modified cured castings is shown in Fig. 9. The percentage of elongation at break of the RS0-CC castings was recorded to be 10.5 ± 1.7 . Compared to RS0-CC castings, there was no difference observed in the elongation at break of RS1-RT-CC (10.2 ± 1.2) castings. A small difference in the elongation at break of RS3-RT-CC ($9.4 \pm 2.0\%$), RS5-RT-CC ($9.8 \pm 1.9\%$), RS1-70-CC (9.9 ± 1.2), RS3-70-CC (9.9 ± 2.0) and RS5-70-CC (9.8 ± 2.0) castings compared to RS0-CC are negligible considering the standard deviation. There was no significant change observed for elongation when comparing RS1-RT-CC and RS1-70-CC; RS3-RT-CC and RS3-70-CC; and RS5-RT-CC and RS5-70-

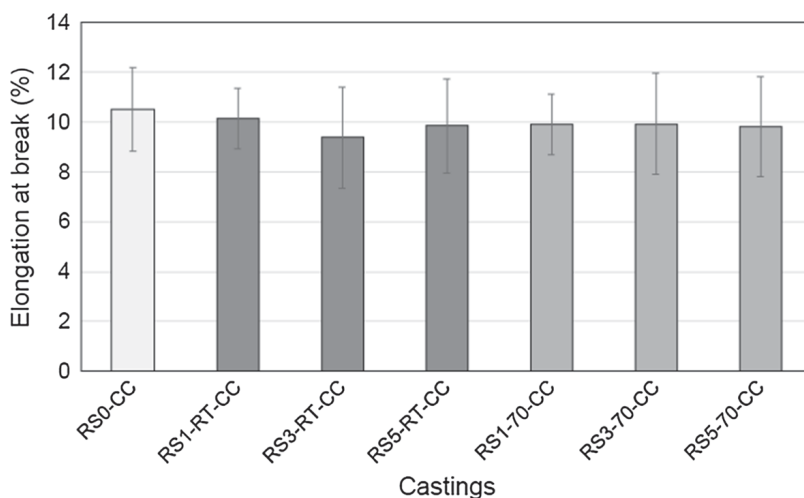


Fig. 9 Effect of APTES modification on elongation at break of cured castings

CC. This indicates that the elongational strength of cured castings was not affected by the content of APTES or the temperature used for modification. Honaman et al. [45] modified epoxy coatings by various silanes and siloxanes to improve the flexibility. They reported that epoxy coatings containing silanes does not improve the flexibility while the flexibility of epoxy coatings containing siloxanes improved. Heng et al. [21] synthesized an epoxy resin containing siloxane bridge and found that the elongation at break improved. The increase in elongation was explained based on the siloxane bond formation. Both studies point out that siloxane bond formation have an essential role in improving the elongation of the epoxy resin modified by organo-silicon compounds. In this study, the modified epoxy resin contains non-hydrolysed ethoxy group and hence siloxane bond formation is not favoured. Thus, the elongation of resin is not affected by the APTES modification.

Tensile properties of composites

The tensile strength of the epoxy/viscose fabric composites is shown in the Fig. 10. The tensile strength of composites prepared from unmodified resin and unmodified fabric (RS0-C) was found to be 71.1 ± 2.3 . The tensile strength of RS1-70-C, RS3-70-C, and RS5-70-C composites was 70.9 ± 1.5 , 81.3 ± 2.7 , and 78.9 ± 1.8 , respectively. The composites prepared from modified viscose fabric (RS0-FS2-C) exhibited a tensile strength of 55.5 ± 2.4 . Compared to RS0-C, no significant difference in strength was noticed for RS1-70-C composites. However, in comparison with RS0-C, the strength of RS3-70-C and RS5-70-C composites increased 14 and 11%, respectively. A trend observed among the composites prepared from APTES-modified resins is that the tensile strength of composites increases up to an APTES content of 3 wt% in modification and then slightly decreases when the APTES content is 5 wt%. The tensile strength of RS0-FS2-C decreased 22% in comparison to RS0-C composite. Compared to RS0-FS2-C, the

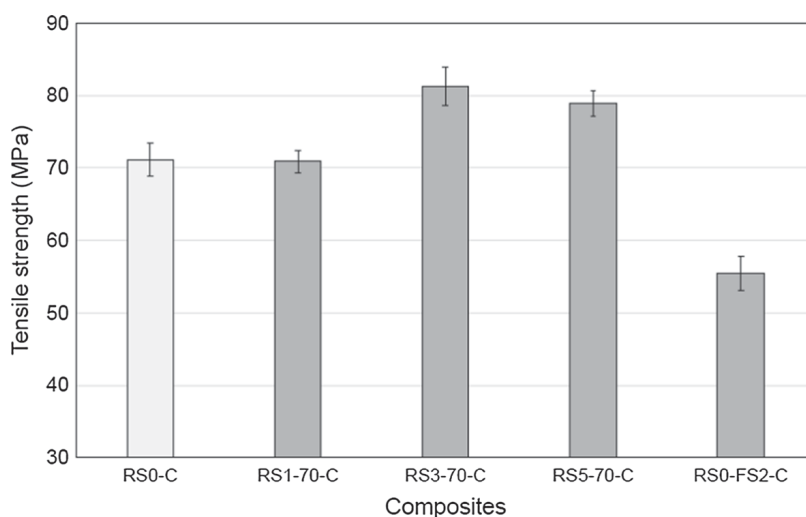


Fig. 10 Effect of APTES modifications on tensile strength of epoxy/viscose fabric composites

strength of RS3-70-C composite is found to be 46% higher. This clearly shows that in this study, the matrix resin modification turns to be better than the chemical fibre surface modification method used.

The elongation at break of the composites (Fig. 11) seems to be increasing with increase in APTES content. Compared to RS0-C composites, the elongation at break increased 29 and 41% for RS3-70-C composite and RS5-70-C composites, respectively. While, there was a decrease of 40% in elongation of RS0-FS2-C. When compared to elongation of cured resin, the elongation of composite depends more on the properties of reinforcement. It could be considered that the elongation at break of the composites is more influenced by the content and elongation of reinforcing fibre [47]. This is reflected from the elongation of composites prepared from modified and unmodified resins, which is lower compared to the RS0-CC. However, the elongation at break for composites made from modified resins is higher than for the epoxy composites reinforced with lignocellulosic fibres and glass fibres. Compared to its lignocellulosic counterparts, the elongation at break of viscose fibre yarns used to make the fabric utilised in this study is significantly higher [48]. The increase in elongation in the case of composites made from modified epoxy resins with respect to RS0-C indicate the improved fibre–matrix adhesion attained after the APTES modification of epoxy resin.

The findings from this study suggest that the interfacial adhesion between a warp knitted viscose fabric and epoxy resin improved after the modification of the epoxy resin by APTES. The coupling mechanism can be explained based on the chemical bond formation between the alkoxy containing epoxy resin and hydroxyl groups in the viscose fabric. The presence of unreacted ethoxy ($\text{CH}_3\text{CH}_2\text{O}-$) after modification of the resin with APTES was confirmed from FTIR analysis (Fig. 5a). The FTIR analysis of cured castings and composites (Fig. 5b, c) show that the absorption band around 1077 cm^{-1} corresponding to (Si–O–C) the ethoxy group, disappears after curing reaction of the epoxy resin. This indicates that the ethoxy groups in the

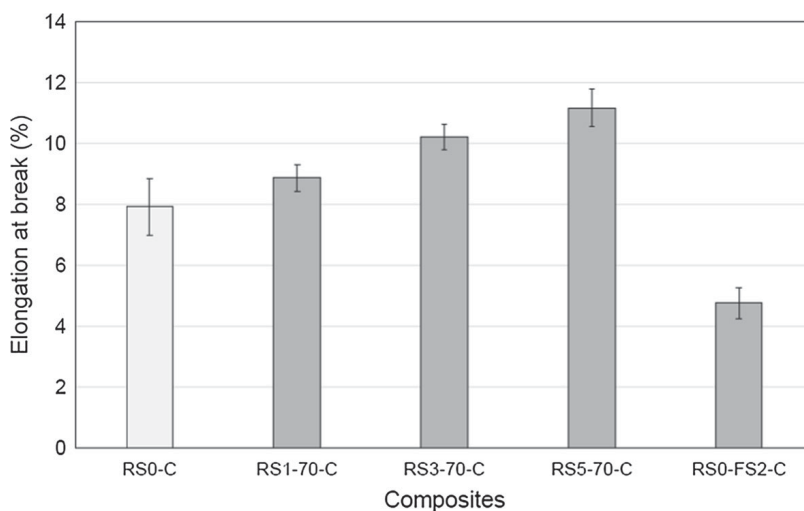


Fig. 11 Effect of APTES modifications on elongation at break of epoxy/viscose fabric composites

APTES-modified epoxy resin have undergone reaction during the curing of the resin. The tensile strength decreased 8% for RS3-70-CC casting and 15% for RS5-70-CC casting when compared to RS0-CC casting. However, the tensile strength of RS3-70-C composite and RS5-70-C composite increased 14 and 11%, respectively. The increase in strength of composites prepared from modified resins with respect to cured castings is obviously due to the improved adhesion between viscose fabric and epoxy resin.

The pre-hydrolysis of the alkoxy group and a temperature above 80 °C are essential for silane modification of cellulose fibre [49]. The low reactivity of Si-OR towards cellulose-OH when compared to Si-OH of the glass surface, was explained based on the poor acidic nature of cellulose-OH [49]. In addition, it is seen in literature that the non-hydrolysed alkoxy group (Si-OR) of silane reacted and formed a chemical bond with glass Si-OH [49, 50]. Instead of fibre modification, matrix modification approach is used in this study and thereby the reaction conditions are different from that of cellulose fibre modification. The modification of resin was done in water free and non-humid conditions. Thus, the silane grafted resin contains unreacted ethoxy group which was evident from the IR results. The disappearance of the unreacted ethoxy group in modified resins after cure reaction hints the possible reaction occurred during the curing of composites involving ethoxy. This is evident from the improvement of up to 14% in tensile strength and 41% in elongation at break of the composites prepared from alkoxy containing epoxy resin.

Since this study used only one chemical modification method to modify the cellulose fibres, the obtained data is compared to the literature. Recently reported data on the effect of the chemical surface modification on the tensile properties of epoxy composites are compared with the results from the current study and are tabulated in Table 5. Only those studies which reported improvement in the tensile properties of epoxy composites are listed to compare the results from this study and those without improvement is omitted. The percent change in tensile strength for the modified epoxy/viscose fabric composites prepared in this study is similar to that of the epoxy composites prepared from silane coupling agent modified lignocellulosic fibres [52, 53]. Whereas, the elongation at break of the composites prepared from modified epoxy resin shows significant increase. The percent change in tensile strength of alkali treated fibre composites obtained from literature is in the range 5.8–32.8%. The results from the modified epoxy resin composites made in this study come within this range of percent change.

The APTES modification of fabric adopted in this study seems to decrease the tensile strength by 22% and elongation at break by 39.8%. The silane treatment method which gave best result with unsaturated polyester resin (UPR) in our previous study was adopted to modify the fabric [5]. This was selected assuming that the chemical affinity of amine in the silane towards epoxy is higher than that to UPR and was expecting to get better results. It is seen from the Table 5 that the tensile strength of APTES-modified *grewia tiliifolia*/epoxy composites shows an increase in strength when the silane content was 1 vol% in acetone. This might be indicating that the 2 vol% APTES in ethanol/water solution used in this study was excess for the modification. The excess silane is reported to form a physisorbed

Table 5 A comparison on influence of fibre modification method and resin modification method on tensile strength and elongation at break of epoxy composites

Composite	Treatment				Tensile strength change (%)	Elongation at break change (%)	References
	Modifier	Content	Time (h)	Drying time (h)			
Sugar palm/epoxy	NaOH	0.25 (M)	1	96	16.4	–	[51]
Grewia tiliifolia/epoxy	NaOH	5 (wt%)	0.5	–	5.8	–	[52]
Flax/epoxy	NaOH	5 (wt%)	0.5	24	21.9	–	[17]
Bamboo/epoxy	NaOH	5 (wt%)	0.5	24	32.8	–	[17]
Grewia tiliifolia/epoxy	APTES	1 (vol%) in (acetone)	6	1	14	–	[52]
Bamboo/epoxy	MPS	0.5 (wt%) in deionized water	4.5	20	15.1	–	[53]
Viscose/epoxy	APTES	2 (vol%) in 95:5 ethanol/water	0.8	0.5	–22.0	–39.8	This study
Viscose/matrix modified epoxy	APTES	3 (wt%)	1	–	14.0	28.9	This study
Viscose/matrix modified epoxy	APTES	5 (wt%)	1	–	10.8	41.2	This study

layer on the chemisorbed silane layer. This layer can act as a lubricant and failure occurs in this region through slippages of physisorbed silane chains [54]. On other hand, the physisorbed layer can prevent the chemisorbed layer from forming chemical bond with the matrix resin [55], which leads to inferior properties.

It is well accepted that chemical treatment methods improve the properties of composites, considering that the optimum treatment conditions are met for each fibre–matrix system under study. However, the established fibre chemical treatment methods are more or less expensive and harmful to environment [56]. The overall time taken from the start of the chemical treatment to drying of the fibres takes minimum 24 h to maximum of 4 days (excluding the time taken for washing and neutralizing the fibres) (Table 5). The modified epoxy castings and composites prepared in this study were fabricated after 24 h of resin modification. Thus, in the matrix modification approach the processing time from resin modification to fabrication of composites is same or even less compared to fibre modification methods listed in Table 5. Since the resin modification only takes 1 h (current study) and because there is no drying step

involved, it is also possible to reduce the time after the modification until the fabrication of composites. More research is needed to optimize the process time. Moreover, the direct mixing of the silane into the resin and using the modified resin in fabrication of composite creates less process waste compared to the hazardous waste generated after the fibre modification. Hence, the improvement in tensile properties of composites attained by resin modification approach indicates that it can be used as an alternative for fibre modification approach. Further research is needed to make both the process cost-effective and environmental friendly.

Tensile fractography

SEM images from tensile fracture surface of composites are shown in Figs. 12, 13 and 14. The bundle pull-off in non-load bearing 90° layer of cross-ply laminate can be observed from Fig. 12a. Single filaments in the 90° layer bundle appears to be clean with less resin covered region and fibre splitting. The polyester yarns used for knitting are also labelled. The appearance of resin rich region is smooth and shiny, but the resin region near polyester knit yarn exhibits micro-textures like river lines. The load bearing 0° plies are observed to be more rugged. The internal cracking within the bundle and bundle de-bonding along the fibre–matrix interface is visible from Fig. 12b. Therefore, from the image analysis of RS0-C composites it is assumed that the adhesion between viscose yarns and the epoxy resin is weak.

The SEM images from the tensile fracture surface of RS3-70-C and RS5-70-C composites are shown in Figs. 13a–c and 14a, b, respectively. Similarly, as in the case of RS0-C composites, pull-out of the non-load bearing 90° fibres and fibre imprints are observed also in the case of RS3-70-C (Fig. 13a). The RS3-70-C seems to be exhibiting surface features like river lines in the region of polyester knit yarn and also in resin rich region. An improved fibre–matrix adhesion can be seen in Fig. 13b through resin smeared bundle as marked. The internal cracking within the bundle in the load bearing 0° layer is seen from the image, but the bundle de-bonding along the fibre–matrix interface is less compared to RS0-C composite as seen from Fig. 13a, b. Moreover, the fracture surface of RS3-70-C is exhibiting more matrix deformations such as cusps and textured micro flow patterns compared to RS0-C composites as seen from Fig. 13c. These observations are indicating the improved adhesion of viscose fibre to APTES-modified epoxy resin.

It can be seen from the comparison of Figs. 12a and 14a that both fracture surfaces are found to be with fibre rich 90° layer. In the case of RS5-70-C composites, the filaments in bundle are well embedded in the matrix resin with less splitting occurring. This point out a better fibre–matrix adhesion in RS5-70-C composite compared to RS0-C composite. As in the case of RS0-C composites, internal cracking within the bundle and the splitting of the load bearing 0° layer are visible from Fig. 14a, but in low degree. It is also seen that the polyester knit yarn exhibit improved adhesion with 5% APTES-modified epoxy resin. This provide a textured appearance of the resin rich area. The 0° bundle smeared with resin can be

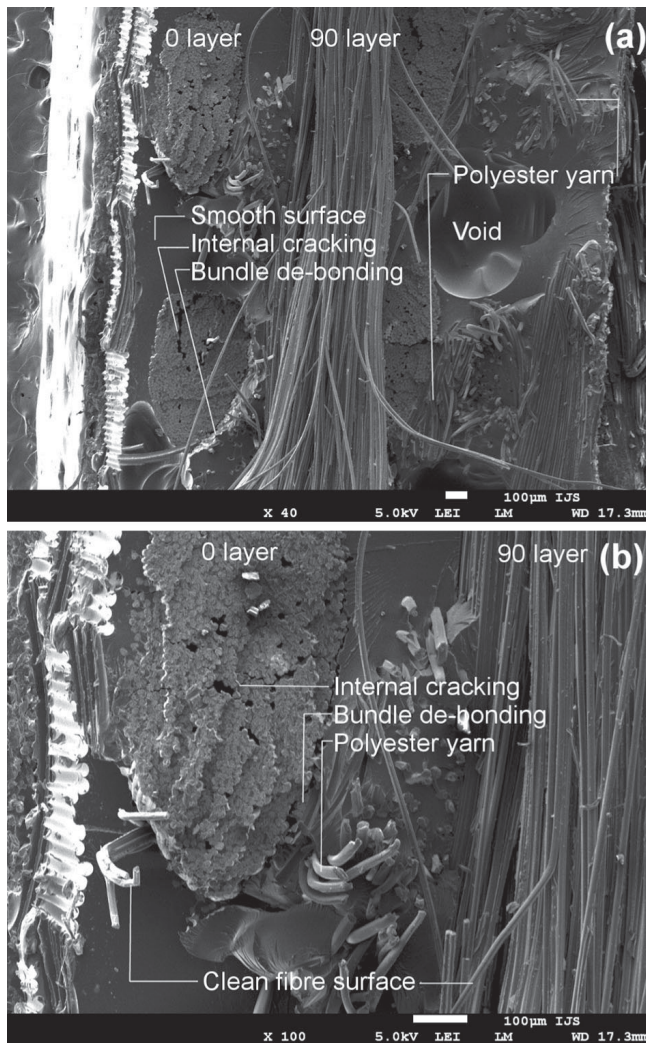
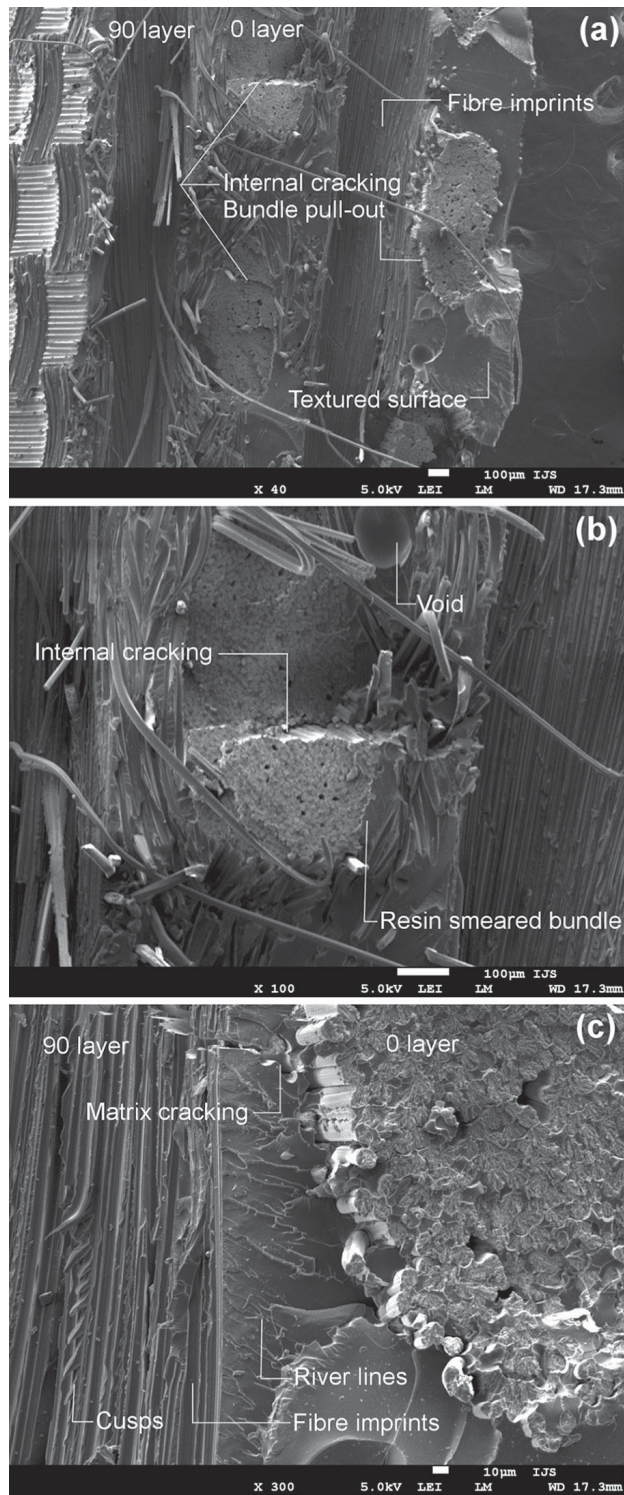


Fig. 12 SEM images from tensile fracture surface of RS0-C composites at different magnifications **a** $\times 40$ and **b** $\times 100$

seen from the Fig. 14b. In addition, resin covered 90° bundle is visible. Although, the fibre–matrix adhesion improved, it is also notable that the presence of the polyester knit yarn has initiated bundle de-bonding in the polyester yarn rich region surrounding the load bearing 0° bundle. From the observations made from the SEM image analysis, it seems that both RS3-70-C and RS5-70-C composites exhibits improved fibre–matrix adhesion compared to the RS0-C composite.

In cross-ply laminated composites, failure modes such as fibre fracture, delamination between the layers, ply splitting or matrix cracking can develop [57, 58]. Under tension, first failure occurring in a cross-ply laminated composite is the ply cracking in the non-load bearing 90° layer. This takes place well before the ultimate failure [59, 60]. In the case of the load bearing 0° layer, the main failures observed are the fibre breakages and bundle internal cracking. Same events are

Fig. 13 SEM images from tensile fracture surface of RS3-70-C composites at different magnifications **a** $\times 40$, **b** $\times 100$ and **c** $\times 300$



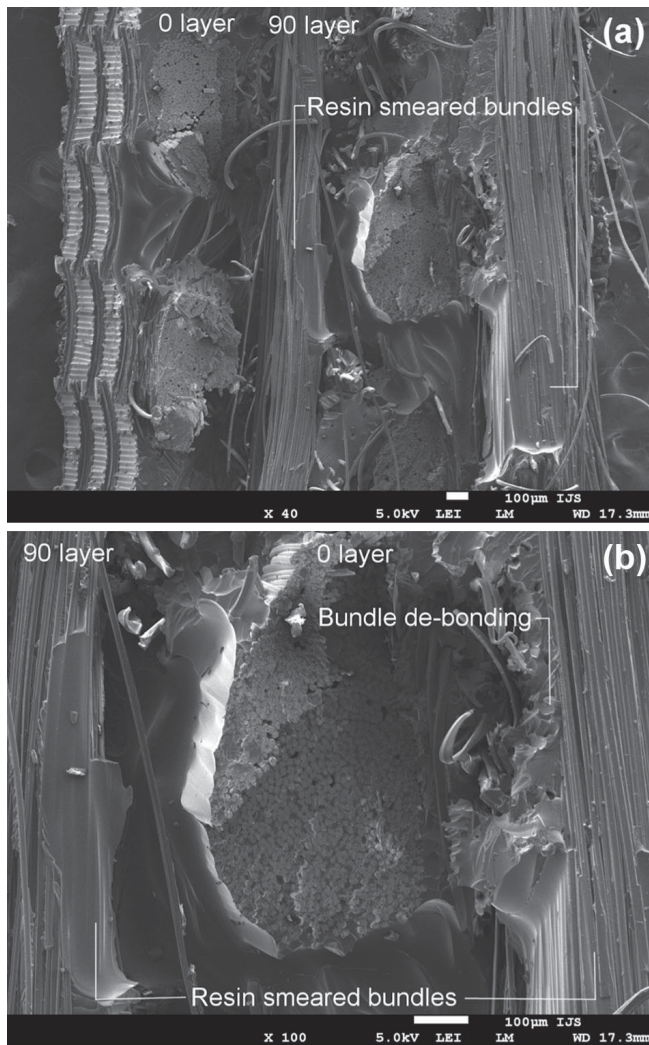


Fig. 14 SEM images from tensile fracture surface of RS5-70-C composites at different magnifications **a** $\times 40$ and **b** $\times 100$

assumed to have happened in case of all the composites under study with varying degree of splitting. Generally, a lack of matrix resin on the fibre surface, higher degree of filament pull-out, and matrix cracking within the fibre bundles are taken as an evidence of poor fibre–matrix adhesion [61, 62]. In addition, a composite with low fibre–matrix adhesion is supposed to exhibit less matrix deformation patterns such as cusps and textured micro-flows like river lines [61–63]. Taking this into account, it could be assumed that the fibre–matrix adhesion improved with the APTES modification of epoxy resin when compared to RS0-C composite. The improvement in fibre–matrix adhesion is evident from the SEM images corresponding to the RS3-70-C and RS5-70-C composites which exhibits resin smeared fibre surfaces with less fibre splitting and lower bundle de-bonding across the fibre–

matrix interface. A notable observation was about the internal cracking within the load bearing 00 yarns. This behaviour was exhibited by all the composites irrespective of modification. This is ascribed to the architecture of the warp knitted viscose fabric. In the case of knitted fabrics, each yarns tends to be fairly filament rich with respect to the overall volume fraction of the composite [64]. Thus, it is susceptible to bundle internal cracking as observed from the tensile fracture surface images of composites. The bundle de-bonding is associated with the rapid change in the compliance across the bundle boundaries [64]. When the fibre–matrix adhesion improved after resin modification, the degree of de-bonding was found to be lower especially in the case of RS5-70-C composites. However, the presence of knit yarn in the boundary of the bundle initiated the de-bonding in that particular region. The knit yarns are reported to act as initiation sites for damage development in composites with knitted fabric as reinforcement [65]. The tensile strength of the RS3-70-C and RS5-70-C composites were 14 and 11% higher than RS0-C composite. SEM analysis alone could not provide evidences for fibre–matrix adhesion in polymer composite materials. The observations made from the image analysis are supplementing the results obtained from the mechanical testing of composites. Thus, it is deduced that the tensile properties of the epoxy/viscose fabric composite improved owing to the improved fibre–matrix adhesion attained after APTES modification of the epoxy resin.

Conclusions

The potential of utilising γ -aminopropyltriethoxysilane (APTES) as epoxy resin modifier to improve the tensile properties of fibre reinforced polymer composites was examined in this study.

- The modification of epoxy resin by silane coupling agent was confirmed through a decrease in epoxide content of modified resin and through ATR-FTIR analysis.
- In comparison with RS0-CC castings, the tensile strength of cured castings prepared from 3 and 5 wt% silane modified epoxy resin decreased 8 and 15%, respectively. This is due to the decrease in crosslink density after resin modification as evident from change in glass transition temperature.
- There was an increase of 14% in tensile strength and 41% in elongation at break of the composites after the modification of resin with 3 wt% APTES. The improvement in the tensile properties is attributed to the improved fibre–matrix adhesion attained after the resin modification. The fracture surface analysis of tensile specimens also justifies the results obtained from the tensile testing of the composites.

The improvement in the tensile properties of composites obtained by resin modification approach is comparable to those attained by fibre modification approach. Moreover, the direct mixing of silane into epoxy resin generates less process waste compared to that generated after the chemical treatments such as alkalization, acetylation and silylation. More research is needed to optimize both resin modification and fibre modification methods to make it more cost-effective

and eco-friendly. Mechanical, water absorption, thermal and burning properties of the viscose fabric composites prepared from silane modified epoxy resin is currently under evaluation. These studies are assumed to provide more insight into the overall performance of these composites.

Acknowledgements This study has received funding from European Union's Seventh Framework Programme (FP7), for the project ECOGEL-CRONOS (Grant No. 609203). The authors gratefully acknowledge the financial support received for the project.

References

1. Kabir MM, Wang H, Lau KT, Cardona F (2012) Chemical treatments on plant-based natural fibre reinforced polymer composites: an overview. *Compos Part B Eng* 43(7):2883–2892. doi:10.1016/j.compositesb.2012.04.053
2. Thomason JL (1995) The interface region in glass fibre-reinforced epoxy resin composites: 1. Sample preparation, void content and interfacial strength. *Composites* 26(7):467–475. doi:10.1016/0010-4361(95)96804-F
3. Sreekala MS, Kumaran MG, Joseph S, Jacob M, Thomas S (2000) Oil palm fibre reinforced phenol formaldehyde composites: influence of fibre surface modifications on the mechanical performance. *Appl Compos Mater* 7(5–6):295–329. doi:10.1023/A:1026534006291
4. Li X, Tabil LG, Panigrahi S (2007) Chemical treatments of natural fiber for use in natural fiber-reinforced composites: a review. *J Polym Environ* 15(1):25–33. doi:10.1007/s10924-006-0042-3
5. Rajan R, Riihivuori J, Rainosalo E, Skrifvars M, Järvelä P (2014) Effect of viscose fabric modification on the mechanical and water absorption properties of composites prepared through vacuum infusion. *J Reinf Plast Compos* 33(15):1416–1429. doi:10.1177/0731684414534748
6. Puliyalil H, Cvelbar U (2016) Selective plasma etching of polymeric substrates for advanced applications. *Nanomaterials* 6(6):108. doi:10.3390/nano6060108
7. Zhou Y, Fan M, Chen L (2017) Interface and bonding mechanisms of plant fibre composites: an overview. *Compos Part B Eng* 101:31–45. doi:10.1016/j.compositesb.2016.06.055
8. Kalia S, Thakur K, Celli A, Kiechel MA, Schauer CL (2013) Surface modification of plant fibers using environment friendly methods for their application in polymer composites, textile industry and antimicrobial activities: a review. *J Environ Chem Eng* 1(3):97–112. doi:10.1016/j.jece.2013.04.009
9. John MJ, Anandjiwala RD (2008) Recent developments in chemical modification and characterization of natural fiber-reinforced composites. *Polym Compos* 29(2):187–207. doi:10.1002/pc.20461
10. Liao M, Yang Y, Hamada H (2016) Mechanical performance of glass woven fabric composite: effect of different surface treatment agents. *Compos Part B Eng* 86:17–26. doi:10.1016/j.compositesb.2015.08.084
11. Ohnishi A, Ohori S, Funami F, Ikuta N (2005) Improvement of resin impregnation into glass cloth by silane treatment in resin transfer molding. *Compos Interfaces* 12(7):683–689. doi:10.1163/156855405774327957
12. Xie Y, Hill CA, Xiao Z, Militz H, Mai C (2010) Silane coupling agents used for natural fiber/polymer composites: a review. *Compos Part A Appl Sci Manuf* 41(7):806–819. doi:10.1016/j.compositesa.2010.03.005
13. Ifuku S, Yano H (2015) Effect of a silane coupling agent on the mechanical properties of a microfibrillated cellulose composite. *Int J Biol Macromol* 74:428–432. doi:10.1016/j.ijbiomac.2014.12.029
14. Asumani OML, Reid RG, Paskaramoorthy R (2012) The effects of alkali–silane treatment on the tensile and flexural properties of short fibre non-woven kenaf reinforced polypropylene composites. *Compos Part A Appl Sci Manuf* 43(9):1431–1440. doi:10.1016/j.compositesa.2012.04.007
15. Sreekumar PA, Thomas SP, Marc Saiter J, Joseph K, Unnikrishnan G, Thomas S (2009) Effect of fiber surface modification on the mechanical and water absorption characteristics of sisal/polyester composites fabricated by resin transfer molding. *Compos Part A Appl Sci Manuf* 40(11):1777–1784. doi:10.1016/j.compositesa.2009.08.013

16. Mahjoub R, Yatim JM, Sam ARM, Hashemi SH (2014) Tensile properties of kenaf fiber due to various conditions of chemical fiber surface modifications. *Constr Build Mater* 55:103–113. doi:10.1016/j.conbuildmat.2014.01.036
17. Yan L, Chouw N, Yuan X (2012) Improving the mechanical properties of natural fibre fabric reinforced epoxy composites by alkali treatment. *J Reinf Plast Compos* 31(6):425–437. doi:10.1177/0731684412439494
18. Ramamoorthy SK, Skrifvars M, Rissanen M (2015) Effect of alkali and silane surface treatments on regenerated cellulose fibre type (Lyocell) intended for composites. *Cellulose* 22(1):637–654. doi:10.1007/s10570-014-0526-6
19. Chikhi N, Fellahi S, Bakar M (2002) Modification of epoxy resin using reactive liquid (ATBN) rubber. *Eur Polym J* 38:251–264. doi:10.1016/S0014-3057(01)00194-X
20. Ratna D (2003) Modification of epoxy resins for improvement of adhesion: a critical review. *J Adhes Sci Technol* 17(12):1655–1668. doi:10.1163/156856103322396721
21. Heng Z, Zeng Z, Chen Y, Zou H, Liang M (2015) Silicone modified epoxy resins with good toughness, damping properties and high thermal residual weight. *J Polym Res* 22(11):1–7. doi:10.1007/s10965-015-0852-x
22. Jin H, Yang B, Jin FL, Park SJ (2015) Fracture toughness and surface morphology of polysulfone-modified epoxy resin. *J Ind Eng Chem* 25:9–11. doi:10.1016/j.jiec.2014.10.032
23. Liu S, Fan X, He C (2016) Improving the fracture toughness of epoxy with nanosilica-rubber core-shell nanoparticles. *Compos Sci Technol* 125:132–140. doi:10.1016/j.compscitech.2016.01.009
24. Heng Z, Chen Y, Zou H, Liang M (2015) Simultaneously enhanced tensile strength and fracture toughness of epoxy resins by a poly (ethylene oxide)-block-carboxyl terminated butadiene-acrylonitrile rubber di-block copolymer. *RSC Adv* 5(53):42362–42368. doi:10.1039/C5RA05124J
25. Ji WG, Hu JM, Liu L, Zhang JQ, Cao CN (2007) Improving the corrosion performance of epoxy coatings by chemical modification with silane monomers. *Surf Coat Technol* 201(8):4789–4795. doi:10.1016/j.surfcoat.2006.09.100
26. Ji WG, Hu JM, Liu L, Zhang JQ, Cao CN (2006) Water uptake of epoxy coatings modified with γ -APS silane monomer. *Prog Org Coat* 57(4):439–443. doi:10.1016/j.porgcoat.2006.09.025
27. Chruściel JJ, Leśniak E (2015) Modification of epoxy resins with functional silanes, polysiloxanes, silsesquioxanes, silica and silicates. *Prog Polym Sci* 41:67–121. doi:10.1016/j.progpolymsci.2014.08.001
28. Yang J, Xiao J, Zeng J, Bian L, Peng C, Yang F (2013) Matrix modification with silane coupling agent for carbon fiber reinforced epoxy composites. *Fiber Polym* 14(5):759–766. doi:10.1007/s12221-013-0759-2
29. Kaynak C, Orgun O, Tincer T (2005) Matrix and interface modification of short carbon fiber-reinforced epoxy. *Polym Test* 24(4):455–462. doi:10.1016/j.polymertesting.2005.01.004
30. Gurit (2016) PRIME™ 20LV—epoxy infusion system. <http://www.gurit.com/prime-20lv-1.aspx>. Accessed 9 Oct 2016
31. Lee A, Lichtenhan JD (1998) Viscoelastic responses of polyhedral oligosilsesquioxane reinforced epoxy systems. *Macromolecules* 31(15):4970–4974. doi:10.1021/ma9800764
32. Kumar SA, Narayanan TS (2002) Thermal properties of siliconized epoxy interpenetrating coatings. *Prog Org Coat* 45(4):323–330. doi:10.1016/S0300-9440(02)00062-0
33. Seraj S, Ranjbar Z, Jannesari A (2014) Synthesis and characterization of an anticratering agent based on APTES for cathodic electrocoatings. *Prog Org Coat* 77(11):1735–1740. doi:10.1016/j.porgcoat.2014.05.018
34. Halley PJ, Mackay ME (1996) Chemorheology of thermosets—an overview. *Polym Eng Sci* 36(5):593–609. doi:10.1002/pen.10447
35. Socrates G (2004) Infrared and Raman characteristic group frequencies: tables and charts. Wiley, New York
36. González MG, Cabanelas JC, Baselga J (2012) Applications of FTIR on epoxy resins—identification, monitoring the curing process, phase separation and water uptake, infrared spectroscopy—materials science, engineering and technology. In: Theophanides T (ed) *InTech*. doi:10.5772/36323
37. Hu JM, Ji WG, Liu L, Zhang JQ, Cao CN (2009) Improving the corrosion performance of epoxy coatings by modification with “active” and “non-active” silane monomers. In: Mittal KL (ed) *Silanes and other coupling agents*, vol 5. CRC Press, pp 203–218
38. Canavate J, Colom X, Pages P, Carrasco F (2000) Study of the curing process of an epoxy resin by FTIR spectroscopy. *Polym Plast Technol* 39(5):937–943. doi:10.1081/PPT-100101414

39. Nikolic G, Zlatkovic S, Cacic M, Cacic S, Laenjevac C, Rajic Z (2010) Fast fourier transform IR characterization of epoxy GY systems crosslinked with aliphatic and cycloaliphatic EH polyamine adducts. *Sensors* 10(1):684–696. doi:10.3390/s100100684
40. Cholake ST, Mada MR, Raman RS, Bai Y, Zhao X, Rizkalla S, Bandyopadhyay S (2014) Quantitative analysis of curing mechanisms of epoxy resin by mid- and near-Fourier transform infrared spectroscopy. *Def Sci J* 64(3):314–321. doi:10.14429/dsj.64.7326
41. Rigail-Cedeño A, Sung CSP (2005) Fluorescence and IR characterization of epoxy cured with aliphatic amines. *Polymer* 46(22):9378–9384. doi:10.1016/j.polymer.2005.04.063
42. Ji WG, Hu JM, Zhang JQ, Cao CN (2006) Reducing the water absorption in epoxy coatings by silane monomer incorporation. *Corros Sci* 48(11):3731–3739. doi:10.1016/j.corsci.2006.02.005
43. Destreri MDG, Vogelsang J, Fedrizzi L (1999) Water up-take evaluation of new waterborne and high solid epoxy coatings by means of gravimetric methods. *Prog Org Coat* 37(1):57–67. doi:10.1016/S0300-9440(99)00055-7
44. Powers DA (2009) Interaction of water with epoxy. Sandia Report SAND2009-4405, Albuquerque, New Mexico. <http://prod.sandia.gov/techlib/access-control.cgi/2009/094405.pdf>. Accessed 18 Oct 2016
45. Honaman LA, de Buyl F, Witucki GL (2004) Improved flexibility of bis-phenol A epoxy paint by crosslinking with amino-functional siloxane resin. Dow Corning Corporation. <http://www.dowcorning.com/content/publishedlit/26-1279-01.pdf?DCWS=Paints%20and%20Inks&DCWSS=Additives%20for%20Paints%20and%20Inksf>. Accessed 18 Apr 2017
46. Dodiuk H, Goodman SH (eds) (2013) Handbook of thermoset plastics. William Andrew, San Diego
47. Colom X, Carrasco F, Pages P, Canavate J (2003) Effects of different treatments on the interface of HDPE/lignocellulosic fiber composites. *Compos Sci Technol* 63(2):161–169. doi:10.1016/S0266-3538(02)00248-8
48. Mader A, Volkmann E, Einsiedel R, Müssig J (2012) Impact and flexural properties of unidirectional man-made cellulose reinforced thermoset composites. *J Biobased Mater Bioenergy* 6(4):481–492. doi:10.1166/jbmb.2012.1229
49. Castellano M, Gandini A, Fabbri P, Belgacem MN (2004) Modification of cellulose fibres with organosilanes: under what conditions does coupling occur? *J Colloid Interf Sci* 273(2):505–511. doi:10.1016/j.jcis.2003.09.044
50. Krasnoslobodtsev AV, Smirnov SN (2002) Effect of water on silanization of silica by trimethoxysilanes. *Langmuir* 18(8):3181–3184. doi:10.1021/la015628h
51. Bachtiar D, Sapuan SM, Hamdan MM (2008) The effect of alkaline treatment on tensile properties of sugar palm fibre reinforced epoxy composites. *Mater Des* 29(7):1285–1290. doi:10.1016/j.matdes.2007.09.006
52. Jayaramudu J, Reddy GSM, Varaprasad K, Sadiku ER, Ray SS, Rajulu AV (2014) Mechanical properties of uniaxial natural fabric *Grewia tilifolia* reinforced epoxy based composites: effects of chemical treatment. *Fiber Polym* 15(7):1462–1468. doi:10.1007/s12221-014-1462-7
53. Kushwaha PK, Kumar R (2010) Effect of silanes on mechanical properties of bamboo fiber-epoxy composites. *J Reinf Plast Compos* 29(5):718–724. doi:10.1177/0731684408100691
54. Park R, Jang J (2004) Effect of surface treatment on the mechanical properties of glass fiber/vinylester composites. *J Appl Polym Sci* 91(6):3730–3736. doi:10.1002/app.13454
55. Hamada H, Fujihara K, Harada A (2000) The influence of sizing conditions on bending properties of continuous glass fiber reinforced polypropylene composites. *Compos Part A Appl Sci Manuf* 31(9):979–990. doi:10.1016/S1359-835X(00)00010-5
56. Fiore V, Scalici T, Nicoletti F, Vitale G, Prestipino M, Valenza A (2016) A new eco-friendly chemical treatment of natural fibres: effect of sodium bicarbonate on properties of sisal fibre and its epoxy composites. *Compos Part B Eng* 85:150–160. doi:10.1016/j.compositesb.2015.09.028
57. Pinho ST, Robinson P, Iannucci L (2006) Fracture toughness of the tensile and compressive fibre failure modes in laminated composites. *Compos Sci Technol* 66:2069–2079. doi:10.1016/j.compscitech.2005.12.023
58. Greenhalgh ES (2009) Fibre-dominated failures of polymer composites. In: Greenhalgh ES (ed) Failure analysis and fractography of polymer composites, 1st edn. Woodhead Publishing Limited, Cambridge, pp 107–163
59. Purslow D (1981) Some fundamental aspects of composites fractography. *Composites* 12:241–247. doi:10.1016/0010-4361(81)90012-4
60. Beaumont PWR (2006) Cracking models; broken parts. *Appl Compos Mater* 13:265–285. doi:10.1007/s10443-006-9022-y

61. Deng S, Ye L (1999) Influence of fiber–matrix adhesion on mechanical properties of graphite/epoxy composites: II interlaminar fracture and in-plane shear behavior. *J Reinf Plast Compos* 18:1041–1057. doi:10.1177/073168449901801106
62. Deng S, Ye L (1999) Influence of fiber–matrix adhesion on mechanical properties of graphite/epoxy composites: I. Tensile, flexure, and fatigue properties. *J Reinf Plast Compos* 18:1021–1040. doi:10.1177/073168449901801105
63. Denault J, Vu-Khanh T (1993) Fiber/matrix interaction in carbon/PEEK composites. *J Thermoplast Compos* 6:190–204. doi:10.1177/089270579300600302
64. Greenhalgh ES (2009) The influence of fibre architecture in the failure of polymer composites. In: Greenhalgh ES (ed) *Failure analysis and fractography of polymer composites*. Woodhead Publishing Limited, Cambridge, pp 279–355
65. Bibo G, Hogg P, Kemp M (1997) Mechanical characterisation of glass- and carbon-fibre-reinforced composites made with non-crimp fabrics. *Compos Sci Technol* 57(9–10):1221–1241. doi:10.1016/S0266-3538(97)00053-5

PUBLICATION III

Mechanical, thermal, and burning properties of viscose fabric composites: Influence of epoxy resin modification

Rathish Rajan, Egidija Rainosaló, Sunil Kumar Ramamoorthy, Selvin P Thomas,
Janez Zavašnik, Jyrki Vuorinen, Mikael Skrifvars

Journal of Applied Polymer Science (2018) 135 (36), 46673

<https://doi.org/10.1002/app.46673>

Publication reprinted with the permission of the copyright holders.

Mechanical, thermal, and burning properties of viscose fabric composites: Influence of epoxy resin modification

Rathish Rajan ^{1,2}, Egidija Rainosallo,¹ Sunil Kumar Ramamoorthy,³ Selvin P. Thomas,⁴ Janez Zavašnik,⁵ Jyrki Vuorinen,² Mikael Skrifvars³

¹Research and Development, Centria University of Applied Sciences, Talonpojankatu 2, Kokkola 67100, Finland

²Department of Materials Science, Tampere University of Technology, P.O. Box589, Tampere 33101, Finland

³Swedish Centre for Resource Recovery, University of Borås, Allégatan 1, Borås 501 90, Sweden

⁴Chemical Engineering Technology Department, Yanbu Industrial College and Advanced Materials Laboratory, Yanbu Research Center, Royal Commission Yanbu-Colleges and Institutes (RCYCI), Yanbu Alsinaiyah 41612, Kingdom of Saudi Arabia

⁵Centre for Electron Microscopy and Microanalysis, Jožef Stefan Institute, Ljubljana 1000, Slovenia

Correspondence to: R. Rajan (E-mail: rathish.rajan@centria.fi)

ABSTRACT: The influence of epoxy resin modification by 3-aminopropyltriethoxysilane (APTES) on various properties of warp knitted viscose fabric is reported in this study. Dynamic mechanical, impact resistance, flexural, thermal properties, and burning behavior of the epoxy/viscose fabric composites are studied with respect to varying content of silane coupling agent. The results obtained for APTES-modified epoxy resin based composites reinforced with unmodified viscose fabric composites are compared to unmodified epoxy resin based composites reinforced with APTES-modified viscose fabric. The dynamic mechanical behavior of the APTES-modified resin based composites indicates improved interfacial adhesion. The composites prepared from modified epoxy resin exhibited a twofold increase in impact resistance. The improved adhesion between the fiber and modified resin was also visible from the scanning electron microscope analysis of the impact fracture surface. There was less influence of resin modification on the flexural properties of the composites. The 5% APTES modification induced early degradation of composites compared to all other composites. The burning rate of all the composites under study is rated to be satisfactory for use in automotive interior applications. © 2018 Wiley Periodicals, Inc. *J. Appl. Polym. Sci.* **2018**, *135*, 46673.

KEYWORDS: cellulose and other wood products; functionalization of polymers; mechanical properties; thermal properties; thermosets

Received 10 January 2018; accepted 27 April 2018

DOI: 10.1002/app.46673

INTRODUCTION

The interest in natural fiber composites is increasing mainly for its potential to replace synthetic fiber reinforced plastics due to low cost, low density, high specific strength, and stiffness, improved sustainability and due to strict environmental regulations.^{1,2} In literature, there are numerous studies which report the use of short lignocellulosic fiber as reinforcement in polymer composites.^{2–4} Continuous fiber reinforcements like unidirectional, non-crimped fabrics, and woven fabrics are a better choice than the short fiber reinforcements when considering the development of high-performance composites.⁵ Regenerated cellulose fibers (RCF) possess high purity, uniformity and reproducibility of their properties compared to lignocellulosic fibers.⁶ These fibers are available as a continuous filament that can be processed into woven or warp-knitted fabrics. RCF could form composites without compromising the environmental benefits

offered by the lignocellulosic fibers, while it can overcome the drawbacks of lignocellulosic fibers. Thus, RCF can be a better alternative or a parallel choice for lignocellulosic fibers in polymer composite manufacturing.^{7,8}

The main approach to improve the interfacial bonding in a composite is surface modification of reinforcement via wet chemical methods and physical methods.^{7,9,10} The chemical methods to modify cellulose fibers include alkali treatment, acetylation, coupling agent treatment, and peroxide treatment to name a few. Physical methods like steam explosion, heat treatment, reactive gas treatment methods like corona treatment and cold plasma treatment are also used to modify the fiber surface.^{7,9,11–14} Among the two methods, chemical modification methods are studied in depth and well-known. The chemical adhesion between a fiber and a matrix resin proceeds through the formation of a covalent bond or hydrogen bonding between

reactive groups in fiber and the matrix. This is achieved by incorporating suitable functional groups and by changing the surface morphology.

Silane coupling agent (SCA) modification is a commonly utilized method to modify the glass fiber surface^{15–17} and also lignocellulosic fiber surfaces.^{7,18–20} SCAs have a general chemical structure of $R(4 - n) - Si - (R'X)_n$ ($n = 1, 2$), where R is ethoxy, methoxy, and so on, X is any functional group such as amine, methacryl, epoxy, or vinyl and R' is the alkyl bridge connecting the silicon atom and the functional group.^{7,19} Trialkoxysilanes are the main type of SCA used in the surface modification of lignocellulosic fibers.¹² The hydrolysable alkoxy group in the SCA can form a chemical bond with the hydroxyl group in the lignocellulosic fiber. The completion of coupling reaction of the SCA on the fiber surface depends on the reactivity of the organic functional group in SCA with the matrix resin. There are several studies which report the lignocellulosic fiber surface modification with SCA.^{15,16} These studies reported that the fiber modification with SCA had resulted in the improvement of various physical properties of the thermoplastic and thermoset composites.

The present study differs from the practice of prior art in a way that the SCA is not used as a fiber surface modifier. Rather, SCA is directly mixed in the thermoset resin to prepare an alkoxy silane containing thermoset resin. From the composite processing point of view, this is a benefit, as resin modification can be done much easily compared to the surface treatment of a reinforcement. It is well understood from the literature that chemical surface modifications weaken the strength of natural fibers.^{17–19} Direct mixing of SCA with epoxy resin and using it in composite preparation is assumed to be eco-friendly and energy efficient. The direct mixing of SCA with resin and using the modified resin in composite preparation creates less process waste compared to the fiber modification method. The reaction medium used to modify the fibers requires waste handling, which includes additional cost and consumes more energy. Through the matrix resin modification, reactive groups having a higher chemical affinity towards hydrophilic cellulose fiber are introduced into matrix resin without weakening the cellulosic fiber strength. The organic functionalities in SCA can form chemical bonds with compatible reactive groups in the matrix resin, while the hydrolysable alkoxy groups can react with the fiber surface. Thus, it is expected to have an improved fiber-matrix adhesion by matrix resin modification approach.

Epoxy resins have been modified by SCA to improve the corrosion resistance and the adhesion of epoxy coatings on aluminum surface.^{21,22} The water resistance of epoxy coatings on metal substrates has been improved through silanes.²³ The potential of SCA, polysiloxanes, silsesquioxanes, silica, and silicates in the modification of epoxy resin has been reported.²⁴ The research related to the silane modification of epoxy resin is mostly in coatings to improve the flexibility, adhesion, corrosion resistance, and water resistance. Patent search using SCA; alkoxy; epoxy resin; modification as keywords yielded studies which report the modification of epoxy resin with SCAs.^{25–28} These studies involve dealcoholization condensation reaction

Table I. Properties of Epoxy Resin According to the Resin Supplier

Properties	Resin	Hardener
Mix ratio (by weight)	100	26
Viscosity at 25 °C (cP)	600–640	15–17
Density (g/cm ³)	1.123	0.936
Cured density (g/cm ³)	1.144	—

between epoxy resin and hydrolyzable alkoxy silane which requires catalysts and solvents. Also, none of these patents report the influence of resin modification on various properties of the fiber reinforced composites. The usage of solvent in the reaction adds another step in composite processing which consumes additional raw material, time, and energy. A recently granted Chinese patent explains a simple method for modification of epoxy resin by direct addition of SCA in to the resin.²⁹ This method of modification of epoxy resin is adoptable for composite processing because of its simplicity. Since this patent reports the application of modified epoxy resin as protective coatings, viability for using the same kind of modification method in the processing of fiber reinforced composites requires an extensive study. The modifications of epoxy resin by SCA to use as matrix resin in polymer composites are seldom found in the literature. Epoxy resins have been modified with different types of SCAs and the resulting mechanical properties of its composite with carbon fiber were studied by Yang *et al.*³⁰ They reported that the matrix modification improved the tensile strength and flexural properties of carbon fiber composites by 4% and 44%, respectively.

The studies on modification of epoxy resin by SCA for using it as the matrix resin in RCF reinforced composites are rarely reported. In a recent study,³¹ we modified an epoxy resin with γ -aminopropyltriethoxysilane (APTES) and studied the properties of the resin and cured castings with respect to neat resin and reaction conditions used. The viscose fabric composites prepared from APTES-modified epoxy resin exhibited increased tensile properties compared to the composites prepared with unmodified epoxy/viscose fabric and APTES-modified viscose fabric/epoxy composites. The main objective of this investigation is to study the effect of APTES-modification of epoxy resin on the mechanical, thermal, and burning properties of epoxy/viscose fabric composite. Finally, the properties of APTES-modified epoxy/viscose fabric composites are compared with the epoxy/APTES-modified viscose fabric to identify the best approach to improve fiber-matrix adhesion.

EXPERIMENTAL

Materials

Prime 20LV, an epoxy resin manufactured by Gurit Ltd. was used for composite preparation. An amine hardener (Prime 20LV slow) was used as curing agent. The main properties of the Prime 20LV resin as given by the manufacturer are listed in Table I.³² The silane-coupling agent for epoxy resin modification was APTES (99% purity).

The fabric used as the reinforcement in the preparation of composites was based on Cordenka 610F viscose yarn with the twist

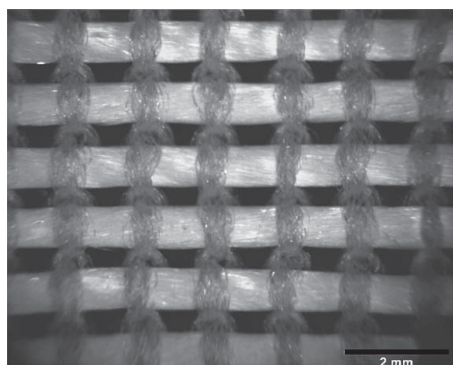


Figure 1. Warp-knitted fabric with thicker weft yarn in the horizontal direction, and thin polyester warp yarn in vertical direction.

Z40, 2440 dtex linear density, and 1350 filaments (Cordenka, Germany). The yarn was processed by warp knitting into uni-directional fabrics with a surface weight of 223 g/m² (Engtex, Sweden). The fabric used in the study is shown in Figure 1.

Modification of Resin and Fabric

The resin modification was done by mixing the epoxy resin with 1, 3, and 5 wt % of APTES without using any solvents or catalysts. An appropriate amount of resin and APTES was weighed into a round bottom flask equipped with a reflux condenser. The mixture was slowly stirred for 1 h on a water bath maintained at 70 °C (± 3). The reaction is assumed to proceed by the primary amine in APTES reacting with oxirane ring forming a secondary amine and a hydroxyl group. The formed secondary amine will further react with another oxirane ring, resulting in the grafting of the silane. More description of the reaction efficiency and scheme can be found from our previous study.³¹

The viscose fabric modification was done according to a method described in our previous study.⁷ APTES was added to an ethanol/distilled water (95:5) solution to yield 2 vol % (2.3 wt %) silane in solution. The silane solution was set aside in a plastic container for 15 min. Then the viscose fabrics were

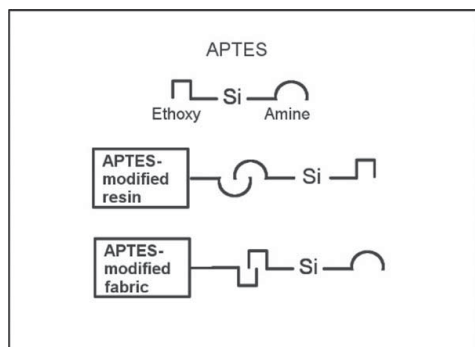


Figure 2. Schematic representation of APTES reaction with epoxy resin and viscose fabric.

immersed in the solution for 5 min and dried at room temperature for 30 min. The fabrics were further dried at 110 °C for 30 min to complete the reaction. The reaction between the viscose fabric and the APTES proceed by hydrolysis of the ethoxy groups and forming highly reactive silanols. The silanols form a hydrogen bond with hydroxyl group on the surface of the fabric. On application of heat, a covalent bond is formed between fabric and APTES. The APTES modification of viscose fabric improved mechanical and water absorption properties of the unsaturated polyester composites.⁷ Thus, it is assumed that the APTES modification of fabric will improve the properties of epoxy/viscose fabric composites since the amino group present in the APTES is compatible with epoxy resin. A schematic representation of the reaction between APTES with epoxy resin and viscose fabric is shown in Figure 2.

Preparation of Composites

All the composite specimens were prepared by vacuum assisted resin infusion method. The steel mold was cleaned and mold releasing agent was applied. Later the mold was polished and used after 30 min. A two-sided sealant tape was attached on the four sides of the mold to fixate the vacuum bag film. Four

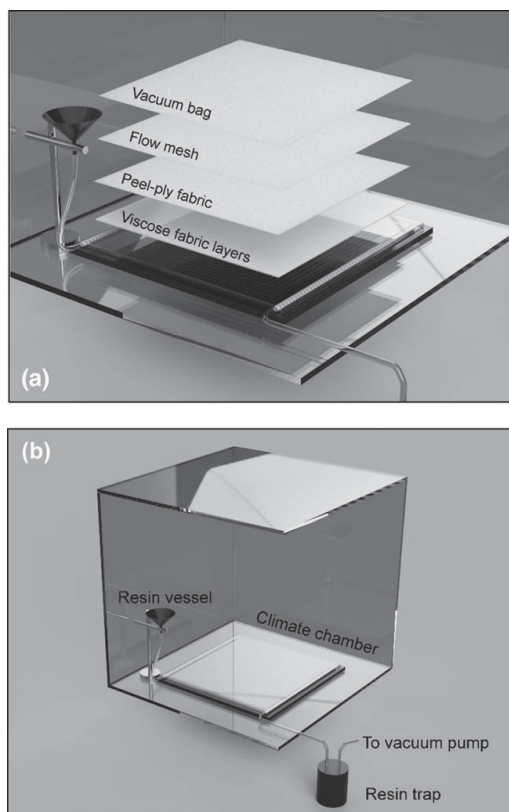


Figure 3. Schematic representation of (a) vacuum bag and (b) composite preparation by vacuum-assisted resin infusion at higher temperature.

Table II. Designations for the Epoxy/Viscose Fabric Composites

APTES	Modification	Designation
	Details	
0 wt %	No modification	RS0-C
1 wt %	Resin modified at 70 °C for 1 h	RS1-70-C
3 wt %	Resin modified at 70 °C for 1 h	RS3-70-C
5 wt %	Resin modified at 70 °C for 1 h	RS5-70-C
2 vol % (2.3 wt %)	Fabric modified at room temperature and dried at 110 °C	RS0-FS2-C

layers of warp knitted unidirectional viscose fabric were carefully placed one over another inside the space formed by sealant tape ($\pm 0/\pm 90/\pm 0/\pm 90$). Then peel-ply fabric was placed on the top layer of viscose fabric and a flow enhancing fabric was laid on the top of the peel-ply fabric. The connection tubes for the resin inlet and vacuum were placed parallel to each other as shown in Figure 3(a). Finally, the mold was carefully sealed using vacuum bag film and vacuum bagging was completed. The sealed mold was placed in a climate chamber having an opening through which the tubes were connected to resin trap to which the vacuum pump was connected. After confirming that there is no leakage, the door of the climate chamber was closed and was heated to 65 °C.

The epoxy resin was mixed with hardener in the ratio 100:26 (by weight). The plastic container containing the resin mix was placed open for 5 min in the climatic chamber heated to 65 °C to remove the trapped air bubbles. Later the resin mix was transferred into the resin vessel which was connected through a flexible plastic tube to the mold. The clamp used to close the resin inlet tube was opened and the resin mix gradually impregnated the viscose fabric layers. The excess resin after proper impregnation was collected in the outlet tube to resin trap or in resin trap. The vacuum pressure applied was 0.1 bar and the temperature in the chamber was maintained at 65 °C for 7 h after the impregnation. After completion of this period, the temperature in the chamber was raised to 80 °C and the composites were post-cured for 2 h. The fiber weight percentage in the composites ranged between 38% and 42%. The thickness of the composites was 2.2–2.4 mm. The designations and the corresponding modification of the viscose fabric composites are listed in Table II.

Characterization

Dynamic mechanical properties of the viscose fabric composites were analyzed using Netzsch DMA 242 analyser. The measurement was conducted under tensile mode at a frequency of 1 Hz. The sample dimension was 30 × 5 mm (length × width). The free length of the sample was 10 mm and thickness was in range 2.2–2.4 mm. The testing temperature ranged from 25–130 °C at a heating rate of 2 K/min. The three-point flexural test was done according to ISO 14125:1998 standard using Tinius Olsen H10KT universal testing machine. The dimensions of the specimens were 80 × 15 mm (length × width). The load cell was 10 kN and rate of loading was 10 mm/min. The support span was 64 mm. Charpy impact test was performed on un-notched specimens according to ISO 179 standard. The specimens were

tested edgewise. Tests were carried out on mechanical impact tester (QC-639D, Cometech testing machines, Taichung Hsien, Taiwan). The dimensions of test specimens used for different tests are shown in Figure 4.

Thermal degradation of the epoxy/viscose fabric composites were studied using a thermogravimetric analyser, Netzsch DMA 242. The test was conducted in a nitrogen atmosphere by heating from 25 to 800 °C at 10 °C/min. The sample mass for all the composites was 20 mg (± 2). Considering the prospects of viscose based fiber composites in automotive application, the burning rate test for all the composites were conducted according to the ISO 3795:1988. The standard describes the method to determine the burning behavior of interior materials in road vehicles, tractors, and machinery for agriculture and forestry. A sample is held horizontally in a U-shaped holder and the free end of the sample is exposed to a low-energy flame for 15 s in a combustion chamber. The test determines when the flame extinguishes or the time in which the flame passes a measured distance. The test sample was 138 in length and 60 mm in width (Figure 5). Three specimens per composites were tested. The measurement starts at the moment when the foot of the flame passed first measuring point. The side (upper or bottom) which burns faster was selected to observe the flame propagation. The measurement completes when the flame reaches the end of the sample. The distance from the first measuring point to the end of the sample was 100 mm.

$$B = \frac{s}{t} \times 60 \quad (1)$$

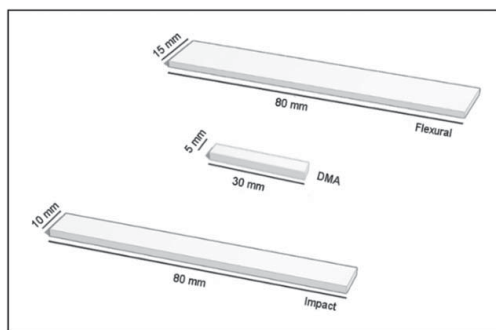


Figure 4. Dimensions of 3-point bending, DMA, and impact test specimens.

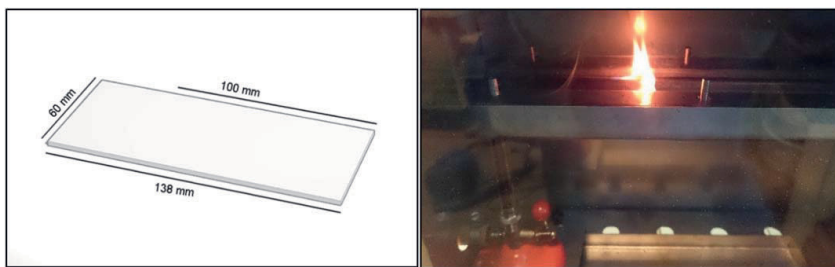


Figure 5. Dimension of test specimen for burning test (left) and a sample under testing (right). [Color figure can be viewed at wileyonlinelibrary.com]

The burning rate B , in mm/minute, is calculated from eq. (1) whereas, s is burnt distance in millimetres and t is the time in seconds taken to burn distance s .

The morphology of the impact fractured samples was studied by scanning electron microscope (SEM; JSM-5800, Jeol Inc., Tokyo, Japan), operating at a low accelerating voltage (5 keV) to minimize beam-damage of the polymer. Prior observation samples were mounted onto Al-support stubs with conductive carbon paint, perpendicular to the support stubs in order to expose the fractured surface. To improve conductivity the samples were sputtered with a thin layer of amorphous carbon (Balzers SCD 050 sputter coater). For observation of the surface of the sample, we used Everhart-Thornley type detector for low-energy (<50 eV) secondary electrons (SE), generated by inelastic scattering interactions with primary (beam) electrons. Due to their low energy, SE originates only from the depth of few nm from the sample surface. While scanning the electron beam in a raster mode over the sample, the intensity map of the signal is constructed, where the number of SE emitted from the surface of the sample is directly related to the angle between the primary electron beam and the sample, resulting in contrasted, well-defined 3D images with a large depth-of-view.

RESULTS AND DISCUSSION

Dynamic Mechanical Analysis

The dynamic storage modulus (E'), is an important property for estimating the load-bearing capacity of the composite material.

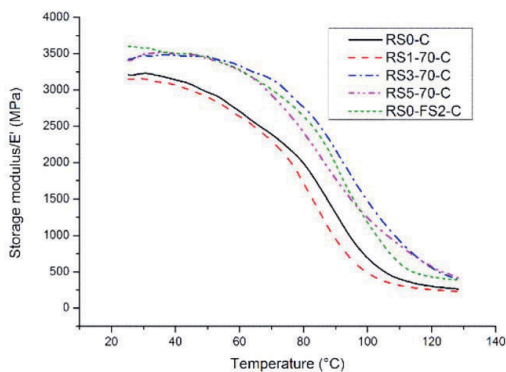


Figure 6. Effect of modification on storage modulus of epoxy/viscose fabric composites. [Color figure can be viewed at wileyonlinelibrary.com]

Figure 6 shows the effect of resin and fabric modification on the storage modulus of epoxy/viscose fabric composites as a function of temperature. In comparison to RS0-C, the storage modulus above the glass transition temperature improved after resin and fabric modification. At 40 °C the storage modulus increases in order of RS0-C < RS1-70-C < RS3-70-C = RS5-70-C < RS0-FS2-C. The storage modulus of all the composites decreases with increase in temperature and the drop is prominent in the transition region. The effect of resin modification by 1% APTES seems to be negligible because its storage modulus in both glassy and rubbery region is unaffected compared to RS0-C. The storage modulus at 120 °C for RS0-FS2-C composites made from modified fabrics is higher than RS0-C and RS1-70-C, but it is relatively lower than RS3-70-C and RS5-70-C.

The increase in storage modulus for the APTES-modified composites compared to RS0-C composites in glassy region and above the glass transition temperature indicates the chemical bond formation between the fiber and matrix. The storage modulus is generally related to Young's modulus and determines the material stiffness.³³ The stiffness in glassy state is more influenced by the intermolecular forces and the packing of polymer chains. The improved stiffness of the composites above the T_g after modification is ascribed to the hindered mobility and deformability of the matrix after APTES-modification. Improved fiber-matrix adhesion is thought to be restricting the molecular mobility resulting the composite to be stiffer.³⁴ The increase in storage modulus of the thermoset composites in glassy region and above the T_g after the modification of fiber and epoxy resin was reported elsewhere.^{35–37}

During the softening of a glassy polymer, intermolecular forces are not suddenly overcome by thermal motions because molecular chains undergo different types of motions. Once the temperature is above the T_g , the micro-Brownian motion becomes so prominent in crosslinked polymers that the material softens and can be deformed by external forces.³⁸ Thus, the decrease in storage modulus near T_g for all the composites can be ascribed to the increased micro-Brownian motion of the crosslinked segments in the matrix. In the transition phase, the storage modulus of APTES-modified composites except RS1-70-C increased than RS0-C. This is due to the restricted chain movement owing to improved interfacial adhesion. The increase in storage modulus at 120 °C for RS3-70-C and RS5-70-C can be related to the change in the structure of epoxy after grafting of alkoxy-silane.

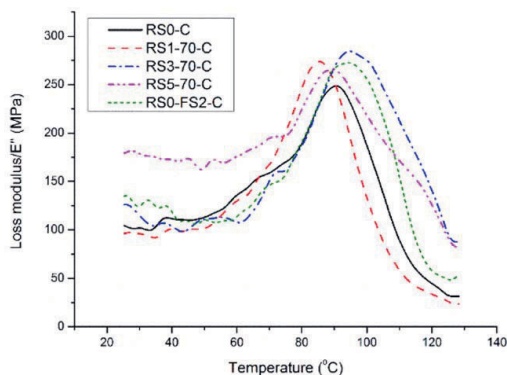


Figure 7. Effect of modifications on the loss modulus of the viscose fabric composites. [Color figure can be viewed at wileyonlinelibrary.com]

The effect of resin and fabric modification on loss modulus of the epoxy/viscose fabric composites as a function of temperature is shown in Figure 7. Loss modulus (E'') or dynamic loss modulus is a measure of energy dissipated or lost and is in fact regarded as the viscous response of the material. In the glassy region, APTES-modification increased the E'' of the composites with respect to RS0-C. There was a notable increase in loss modulus of the RS5-70-C composites in the glassy region. Below the glass transition temperature, the energy dissipated or lost as heat per cycle of sinusoidal deformation increased in the order of RS0-C < RS1-70-C < RS3-70-C < RS0-FS2-C < RS5-70-C. The loss modulus of RS0-C, RS1-70-C, and RS0-FS2-C composites at 120°C is almost similar whereas, the loss modulus E'' of RS3-70-C and RS5-70-C composites is significantly higher at 120°C. The E'' peak of the composites increased in the order of RS1-70-C < RS0-C < RS0-FS2-C < RS5-70-C < RS3-70-C. The broadening of the E'' peak is seen from Figure 7 and it is wider in the case of RS5-70-C, followed by RS3-70-C and RS0-FS2-C composites, respectively.

The interaction of modified resin with fiber is assumed to occur via a covalent bonding between cellulose hydroxyl and ethoxy group present in the modified epoxy resin. Thus, the fiber-matrix interaction is similar as in the case of composites prepared from fiber modified by SCAs. The increase in loss modulus E'' of RS5-70-C composites below and that of both RS3-70-C and RS5-70-C composites above the T_g , when compared to RS0-FS2-C, can be ascribed to the improved fiber-matrix adhesion attained through the matrix modification approach. The E'' peak broadening can be ascribed to the inhibition of relaxation process within the composites due to the presence of an increased order.³⁹ The greater restrictions on the amorphous phase may result in increase or broadening of the glass transition temperature.⁴⁰ There was a shift in the T_g towards the higher temperature in the case of RS3-70-C and RS0-FS2-C indicating increased crosslinking in both composites. The increase in loss modulus of natural fiber reinforced composites after chemical modification of fiber was reported by d'Almeida *et al.*⁴¹ and Saha *et al.*⁴² The increase in loss modulus of SAN

(polystyrene-*co*-acrylonitrile) modified epoxy/glass fiber composite was also reported.³⁷

Tangent δ or $\tan d$ is a dimensionless number regarded as the mechanical damping factor which is the ratio of the loss modulus to the storage modulus. The influence of fiber or matrix modification on the variation in $\tan d$ of the composites with increasing temperature is shown in Figure 8. For all the composites, it is seen that with an increase in temperature, damping increases by reaching maximum value in the transition region and above the T_g , damping value again decreases. The high damping in the transition region can be ascribed to the micro-Brownian motions of molecular chain segments and their stress relaxation. The $\tan d$ peak position and height provides information on the structure and properties of composites. The $\tan d$ peak height is in the order of RS1-70-C > RS0-C > RS0-FS2-C > RS3-70-C > RS5-70-C. The increase in peak height of RS1-70-C composite compared to RS0-C composite indicate that 1% APTES modification of resin resulted in decreased interfacial bonding. However, the resin modification with 3% (RS3-70-C) and 5% (RS5-70-C) APTES seems to have improved the interfacial adhesion in the composites as seen from the lowering of the $\tan d$ peak. The increase in interfacial adhesion in thermoset composites with lowering of $\tan d$ peak and vice versa has been reported elsewhere.^{40,43} The maximum damping occurs in the region where most of the chain segments take part in the micro-Brownian motion. The improved interfacial adhesion might have restricted the molecular movement and thereby lowered the damping peak height. A shift in glass transition temperature is observed in the composites after the APTES-modification. There was about 7°C decrease in T_g of RS1-70-C composite with respect to RS0-C composite. The glass transition temperature T_g of RS3-70-C and RS5-70-C composites increased 16°C when compared to RS0-C composite. There was an increase of 6°C in T_g of RS0-FS2-C composite with respect to RS0-C composite. The increase in glass transition temperature of the composite can be taken as a measure of interfacial interaction. Higher the T_g , stronger the fiber-matrix adhesion. Similar kinds of observations for natural fiber reinforced composites have been reported in the literature.^{40,43}

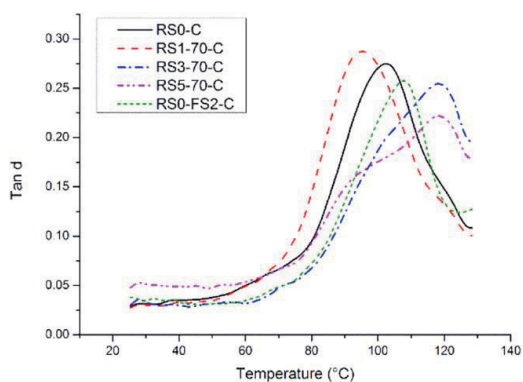


Figure 8. Effect of modifications on the $\tan d$ value of the viscose fabric composites. [Color figure can be viewed at wileyonlinelibrary.com]

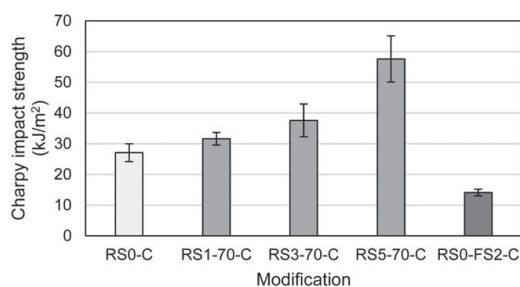


Figure 9. Effect of modifications on the Charpy impact strength of the viscose fabric composites.

Charpy Impact Strength

The Charpy impact strength is shown in Figure 9. It is observed that the addition of APTES into epoxy resin increased the impact strength of composites. There was an increase in strength by increasing the APTES content in the modification. When compared to RS0-C composite, the strength of RS1-70-C and RS3-70C increased 18% and 37%, respectively. Maximum improvement in strength was recorded for RS5-70-C composite in which the impact strength almost doubled compared to the RS0-C composites. The epoxy composite prepared from fabric modified with APTES (RS0-FS2-C) exhibited the lowest strength among all the composites. Compared to RS0-C composite there was a decrease of 48% in the strength of the RS0-FS2-C composite.

Literally, these results show that the modification of the resin with APTES is more effective than fabric modification method in improving the impact resistance of viscose fabric/epoxy composites. There are several factors governing the impact resistance of the composite materials. Among those, strength and stiffness of fiber, matrix toughness, thickness, lay-up, impact velocity, and support conditions are of importance.³⁹ The damping factor $\tan d$ has found to be often correlated to the impact resistance of the natural fiber composites.⁴⁰ The lowering of the $\tan d$ peak height can be related to an increase in impact resistance of the composites. Among all the composites, the lowest $\tan d$ peak was observed for RS5-70-C composite (Figure 9). The result from $\tan d$ curve very well correlates with the results obtained from the Charpy impact test for RS0-C, RS1-70-C, RS3-70-C, and RS5-70-C composites. On contrary to this, although the $\tan d$ height for RS0-FS2-C composite is lower than that of RS0-C composite, the impact resistance of RS0-FS2-C was the lowest among all the composites. The lowering of $\tan d$ has been explained as an indication of the improved interfacial adhesion as reported elsewhere.⁴⁰ Thus, it could be assumed that the epoxy resin modification by 3% and 5% APTES have improved the fracture toughness of the epoxy/viscose composites and improved interfacial adhesion. However, the interfacial adhesion in RS0-FS2-C composite decreased with the fiber modification approach employed in this study. This ultimately decreased the impact resistance of RS0-FS2-C composites. When a composite is tested under impact, a part of energy related to impact is used for elastic deformation of the composite. The remaining energy is dissipated through different failure

mechanisms like fiber breakage, fiber-matrix de-bonding, delamination, and matrix resin cracking.³⁹ The impact fracture surface analysis through SEM is supposed to provide the information on the type of fractures occurred in the composites.

3-Point Bending Test

The capability of composites to withstand the bending before reaching the breaking point is represented in terms of flexural strength. Average flexural strength for composites under study is shown in Figure 10. There was only negligible influence of resin modification on flexural strength of RS1-70-C composite when compared to RS0-C. Even though the average strength of RS3-70-C composite (85.5 MPa) decreased compared to RS0-C composite (93.7 MPa), the larger standard deviation makes it insignificant. However, there was a clear drop in flexural strength of RS3-70-C composites with respect to RS0-C composites. About 20% drop in the strength of RS3-70-C was recorded. The composite prepared from APTES-modified fabric (RS0-FS2-C) shows flexural strength similar to RS0-C composites indicating insignificant influence of fabric modification on flexural strength.

The trend obtained for tensile strength of the APTES-modified resin composites was RS0-C = RS1-70-C < RS5-70-C < RS3-70-C.³¹ While considering the average flexural strength values, the trend obtained for APTES-modified resin composites is in order of RS3-70-C < RS5-70-C < RS1-70-C < RS0-C. Thus, 3% APTES-modification of resin decreased the flexural strength, while the same increased the tensile strength of the viscose composites. The common failures under bending are compressive, tensile, and/or shear failure related to interlaminar crack propagation, matrix failure, and fiber breakage.⁴⁴ It is evident from the dynamic mechanical analysis, tensile test, and Charpy impact test that the improvement in corresponding properties of composites is achieved through an improved interfacial adhesion. Hence, other than interfacial adhesion, the change in property of matrix after 3% APTES modification might be influencing more on the 3-point bending test results. Ahmad *et al.*⁴⁴ toughened thermoset resin and studied its influence on impact and flexural properties of kenaf fiber composites. They reported that the composites prepared from toughened polyester exhibited improved impact resistance while the flexural properties decreased.

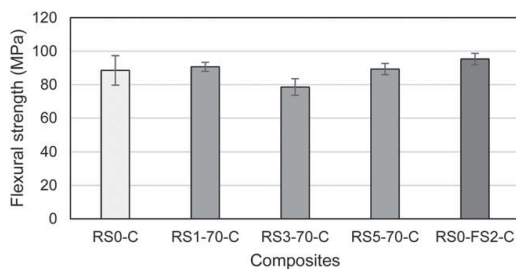


Figure 10. Effect of modifications on the flexural strength of the viscose fabric composites.

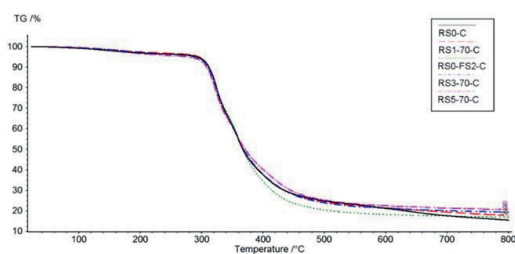


Figure 11. Thermogram of epoxy/viscose fabric composites. [Color figure can be viewed at wileyonlinelibrary.com]

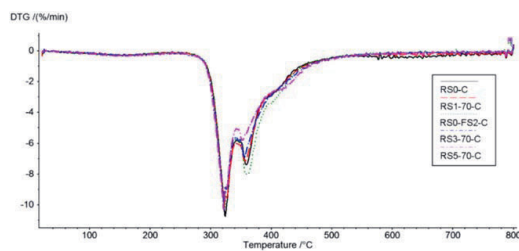


Figure 12. DTG curve of epoxy/viscose fabric composites. [Color figure can be viewed at wileyonlinelibrary.com]

Thermogravimetric Analysis

The thermogram (TG) and derivative of thermogravimetry (DTG) for epoxy/viscose fabric composites are shown in Figures 11 and 12. As seen from Figure 11, a two-stage degradation is followed by all the composites. The first degradation stage is mainly related to the degradation of viscose fabric in the composite. A mass loss of approximately 30% occurred during this stage for all the composites. The second degradation stage is mainly due to the degradation of epoxy resin in the composite. When compared to RS0-C composite, the main difference noticeable in this stage is an increase in mass loss percent of 3.0% and 6.8% in the case of RS3-70-C and RS0-FS2-C composites, respectively. The residual mass obtained for the composites prepared from modified epoxy resin increases with the increase in APTES content in the modification. Compared to RS0-C composite, there was an increase in residual mass of 3.9% and 5.2% for RS3-70-C and RS5-70-C composites, respectively.

The onset degradation temperature is taken at 5% mass loss, see Table III. Compared to RS0-C, the main difference observed

is a significant decrease of 15 °C in the case of the RS5-70-C composite. However, at 50% mass loss, the temperature of the RS5-70-C composite is 5 °C higher than the RS0-C composite. Mainly two degradation stages are seen from DTG curve in Figure 12. The first peak corresponds to the degradation of viscose fabric in composites. There is no significant change observed in the maximum degradation temperature for all the composites in this stage according to Table III.

The initial mass loss in cellulose-based composites is reported due to evaporation of the moisture in the fiber.^{45,46} The RCF are reported to exhibit a two-step degradation excluding the water loss.⁴⁷ The second degradation step around 325 °C is related to cellulose degradation. This is associated with the dehydration and decarboxylation reactions producing combustible gases like aldehydes, ketones, and ethers.⁴⁸ A notable decrease in the case of onset temperature was observed for RS5-70-C compared to RS0-C composite. Also, it was noticed that at higher temperature the mass loss is delayed for RS5-70-C with respect to RS0-C composite. Among all the composites, the silane content is highest in RS5-70-C composite. The decrease in onset temperature of RS5-70-C might be due to the initial degradation of APTES occurring at a lower temperature. The lowering of onset temperature (at 5% mass loss) is reported for epoxy resin modified with triglycidylxyphenylsilane.⁴⁹ The initial degradation of silane group forms a silicon-containing residue which slows down the degradation of epoxy resin occurring in next stage in the case of RS5-70-C composite.^{49,50} This is reflected by the increase in temperature at 50% mass loss corresponding to the epoxy resin and an increase of 5.2% residual mass with respect to RS0-C.

Burning Rate Test

The burning rate of the composites determined through ISO 3795-1988 is shown in Figure 13. The burning rate of the composites prepared from APTES-modified epoxy resins shows an increase in the burning rate. There is around 18% increase in the burning rate of the RS5-70-C composite when compared to RS0-C composite. These results indicate that with an increase in APTES content in the modification of resin, the burning rate of the composites increased. The composite prepared from APTES-modified viscose fabric (RS0-FS2-C) was showing the lowest burning rate among the entire composites. Compared to RS0-C composite, there was a decrease of about 8% in the burning rate for RS0-FS2-C composite. This is indicating that the APTES fabric modification has effectively reduced the burning rate of the composite. During the test, it was also observed

Table III. Results from Thermogravimetric Analysis of Epoxy/Viscose Fabric Composites

Composites	Temperature (°C) (5% mass loss)	Temperature (°C) (50% mass loss)	1st DTG peak (°C)	2nd DTG peak (°C)	Residual mass (%)
RS0-C	294	368	327	359	15.5
RS1-70-C	297	368	324	356	17.8
RS3-70-C	292	370	324	356	19.4
RS5-70-C	279	373	324	354	20.7
RS0-FS2-C	296	368	324	361	17.0

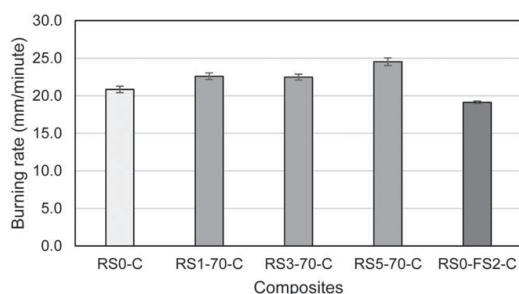


Figure 13. Effect of modification on burning behavior of epoxy/viscose fabric composites.

that after self-extinguishing, the RS3–70-C and RS5–70-C composites deformed more compared to other composites under study. Also, another important observation during the test was the change in maximum temperature inside the chamber during the test. The maximum temperature was recorded as 165, 168, 184, 189, and 175 °C for RS0-C, RS1–70-C, RS3–70-C, RS5–70-C, and RS0-FS2-C, respectively.

After exposure to sufficient heat energy, polymers undergo thermal degradation through pyrolysis. The evolved flammable volatiles when mixed with air at an optimal temperature they will ignite. If the energy feedback into the system from the exothermic burning process is sufficient, an endothermic pyrolysis process is activated and result in flame spread.⁵¹ Whereas, in the case of cellulosic fiber, the pyrolysis results in the formation of levoglucosan which usually evolves in the form of an extremely flammable fluid tar.⁵² Hence, both viscose fabric and the epoxy resin are involved in the burning of the composite. In the composites prepared from APTES-modified resins, the influence of viscose fabric on the burning rate is less significant because it has not undergone any modification. However, it is relevant in the case of the composite prepared from APTES-modified viscose fabric.

The result obtained from DMA shows an increase in T_g obtained from the tan δ curve (Figure 8) which indicate an increase in crosslink density of RS3–70-C and RS5–70-C composites among the resin-modified composites. The flame retardant property of epoxy resin is reported to be adversely affecting by high crosslink density.^{53,54} High crosslink density can make the network structure too rigid to produce charred layers during combustion and thereby decreasing the flame retardant property. Since high energy is needed to break highly crosslinked structures, the maximum temperature in the chamber recorded during the test for RS3–70-C and RS5–70-C composites was higher compared to other composites. Thus, it is assumed that the energy fed back from the exothermic burning process is enough to activate the endothermic pyrolysis process and this increased the burning rate of RS3–70-C and RS5–70-C composites.

The T_g obtained for RS0-FS2-C composite is lower than RS3–70-C and RS5–70-C composites. Thus, it is assumed that crosslink density is low in RS0-FS2-C composites compared to RS3–70-C and RS5–70-C composites. Other than the crosslink

density of composite, the lowering of burning rate in RS0-FS2-C can be more influenced by the structure of viscose fabric after modification. In the case of chemical modification of cellulose, the reaction takes place in the amorphous region or at the edge of the crystalline region. Since the reagent is not able to diffuse into the crystalline region the reaction takes place at the chain ends close to the surface of crystallites resulting in the opening of some of the hydrogen bonded cellulose chains. Consequently, new amorphous domains are formed from the crystalline region.⁵⁵ The increase in amorphous region in cellulose after silane treatment is reported in the literature.⁷ Higher the crystallinity of fiber, higher the levoglucosan formation during the pyrolysis of cellulose. As already mentioned levoglucosan is usually evolved as highly flammable fluid tar. One recommendation made by Kozłowski and Władysław-Przybylak⁵² to decrease the flammability of the cellulose fiber is to decrease the crystallinity of the cellulosic fibers. RS0-FS2-C composites were made from APTES-modified viscose fabric and it is assumed that the silane treatment decreased the crystallinity of the viscose fabric. This eventually decreased the formation of the levoglucosan, which resulted in a composite with the lower burning rate among all the composites tested in the study. Thus, it is notable that the APTES modification of epoxy resin increased the burning rate and the APTES-modification of viscose fabric effectively decreased the burning rate. According to ECE Reg. No 118 and directive 95/28/CE,⁵⁶ the result of the horizontal burning tests conducted according to ISO 3795 shall be satisfactory if the burning rate is not more than 100 mm/min.⁵⁶ Then all the epoxy/viscose fabric composites studied in this study is exhibiting satisfactory performance in the burning test.

Impact Fractography

The SEM images from impact fracture surface of the RS0-C composite is shown in Figure 14(a–d). Matrix fracture in the load bearing 90° layers is visible from Figure 14(a). One among the two 90° layers seen from Figure 14(a,b) show fiber or bundle pull-out, bending, shearing fiber end and region where the filaments are completely pulled-out whereas, the bundles in another 90° layers as seen from the image is assumed to be fractured under compression. In Figure 14(c), radials which are characteristic of tensile failure is observed. In the case of both 0° layer, the partially pulled out filaments, micro-textures related to sheared surfaces, and fiber imprints are seen [Figure 14(d)]. Another notable observation made from the fracture surface of the RS0-C composite is the crack in the matrix after impact [Figure 14(a)] indicating brittle nature of the composite.

The breakage of load bearing 90° bundles and filament pull-out from 0° layers was also observed in the case of RS5–70-C composites. The SEM images from impact fracture surface of RS5–70-C composites are shown in Figure 15(a–d). The broken parts of the bundle are visible in Figure 15(b). Among the load bearing 90° layers, one shows terraced bundle pull-out and other layer do not show bundle pull-out similarly as in the case of RS0-C composites. The first layer is undergoing failure in tension/shear and other layer failed under compression. The appearance of the radials as seen from the Figure 15(c) is confirming the failure of one of the 90° layer in tension. Both the 0° layers from the fracture surface seems to be failed under

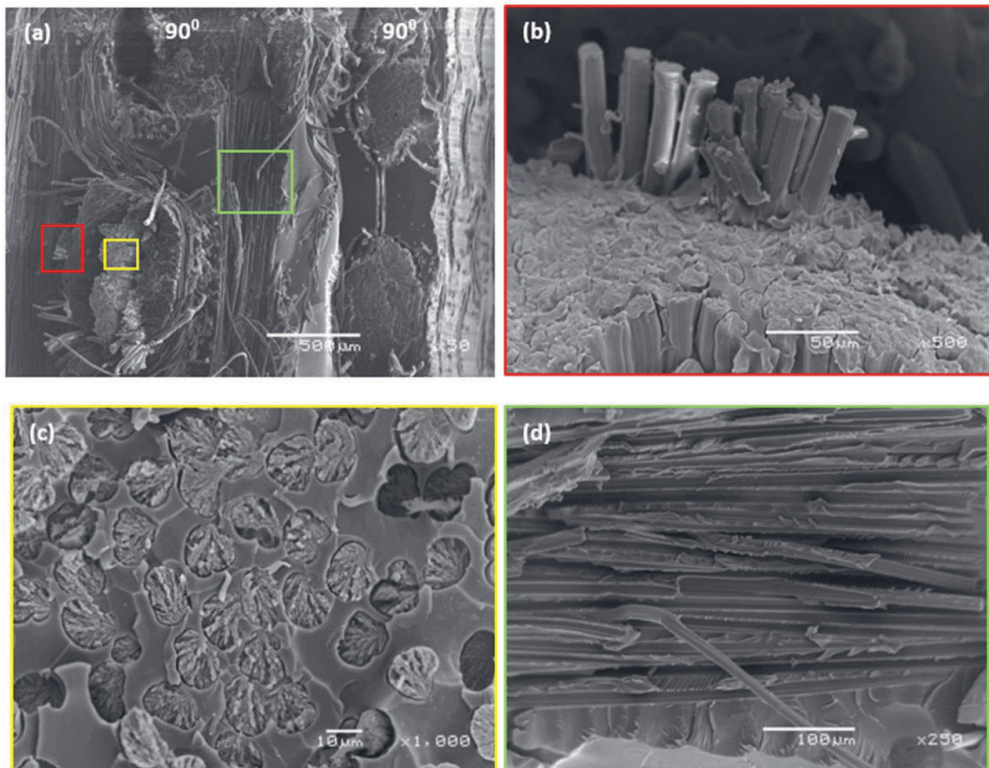


Figure 14. SEM images from impact fracture surface of RS0-C composites (a) $\times 50$, (b) $\times 500$ red square in $\times 50$ image, (c) $\times 1000$ yellow square in $\times 50$ image, (d) $\times 250$ green square in $\times 50$ image. [Color figure can be viewed at wileyonlinelibrary.com]

shearing [Figure 15(a,d)]. One notable difference compared to RS0-C composite is that the matrix cracking in the resin-rich region was not observed during the fracture surface analysis of RS5–70-C composites [Figure 15(d)]. Another observation was the microtextures supporting the shearing of the matrix [Figure 15(a)] in resin rich area.

When a composite material is tested under impact, some part of the energy related to impact is used for elastic deformation of the composite material. The energy in excess is dissipated in forms of fiber/bundle breakage, delamination, fiber–matrix debonding, and matrix cracking.⁴⁴ The failure modes occurring in Charpy impact test of composite materials is often complex. All three basic failures; tension, compression, and shear is exhibited by the tested specimen.⁴⁴ The results obtained from this study are supporting the above observations. One of the two 90° layers failed under combined tension/shear mode, while the other 90° layers failed under compression. Hence in the edgewise impact testing, the load bearing bundles on the opposite side of the impact fails under tension/shear and the other fails under compression. This was commonly observed from all the analyzed failure surfaces irrespective of the type of the resin modification. The fractography analysis supports the experimental results obtained from the

Charpy impact testing. There was an increase in impact strength of the composites prepared with APTES-modified resin. Among the modified resin-based composites, the impact strength of RS5–70-C composites almost doubled compared to RS0-C composites. The improvement in the toughness of the resin is evident when comparing the resin rich areas of the RS0-C composites and RS5–70-C composites. The resin-rich region in the RS5–70-C composite was much more impact resistance when considering the matrix crack formation observed in the RS0-C composites. Also, the microtextures indicating the shear failure in the resin-rich region is also indicating the improved impact resistance of the epoxy composite after the APTES-modification. The impact failure surface with evidence of shear failure shows improved impact resistance. Thus, it is assumed that the epoxy resin modification with compatible SCAs like APTES improves the toughness of the resultant composite.

CONCLUSIONS

In our previous study, an epoxy resin was modified with APTES. The results from that study showed that the APTES-modified epoxy resin increased the tensile strength and elongation of the viscose fabric composite. It is a necessity to know

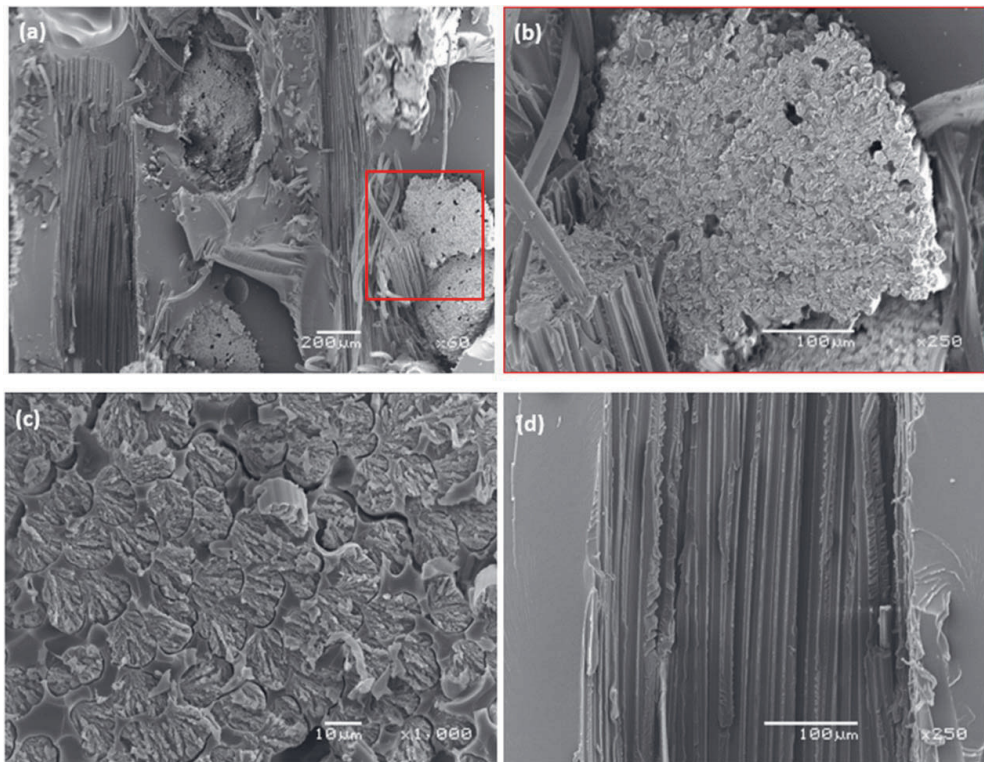


Figure 15. SEM images from impact fracture surface of RS5-70-C composite. [Color figure can be viewed at wileyonlinelibrary.com]

the effect of resin modification on different properties of composites, to confirm the viability of using resin modification over existing fiber modification method in composite preparation. The main conclusions from the current study are listed below.

The storage modulus and $\tan \delta$ results point out an increase in interfacial adhesion between the viscose fabric and the APTES-modified epoxy resin.

The impact resistance of the composites increased with increasing APTES content. Impact resistance of composites prepared from epoxy resin modified with 5 wt % APTES almost doubled compared to RS0-C composites.

The effect of resin modification and fabric modification on flexural strength except for RS3-70-C was insignificant compared to unmodified composite.

The burning rate of the RS0-FS2-C composites was lower than all other composites owing to the fabric modification. However, the burning rate of all the composites irrespective of modifications is rated to be satisfactory for use in automotive applications.

The modification of the epoxy resin by APTES seems to be a better option when considering the less process waste and low energy consumption compared to wet chemical fabric modification methods like alkali, acetylation, and silane treatments. In our studies, it was found that the epoxy resin modification by APTES improved the tensile and impact resistance properties

compared to unmodified and fabric-modified composites. It is worth mentioning that the epoxy resin modification by APTES has doubled the toughness of the viscose fabric composites. Thermal stability of the resin-modified composites and fabric-modified composites are unchanged compared to unmodified composites. While the burning rate was higher for resin-modified composites compared to fabric-modified composites.

ACKNOWLEDGMENTS

This study has received funding from European Union's Seventh Framework Programme (FP7), for the project ECOGEL-CRONOS (Grant No. 609203). The authors gratefully acknowledge the financial support received for the project.

REFERENCES

- Pickering, K. L.; Efendy, M. G. A.; Le, T. M. *Compos. Part A* **2016**, *83*, 98.
- Anbukarasi, K.; Kalaiselvam, S. *Mater. Des.* **2015**, *66*, 321.
- Gunning, M. A.; Geever, L. M.; Killion, J. A.; Lyons, J. G.; Higginbotham, C. L. *Polym. Test.* **2013**, *32*, 1603.
- Etaati, A.; Pather, S.; Fang, Z.; Wang, H. *Compos. Part B* **2014**, *62*, 19.
- Scida, D.; Bourmaud, A.; Baley, C. *Mater. Des.* **2017**, *122*, 136.

6. Ramamoorthy, S. K. PhD Thesis, University of Borås (2015).
7. Rajan, R.; Riihivuori, J.; Rainosalo, E.; Skrifvars, M.; Jarvela, P. *J. Reinf. Plast. Compos.* **2014**, *33*, 1416.
8. Mader, A.; Volkmann, E.; Einsiedel, R.; Müssig, J. *J. Biobased Mater. Bioenergy* **2012**, *6*, 481.
9. Li, X.; Tabil, L. G.; Panigrahi, S. *J. Polym. Environ.* **2007**, *15*, 25.
10. John, M. J.; Anandjiwala, R. D. *Polym. Compos.* **2008**, *29*, 187.
11. George, J.; Sreekala, M. S.; Thomas, S. *Polym. Eng. Sci.* **2001**, *41*, 1471.
12. Sreekala, M. S.; Thomas, S. *Compos. Sci. Technol.* **2003**, *63*, 861.
13. Zhou, Y.; Fan, M.; Chen, L. *Compos. Part B: Eng.* **2016**, *101*, 31.
14. Sun, D. In *Biodegradable Green Composites*; Kalia, S., Ed.; John Wiley & Sons, Inc.: Hoboken, NJ, **2016**; Chapter 2.
15. Wu, H. F.; Dwight, D. W.; Huff, N. T. *Compos. Sci. Technol.* **1997**, *57*, 975.
16. Park, S.-J.; Jin, J.-S. *J. Polym. Sci. Part B: Polym. Phys.* **2003**, *41*, 55.
17. Cui, H.; Kessler, M. R. *Compos. Part A: Appl. Sci. Manuf.* **2014**, *65*, 83.
18. Shokoohi, S.; Arefazar, A.; Khosrokhavar, R. *J. Reinf. Plast. Compos.* **2008**, *27*, 473.
19. Xie, Y.; Hill, C. A.; Xiao, S.; Miltz, Z. H.; Mai, C. *Compos. Part A: Appl. Sci. Manuf.* **2010**, *41*, 806.
20. Abdelmouleh, M.; Boufi, S.; Belgacem, M. N.; Duarte, A. P.; Ben Salah, A.; Gandini, A. *Int. J. Adhes. Adhes.* **2004**, *24*, 43.
21. Jiang, M.-Y.; Wu, L.-K.; Hu, J.-M.; Zhang, J.-Q. *Corros. Sci.* **2015**, *92*, 118.
22. Bera, S.; Rout, T.; Udayabhanu, K. G.; Narayan, R. *Prog. Org. Coatings* **2016**, *101*, 24.
23. Ji, W.-G.; Hu, J.-M.; Liu, L.; Zhang, J.-Q.; Cao, C.-N. *Prog. Org. Coatings* **2006**, *57*, 439.
24. Chruściel, J. J.; Leśniak, E. *Prog. Polym. Sci.* **2015**, *41*, 67.
25. Coltrain, B. K.; Rakes, G. A.; Smith, V. K. (Eastman Kodak Co.). U.S. Pat. 5019607A (1991).
26. Goda, H.; Higashino, T. (Arakawa Chemical Industries Co. Ltd.). U.S. Pat. 6525160B1 (2003).
27. Aida, H.; Tsuchiya, K. (Arakawa Chemical Industries Co. Ltd.). Jpn. Pat. 3570380B2 (2004).
28. Aida, H.; Tsuchiya, K. (Arakawa Chemical Industries Co. Ltd.). Jpn. Pat. 3458379B2 (2003).
29. Min, Q.; Yihui, Y.; Nankai, G.; Qianping, Q.; Jiaping, L. (Jiangsu Subotic New Material Co. Ltd.; Bote Building Materials (Tianjin) Co. Ltd.). Chin. Pat. 103468095B (2016).
30. Yang, J.; Xiao, J.; Zeng, J.; Bian, L.; Peng, C.; Yang, F. *Fibers Polym.* **2013**, *14*, 759.
31. Rajan, R.; Rainosalo, E.; Thomas, S. P.; Ramamoorthy, S. K.; Zavasnik, J.; Vuorinen, J.; Skrifvars, M. *Polym. Bull.* DOI 10.1007/s00289-017-2022-2.
32. Available at: <http://www.gurit.com/sitecore/content/Old-Product-Pages/Other-Products/Laminating-Infusion-Systems/PRIME-20LV> (accessed December 2017).
33. Cheng, Q.; Wang, S.; Rials, T. G.; Lee, S. H. *Cellulose* **2007**, *14*, 593.
34. Suresh Kumar, S. M.; Duraibabu, D.; Subramanian, K. *Mater. Des.* **2014**, *59*, 63.
35. SabaJawaid, N. M.; Allothman, O. Y.; Paridah, M. T. *Constr. Build. Mater.* **2016**, *106*, 149.
36. Pothan, L. A.; Thomas, S.; Groeninckx, G. *Compos. Part A: Appl. Sci. Manuf.* **2006**, *37*, 1260.
37. Hameed, N.; Sreekumar, P. A.; Francis, B.; Yang, W.; Thomas, S. *Compos. Part A: Appl. Sci. Manuf.* **2007**, *38*, 2422.
38. Braun, D.; Cherdron, H.; Ritter, H. In *Polymer Synthesis: Theory and Practice*; Braun, D.; Cherdron, H.; Rehahn, M.; Ritter, H.; Voit, B., Eds.; Springer: Berlin, Heidelberg; **2001**; Chapter 2.
39. Woo, E. M.; Seferis, J. C.; Schaffnit, R. S. *Polym. Compos.* **1991**, *12*, 273.
40. Pothan, L. A.; Zachariah, O.; Thomas, S. *Compos. Sci. Technol.* **2003**, *63*, 283.
41. d'Almeida, L. F. S.; Calado, V.; Barreto, D. W.; d'Almeida, J. R. M. *J. Therm. Anal. Calorim.* **2011**, *103*, 179.
42. Saha, K.; Das, S.; Bhatta, D.; Mitra, B. C. *J. Appl. Polym. Sci.* **1999**, *71*, 1505.
43. Jawaid, M.; Abdul Khalil, H. P. S.; Alattas, O. S. *Compos. Part A: Appl. Sci. Manuf.* **2012**, *43*, 288.
44. Ahmad, S. H.; Rasid, R.; Bonnia, N. N.; Zainol, I.; Mamun, A. A.; Bledzki, A. K.; Beg, M. D. H. *J. Compos. Mater.* **2011**, *45*, 203.
45. Sreekumar, P. A.; Saiah, R.; Saiter, J. M.; Leblanc, N.; Joseph, K.; Unnikrishnan, G.; Thomas, S. *Compos. Interfaces* **2008**, *15*, 629.
46. Gopalakrishnan, P.; Saiah, R.; Gattin, R.; Saiter, J. M. *Compos. Interfaces* **2008**, *15*, 759.
47. Carrillo, F.; Colom, X.; Suñol, J. J.; Saurina, J. *Eur. Polym. J.* **2004**, *40*, 2229.
48. Gaan, S.; Rupper, P.; Salimova, V.; Heuberger, M.; Rabe, S.; Vogel, F. *Polym. Degrad. Stab.* **2009**, *94*, 1125.
49. Wang, W. J.; Perng, L. H.; Hsue, G. H.; Chang, F. C. *Polymer* **2000**, *41*, 6113.
50. Hsue, G.-H.; Wei, H.-F.; Shiao, S.-J.; Kuo, W.-J.; Sha, Y.-A. *Polym. Degrad. Stab.* **2001**, *73*, 309.
51. Chai, M. PhD Thesis, The University of Auckland (2014).
52. Kozłowski, R.; Władysław-Przybylak, M. *Polym. Adv. Technol.* **2008**, *19*, 446.
53. Levchik, S. V.; Weil, E. D. *Polym. Int.* **2004**, *53*, 1901.
54. Iji, M.; Kiuchi, Y. *J. Mater. Sci. Mater. Electron.* **2001**, *12*, 715.
55. Tserki, V.; Zafeiropoulos, N.; Simon, E. F.; Panayiotou, C. *Compos. Part A: Appl. Sci. Manuf.* **2005**, *36*, 1110.
56. Försth, M.; Modin, H.; Sundström, B. *Fire Mater.* **2013**, *37*, 350.

PUBLICATION IV

Wood plastic composites with improved electrical and thermal conductivity

Rathish Rajan, Jonne Näkki, Rama Layek, Egidija Rainosalo

Wood Science and Technology (2021) 55 (3), 719-739

<https://doi.org/10.1007/s00226-021-01275-9>

Publication reprinted with the permission of the copyright holders.

Wood plastic composites with improved electrical and thermal conductivity

Rathish Rajan^{1,2}  · Jonne Näkki¹ · Rama Layek^{2,3} · Egidija Rainosalu¹

Received: 3 August 2020 / Accepted: 16 February 2021

© The Author(s), under exclusive licence to Springer-Verlag GmbH Germany, part of Springer Nature 2021

Abstract

Graphene nanoplatelets (GNP) are used to produce wood plastic composites (WPC) with improved electrical and thermal conductivity. The polypropylene/wood/GNP hybrid composites are produced by melt compounding followed by hot pressing. The effect of GNP loadings (5, 10 and 15 wt%) on electrical conductivity, thermal conductivity, tensile properties, and thermal degradation of hybrid WPC containing 20 wt% of wood flour is studied. The effect of fast and slow cooling rates during hot pressing on the surface resistivity of hybrid WPC is evaluated. Scanning electron microscopy of the tensile fracture surface and polished cross-sections of hybrid WPC is analysed. The hybrid WPC containing 20 wt% wood flour and 15 wt% of GNP (PP-W20-G15) is measured to show surface resistivity of $2.05E+06 \Omega/\text{sq}$ and thermal conductivity of 0.61 W/m.K . There is a significant increase in electrical and thermal conductivity of PP-W20-G15 when compared to WPC containing 20 wt% of wood flour (PP-W20). The wood flour helps with the distribution of GNP in PP-W20-G15 by which the surface resistivity is improved when compared to PP filled with 15 wt% GNP. It was found that the surface resistivity of PP-W20-G15 was dependent on the cooling rate used during the hot pressing. There is a considerable decrease in tensile strength and an increase in the tensile modulus of hybrid WPCs compared to PP-W20 and neat polypropylene.

✉ Rathish Rajan
rathish.rajan@centria.fi

¹ Research and Development, Centria University of Applied Sciences, Talonpojankatu 2, 67100 Kokkola, Finland

² Department of Materials Science, Tampere University of Technology, P.O. Box 589, 33101 Tampere, Finland

³ Department of Separation Science, School of Engineering Science, LUT University, Mikkulankatu 19, 15210 Lahti, Finland

Introduction

The demand for electrically conductive composites is on the rise due to the growing need for antistatic materials for various applications including packaging and electronics that are susceptible to electrostatic damage or in electromagnetic shielding applications (Choi et al. 2019; Yadav et al. 2019). Compared to conventional antistatic materials that are used currently, conductive polymer composites are cheap, lightweight, flexible, and easy to design and manufacture. Electrically conductive composites prepared from polymers other than intrinsically conducting polymers usually incorporate electrically conductive fillers to introduce the electrical functionality in the polymer. Commonly used electrically conductive fillers include carbon black (Al-Saleh et al. 2013; Choi et al. 2019; Yang et al. 2015), carbon nanotubes (Al-Saleh et al. 2013), carbon fibres (Yang et al. 2015), and graphene (Haznedar et al. 2013).

The electrical resistance of air-dried wood is higher than $10^{12} \Omega$ and for insulating plastics, it is equal to or higher than $10^{11} \Omega$ (Fu and Yuan 2017). The electrostatic charge is generated on the surface of insulating material due to the piezoelectric effect caused by friction or mechanical effect. Due to high electrical resistance, electrostatic charges are prevented from escaping by allowing electrostatic charge build up on the surface. The electrostatic discharge (ESD) can occur through the high-intensity transfer of charge between two objects of different electrostatic potential when contacted (Moultif et al. 2017). Antistatic agents when applied as a surface coating or as an internal additive with polymers can prevent the electrostatic charge accumulation by decreasing the bulk volume or surface resistivity. The resistance of packaging materials according to ANSI/ESD S541 is tabulated in Table 1.

Bio-composites play an essential role in various industries as an alternative to materials from fossil-fuel (Alemdar and Sain 2008). Wood-plastic composites (WPC) are bio-composites produced from wood fibre and synthetic or bio-based plastics. Currently, WPC is used in building and construction, automotive, and household applications. The applications of WPC can be expanded to new industries by tailoring the properties of wood-plastic composites. As an example, incorporating electrical and thermal conductivity in WPC can open its application to products demanding these functional properties. Conductive (electrical and/or thermal) thermoplastic compounds are available in the market for producing products requiring antistatic properties, electromagnetic interference shielding (EMI shielding), and for those products used in thermal management in the electrical and electronic industry (Biron 2018).

Table 1 Classification of packaging materials based on surface resistance

Material designation	Surface resistance (Ω)
Electric field shielding	$< 10^3$
Conductive	$< 10^4$
Dissipative/Antistatic	$\geq 10^4 - < 10^{11}$
Insulative	$\geq 10^{11}$

Hybridization of WPC with functional inorganic fillers and nanofillers are of interest since these fillers can impart special functionality to the WPC. Hybrid polymer composites are those with two or more reinforcing materials embedded in a matrix polymer. Most of the literature studies related to hybrid composites indicate that the hybridization results in multifunctional polymer composites. It is also understood from the related literature that there is a synergic effect of reinforcing fillers, which may increase certain properties of the composites (Lee et al. 2011; Papageorgiou et al. 2016; Pedrazzoli and Pegoretti 2013; Pedrazzoli et al. 2015; Thwe and Liao 2003).

Graphene has received a lot of interest in recent years due to its exceptional mechanical, thermal, and electrical properties. Graphene is a two-dimensional allotrope of carbon made up of a single layer of sp^2 hybridized carbon atoms (Phiri et al. 2017). The structures with several layers of carbon atoms are called graphene nanoplatelets (GNPs) which are reported to be used as nanofillers to improve the various properties of polymer nanocomposite even at a low filler loading (Tripathi et al. 2017). A major challenge of using graphene as filler in polymer composites remains the high price compared to alternatives like carbon black. According to a recent study (Batista et al. 2019), the research-grade graphene powder is priced at 1–50 \$/g and mass-produced graphene is available from as low as \$20/kg to \$800/kg. The specialty carbon black is sold for \$50/kg and high conductive carbon black cost around \$25/kg (Mertens 2017). Considering that the desired property is reached at a much lower graphene loading compared to carbon black and the multi functionalities offered, graphene is a reasonable choice as filler for developing polymer composites. Several processing methods such as in-situ, solution casting, and melt mixing are used to prepare thermoplastic polymer-based nanocomposites (Tripathi et al. 2017). Since melt mixing is a well-established processing technique in the plastic industry, a lot of research has been devoted to graphene-based polymer nanocomposites (Kalaitzidou et al. 2007; Kim and Macosko 2009; Zhang et al. 2010; Zhao et al. 2007; Zheng et al. 2004). These studies indicate that graphene addition improves the mechanical properties of nanocomposites at a lower filler content. The percolation threshold in terms of electrical conductivity for the composites prepared by the melt mixing method is reached at a higher GNP loading compared to in-situ and solution mixing methods (Khanam et al. 2016). Hence, the electrically conductive graphene-based nanocomposites (GNP loading above 10 wt%) prepared by the melt mixing method show low mechanical properties due to graphene agglomeration.

Few studies have reported on the influence of GNP's on the properties of WPC. Most of those were focused on the influence of GNP's on mechanical and thermal properties. Sheshmani et al. (2013) studied the polypropylene/wood/GNP system and reported that the tensile and flexural properties of the hybrid composites increased at 0.8 wt% of GNP content. They also indicated that strength decreased due to agglomeration when the content of GNP's was increased to 3–5 wt%. In another study, polyvinylchloride/wood/GNP system was developed to be used as electromagnetic interference shielding material (Karteri et al. 2017).

To the best of the author's knowledge, studies that address the electrical and thermal conductivity of polypropylene/wood flour/GNP hybrid composites produced through the melt mixing method followed by compression moulding have not been

published. The electrical and/or thermally conductive fillers used to introduce electrical or thermal conductivities in WPC may favourably or adversely affect other important properties of the hybrid WPC. Thus, it is important to study the electrical/thermal conductivities and the mechanical properties of the hybrid WPC. The overall objective of this study is to prepare and characterize the polypropylene-based antistatic wood plastic composites containing GNP's that can be utilized to produce ESD safe products such as ESD safe enclosures or containers and ESD safe WPC composite decking.

Experimental

Materials

The WPC masterbatch (WPC-MB) containing 50 wt% wood flour and polypropylene (PP) was purchased from a WPC granulate manufacturer. The softwood flour consists of spruce and fir with a maximum size of 500 μm . The masterbatch contains 3 wt% of additives including MAPP. The GNP masterbatch (GNP-MB) PP @ 30% heXo-G V20 was purchased from NanoXplore Inc, Canada. The GNP in the masterbatch is heXo-G V20 with an average thickness of 20 nm (40 layers) and a flake size of 50 μm . The heXo-G V20 is commercially sold for \$20/kg. The PP used in the masterbatch is an impact copolymer 4220H from Pinnacle Polymers. The polypropylene in WPC and the PP used to dilute WPC masterbatch was Moplen EP240H, which is an impact-resistant copolymer produced by LyondellBasell.

Preparation of hybrid wood plastic composites

The hybrid WPC's were prepared by two-stage melt compounding in a co-rotating twin-screw extruder ZSK 18 MEGAlab from Coperion, Germany. The barrel length of the extruder was 72 mm and the outer diameter of the screw was 18 mm ($D_o/D_i=1.55$). The pre-mixed wood plastic composites containing 24 wt% (WPC1), 30 wt% (WPC2), and 40 wt% (WPC3) of wood flour were prepared by diluting WPC-MB (50 wt% wood flour) with Moplen EP240H. In the second stage, WPC1 (83.5 wt%)/GNP-MB (16.5 wt%), WPC2 (66.6 wt%)/GNP-MB (33.4 wt%), and WPC3 (50 wt%)/GNP-MB (50 wt%) were melt mixed to produce PP-W20-G5, PP-W20-G10, and PP-W20-G15, respectively. The pre-mix was fed from the main feeder and GNP-MB was fed from the side feeder. The compounding was done at a screw speed of 150 rpm and the total feed rate was 5 kg/h. The extruder temperature was set to 190 °C until the melting zone and then it was set to 200 °C in the discharge zone. The extrudate was cooled in water and finally pelletized and saved for further use. The designations and composition of hybrid wood plastic composites are listed in Table 2.

The WPC plates were made by hot pressing the hybrid WPC pellets. The pressing was done in a manual hydraulic hot press at a temperature of 220 °C for 3 min with a press load of 3.5 MPa. Initially, a pre-heating time of 15 min was given before the

Table 2 Designations and composition of hybrid wood plastic composites

Composites	PP (%)	Wood flour (%)	GNP (%)
PP	100	0	0
PP-W20	80	20	0
PP-W20-G5	75	20	5
PP-W20-G10	70	20	10
PP-W20-G15	65	20	15

load was applied. The size of the plates was 200 mm × 200 mm with a thickness of 3.6–3.8 mm. These plates were later CNC machined to test specimens.

Characterization

The surface resistivity measurement was done according to ASTM D257—07: Standard Test Method for DC Resistance or Conductance of Insulating Materials. Surface resistivity was measured by applying a voltage potential across the surface of the insulator sample and measuring the resultant current (I) as shown in Fig. 1.

The electrode system is a circular flat metal plate type concentric ring electrode Vermason H108C (upper electrode) and H116BC (lower electrode). The power supply was TRACOPOWER MHV12—0.5 K6000P, 500 V. Voltmeter used was Fluke 45 Dual display multimeter and ammeter was Keithley model 6485 Picoammeter. The measurement was taken at 500 V and was done in a room maintained at a temperature of $21\text{ }^{\circ}\text{C} \pm 2$. The current reading from picoammeter was noted 60 s after the start of measurement. The surface resistivity measurement of all other samples was taken following the same procedure. Two plates each with 100 mm × 100 mm and thickness of 3.6–3.8 mm were measured for all the samples. Results are an average of four measurements taken from both surfaces of the two plates. The surface resistance of PP-W20-G15 prepared by slow and fast cooling was measured

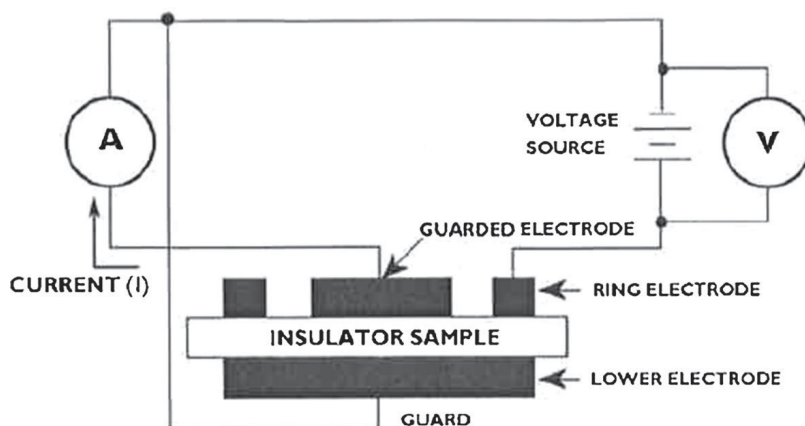


Fig. 1 Surface resistivity measurement method

following the same procedure explained above except that the thickness of the test samples was 2 mm and test voltage was 100 V. The surface resistivity was calculated from Eq. (1).

$$\text{Surface resistivity } \rho_s = \frac{\pi(D1 + D2)}{(D2 - D1)} R_s \quad (1)$$

where $D1$ is the outer diameter of the inner ring in cm; $D2$ inner diameter of the outer ring in cm; R_s is measured resistance in ohms.

Netsch LFA 467 device with Proteus LFA software was used to measure the thermal diffusivity and $C_p(T)$ of the samples at 25 °C. Prior to the measurements, the surface of the sample was coated using a graphite spray. The rear surface of the samples was heated by exposing a short light xenon laser pulse on the rear surface and the temperature change of the opposite side of the sample was detected using an infrared detector. The thermal diffusivity was calculated using Eq. (2) (Parker et al. 1961).

$$\alpha = 0.1338d^2/t_{1/2} \quad (2)$$

where α = the thermal diffusivity; d = thickness of the sample, and $t^{1/2}$ = time at the half signal height.

$$\kappa(T) = \alpha(T) \times c_p(T) \times \rho(T) \quad (3)$$

The thermal conductivity of the samples was computed at 25 °C using Eq. (3). Where $\kappa(T)$, $\alpha(T)$, $c_p(T)$, and $\rho(T)$ are the thermal conductivity, thermal diffusivity, specific heat capacity, and experimental density of the sample, respectively. The density of PP, PP-W20, PP-G15, and PP-W20-G15 was measured as 0.90, 0.94, 0.97, and 1.04, respectively. The size of the specimens was 9.8 mm in diameter and 1.3 mm in thickness and the result presented is an average of 5 specimens.

The tensile test was performed according to ISO 527–2:2012 using a Tiratest 2705 tensile testing machine equipped with a 5kN load cell. The test was carried out at room temperature with a speed of 5 mm/minute. The length of the sample was 150 mm and the length of the narrow portion was 80 mm. The thickness of tensile specimens was 3.6–3.8 mm. Tensile properties are calculated as an average of 5 specimens. Tensile modulus is calculated from the slope of the stress/strain curve in the strain interval between 0.05% and 0.25%.

The examination of the platinum-coated tensile fracture surface was performed on JEOL JCM-6000 Neoscope scanning electron microscope with an electron acceleration voltage of 15 kV. For polished cross-section surfaces, the examination was made without a coating and with an acceleration voltage of 1 kV to reduce charging of the surface on Zeiss EVO 50VP scanning electron microscope.

Thermal degradation of the hybrid WPC was studied using a thermogravimetric analyzer, Netsch TG 209. The test was conducted in a nitrogen atmosphere by heating from 25 °C to 800 °C at 10 °C/minute. The sample mass for all the composites was 20 mg (± 2). The results from one of the two specimens tested are reported. The effect of cooling rate on melting and crystallization behaviour of the PP-W20-G15

was determined using Netzsch DSC 204 in a nitrogen atmosphere. The sample mass for all the composites was 10 mg (± 2), and the results from one of the two specimens tested are reported. The first heating was done from a temperature of 25 to 220 °C at a rate of 40 °C/min followed by isothermal heating for 20 min representing the press time of the composites. The cooling was done at two different cooling rates of 2 °C/min or 40 °C/min. The second heating was performed at 40 °C/min.

A one-way analysis of variance (ANOVA) was performed on the collected data to determine the statistically significant differences ($p = < 0.05$) among the surface resistivity, thermal conductivity, and tensile properties of the composites. A paired *t*-test was performed on surface resistivity data to determine the statistical significance between the slow and fast cooling rate on the surface resistivity of composites containing 20 wt% of wood fibre and 15 wt% GNP (PP-W20-G15). The statistical analyses were performed using a free and open-source statistical analysis software JASP (Version 0.14.1).

Results and discussions

Surface resistivity

The surface resistivity of PP/GNP and functionalized WPC is listed in Table 3. The percolation threshold is reached at 15% by weight in the case of PP/GNP and hybrid composites. The surface resistivity of PP-G15 and PP-W20-G15 decreased several orders of magnitude to $10^8 \Omega/\text{sq}$ and $10^6 \Omega/\text{sq}$, respectively. The results from surface resistivity measurements indicate that the surface resistivity decreased by the incorporation of 15 wt% GNP in both PP and WPC containing 20% by weight of wood filler.

The electrical conduction mechanism in the insulating polymer/conductive filler composites is described based on the percolation theory. The electrical conductivity in those composites is due to free electron movement through the conductive path formed by conductive fillers at a critical filler loading. At this critical filler loading, there is a sudden increase in electrical conductivity after which

Table 3 Effect of GNP on the surface resistivity of PP/GNP and wood plastic composites

Composites	Surface resistivity (Ω/sq)	SD
PP neat	1.19E + 14	5.34E + 12
PP-W20	1.08E + 14	6.19E + 12
PP-G5	1.05E + 14	7.25E + 12
PP-G10	1.00E + 14	3.55E + 12
PP-G15	8.83E + 08	8.43E + 08
PP-W20-G5	4.96E + 14	6.67E + 12
PP-W20-G10	4.48E + 14	1.90E + 13
PP-W20-G15	2.90E + 06	2.05E + 06

it gets saturated. This critical filler concentration is known to be the electrical percolation threshold concentration (Tripathi et al. 2017).

The result from this study is in agreement with the findings in the literature related to PP/GNP composites. The percolation threshold for PP/GNP composites prepared through melt extrusion was found to be above 10 wt% (4.4 vol%) (Imran et al. 2018) and 15 wt% (6.7 vol%) (Park et al. 2007). The percolation threshold for PP/GNP and hybrid composites in this study is reached at 15 wt% (6.7 vol%). The size of the GNP is an important factor affecting the electrical conductivity of extrinsically conductive polymers. The percolation threshold in PP/GNP composites was reported to decrease with increasing flake size (Jun et al. 2018). The percolation threshold for PP composites containing GNP with flake sizes of 150 μm and 2 μm is 2.99 vol% and > 9.29 vol%, respectively, as reported in the literature (He et al. 2017). They also found that a lower thickness of layers improves electrical conductivity. The GNP used in this study has an average flake size of 50 μm and an average thickness of 20 nm. Since the percolation threshold for hybrid WPC was the same as for PP/GNP as found in the present study, it is assumed that using GNP with a larger flake size will initiate the formation of the conductive network at a low percolation threshold and the thinner GNP can facilitate fast electronic movement between the layers resulting in improvement of electrical conductivity in hybrid WPC's.

The WPC containing 20 wt% of fibre and 15 wt% GNP is more conductive than PP with the same loading (15 wt%) of GNP alone (Fig. 2). The total insulating components (PP and/or wood) in both PP-G15 and PP-W20-G15 are 85 wt%. The total amount of conductive filler in both PP/GNP and hybrid composite being the same, the decreased surface resistivity of hybrid composite is due to the good distribution of GNP in the presence of wood filler. The SEM images from the polished surface of PP neat and hybrid WPCs are seen in Fig. 3d. It is evident that in the presence of wood fibre, the GNP was well distributed compared to the PP-G15 composite (Fig. 3c). Good distribution of GNP helped with forming a more effective conductive path in PP-W20-G15 hybrid composite.

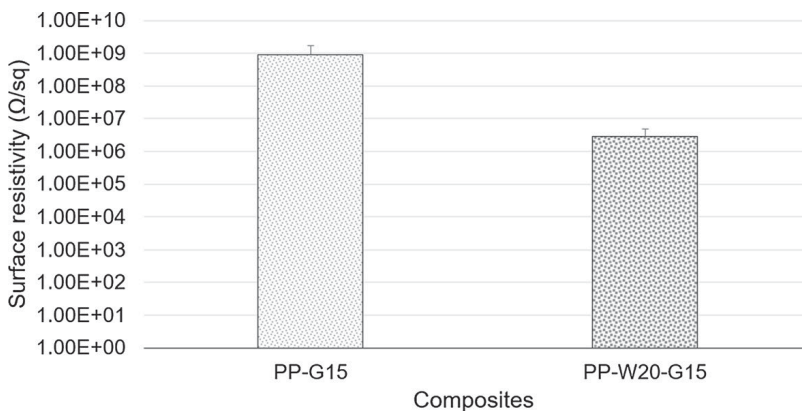


Fig. 2 Surface resistivity of PP and wood plastic composites containing 15 wt% of graphene nanoplatelets

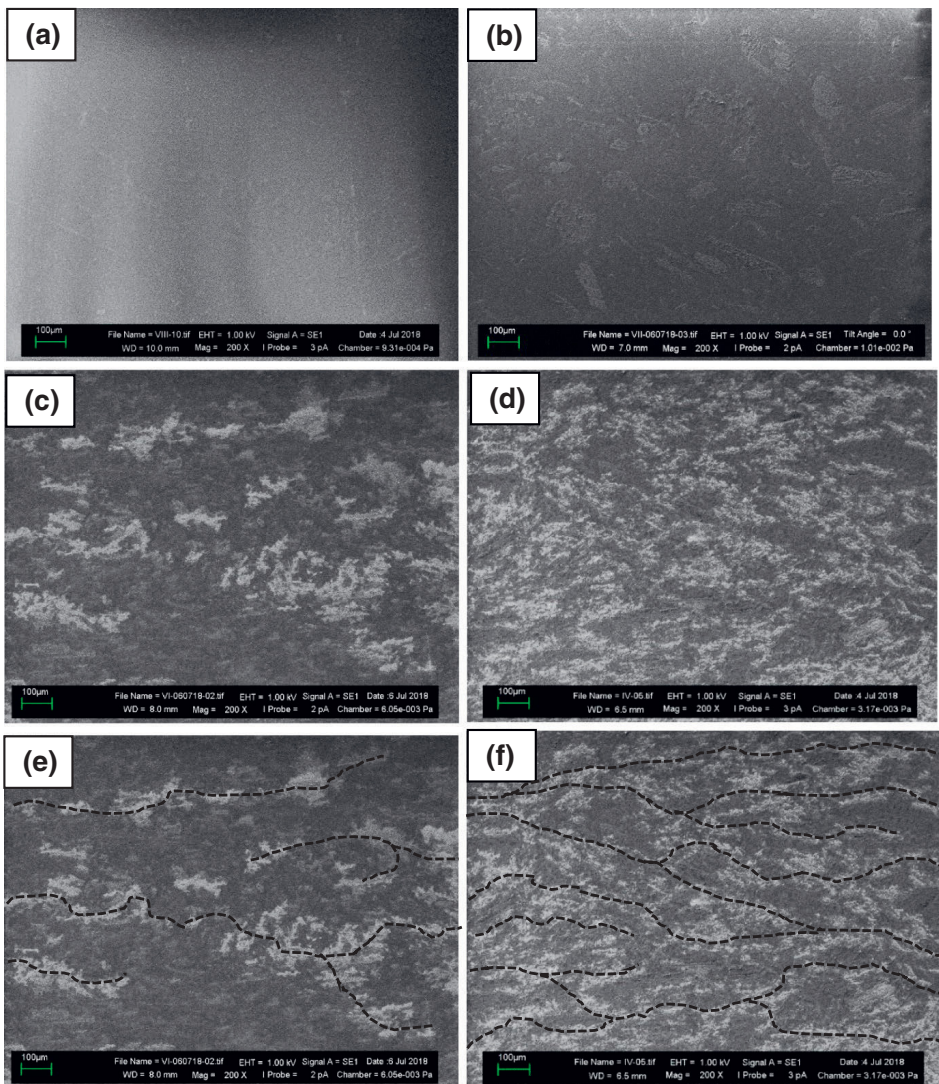


Fig. 3 SEM images from the polished surface of (a) PP neat (b) wood plastic composite—PP-W20 (c) antistatic composites filled with GNP (PP-G15) (d) antistatic/dissipative wood plastic composite filled with wood flour and GNP (PP-W20-G15) (e) dotted lines representing the continuous conductive path of GNP in PP-G15 and (f) dotted lines representing continuous conductive path of GNP in PP-W20-G15

In general, an uncoated insulator sample accumulates charge during the examination. SEM images from a cross-section of GNP-filled PP-G15 and PP-W20-G15 that were acquired with 1 kV show brighter areas. This can be explained as the “reverse” charging characteristic, where the local field effect in a conductive composite enhances the relative secondary electron emission in the isolated conductive grains (Chung et al. 1983). Similar observations in polymer/carbon nanofillers filled composites are reported elsewhere (Syurik et al. 2012, 2013). Due to this phenomenon, the conductive filler is seen brighter in a dark insulating

matrix. Due to a low acceleration voltage of 1 kV, both the penetration depth of primary electrons and the escape depth of secondary electrons (SE) are low, and only near-surface information is obtained.

The brighter GNP (15 wt%) is seen from Fig. 3c, d. In Fig. 3d, the GNP is seen to be even better distributed in the presence of 20 wt% wood fibre. The charging phenomenon directly represents the electrically conductive path of the GNP in the PP matrix as seen from the dotted lines marked in Fig. 3e, f. The results from SEM analysis support the findings from the surface resistivity measurements.

The surface resistivity of PP-W20-G15 was found to be influenced by the processing conditions during the hot pressing (Fig. 4). Two different cooling rates were used during the compression moulding; (1) fast cooling in which the composites were cooled at a rate of ≈ 14 °C/minute by running water and air through the channels in top and bottom platens in the hydraulic press and (2) slow cooling at a rate of ≈ 0.7 °C/minute, in which the composites were left in the press to cool down to 23 °C without using cooling water or air. The composite produced under slow cooling exhibits low surface resistivity ($6.97E+05$) compared to the composite produced under fast cooling ($2.52E+07$). Since there is no variation in GNP or wood flour content in the two composites, the lowering of resistivity can be related to the crystallization behaviour of the polypropylene.

DSC analysis was done on the granulates of neat polymer and hybrid WPC to study the effect of fast and slow cooling on its thermal behaviour. A cooling rate of 2 °C/minute and 40 °C/minute was used to represent slow cooling and fast cooling, respectively. It should be noted that the result presented in Table 4 does not represent the cooling rate used to produce composites. When comparing two different cooling rates, a notable difference in the case of crystallization temperature and the degree of crystallinity of PP can be observed from Table 4. The decrease in surface resistivity of PP-W20-G15-Slow produced using slow cooling can be correlated to the increase in the degree of crystallinity and crystallite size.

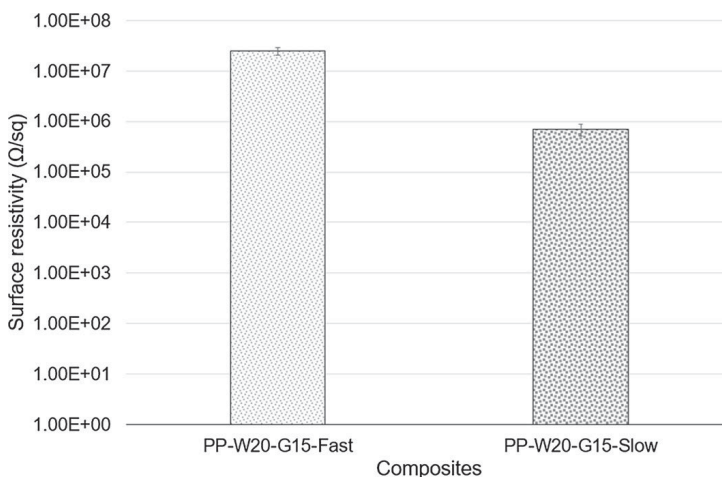


Fig. 4 Effect of cooling rate of surface resistivity of hybrid wood plastic composites

Table 4 Effect of cooling rate on the melting and crystallization behaviour of composites

Composites	T _m (°C)		T _c (°C)		χ (%)	
	Fast	Slow	Fast	Slow	Fast	Slow
PP neat	169	170	106	128	30	34
PP-W20	172	169	104	129	29	34
PP-G15	175	174	106	131	30	37
PP-W20-G15	170	172	108	132	30	36

It is documented that the formation of the conductive path is easier in the case of highly crystalline thermoplastics compared to thermoplastics with a higher amorphous phase (Chodak and Krupa 1999). According to Kalaitzidou et al. (2008), not only the degree of crystallinity but also the type of crystals, size of the crystals, and nucleating effect of GNP can affect the percolation threshold and electrical resistivity of PP-based composites. They found that the slow cooling resulted in the formation of larger, but fewer crystals compared to fast cooling in which a large number of small crystals were formed (Kalaitzidou et al. 2008). A similar observation about decreased resistivity in the case of slow cooled PP/CNT composites was made by Wang et al. (2020). They reported that by using an external nucleating agent, most CNT was prevented from participating in the nucleation of PP crystals and therefore more CNT was available for forming a conductive path. Thus, the decreased resistivity of PP-W20-G15-Slow compared to PP-W20-G15-Fast is due to an increase in crystallinity and fewer, but large crystallites formed during slow cooling. It is assumed that the wood flour participated in the nucleation of PP crystals sparing most of the GNP to form a conductive path in the case of slow cooled PP-W20-G15 by decreasing the surface resistivity. Based on the results obtained from surface resistivity measurements and according to the literature (Gulrez et al. 2014), the PP filled with 15 wt% of GNP and WPC containing 15 wt% GNP can be used in applications such as antistatic packaging for electronics and in wood plastic composites to prevent the static electricity build-up.

Thermal conductivity

The thermal conductivity of polypropylene (PP neat) and composites are shown in Fig. 5. The incorporation of 15 wt% GNP in wood plastic composites with 20 wt% of wood filler has significantly increased thermal conductivity by 130% (PP-W20-G15). The increase in thermal conductivity is attributed to the better distribution of GNP in hybrid composites in the presence of wood flour as seen from Fig. 5.

The GNP has high thermal conductivity and it is reported that incorporation of GNP in the polymer matrix can lead to an increase in thermal conductivity (Li et al. 2017). The main factors affecting the heat conduction in polymer composites containing GNP are lateral size and thickness, interfacial thermal resistance, dispersion of GNP, surface functionalization, and GNP concentration (Li et al. 2017). The heat transfer in polymer composites containing low GNP in which the fillers are unable to connect each other is highly dependent on the interfacial interaction of graphene and

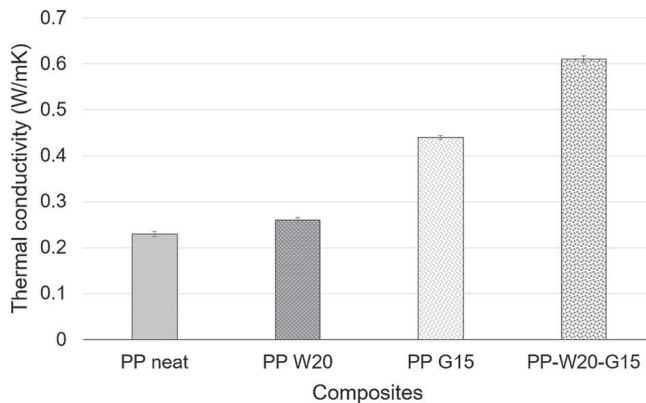


Fig. 5 Effect of GNP loading on the thermal conductivity of wood plastic composites

polymer (Li et al. 2017). Effective interaction between polymer and graphene can decrease the interfacial thermal resistance and improve the phonon transfer between polymer and graphene. In the case of polymer composites with higher GNP loading like those used in this study, the heat conduction is through the thermally conductive path formed by the GNP-GNP contact. Once the composite contacts with the heat source, the heat transfers quickly through the thermal conduction path formed by GNP. In the case of PP/GNP and PP/GNP/wood flour hybrid composites, there was no critical loading or percolation threshold identified. An increase in the thermal conductivity in both systems containing 15 wt% of GNP was observed.

A similar observation was made by other researchers in the case of hybrid WPC based on PE (Zhang et al. 2019). The wood fibre content in this study was kept at a constant loading of 40 wt.% and the GNP content in this study was 3, 6, 9, and 12 wt%. The thermal conductivity of the composite increased to ≈ 0.9 W/m.K at a GNP loading of 12 wt%. The thermal conductivity of PP/GNP composite was reported to be improved by the addition of GNP (Imran et al. 2018). The thermal conductivity increased from 0.2 to 0.25 W/m.K for PP to approximately above 0.8 W/m.K at a GNP loading of 16.7 wt%. In the present study, the introduction of 15 wt% GNP has shown an increase in thermal conductivity of PP and WPC to 0.44 W/m.K and 0.61 W/m.K respectively. Although there was an increase in thermal conductivity of PP and WPC after the addition of 15 wt% GNP, these materials are still not suitable for use in applications requiring heat dissipation.

Tensile properties

The tensile strength of PP-W20 and PP-Wood-GNP hybrid composites is shown in Fig. 6. The strength of hybrid composites decreased gradually by increasing the GNP content. The strength of PP-W20-G10 and PP-W20-G15 decreased by 10% and 20% respectively when compared to PP-W20.

The capability of GNP in enhancing the tensile properties of composites is described based on graphene structure, dispersion of fillers, and filler-matrix adhesion (Papageorgiou et al. 2017). The analysis of hybrid composites indicates that

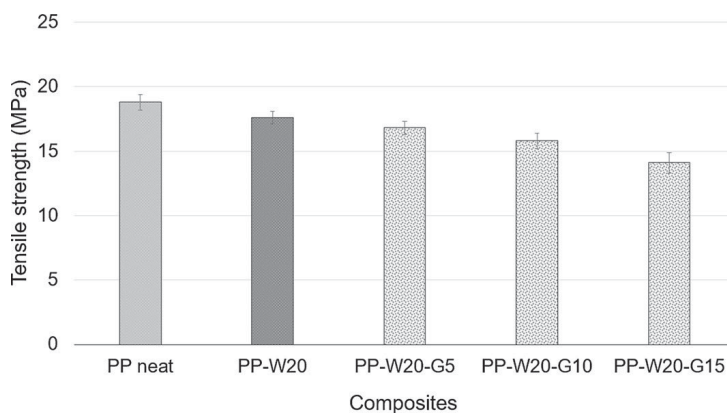


Fig. 6 Effect of GNP loading on the tensile strength of hybrid WPC

the composite's tensile strength is influenced by the presence of GNP fillers. The strength of PP-W20-G10 and PP-W20-G15 decreased (approx. 2 MPa and 4 MPa respectively) when compared to the tensile strength (18 MPa) of PP-W20. However, because of the total filler content of PP-W20-G10 and PP-W20-G15 composites (30 wt% and 35 wt% respectively), the decrease in tensile strength is quite obvious. The WPC masterbatch used to produce PP-W20 and the hybrid WPCs contained 3 wt% of additives including MAPP. A widely accepted reaction mechanism of MAPP in WPCs proceeds with the reaction of maleic anhydride in MAPP with the free hydroxyl groups in wood flour to form an ester bond. The PP segment in the MAPP then becomes entangled with the melted neat PP resulting in a mechanical link between the hydrophilic wood flour and the hydrophobic PP (Rowell 2006). However, there is an optimal concentration of MAPP until which the tensile strength increases. Excess addition of MAPP results in decreased tensile strength of composite (Leu et al. 2012). Compared to neat PP, there was no significant decrease in tensile strength of PP-W20.

Idumah and Hassan (2016) studied kenaf fibre/GNP/PP composite system and reported that usage of 5 wt% MAPP improved polymer to kenaf fibre adhesion. However, the adhesion of GNP to polymer was weak due to a lack of any chemical bond formation between GNP and MAPP. A similar observation is made from the tensile fracture surface analysis of the wood flour/GNP/PP composite system under this study. The nature of graphene to agglomerate has created stress concentration in the composite that leads to failure of composites in tensile load. The decrease in tensile properties due to the restacking of GNP at 5 wt% loading has been reported elsewhere (Idumah and Hassan 2016). In this study, the GNP loadings in hybrid WPC are above 5 wt%. The decrease in tensile strength thus can be attributed to the agglomeration of the GNP and lack of chemical interaction between GNP and polymer.

The Young's modulus of hybrid composites increased 35% when compared to PP neat and 14% compared to PP-W20 (Fig. 7). The graphene is a two-dimensional layer of carbon that possesses high stiffness (Potts et al. 2011). It seems that the reinforcing effect of graphene is increasing with increasing graphene content up to

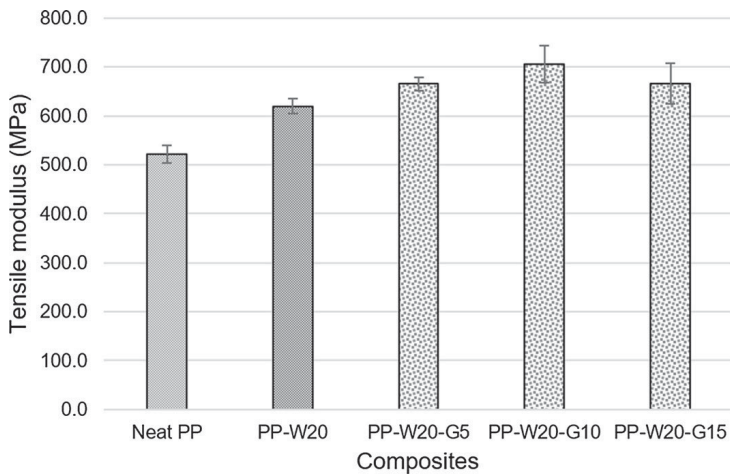


Fig. 7 Effect of GNP content on tensile modulus of hybrid WPC

10% by weight and then decreased. When compared to PP-W20, the elastic modulus of hybrid composite has improved. This indicates that the incorporation of GNP into wood plastic composite improved the stiffness of composites. The tensile modulus of graphene is 1 TPa (de Sousa et al. 2015), and the increase in stiffness with the incorporation of GNP up to an optimal concentration of filler in nanocomposites and hybrid composites is also reported in the literature (Kim et al. 2010; Sheshmani et al. 2013). The enhancement in the modulus can be attributed to the stiffness difference between the polymer and the graphene.

SEM images from the tensile fracture surface are shown in Fig. 8a–d. The surface of wood flour in the wood plastic composite containing 20 wt% flour seems to show good compatibility with PP (Fig. 8a, b). The wood flour surface seems to be rough and wetted with the polymer. Further, there is less fibre pull out observed from the SEM analysis. These observations indicate good adhesion between PP and wood fibre in the presence of MAPP as a compatibilizing agent. The analysis of both PP-G15 and PP-W20-G15 revealed clusters of agglomerated particles appearing in different sizes. The surface of GNP was found to be clean without any polymer covering which indicates low compatibility between polymer and the GNP. From Fig. 8d, the partially pulled out and broken fibres seemed to be covered with polymer indicating better adhesion between wood flour and PP in the hybrid composites. At the same time, the GNP surface is found to be without any polymer covering which indicates low compatibility with the PP in PP-W20-G15. The observations from SEM images support the finding from tensile testing which indicated the lack of adhesion between the polymer and GNP in the PP/wood/GNP system.

Thermogravimetric analysis

The TG and DTG curves from the thermogravimetric analysis are shown in Figs. 9, 10, respectively. It is evident from the TGA analysis that the introduction of GNP increased the initial degradation temperature (2% mass loss) of PP by 78 °C at a

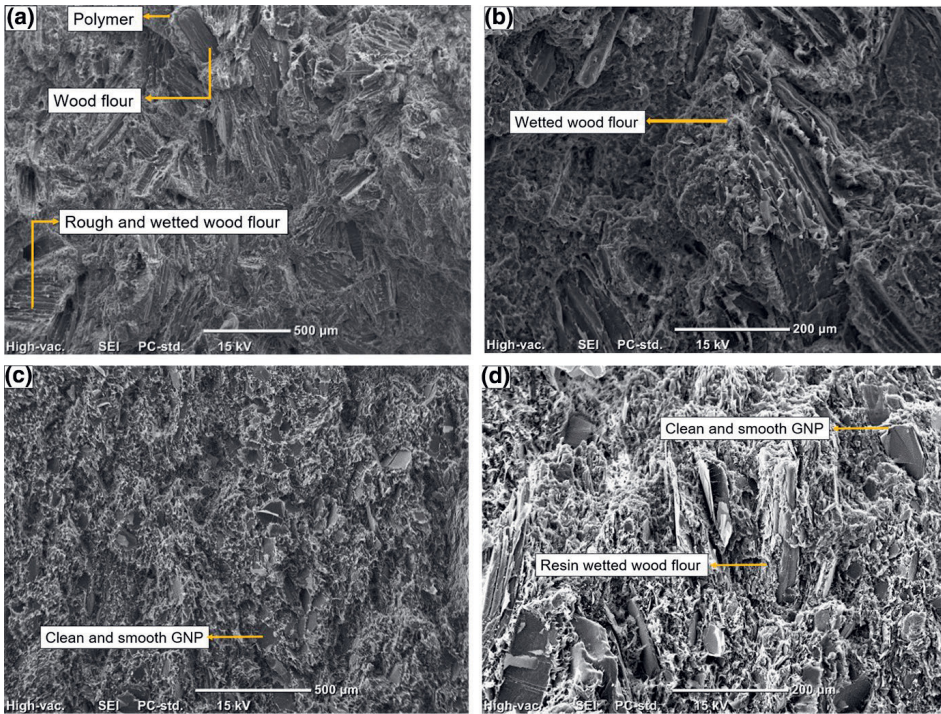


Fig. 8 SEM images from the tensile fractured surface of PP-W20 (a), (b) and PP-W20-G15 (c), (d)

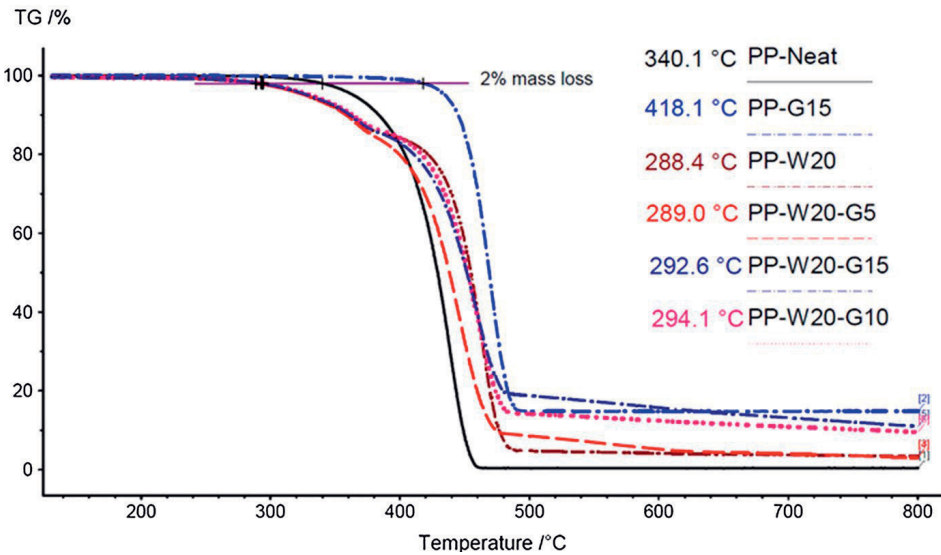


Fig. 9 TGA thermograms of polypropylene (PP-neat), polypropylene/graphene nanoplatelets composite (PP-GNP15), polypropylene/wood flour composite (PP-W20) and polypropylene/wood flour/graphene nanoplatelets hybrid composites (PP-W20-G5, PP-W20-G10, PP-W20-G15)

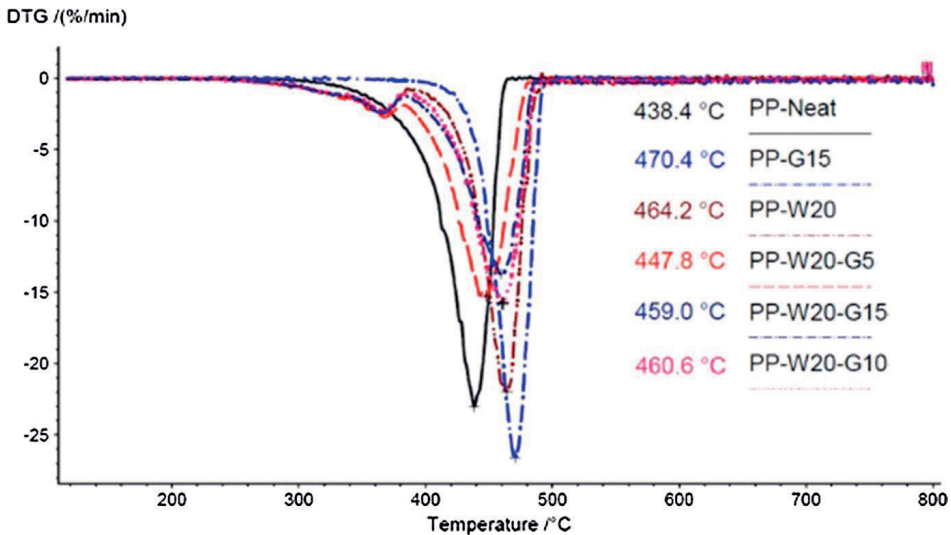


Fig. 10 DTG curve of polypropylene neat (PP-neat), polypropylene/graphene nanoplatelets composite (PP-GNP15), polypropylene/wood flour composite (PP-W20) and polypropylene/wood flour/graphene nanoplatelets hybrid composites (PP-W20-G5, PP-W20-G10, PP-W20-G15)

GNP loading of 15 wt% (PP-GNP). The initial degradation temperature of PP-W20 was determined to be 288 °C and was found to be 52 °C lower than PP neat. The PP neat and PP-G15 thermally decompose in a single stage. The increase in the initial degradation temperature of composites after the addition of GNP is reported in the literature (Li et al. 2011). This is attributed to the barrier effect created through the tortuous path of GNPs formed in the matrix. The tortuous path can delay the diffusion of the condensed phase decomposition products to the surface or gas phase (Liang et al. 2015). In addition, the absorption of free radicals produced during the decomposition by GNPs plays a key role in improving the thermal stability of PP-G15 (Li et al. 2011; Liang et al. 2015).

The thermal decomposition of PP-W20 occurs in two stages as seen from Fig. 10 (DTG). The first decomposition stage is mainly related to the degradation of wood flour in the composite and the second degradation stage mainly corresponds to the degradation of the polymer and remaining components of wood. In general, the wood fibre thermal decomposition occurs in three stages. (1) 250–340 °C is related to decomposition and depolymerization of hemicellulose and pectins; (2) 340–370 °C is ascribed to the decomposition of cellulose; (3) 370–500 °C is related to the decomposition of lignin (Li et al. 2014). The first DTG peak (Fig. 10) shows that the maximum degradation of wood flour in PP-W20 and all the three hybrid composites occurs between 360 and 380 °C.

The initial decomposition temperature (2% mass loss) of WPC increased slightly for PP-W20-G10 (294 °C) and PP-W20-G15 (293 °C) when compared to PP-W20 (288 °C). Although the improvement in thermal stability of hybrid composites is low compared to PP-G15, the increase in initial thermal decomposition temperature of hybrid WPCs is due to the presence of GNP. As discussed earlier, GNP can delay

the thermal decomposition by inhibiting the diffusion of oxygen and other volatiles formed during the decomposition of the hybrid WPCs.

The maximum degradation temperature (T_{max}) of all the studied composites increased compared to PP neat (Fig. 10). The increase in maximum degradation temperature of the composites compared to PP neat is due to the lignin content in wood flour and due to the increasing GNP content. The thermal stability of lignin is due to the presence of phenylpropanoid units consisting of highly stable aromatic phenyl groups (Gordobil et al. 2015). The increase in T_{max} for WPC compared to PP was reported elsewhere (Sheshmani et al. 2013). They studied the thermal decomposition of the PP/WF/GNP system and reported an increase in initial decomposition temperature and T_{max} after the addition of GNP. The maximum improvement in thermal stability was observed in the case of the hybrid composite containing 0.8 wt% GNP. Increasing the GNP content above 0.8 wt% decreased the thermal stability of hybrid composites. The maximum GNP loading used in their study was 5 wt% and in this study, it was 15 wt%. Thus, it is assumed that the higher content of GNP in hybrid WPCs lowered its effect on thermal stability due to the agglomeration of GNP.

Statistical analysis

The detailed results from statistical analysis are included as supporting information (see Electronic Supplementary Material). The test assumptions for one-way ANOVA on surface resistivity of composites were checked. Levene's test was significant ($p < 0.001$), indicating that the assumption of homogeneity of variance was violated. Normality was checked with a Q–Q plot and no deviations were noted. Since the assumption of homogeneity of variance was violated, Brown-Forsythe homogeneity correction was applied. According to ANOVA, there was a statistically significant difference among the composites on the surface resistivity ($p < 0.001$). Games-Howell post-hoc test revealed that the surface resistivity results are statistically significant ($p < 0.001$) except for PP-neat vs PP-W20 ($p = 0.225$), PP-G15 vs PP-W20-G15 ($p = 0.459$) and PP-W20-G5 vs PP-W20-G10 ($p = 0.079$). Although the post-hoc test shows no statistical difference between PP-G15 and PP-W20-G15, the experimental results indicate a difference between the two groups of composites. This is based on the findings from the cross-section SEM analysis of these two composites which supports the results from surface resistivity that PP-W20-G15 is more electrically conductive than PP-G15. The paired t-test was performed to differentiate the statistical significance between slow cooling and fast cooling of PP-W20-G15 on the surface resistivity. There was no deviation from normality as found from the (Shapiro–Wilk) test of normality. The t-test results show that there is a statistically significant difference in surface resistivity of fast cooled PP-W20-G15 and slow cooled PP-W20-G15 ($p = 0.001$).

As mentioned above, the test assumptions for ANOVA were checked and no deviations were noted in the case of thermal conductivity results. The ANOVA shows that there are statistically significant differences among the composites ($p < 0.001$) in terms of thermal conductivity. Since there were no violations of assumptions, a

Tukey post-hoc test was performed and the comparisons show that the thermal conductivity results have statistically high significance ($p = < 0.001$ for all the comparisons except PP vs PP-W20 with $p = 0.005$). The comparison is considered as statistically significant when the p -value is < 0.05 .

The ANOVA shows that there are statistically significant differences among the composites in terms of the tensile strength ($p = < 0.001$). Tukey's post-hoc comparisons show that compared to PP-neat, the tensile strength of all the hybrid WPC is statistically significant ($p = < 0.001$). When comparing to PP-W20, the tensile strength of PP-W20-G10 and PP-W20-G15 is statistically significant ($p = 0.002$ and $p = < 0.001$). There was no statistical significance between PP-W20-G5 and PP-W20-G10 ($p = 0.139$). Since the assumption of homogeneity of variances was violated, Brown-Forsythe homogeneity correction was applied in the case of tensile modulus of the composites. The ANOVA shows a statistically significant difference among the composites in terms of tensile modulus ($p = < 0.001$). Games-Howell post-hoc comparisons revealed that there is a statistically significant difference in hybrid WPC when compared to PP-W20. However, there was no statistically significant difference when comparing the hybrid WPC between each other.

Conclusion

The objective of this study was to develop wood plastic composites (WPC) with improved electrical and thermal conductivity. The graphene nanoplatelet used as conductive filler is found to be efficient in decreasing the surface resistivity of hybrid wood plastic composites. The percolation threshold for the studied composite is identified to be 15 wt% in the presence of 20 wt% wood flour. The conductive path formation in the PP-W20-G15 composite is explained from the charge contrast in the SEM image taken at low voltage and high vacuum. The difference in the conductive path formation in PP-G15 and PP-W20-G15 is clear from the SEM images from the polished cross-section. The thermal conductivity shows an increasing trend with an increase in GNP loading. However, the increase in thermal conductivity from 0.23 W/m.K (PP neat) to 0.61 W/m.K (PP-W20-G15) is of less significance when considering the practical applications like heat sink materials requiring a minimum thermal conductivity of 2.0 W/m.K. The decrease in the tensile strength of hybrid WPC is due to the weak interfacial adhesion between the PP and GNP. The adhesion between PP and wood in hybrid WPC was found to be good due to MAPP. This points out the need for using functionalized GNP while developing hybrid WPC. Improved interfacial adhesion cannot only improve the mechanical properties but will also increase the thermal conductivity by decreasing the interfacial thermal resistance.

The antistatic wood plastic composite produced in this study can be utilized in producing ESD safe enclosures for sensitive electronic parts and in other applications demanding controlled electrostatic discharge. In the future, efforts should be focused on reaching the percolation threshold at lower GNP content considering the cost of GNP compared to conductive carbon black. In future, wood plastic composites containing conductive carbon black will be developed and studied as a cheaper

alternative to graphene. Considering the moisture absorption ability of wood flour, a detailed study is required to see how the moisture absorption is affecting the various properties of electrically and thermally conductive wood plastic composites.

Supplementary Information The online version contains supplementary material available at <https://doi.org/10.1007/s00226-021-01275-9>.

Acknowledgements This study has received funding from EU Interreg IV North program 2014–2020 by The county Administrative Board of Norrbotten, Sweden and Regional Council of Lapland, Finland, for project SMART-WPC. The authors gratefully acknowledge the financial support received for the project. Authors are thankful to Ms. Zainab Al-Maqdasi, Luleå University of Technology for fracture surface SEM images and Mr. Juha Junkala, Centria UAS for assistance in laboratory.

References

- Alemdar A, Sain M (2008) Biocomposites from wheat straw nanofibers: morphology, thermal and mechanical properties. *Compos Sci Technol* 68:557–565. <https://doi.org/10.1016/j.compscitech.2007.05.044>
- Al-Saleh MH, Saadeh WH, Sundararaj U (2013) EMI shielding effectiveness of carbon based nanostructured polymeric materials: a comparative study. *Carbon* 60:146–156. <https://doi.org/10.1016/j.carbon.2013.04.008>
- Batista NL, Helal E, Kurusu RS, Moghimian N, David E, Demarquette NR, Hubert P (2019) Mass-produced graphene—HDPE nanocomposites: thermal, rheological, electrical, and mechanical properties. *Polym Eng Sci* 59:675–682. <https://doi.org/10.1002/pen.24981>
- Biron M (2018) Chapter 7 - plastics solutions for practical problems. In: Biron M (ed) *Thermoplastics and thermoplastic composites* (Third Edition). William Andrew Publishing, New York, pp 883–1038
- Chodak I, Krupa I (1999) “Percolation effect” and mechanical behavior of carbon black filled polyethylene. *J Mater Sci Lett* 18:1457–1459. <https://doi.org/10.1023/A:1006665527806>
- Choi H, Kim MS, Ahn D, Yeo SY, Lee S (2019) Electrical percolation threshold of carbon black in a polymer matrix and its application to antistatic fibre. *Sci Rep* 9:1–12. <https://doi.org/10.1038/s41598-019-42495-1>
- Chung KT, Reisner JH, Campbell ER (1983) Charging phenomena in the scanning electron microscopy of conductor-insulator composites: a tool for composite structural analysis. *J Appl Phys* 54:6099–6112. <https://doi.org/10.1063/1.331946>
- de Sousa D, Salvador E, Scuracchio CH, de Oliveira Barra, Guilherme Mariz, Lucas AdA, (2015) Chapter 7 - expanded graphite as a multifunctional filler for polymer nanocomposites. In: Friedrich K, Breuer U (eds) *Multifunctionality of polymer composites*. William Andrew Publishing, Oxford, pp 245–261
- Fu F, Yuan Q (2017) 12 - Electricity functional composite for building construction. In: Fan M, Fu F (eds) *Advanced high strength natural fibre composites in construction*. Woodhead Publishing, UK, pp 287–331
- Gordobil O, Delucis R, Egiúés I, Labidi J (2015) Kraft lignin as filler in PLA to improve ductility and thermal properties. *Ind Crops Prod* 72:46–53. <https://doi.org/10.1016/j.indcrop.2015.01.055>
- Gulrez SKH, Mohsin MEA, Shaikh H, Anis A, Pulose AM, Yadav MK, Qua EHP, Al-Zahrani SM (2014) A review on electrically conductive polypropylene and polyethylene. *Polym Compos* 35:900–914. <https://doi.org/10.1002/pc.22734>
- Haznedar G, Cravanzola S, Zanetti M, Scarano D, Zecchina A, Cesano F (2013) Graphite nanoplatelets and carbon nanotubes based polyethylene composites: electrical conductivity and morphology. *Mater Chem Phys* 143:47–52. <https://doi.org/10.1016/j.matchemphys.2013.08.008>
- He S, Zhang J, Xiao X, Hong X, Lai Y (2017) Investigation of the conductive network formation of polypropylene/graphene nanoplatelets composites for different platelet sizes. *J Mater Sci* 52:13103–13119. <https://doi.org/10.1007/s10853-017-1413-y>

- Idumah CI, Hassan A (2016) Characterization and preparation of conductive exfoliated graphene nanoplatelets kenaf fibre hybrid polypropylene composites. *Synth Met* 212:91–104. <https://doi.org/10.1016/j.synthmet.2015.12.011>
- Imran KA, Lou J, Shivakumar KN (2018) Enhancement of electrical and thermal conductivity of polypropylene by graphene nanoplatelets. *J Appl Polym Sci* 135:45833. <https://doi.org/10.1002/app.45833>
- Jun Y, Um JG, Jiang G, Yu A (2018) A study on the effects of graphene nano-platelets (GnPs) sheet sizes from a few to hundred microns on the thermal, mechanical, and electrical properties of polypropylene (PP)/GnPs composites. *Express Polym Lett* 12:885–897. <https://doi.org/10.3144/expresspolymlett.2018.76>
- Kalaitzidou K, Fukushima H, Askeland P, Drzal LT (2008) The nucleating effect of exfoliated graphite nanoplatelets and their influence on the crystal structure and electrical conductivity of polypropylene nanocomposites. *J Mater Sci* 43:2895–2907. <https://doi.org/10.1007/s10853-007-1876-3>
- Kalaitzidou K, Fukushima H, Drzal LT (2007) A new compounding method for exfoliated graphite–polypropylene nanocomposites with enhanced flexural properties and lower percolation threshold. *Compos Sci Technol* 67:2045–2051. <https://doi.org/10.1016/j.compscitech.2006.11.014>
- Karteri I, Altun M, Gunes M (2017) Electromagnetic interference shielding performance and electromagnetic properties of wood-plastic nanocomposite with graphene nanoplatelets. *J Mater Sci Mater Electron* 28:6704–6711. <https://doi.org/10.1007/s10854-017-6364-1>
- Khanam NP, AlMaadeed MA, Ouederni M, Harkin-Jones E, Mayoral B, Hamilton A, Sun D (2016) Melt processing and properties of linear low density polyethylene-graphene nanoplatelet composites. *Vacuum* 130:63–71. <https://doi.org/10.1016/j.vacuum.2016.04.022>
- Kim H, Abdala AA, Macosko CW (2010) Graphene/polymer nanocomposites. *Macromolecules* 43:6515–6530. <https://doi.org/10.1021/ma100572e>
- Kim H, Macosko CW (2009) Processing-property relationships of polycarbonate/graphene composites. *Polymer* 50:3797–3809. <https://doi.org/10.1016/j.polymer.2009.05.038>
- Lee S, Choi O, Lee W, Yi J, Kim B, Byun J, Yoon M, Fong H, Thostenson ET, Chou T (2011) Processing and characterization of multi-scale hybrid composites reinforced with nanoscale carbon reinforcements and carbon fibers. *Compos A Appl Sci Manuf* 42:337–344. <https://doi.org/10.1016/j.compositesa.2010.10.016>
- Leu S, Yang T, Lo S, Yang T (2012) Optimized material composition to improve the physical and mechanical properties of extruded wood–plastic composites (WPCs). *Constr Build Mater* 29:120–127. <https://doi.org/10.1016/j.conbuildmat.2011.09.013>
- Li A, Zhang C, Zhang Y (2017) Thermal conductivity of graphene-polymer composites: mechanisms, properties, and applications. *Polymers* 9:437. <https://doi.org/10.3390/polym9090437>
- Li X, Lei B, Lin Z, Huang L, Tan S, Cai X (2014) The utilization of bamboo charcoal enhances wood plastic composites with excellent mechanical and thermal properties. *Mater Des* 53:419–424. <https://doi.org/10.1016/j.matdes.2013.07.028>
- Li Y, Zhu J, Wei S, Ryu J, Sun L, Guo Z (2011) Poly(propylene)/graphene nanoplatelet nanocomposites: melt rheological behavior and thermal, electrical, and electronic properties. *Macromol Chem Phys* 212:1951–1959. <https://doi.org/10.1002/macp.201100263>
- Liang JZ, Wang JZ, Tsui GCP, Tang CY (2015) Thermal decomposition kinetics of polypropylene composites filled with graphene nanoplatelets. *Polym Test* 48:97–103. <https://doi.org/10.1016/j.polymertesting.2015.09.015>
- Mertens R (2017) NanoXplore plans a 10,000 ton graphene powder facility. In: <https://www.graphene-info.com/nanoxplore-plans-10000-ton-graphene-powder-facility>. Accessed Dec 31, 2020
- Moultif N, Masmoudi M, Joubert E, Latry O (2017) 5 - reliability and qualification tests for high-power MOSFET transistors. In: El Hami A, Delaux D, Grzeskowiak H (eds) *Reliability of high-power mechatronic systems 2*. Elsevier, Amsterdam, pp 155–197
- Papageorgiou DG, Kinloch IA, Young RJ (2017) Mechanical properties of graphene and graphene-based nanocomposites. *Prog Mater Sci* 90:75–127. <https://doi.org/10.1016/j.pmatsci.2017.07.004>
- Papageorgiou DG, Kinloch IA, Young RJ (2016) Hybrid multifunctional graphene/glass-fibre polypropylene composites. *Compos Sci Technol* 137:44–51. <https://doi.org/10.1016/j.compscitech.2016.10.018>
- Park HM, Kalitzidou K, Fukushima H, Drzal LT (2007) Exfoliated graphite nanoplatelet (xGnP)/polypropylene nanocomposites. SPE 7th annual automotive composites conference and exhibition, ACCE 2007—driving performance and productivity

- Parker WJ, Jenkins RJ, Butler CP, Abbott GL (1961) Flash method of determining thermal diffusivity, heat capacity, and thermal conductivity. *J Appl Phys* 32:1679–1684. <https://doi.org/10.1063/1.1728417>
- Pedrazzoli D, Pegoretti A, Kalaitzidou K (2015) Synergistic effect of graphite nanoplatelets and glass fibers in polypropylene composites. *J Appl Polym Sci*. <https://doi.org/10.1002/app.41682>
- Pedrazzoli D, Pegoretti A (2013) Silica nanoparticles as coupling agents for polypropylene/glass composites. *Compos Sci Technol* 76:77–83. <https://doi.org/10.1016/j.compscitech.2012.12.016>
- Phiri J, Gane P, Maloney TC (2017) General overview of graphene: production, properties and application in polymer composites. *Mater Sci Eng, B* 215:9–28. <https://doi.org/10.1016/j.mseb.2016.10.004>
- Potts JR, Dreyer DR, Bielawski CW, Ruoff RS (2011) Graphene-based polymer nanocomposites. *Polymer* 52:5–25. <https://doi.org/10.1016/j.polymer.2010.11.042>
- Rowell RM (2006) Advances and challenges of wood polymer composites. Proceedings of the 8th pacific rim bio-based composites symposium, advances and challenges in biocomposites: 20–23 November 2006, Kuala Lumpur, Malaysia. Kepong, Malaysia : Forest Research Institute Malaysia, c2006: ISBN: 9832181879: 9789832181873: pp 2–11
- Sheshmani S, Ashori A, Arab Fashapoyeh M (2013) Wood plastic composite using graphene nanoplatelets. *Int J Biol Macromol* 58:1–6. <https://doi.org/10.1016/j.ijbiomac.2013.03.047>
- Syurik J, Ageev OA, Cherednichenko DI, Konoplev BG, Alexeev A (2013) Non-linear conductivity dependence on temperature in graphene-based polymer nanocomposite. *Carbon* 63:317–323. <https://doi.org/10.1016/j.carbon.2013.06.084>
- Syurik YV, Ghislandi MG, Tkalya EE, Paterson G, McGrouther D, Ageev OA, Loos J (2012) Graphene network organisation in conductive polymer composites. *Macromol Chem Phys* 213:1251–1258. <https://doi.org/10.1002/macp.201200116>
- Thwe MM, Liao K (2003) Durability of bamboo-glass fiber reinforced polymer matrix hybrid composites. *Compos Sci Technol* 63:375–387. [https://doi.org/10.1016/S0266-3538\(02\)00225-7](https://doi.org/10.1016/S0266-3538(02)00225-7)
- Tripathi SN, Rao GSS, Mathur AB, Jasra R (2017) Polyolefin/graphene nanocomposites: a review. *RSC Adv* 7:23615–23632. <https://doi.org/10.1039/C6RA28392F>
- Wang J, Kazemi Y, Wang S, Hamidinejad M, Mahmud MB, Pötschke P, Park CB (2020) Enhancing the electrical conductivity of PP/CNT nanocomposites through crystal-induced volume exclusion effect with a slow cooling rate. *Compos B Eng* 183:107663. <https://doi.org/10.1016/j.compositesb.2019.107663>
- Yadav R, Tirumali M, Wang X, Naebe M, Kandasubramanian B (2019) Polymer composite for antistatic application in aerospace. *Def Technol*. <https://doi.org/10.1016/j.dt.2019.04.008>
- Yang H, Gong J, Wen X, Xue J, Chen Q, Jiang Z, Tian N, Tang T (2015) Effect of carbon black on improving thermal stability, flame retardancy and electrical conductivity of polypropylene/carbon fiber composites. *Compos Sci Technol* 113:31–37. <https://doi.org/10.1016/j.compscitech.2015.03.013>
- Zhang H, Zheng W, Yan Q, Yang Y, Wang J, Lu Z, Ji G, Yu Z (2010) Electrically conductive polyethylene terephthalate/graphene nanocomposites prepared by melt compounding. *Polymer* 51:1191–1196. <https://doi.org/10.1016/j.polymer.2010.01.027>
- Zhang X, Zhang J, Wang R (2019) Thermal and mechanical behavior of wood plastic composites by addition of graphene nanoplatelets. *Polymers* 11:1365. <https://doi.org/10.3390/polym11081365>
- Zhao YF, Xiao M, Wang SJ, Ge XC, Meng YZ (2007) Preparation and properties of electrically conductive PPS/expanded graphite nanocomposites. *Compos Sci Technol* 67:2528–2534. <https://doi.org/10.1016/j.compscitech.2006.12.009>
- Zheng W, Lu X, Wong S (2004) Electrical and mechanical properties of expanded graphite-reinforced high-density polyethylene. *J Appl Polym Sci* 91:2781–2788. <https://doi.org/10.1002/app.13460>

Publisher's Note Springer Nature remains neutral with regard to jurisdictional claims in published maps and institutional affiliations.

